The Synthesis and Application of Dendritic Polymer for Photodynamic Therapy

Fatema Aboshnaf

PhD Thesis

2017

The Synthesis and Application of Dendritic Polymer for Photodynamic Therapy

Fatema Aboshnaf

A thesis submitted for the degree of Doctor of Philosophy

Department of Chemistry, The University of Sheffield

Sheffield, S3 7HF

England

June 2017

SUPERVISOR

Dr L J TWYMAN

To my father,

Thank you for your endless love…

Acknowledgement

The present work could not have been accomplished without the help of a number of people. I would firstly like to extend my sincere and deepest gratitude to my supervisor Dr. Lance Twyman whom his support and guidance from the initial to the final level enabled me to develop an understanding of the subject.

My deepest gratitude to my husband, Abdulsallam and our five children; Safe, Faisel, Faizah, Makzhoum and Hamudi who have given me the opportunity to complete my project. Their deepest love, assistance and courage have made to finish my thesis. It would like also to thank the entire Twyman group who supported me through all these years, notably Samira Hussein, Alaa Kadhim, Devanshi Singh, Azrah Abdul Aziz, Hamza Qasem, Greg Clixby, Jawad K Abaies , Bunian Shareef, Talal Alghassab Ibrahim Althobaiti, and Fan Meng

I would like to extend a special appreciation to the staff of the Department of Chemistry at the University of Sheffield, Special thanks go to Heather Grievson for her dedication and assistance on lab management and instrumentation, Susan Bradshaw for the help with NMR, Simon Thorpe for Mass Spectroscopy Pete Farran, Nick Smith for their help in orders, chemical collections in the department. Many thanks to Mr Luke Mckenzie from medical school for the cell culture work and discussions made for my further knowledge. I would also like to convey my sincere appreciation to Lynne Newcombe for her help.

I offer my regards and blessings to all of those who supported me in any respect during the completion of the thesis, special thanks to my lovely friend Laila Alhaidari who really supported me during writing up my thesis. Lastly, my thanks go to my brothers, sisters, my uncle Amer and all my relatives for their unlimited support during the journey of my PhD.

Contents

List of Figures

List of Tables

Abstract

Dendrimers and dendrons are highly branched polymers with a three-dimensional structure and diameters around 1-10 nm. Their properties, include, easy modification of the core, surfaces and interior, the ability to control polymer size and high water solubility. Because of these characteristics, these macromolecules have been used for several applications. This research has studied these materials as drug delivery systems for photodynamic therapy (PDT) in cancer dieses. In oncology, photosensitizers (PS) are specific drugs used in PDT. The problems with drugs are poor solubility and they are taken up by healthy as well as cancerous tissues therefore, the success of PDT is limited with these issues. To overcome this problem, dendrimers were synthesised and used to improve the drug solubility and carry drugs to the specific targeted cell. Accordingly, the essential goal of PDT is to induce efficient damage to tumour tissue without any negative effect on healthy cells.

Initially, the first part includes the synthesis of water-soluble PAMAM dendrimers from G0.5 to G4.5 via the divergent approach, which involves two steps; a 1,4-Michael addition to yield half-generation dendrimers (ester terminated dendrimers) and an amidation step to synthesise whole generation dendrimers (amine terminated dendrimers). Ethylenediamine (EDA) was chosen as a core for the dendrimers to generate primary and secondary amines within the dendrimer structure. The half-generation dendrimers from G0.5 to G4.5 were successfully converted to OH terminated dendrimers using hydroxymethyl amino methane (TRIS). To investigate our dendrimer as the solubility enhancer, ibuprofen was studied. The study exploits water-soluble PAMAM dendrimers ranging from G 0.5 to G 3.5 for encapsulation of ibuprofen. The G3.5 (96OH) PAMAM dendrimer systems recorded the highest encapsulation when compared to the smaller G1.5 (24OH) and G2.5 (48OH). Encapsulation studies using excess ibuprofen and a dendrimer concentrations ranging from $1\times10^{-4} – 6\times10^{-4}$ M. These experiments showed that ibuprofen loading was not linear, with a maximum loading of 1.00×10^{-4} M observed, at all dendrimer concentrations above $2x10^{-4}$ M. The reason for this was aggregation of the dendrimers at the higher concentrations. This was confirmed by DLS, which showed 200 nm-sized aggregates, at 1×10^{-4} M and above.

The second part of the work utilises the OH-terminated PAMAM dendrimer from G1.5 to G3.5 for encapsulation of two hydrophobic molecules namely; tetra-phenyl porphyrin (TPP) and zinc Tetraphenylporphyrin (ZnTPP). Both molecules are used as drugs in photodynamic therapy, but have zero solubility in water. The dendrimers were able to solubilize and encapsulate TPP

and ZnTPP, but the dendrimers were able to solubilize ten times more of the metalated ZnTPP. The increased solubility came from a secondary interaction generated via coordination between the dendrimer's internal nitrogen(s) and the zinc metal within ZnTPP. As with the ibuprofen, the level of ZnTPP encapsulation increased with the size of the dendrimers, with G3.5 OH being the best host ZnTPP. Despite these results, the solubility of the drug remains below the desired limit for therapeutic applications, with dendrimer to ZnTPP ratios being very low (around 10 dendrimers to 1 ZnTPP). Thus, to increase drug loading, coordination bonding was further exploited and used as an integral part of the dendrimer synthesis.

The third part describes the synthesis of PAMAM dendrons, ranging from G 0.5 to G 3.5, and their use as ligands that could assemble around a porphyrin or a phthlocyanine photosensitizer. Tin cored porphyrin $SnTPP(OH)_2$ and tin cored phthlocyanine $SnPC(Cl)_2$ were synthesized as the photosensitiser (PS). When the dendrons were added they could replace the OH or Cl ligands and assemble on either face of the PS. The aqueous solubility of the dendronized photosensetizers was higher than either $SnTPP(OH)_2$ or $SnPC(Cl)_2$, and experiments showed that they could be taken up and internalised by cancer cells. However, they were not soluble at the level required to perform PDT experiments. In addition, the phthalocyanin-dendron systems showed aggregation characteristics in aqueous solution, which may have been good for PDT. However, although soluble, λ_{max} had shifted from 750 nm to 350 nm. At the shorter wavelength they are no longer useful for PDT and were not tested.

Keywords: PAMAM dendrimers, and PAMAM dendrons a carrier, drug delivery systems, Photodynamic Therapy, Enhanced permeation and retention (EPR) effect, Encapsulation study.

Standard Abbreviations

PK……. Pharmacokinetics.

PD……. ...Pharmacodynamics.

PDT……...Photodynamic therapy.

ROS…….....Reactive oxygen species.

LD……. Light delivery.

PS……. Photosensitizer.

PS_{Es}……Excited singlet state

PS_{Et}……Long lived triplet.

DDS……Drug delivery system.

1O2……...…. Reactive singlet oxygen.

DDS……Drug delivery system

EPR…….....Enhanced permeation and retention effect.

MTX……...Methotrexate.

HPB……Hyperbranched Polymer

MA…… Methyl acrylate

EDA……. Ethylenediamine

PAMAM……Polyamido amine.

G…….……Generation

OH……. hydroxyl group

12-OH……. PAMAM dendrimer with 12 hydroxyl groups

24-OH……PAMAM dendrimer with 24 hydroxyl groups

48-OH……PAMAM dendrimer with 48 hydroxyl groups

DCM……. Dichloromethane.

mg……..……Milligram

mmol……...……millimole

MeOH…….....Methanol

$MgSO_4$……Magnesium Sulphate

K_2CO_3……Potassium Carbonate

h……...……Hour

sec……. second

DMSO……. Dimethyl Sulphoxide

^{1}H NMR.....Proton Nuclear Magnetic Resonance Spectroscopy

^{13}C NMR.....Carbon Nuclear Magnetic Resonance Spectroscopy

ESMS…….....Electrospray Mass Spectrometry

MALDI-TOF-MS……Matrix Assisted Laser Desorption Ionisation Time of Flight Mass Spectroscopy

FTIR..... Fourier Transform Infrared Spectrophotometry.

UV/Vis..... Ultraviolet, Visible Light Spectrophotometry.

Ɛ……Extinction coefficient

nm……Nanometre.

DLS……...Dynamic light scattering

TRIS…….....Tris(hydroxymethyl)aminomethane.

TPP……Tetraphenyl porphyrin.

ZnTPP……Zinc tetraphenylporphyrin.

Sn(IV)……. Tin(IV).

$Sn(OH)_2TPP$……..... Dihydroxy tetra phenyl porphyrin tin (1V).

$CHCl_3$…… …Chloroform

$PcCl_2$……. Dichloride(Phthalocyanato)tin(IV)

1-CNP…….1-chloronaphthalene

$SnCl_2$……. Tin (II)chloride

$SnPc(Cl)_2$……. Tinphthalocyaninedichloride

HCl ……Hydrochloride Acid

d6-DMSO.…… Deuterated Dimethyl Sulphoxide.

NH_2……Amine

NH…… Amide.

°C……. Degree Celsius

NMR Abbreviations

Br……. broad

d……. doublet

dd……... doublet of doublets

m……. multiplet

o- …… ortho

m- ……meta

p-……. para

Q……..…quartet

s……singlet

t…… triplet

Chapter 1

Introduction

1.1 - Forward

The objective of this chapter is to present the necessary information related to this project from the existing literature. The first section will focus on the essential information related to photodynamic therapy for cancer treatment and difficulties associated with therapeutic compounds. The second section aims to offer background information about dendrimers and their importance in this project.

1.2 Concerns with therapeutic compounds

Drugs are chemical substances that are used for treatment, prevention and diagnosis of illnesses. They work by interfering with biological operations, such as acting on an enzyme or a transporter protein. All drugs have side effects; large doses can be toxic and deadly. Many medications are unable to perform their desired objective due to poor drug solubility, inadequate bioavailability or high toxicity [1]. To effectively treat humans and animals, pharmaceutical companies must accurately design drugs to reach the desired location in the body [2].

Drug delivery can occur in several ways depending on the drug and place of the target in the body. The most common forms of drug administration are oral, nasal, sublingual, vaginal, rectal, optical or by intravenous injection. The method of administrating a medication can depend on the drug properties; such as solubility and the extent of ionisation. The physiological action of a drug action is studied in pharmacology, a branch of biology [3]. There are two main areas of pharmacology to consider; the first is pharmacokinetics (PK) which studies the action of a drug in the body and how a drug reaches its target [4]. It includes adsorption, distribution, metabolism and excretion of the drug molecules. The second topic is pharmacodynamics (PD) which is related to the drug concentration at the site of action and the effect on the body. The major challenges that face the pharmacologist are bioavailability and absorption of drugs within the body; both these obstacles have a direct relationship with solubility [5]. For instance, therapeutic compounds with a low aqueous solubility are problematic and have poor absorption, a short half-life and a high clearance rate in the body. In addition, as a drug travels through the body it will indiscriminately enter healthy and cancerous tissues. This research will assess drug delivery systems for photodynamic therapy. The next section will highlight photodynamic therapy, mechanisms of PDT and drug target for cancer cells.

1.3 Photodynamic therapy (PDT) for cancer

Cancer is one of the deadliest diseases in the world, in 2015 it is estimated there were 8.8 million cancer-related deaths. To combat this, billions of dollars spent on research and improvements to cancer treatment standards every year. Photodynamic therapy (PDT) is a comparatively new therapy compared to traditional treatments, for instance, radiation therapy, surgery, and chemotherapy [6] It is a promising method for treating numerous cancers particularly for the treatment of skin, respiratory, bladder [7,8], neck and head cancers [9]. It includes three components; photosensitizers (PS), light and oxygen (O2) [10- 12]. PS is essential to PDT [13], they have unique characteristics such as the ability to produce singlet oxygen, no dark toxicity, high stability [14], the ability to be accumulated and retained to target cancerous cells and high absorption in the long wavelength area (600-700nm) which makes them useful for therapy [15]. In this type of treatment, cancerous cells are damaged via reactive oxygen species (ROS) which form when a photosensitizer is excited by light at a specific wavelength (in the visible region or near-infrared region of the spectrum) [16-18]. PDT has several benefits over traditional treatments; the most important are its ability to selectivity damage cancerous tissues and vasculature associated with the tumour itself is reachable to the light. More significantly, in the absence of light, it is not activated which leads to very low toxicity [19]. Light delivery (LD) to the target tissues is another important factor of PDT. Deep cancerous cells are difficult to treat because of low tissue penetration of visible light. Hence, to overcome this obstacle, the LD can be enhanced by using deeper wavelengths of compounds.

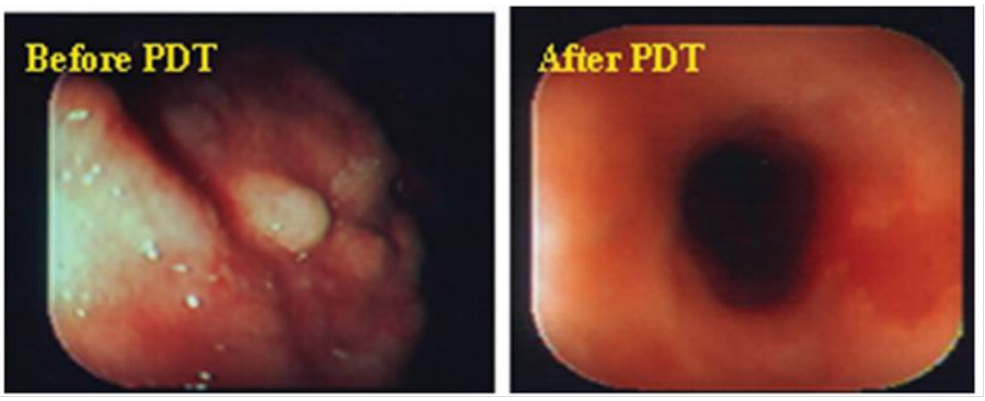

Figure 1.1. Esophageal tumor before PDT and after treated with HPPH-PDT. Taken from Ethirajan, M; Yihui, C.; Penny, J.; Ravindra, K. P. Chemical Society Reviews .2011,40 (1) 340-362).

1.3.1 PDT mechanism

A known mechanism used in PDT involves three main elements: PS, O_2, and light. Combining these elements causes the death of cancer cells in the body [20-22]. After the absorption of an appropriate wavelength of light, the PSs in the ground state are electronically excited and transferred to excited singlet state (PS_{Es}) and lose their energy by emission of fluorescence. The excited PS relaxes to a long-lived triplet state (PS_{Et}) and the energy is dissipated via emission of phosphorescence. The triplet excited state can interact with surrounding biomolecules via two pathways. In the first pathway, reaction type (I), the PS_Et interact with molecules which produce hydrogen atoms or free radicals which in turn interact with oxygen leading to the formation of reactive oxygen species (ROS). In the second pathway, the PSEt interact with oxygen to generate highly reactive singlet oxygen ($^1O_2$), reaction type (II). These reactions take place simultaneously although successful therapy is more dependent on the reaction type (II) Figure 1.2 [9, 10, 19, 23].

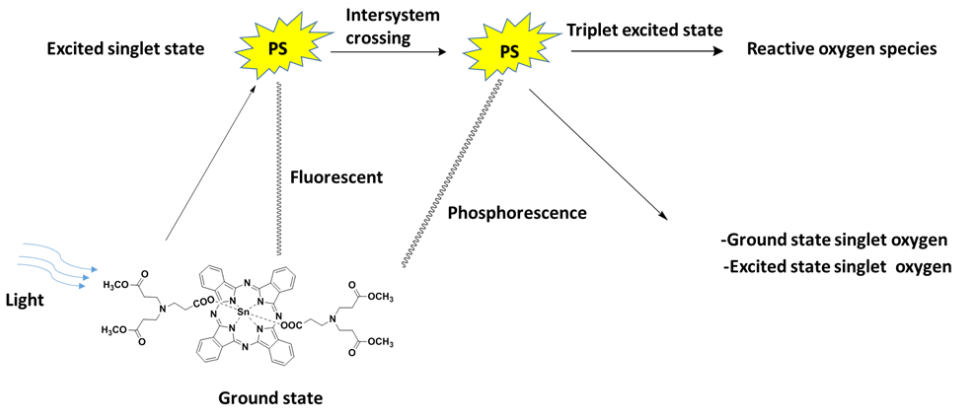

Figure 1.2. Photodynamic therapy mechanism

The success of photodynamic therapy relies on targeting diseased cells, without targeting it is toxic to the body. Targeting is a precise way of drug delivery to the specified location in an efficient and safe manner. The concept of tumour targeting first appeared in 1906 by Ehrlich who conceived the “magic bullet”. However, successful targeting requires identification of a medication appropriate for treatment, drug carriers and a precise way to target the drugs to

therapeutic sites [24]. In various laboratories, drug design depends on drug targeting mechanisms [17].

1.3.2 Mechanisms targeting

The systems under development can be modified to target specific sites, slowly degrade and be stimuli responsive i.e. respond to vicissitudes such as light and temperature. There are two main approaches used to target the delivery of drugs to cancers these are: passive and active targeting.

1.3.2.1 Active targeting

In this strategy, targeting is performed by specific ligands attached to the surface of the nano carries (Figure 1.3). These ligands can selectively bind to suitable receptors on cancerous cells. One the most influential elements of the effectiveness of active targeting is the binding affinity of the ligands; high affinity is better for targets and enhanced delivery of nanocarrier systems [24,25]. In vitro, this approach has displayed promising efficacy however, its effectiveness is limited in vivo activity and tumour-selectivity [9]. This strategy doesn't enhance the tumour accumulation of cytotoxic therapeutic compounds at the target site and delivers only a small portion of the drugs to the tumour [26]. Passive targeting depends on the use of a specific size to avoid penetration into normal tissue. This approach has been more successful in vivo in tumour-selectivity [9]; we will more focus on this method in this project.

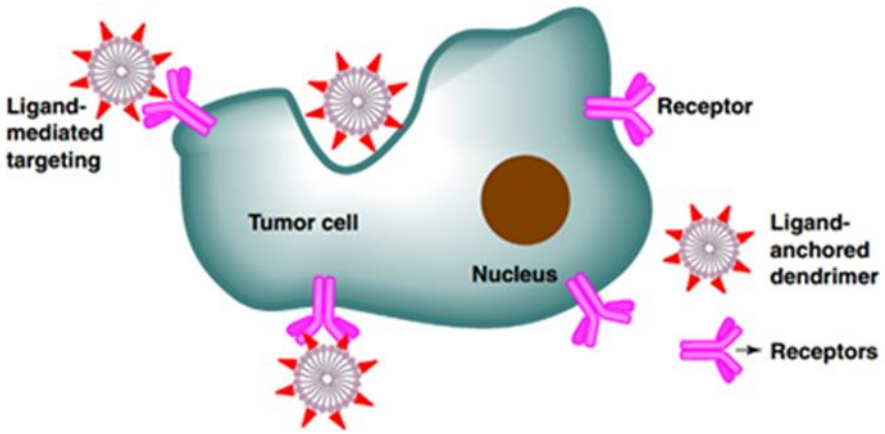

Figure 1.3. Ligand-anchored dendrimer mediated active targeting. Taken from Sharma, A. K.; Dendrimer Nano architectures for cancer diagnosis and anticancer drug delivery. Drug discovery today 2017: 22 (2), 314-326.

1.3.2. 2 Passive drug targeting: EPR effect

During the past fifty years, anticancer drugs with low molecular weights have been the treatment for many advanced cancers, but they result in massive toxicity because of the lack of selectivity. At the end of the 20th century, scientists agreed that cancer-selective targeting is one of the most important aims for tumour therapy [17]. A passive targeting mechanism was discovered in the 1980s by Maeda et al. based on the structure and size of the drug. A selective accumulation process of nanocarriers and drugs in tumour cells via leaky vasculature is called passive targeting, it also is known as an enhanced permeation and retention (EPR) effect [27]. This phenomenon results from the formation of new, irregular blood vessels in the tumour which only allow a certain size of molecule, nanoparticle or macromolecule, to accumulate in the cancerous cells as shown in Figure 1.4. [9,28,29].

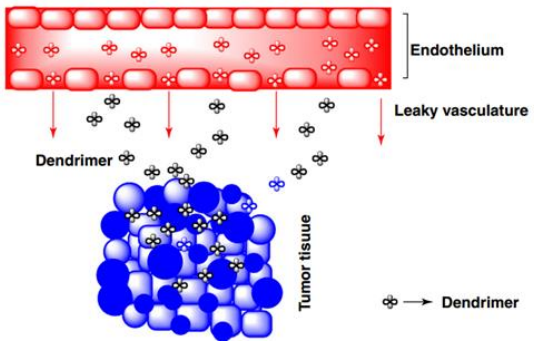

Figure 1.4. passive targeting through leaky blood vessels. Taken from Sharma, A. K.; Dendrimer nanoarchitectures for cancer diagnosis and anticancer drug delivery. Drug discovery today 2017: 22 (2), 314-326.

1.4 Drug delivery system (DDS) for PDT of cancer

Drug delivery systems are mechanisms to introduce a drug into the body to accomplish the desired results of the treatment while limiting the side effects. They involve multidisciplinary methods, such as pharmaceutics, polymer science, and molecular biology. Great effort was made to improve polymer architectures which led to the control of the size and shape of the polymers. These developments highlighted the importance of macromolecules in advanced

drug delivery systems [30]. To improve the effectiveness of therapeutic compounds, these systems focus on the synthesis of target therapy specifically tumour targeting [31,32]. At the present time, the use of nanocarriers for hydrophobic drugs is very attractive due to many new drugs being poorly soluble in water. Nanocarriers have revolutionised cancer therapy; there are many different nanosize structures used in this field such as nanoparticles, liposomes and polymeric micelles [25,33]. The size of nanocarriers (1-100 nm) [34] and their formulation in biocompatibility play the largest role as delivery systems [35-37]. Nevertheless, to create these systems synthetically is very challenging, they are difficult to make and inconsistent [38], they can be unstable under environmental conditions, such as temperature, high dilution, and pressure [39]. For example, the liposomes are self-assembled and formed by one or numerous phospholipid bilayers surrounding an aqueous core; these vesicles can encapsulate therapeutic compounds in their hydrophilic interior or hydrophobic exterior [40]. These liposomes can be used for passive and active pathway [41], but, they have disadvantages such as low drug loading ability, it can also cause cell toxicity, this is due to limited control of drug release [8] and problems in sterilisation [26,42,43]. Another example is micelles; these are self-assembled from surfactant molecules dispersed in a liquid colloid. They have the ability to overcome problems associated with liposomes, for instance, control over drug release and instability. However, obstacles such as instability in aqueous media and early drug release from the carrier [26,44,45] can reduce the importance of the micelles as a nanocarrier. These nanocarriers are illustrated in figure1.5.

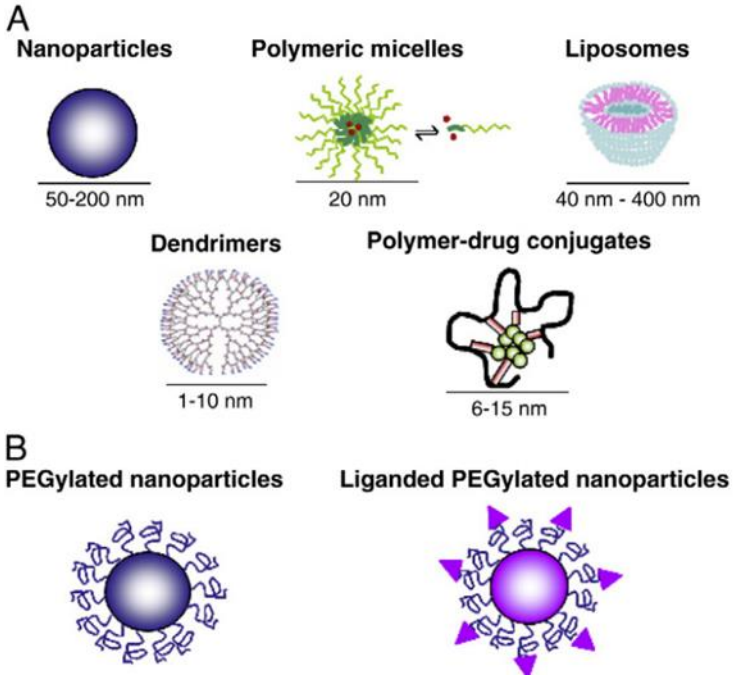

Figure 1.5. Schematic representation of Nanomedicine -based drug delivery systems. A. nanocarriers described in preclinical and clinical studies. B. PEGylation and ligand Grafting. Taken from Danhier, F.; Olivier, F.; Véronique, P. Journal of Controlled Release. 2010,148 (2),135-146.

difficult to achieve all these elements in one drug delivery system [17,46]. Dendrimers are another example of nanocarriers and will be the focus of this study. They have been recommended as a novel and 'smart' nanocarrier, as they have the ability to encapsulate a hydrophobic drug within the internal cavities of their structure or conjugated on the surface of the dendrimers [47]. Dendrimers have previously been used as a passive anticancer nanocarrier for PDT [25]. The next section will discuss the synthesis, properties, and applications of dendrimers.

1.4.1 Dendrimers

The term, dendrimer, is derived from the Greek words 'dendron' meaning tree and 'meros' meaning part. The 20th century has seen most of the innovations in polymer synthesis and advances in the design of the macromolecules of biodegradable polymers [48-49]. These advances in the field of polymer science resulted in dendrimers which were synthesised by different research groups. In the 1940s, Flory presented his first theoretical proposal for a highly branched macromolecule with a 3D structure [50.] After Flory, the first dendrimer to be synthesised as a branched polypropylene–amine (PPI) described by Vogtle and referred to the molecule as a "cascade polymer. Between 1983 and 1985, the Tomalia group synthesised polyamidoamine (PAMAM), Tomalia who generated the dendrimers term and Newkome created the term "arborols" in 1985. Moreover, Tomalia presented the creation of dendrimers at the first International Polymer Conference in 1984 [51]. This was closely followed by a paper detailing the dendrimer preparation; it described the synthesis of a starburst molecule using the divergent approach. In addition, Tomalia suggested the possibility of using a dendritic polymer to encapsulate hydrophobic molecules as the dendritic box. Hawker and Frechet in 1990 documented the convergent method to synthesise dendrimers.

1.4.1.1 Structure of dendrimers

Hermann Staudinger presented the macromolecule term which refers to the polymeric materials that included long chains or repeating units linked by covalent bonds by a reaction that he called polymerization. In 1922, Staudinger published a paper on the macromolecular hypothesis and was awarded the Nobel Prize for this work in 1953[52]. Polymers have a significant role in the advancement of drug delivery systems; they have the ability to control the release of therapeutic agents to provide a constant dose over long periods. There are four macromolecular architectures of polymeric molecules; three of the four categories are traditional synthetic

polymers: linear polymers, branched polymers and cross-linked polymers as shown in Figure 1.6.

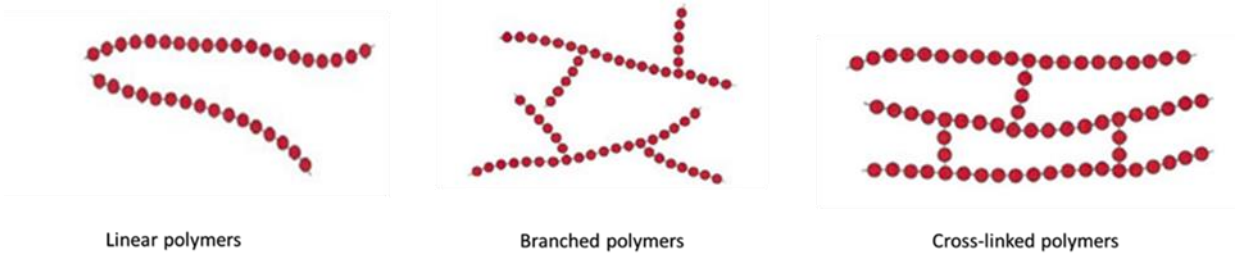

Figure 1.6 Three main types of traditional synthetic polymers: (a) linear polymer, (b) branched polymer and(c) cross-linked polymer

The fourth category is dendritic polymers [36]. Many dendritic polymers have been used for controlled release formulations and drug targeting systems. These molecules can be divided into four dendritic molecules: (a) random hyper branched polymers, (b) dendrigrafts, (c) dendrons, and (d) dendrimers Figure 1.7.

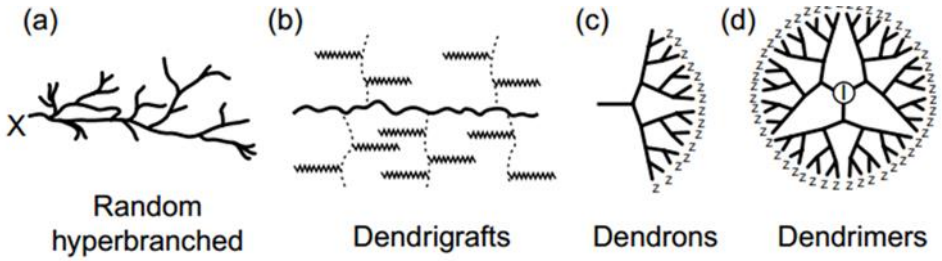

Figure 1.7. Three main types of traditional synthetic polymers: (a) Random hyperbranched, (b) Dendrigrafts, (c) dendrons and (d)dendrimers

In the past decade, there have been many attempts to design dendrimers, and after synthesis, these macromolecules have been attractive to the pharmaceutical industry due to their various chemical and physical properties that make them suited to drug delivery systems. The most important properties are low polydispersity, a high degree of branching, well-defined molecular

weight, globular architecture, biological activity, and they have hydrophilic exteriors and hydrophobic interiors [5,53,54].

Dendrimers and dendrons are a new class of the polymeric family; they are highly branched, symmetric macromolecules with a well-defined three-dimensional structure [55-57]. They are nanometres in size (around 1-10 nm), which allows for their passage through biological barriers [23]. Their nanostructure consists of three main units: the focal point or core, dendritic units and terminal units at the periphery [54,58]. Similar fragments of the dendrimer are called "dendrons" (Figure 1.8). Each dendrimer layer is called a generation; the first generation is synthesised from a core which is attached to repeat units (as a single layer). However, the second generation has two layers of repeat units, and the third generation three layers. The increasing number of layers leads to an increase in the size of generations and end groups at the dendrimer's surface [59]. They possess many functional groups in comparison with the traditional linear polymers which only have two end groups per molecule. Higher generation dendrimers have a more flexible and a globular structure in comparison with lower generations which have a flat conformation [60].

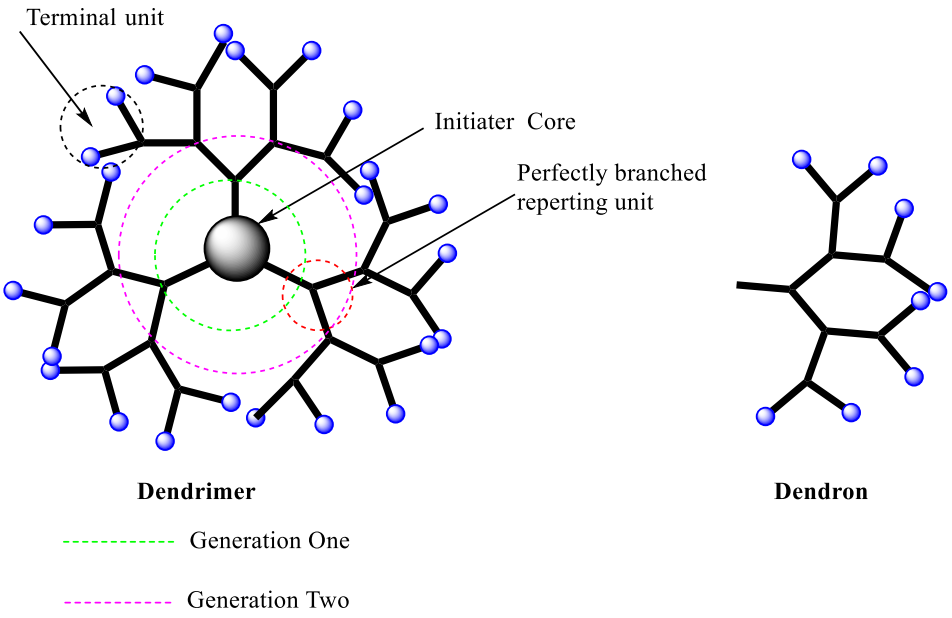

Figure 1.8. Basic structure of dendrimer

Each generation displays a different level of container property. Highly crowded branches in dendrimers can offer hollow spaces which have been used by numerous scientists to encapsulate

hydrophobic molecules. However, generations larger than G4 are extra-densely packed and have a closed structure, while the smaller generations are more open [61-62] for direct solvent contact within its interior. Dendrimers are stable under many conditions. Unlike classical micelles dendrimers are not affected by temperature, concentration, and pH.

1.4.1.2 Synthesis of dendrimers

Since 1979, two main approaches have been developed to synthesise dendrimers that often involve difficult purification steps. These methods are commonly named the divergent and convergent approach, construction notions of these methods are different [63-66].

1.4.2.2.1 Divergent approach

The divergent method was the first approach to synthesise dendrimer and was introduced by Tomalia in 1983. In this approach, dendrimer generation is built in a stepwise layer-by-layer manner which starts from a multifunctional core unit (inside) to the outer surfaces (outside) (Figure 1. 9) The first generation dendrimer is formed when a reactive core unit reacts with monomers containing one reactive and two inactive groups. After that, one reactive group on the periphery reacts with another monomer unit to form second generation dendrimers. These steps are repeated until the desired generation is achieved. The molecular weight of the dendrimer doubles after every separate generation. Large quantities of dendrimers can be produced by this method, and due to this, this method became the commercial route used to synthesise dendrimers. Despite the advantages of this strategy, there are some disadvantages associated with it, such as incomplete reactions and the side reactions which cause defects in the structure of the dendrimer. Thus to avoid these defects, an excess amount of reagent is needed to complete both reaction steps [65-70].

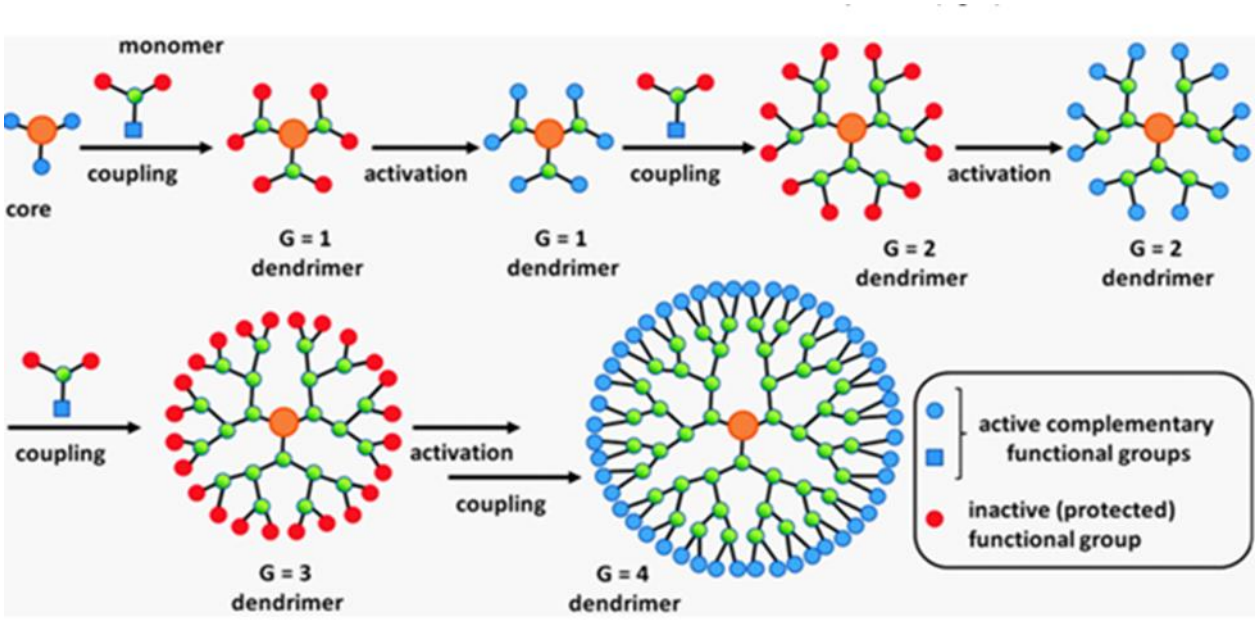

Figure 1.9. Divergent Growth Method. Taken from Singh, U.; Mohammad, M.D.; Athar, A. H.; Oriental Journal of Chemistry2014. 30 (3), 911-922

1.4.2.2.2 Convergent approach

The convergent method was an alternative approach used to synthesise dendrimers, introduced by Fréchet et al in 1990 [70-72]. The synthesis of the dendrimer by this approach starts from the outside (periphery) to the inside (core unit). The surface molecules are combined together to generate large surface molecule (dendrons), and these surface molecules link to multifunctional core molecules (Figure 1.10). Unlike the divergent approach, equal molar quantities are needed to complete the synthesis, without a large excess of branching units. The convergent method has a low number of coupling reactions at each growth step resulting in more constructive control than the divergent method. Thus, the products that form by this method have fewer defects and purification is simplified. One disadvantage associated with this method is the steric hindrance on the external surfaces that prevents the formation of high generation dendrimers [64, 71,73].

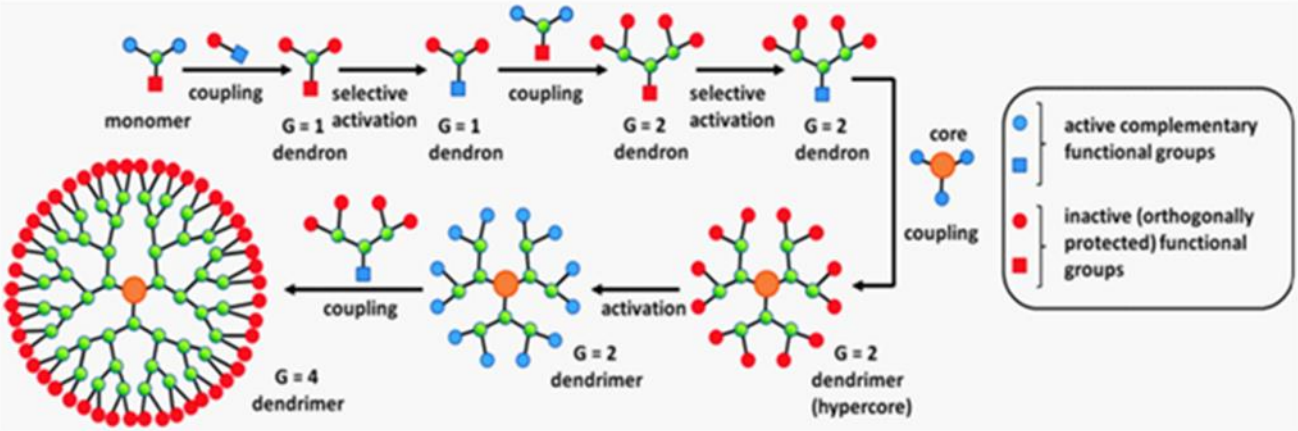

Figure 1.10. Convergent Growth Method. Taken from Singh, U.; Mohammad, M.D.; Athar, A. H.; Oriental Journal of Chemistry2014. 30 (3), 911-922

1.4.3 Properties of dendrimers

Dendrimers have a regular shape and size, unlike linear polymers. They are nondispersive macromolecules; polymerised by a specific process and precise control during synthesis. Their distinctive globular structure and dimensions make them very similar to numerous significant biological polymers [62, 74]. Biological properties are essential because these macromolecules are used in biomedical applications [75].

1.4. 3.1 Solubility

In many different dendrimer applications, solubility plays the vital role in achieving the goal. This property depends on the nature of the functional groups on the dendrimer surfaces. Solubility can be improved by modification of the dendrimer's end groups with suitable functional groups. The presence of many modified functional groups on the surfaces can provide the desired solubility in certain solvents [68]. These depend on the alternative groups used for this purpose. Also, the reactivity and binding capacity of dendrimers can improve with the presence of many functional groups. Due to their globular nature and internal cavities, particularly higher generations, dendrimers have become an attractive molecule to encapsulate hydrophobic drugs.

1.4. 3.2 Biocompatibility

In general, any polymeric carrier used in biomedical applications should be non-toxic and biodegradable. Dendrimer cytotoxicity is dependent significantly on the nature of the dendrimer external groups which are exposed to interactions with the biological cells [76]. In several published studies, dendrimer cytotoxicity has been tested in vitro, as for in vivo, published studies were limited [77]. The cationic surface of PAMAM dendrimers can damage the cell membrane which leads to cell lysis. The cytotoxicity of the cationic dendrimers displayed more cytotoxic than anionic dendrimers and the lowest cytotoxicity was revealed by PAMAM–OH dendrimers [78,79]. Another characteristic that affects dendrimer toxicity is the size of generation; some studies show that higher generations are more toxic [80]. A recent study was conducted on G4 amino terminated dendrimers concluded that toxicity was a result of their end groups. In addition, dendrimers with amine terminal groups have different levels of cytotoxicity, whereas primary amine dendrimers are more toxic than secondary amine dendrimers [81,82]. The most effective strategy to improve the biocompatibility of dendrimer is through conjugation of the dendrimer with biocompatibility units, such as polyethylene glycol (PEG) chains (Figure 1.11) [55]. For example, poly benzyl ether dendrimers conjugated with (PEG) show lower cytotoxicity than free poly benzyl ether dendrimers [26,83.]

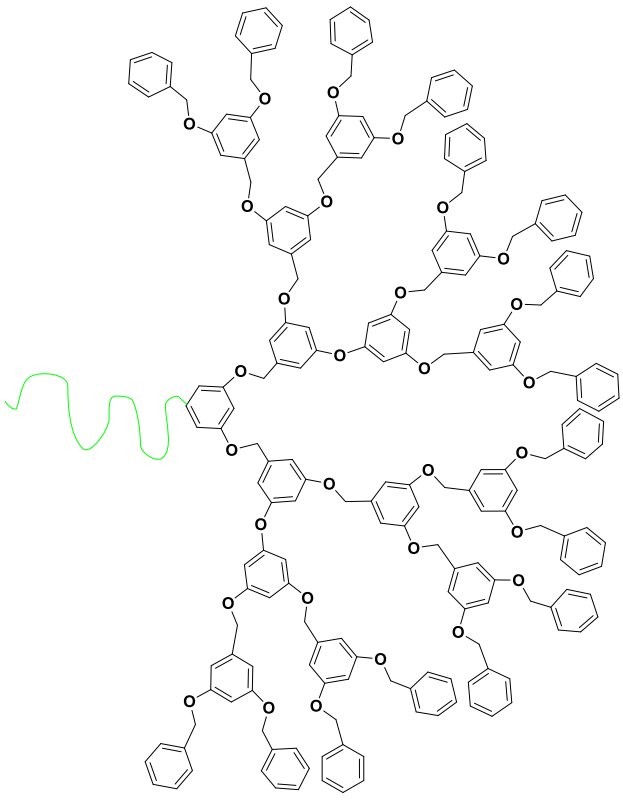

Figure 1.11. Poly benzyl ether dendrimers conjugated with (PEG)

1.4. 3.3 Biodegradability

Dendrimer degradability is an important characteristic in the drug delivery field [83- 85]; it will prevent any toxic effects likely to occur due to bioaccumulation of the macromolecule in the body. In medical use, more focus was on improvement of dendritic architectures with hydrolyzable bonds. Pharmacokinetic studies have proven that dendrimers with higher molecular weights >~40 kDa stay in the blood for longer than dendrimers with lower molecular weights. This highlights the importance of the size of the polymer, which must be in the required range for renal filtration. Significant research has been carried out into the use of polyester dendrimers because of their biocompatibility and biodegradability under biological conditions [2,82]. Polyester dendrimers, based on (R)-3-hydroxybutanoic acid and trimesic acid, undergo enzymatic degradation and it was the first published biodegradable dendrimer in 1996 [82].

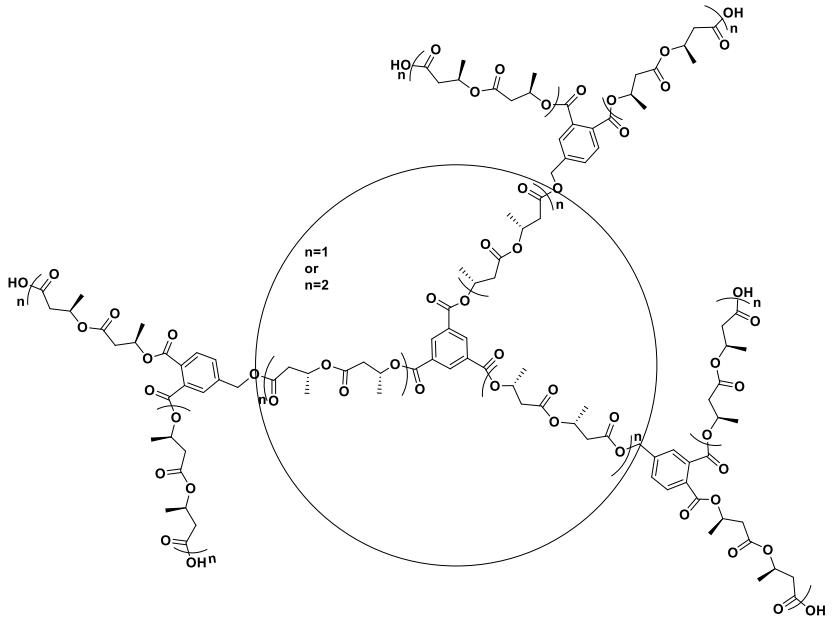

Figure 1.12. The first published biodegradable dendrimer

1.4. 3.4 Distribution

Distribution is one pharmacokinetic property which describes diffusion of substances throughout the tissues and fluids of the body [86]. Controlling polymer carriers size and conformation means that distribution can be modified. For a polymeric carrier such as dendrimers to be suitable for in vivo application, it must display body distribution that inherent allows proper tissue targeting [79]. Distribution of the free drug molecules leads to a short half-life in the blood stream and the drug is not retained long enough to show its therapeutic effect.

Many studies have shown that organ bio distribution, passive tumour targeting and circulation time, depends on the physicochemical properties of the dendrimers, extent of PEGylation, and presence of ligands etc. successful drug delivery to cancer cells needs extended circulation times of water-soluble polymers, this interaction of the macromolecule drug conjugates with the desired targeted site which depends on size and polymer construction. the design smart carriers with the ability to reduce drug exposure to healthy tissues lead to improved therapeutic efficacy [87].

1.4.4 Applications of dendrimers

Dendrimers are a family of highly branched polymers with a static globular construct [29]. There is much interest focused on this type of dendritic polymer because of their intrinsic characteristics, such as a high degree of control of their shape and molecular weight. However, the focus was on their synthesis and analysis [86]. Lately, there have been several studies that have explored many fields including biomedicine and industry. Dendrimers have been called 21st-century polymers for their importance and widespread use in the field of medicine [87]. In biomedical applications, dendrimers have been used as a solubility enhancer for drugs [2], blood substitutes and many other applications [88-95] are shown schematically in (Figure 1.13).

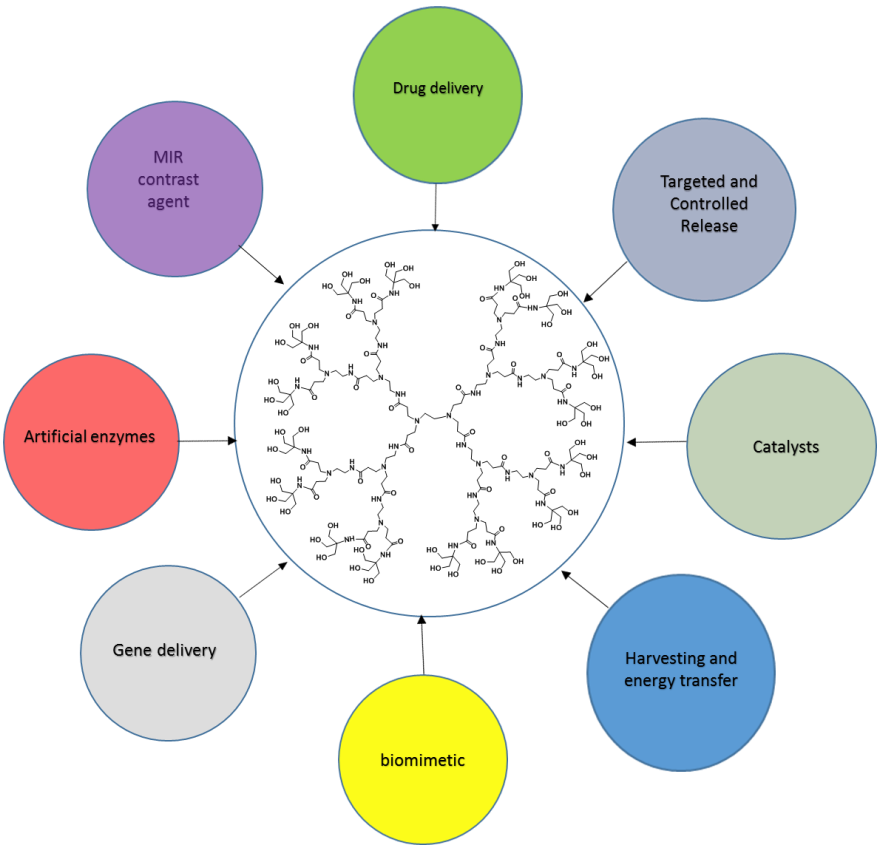

Figure 1.13. Schematic representation of the diagnostic and biomedical applications of dendrimers

1.4.4.1 Dendrimers as carrier in drug delivery

In addition to the aforementioned characteristics of dendrimers, they have other certain unique dendritic features that make them suitable as a carrier for drug delivery: water solubility, encapsulation ability, permeability across a biological membrane, a large number of peripheral function groups and polyvalency. They have been used as carriers in many studies regarding cancer therapy, for instance, photodynamic therapy drugs and anticancer drugs [29,25]. Amphiphilic dendrimers with different interiors containing poly(amidoamines) (PAMAM), poly(esters), poly(ethers), poly(amide) have been used as drug delivery systems [96]. These macromolecules have the ability to solubilize insoluble drugs in water. Dendrimers can be considered static, covalent micelles and have also been referred to as unimolecular micelles [97] There are two types of interaction between the dendrimers and hydrophobic drug these are:

(1) non-covalent interaction (Host-Guest) via encapsulation (by hydrophobic interactions, physical entrapment, or hydrogen bonding) or surface interaction between drugs and dendrimers (electrostatic interactions). Drugs can be physically entrapped in the interior of dendrimers with rigid shells, for example, encapsulation of 2'-(benzo[1,2-c] 1,2,5- oxadiazol-5(6)-yl (N1-oxide) methylene)-1-methoxy methane hydrazide resulted good drug solubilisation [2,36,97,98].

(2) covalently by conjugation of the drug to a dendrimer using via a spacers or cleavable linkage [99], such as the conjugation of G-3.5 a sodium carboxyl terminated PAMAM dendrimer with cisplatin which results in enhanced antitumor efficiency targeting compared to the drug without dendrimers; this was for passive targeting in vivo [26]. Non-covalent and covalent systems can exploit the EPR phenomenon [66,100].

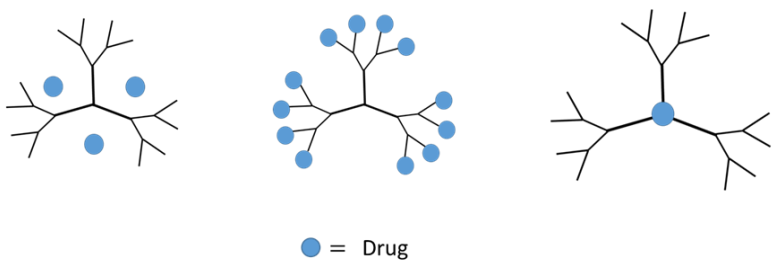

Figure 1.14. Different interactions of dendrimer structures

Polyester dendrimers are chiefly promising as drug nanocarriers which have shown to be biocompatible and non-toxic [2,97]. These dendrimers can be used to incorporate small molecule drugs or imaging moieties into interior spaces; the encapsulation process can control the release and therefore increase the half-life of the treatment in the bloodstream. There are many types of dendrimers that have been used to dissolve anti-cancer agents. For instance, methotrexate (MTX) has been encapsulated using a melamine dendrimer; this study demonstrated the efficacy of the dendrimers to improve solubility and drug efficacy [101]Figure 1.15.

Successful encapsulation of small organic molecules acid [102], such as p-nitrobenzoic within the interior of the poly (propylene imine) dendrimer which have been stated by Meijer [65,103].

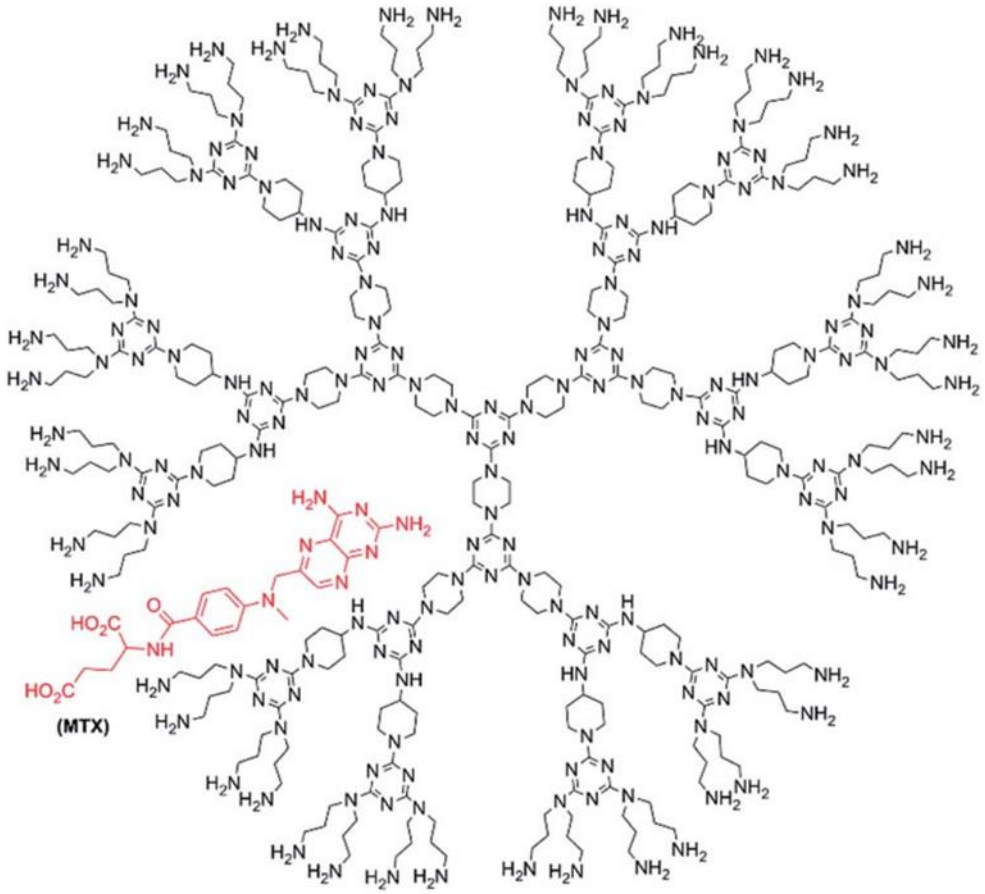

Figure 1.15 Encapsulated o f methotrexate using a melamine dendrimer

Dendrimers have been used as cellular drug delivery systems, in a comparison between free ibuprofen and dendrimer ibuprofen complexes to enter the cell. The results show that free ibuprofen took three hours to enter the cell, while dendrimer ibuprofen complexes took only

one hour. In photodynamic therapy (PDT) for cancer treatment, dendrimers have been used in many studies, for example, the photosensitizer 5-aminolevulinic acid linked to the surface of dendrimers was used as an agent for PDT of cancer cells [105]. In this regard, they have the ability to enhance both the permeability and retention of compounds within the tumour cells and enhanced permeation and retention (EPR) of the drug inside the cancer cells which leads to reduced cytotoxicity of the anticancer drug (e.g. Doxorubicin) [26]. Some types of dendrimers, such as PAMAM dendrimers, have been tested as a genetic material vector in gene therapy, they have terminal amino groups, and this group interacts with the phosphate group of nucleic acid which showed no significant accumulation in any vital organ [2].

Chapter 2

Aims and Objectives

2.1. Part one: Dendrimer as Solubilisation Enhancer for Hydrophobic Drug

In the initial stage of the project, we will investigate whether the dendrimers have the capability to improve the solubility of hydrophobic drugs. This part will highlight my contribution towards a larger project within my research group. A great number of hydrophobic drug molecules are rejected by the pharmaceutical industry. Their assessment reveals that, up to 60% of potential drug candidates [105] show low aqueous solubility and poor delivery of hydrophobic drugs to a specific target. Poor drug solubility can cause many problems, such as poor biocompatibility and low bioavailability due to incomplete release from the dosage form, which leads to harmful side effects in patients. Numerous pharmacological properties such as solubility, biocompatibility, and bioavailability can be improved by the use of drug delivery systems (DDS) [35]. DDS include several types of polymeric carriers, for instance, dendritic polymers, block copolymers and linear polymers.

Dendrimers are highly branched with a well-defined structure; they are monodispersed macromolecules [107]. Dendrimers have been stated to successfully encapsulate small organic molecules within a hydrophobic interior or surface of dendrimers (interaction between drugs and dendrimers) [108,109]. Their functional groups on their periphery, can be simply modified to achieve the desired solubility in the chosen solvent. The interaction between the dendrimer and drug could be by non-covalent interaction (drug encapsulated within interior cavity of dendrimer), or surface interaction between drugs and dendrimer as shown in Figure 2.1. Encapsulation of hydrophobic molecules has previously been presented as a way to improve poor solubility of drugs; Therefore, we propose the use of water soluble dendrimers as the drug delivery carriers. The requirements for these dendrimers are high solubility, a hydrophobic interior capable of interacting with drugs and they must be non-toxic to living organisms [2,44, 110-113]. In particular, the use of the neutral dendrimers is a key focus of my work, as this limits toxicity associated with multiple charges [26,81,82].

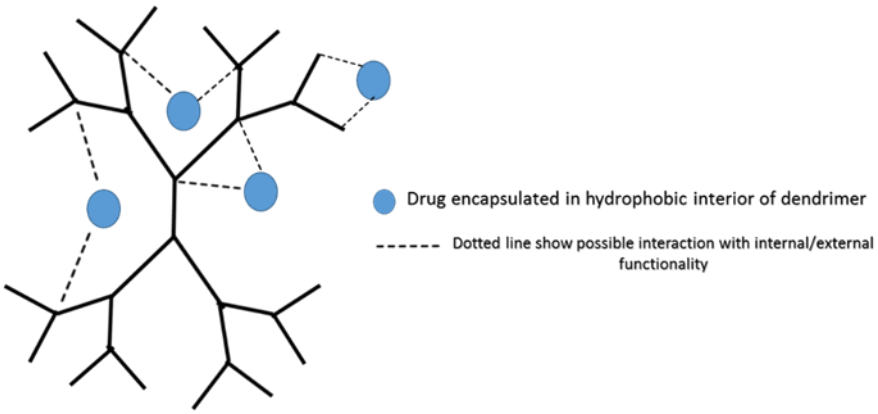

Figure 2.1. Non-covalently encapsulated drug within water soluble dendrimers

The size of dendrimer depends on the generation, in other words, the size of dendrimer increases with an increase generation. Larger sized dendrimers provide an increased hydrophobic interaction but, also, increased in steric hindrance. In this part of the work, G3.5 OH ended dendrimers with a molecular weight of 8149 Da will be the largest dendrimers used to investigate the effect of dendrimer concentration on their ability to solubilize and bind hydrophobic drug molecules.

G3.5 ester terminated PAMAM dendrimers will be the largest dendrimers used for our study. Previous work has shown that this dendrimer was the best compromise between provision of a good binding environment and enough space to accommodate drugs or catalytic species/substrates [110]. This work will investigate the use of OH ended neutral of dendrimers on encapsulation. These will be synthesised from ester terminated dendrimers after reaction with Tris. Initially, an investigation into the encapsulation ability will be carried out using ibuprofen (Figure2.3); due to its wide availability and (extensive) use in similar studies [89,111]. In addition to being hydrophobic, ibuprofen also possess a carboxylic acid group. As such we were interested to see what this acidic group could be contribute to binding, via an acid/base reaction with the internal and basic amine. In order to determine the maximum loading of the dendrimer, different concentrations of ibuprofen will be used with a constant concentration of polymer at $1x10^{-4}$. Also, G3.5 PAMAM dendrimers will be studied at different concentrations of polymer, and an excess of the drug. Increasing the amount of the drug encapsulated (percent loading) with the increase in the concentration of dendrimer is a predictable consequence of the process of encapsulation (Figure 2.2).

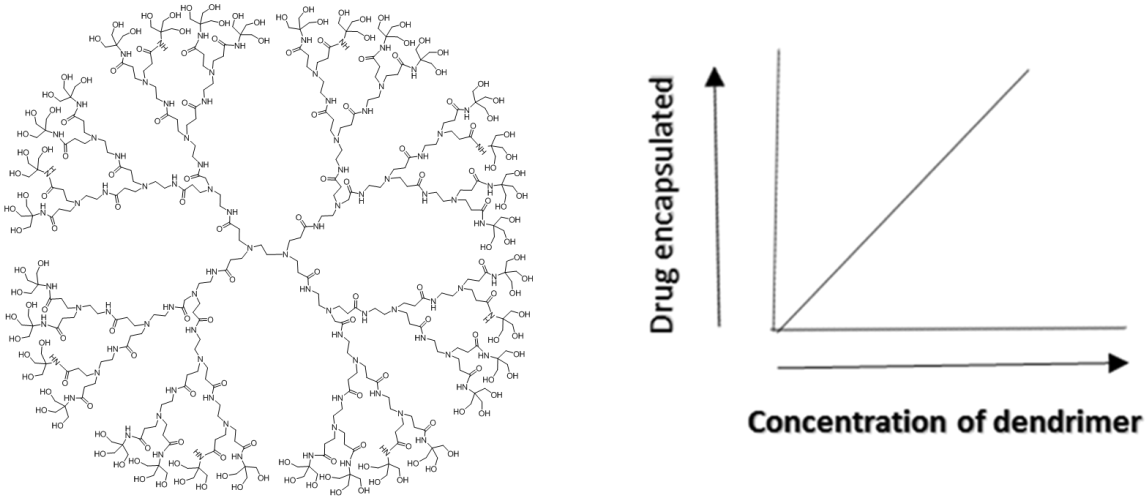

Figure 2.2. The expected linear relationship is to increase the concentrations of the encapsulated drug with increased polymer concentrations

The encapsulation of the drug will be via a simple hydrophobic interaction, with additional binding from acid/base and hydrogen binding possibly being. After establishing the ability of dendrimers to encapsulate a simple drug molecule, we will further explore the effect of secondary interaction by two the study two similar drugs that differ in their ability to provide a strong secondary interaction. Specifically, we will compare TPP with ZnTPP. Both drugs are used in PDT and only differ in their ability to coordinate to the internal tertiary nitrogen within the PAMAM dendrimers.

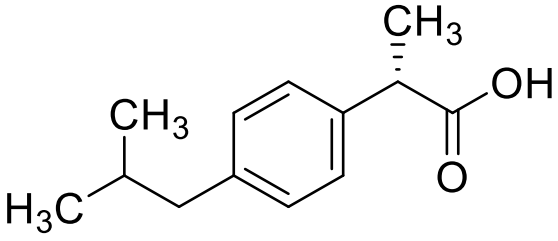

Figure 2.3 Ibuprofen structure

2.2. Part two: Water soluble dendrimers with free base Porphyrin and metal Porphyrin via Non-Covalent encapsulation for PDT

In the second part, we will try to increase encapsulation via a strong interaction, specifically metal ligand coordination using amine containing dendrimers. From this point, we can determine how important secondary interaction with regards to encapsulation efficacy. Many derivatives of porphyrin can be used as photosensitizers (PS); They are macrocyclic, conjugated compounds and have an intense absorption peak in the visible region spectrum, at the wavelength useful for therapeutic action. Disadvantages include a lack of solubility under physiologic conditions and poor targeting for cancerous cells [10]. An offered resolution is to attach the drug to a suitable carrier that is soluble and can deliver the drug to specific target location.

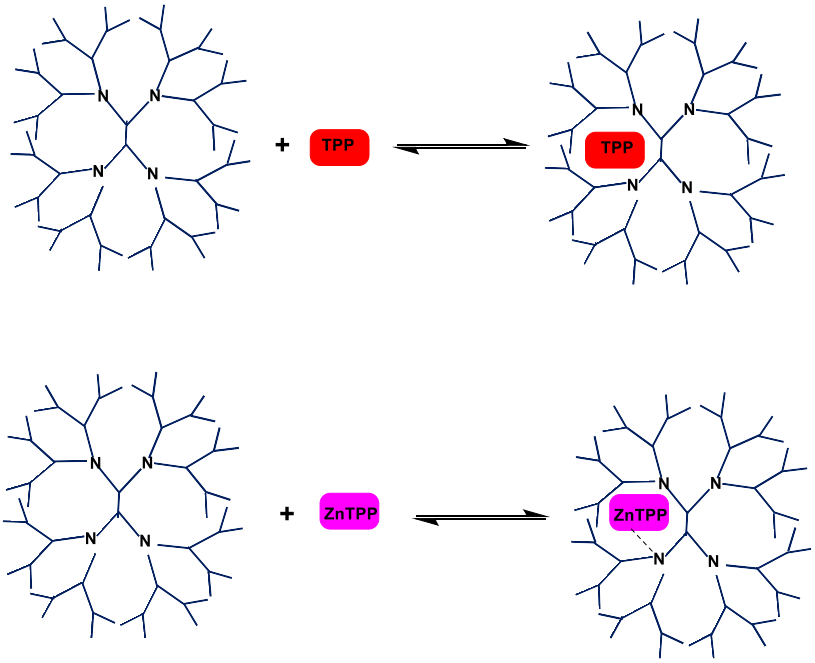

Figure 2.4. Non-covalently encapsulated free porphyrin and Zinc porphyrin using dendrimers

The first strategy in this part is to study guest–host interactions of a drug with a dendrimer, which results in improved drug solubilisation; a porphyrin can be as used the hydrophobic drug (guest). In this initial study, the guest molecules encapsulated within the hydrophobic cavity of the dendrimer using just hydrophobic interaction and no other interaction will be engaged. The

drawbacks of drug delivery carriers based on hydrophobic entrapment of drugs into hydrophobic (internal) cavities is a poor drug loading capacity. To overcome this problem and to increase the capacity of drug loading, a different method is required. The second strategy will involve encapsulation of metal cored porphyrin; the insertion of the metal into the cavity of porphyrin is important step because the metal can provide coordination binding (secondary interaction) with the polymer. This will produce additional binding to support the weak hydrophobic interaction, hence the use of metal porphyrin can offer a potentially good result for drug encapsulation. Based on this, the third the project will be to use the coordination to the drug delivery system (self-assemble self-assembly between a metal porphyrin and dendrons ligand). Therefore, the use of self-assembly/ coordination chemistry will give us control of with regards to encapsulation level. Also this approach will allow the same dendrimer to use with many different porphyrins bonded Ps.

2.3. Part three: Self-assembled Drug for PDT

In the third stage of this research project we intend to increase the capacity of drug encapsulation, improving the solubility of PS compounds by synthesising a self-assemble drug to specifically target cancer cells.

2.3.1. Selection of polymer

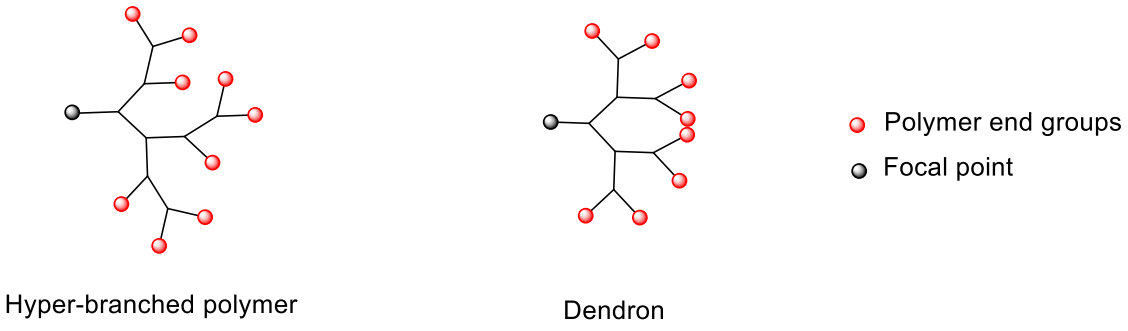

Figure 2.5. Structure of dendritic polymers

Either hyper-branched polymers or dendrimers can be selected at this stage as both have similar chemical and physical properties, such as high water-solubility, presence of internal cavities which can be used as drug binding sites and big numbers of controllable surface functionalities

[114]. However, HPBs have random structures and uncontrolled molar mass compared with dendrimers [115]. The molar mass and size of the dendrimer can easily be controlled therefore they are the preferable candidates for an ideal, water-soluble delivery system. To achieve our aims in the synthesis of photosensitizers for PDT, an acid core with ester terminal groups PAMAM dendrons were selected. Undoubtedly, an ideal nanoscale carrier in medical uses should be non-toxic and biocompatible, biodegradable with acceptable bio elimination, these features are characterized by polyester dendrimers [115]. This is due to the fact that the ester group readily hydrolysis by an autocatalytic process and be convert to an acid group and be water soluble similar dendrimers have been to inter cells [2]. The Dendron with one focal point (acid core) can facilitate the non-covalent bonding with metal porphyrins.

2.3.2. Selection of chromophores as photosentizier for PDT

Many photosensitizers(PSs) are either porphyrins or phthalocyanines. These compounds are molecules that are activated when excited by absorbing a specific wavelength of light. Then the excited PS transfers its energy to oxygen in the cell to generate the extremely reactive oxygen species that can kill the cancer cell.

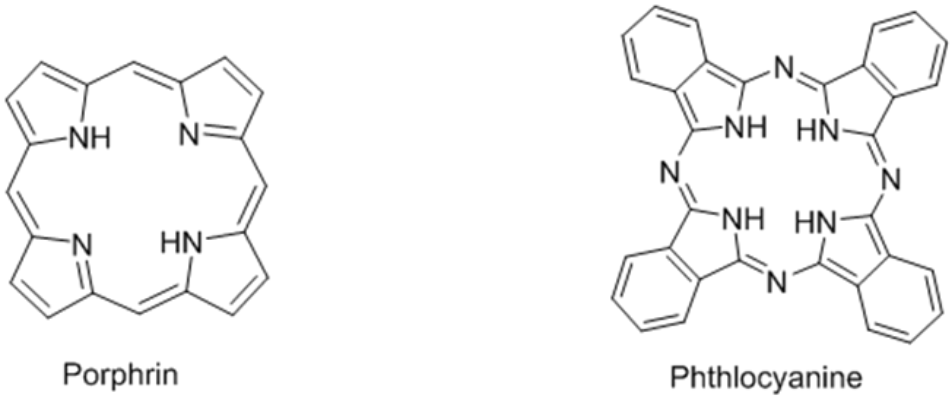

Figure 2.6. Different chromophores can be as photosentizier

The hydrophobicity of these PSs makes them insoluble in water [116]. Therefore, the PSs are difficult to use in a pharmacological system [117]. To overcome this drawback [19] [13] and to yield positive results, we propose to use a self-assembled targeting system for photodynamic therapy. As stated in the literature, a dendrimer with terminal anionic functional groups has presented good results as drug delivery agents which can be used to improve the solubility of Ps in an

aqueous medium [13]. The use of dendrimers appears the most appropriate strategy to produce the required large molecular weight molecules that can accumulate at high levels in a tumour [2].

2.3.3 Self-assembly of Dendron and Chromophores (poryrins & phthalocyanines)

Self-assembly is spontaneous and reversible; structure formation involves non-covalent bonds of two or more components [118]. The intermolecular interactions include hydrogen bonding, electrostatic interactions, Van der Waals interactions, and metal coordination. In various studies, coordination chemistry has been used to synthesise a variety of supramolecular dendrimers; and this will be used for the self-assembly of the drug with the appropriate metal porphyrin and ligand (dendrons) [90]. This part of the study will involve a self-assembled study using the Pc as the core. Self-assembly was selected as the favoured strategy because each dendrimer can contain a porphyrin molecule; thus increasing the efficiency of encapsulation. Furthermore, it is simple to produce a large molecule for EPR, using the porphyrin as a core to grow the large dendrimer/drug complex around, and increases solubility. Strong intermolecular forces between porphyrin and ligands (dendrons) can be obtained using metal coordination over other supramolecular assemblies. Also, the suitable metal phthalocyanines will be use to improve performance of PDT.

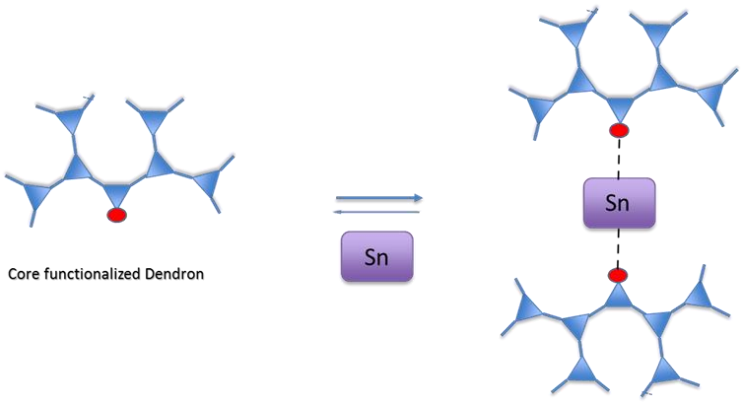

Figure 2.7. Self-assembly between dendron and tin porphyrin (or phthalocyanine)

Tin porphyrin will be used due to the fact that tin metal can be easily inserted in the porphyrin and is 6 coordination 4 of which are coordinated to the porphyrin, allowing 2 axial carboxylates ligands (dendrons) to be added [119]. In other words, the complexes of porphyrins with tin(IV) are readily synthesised and very stable [12]. The tin metal provides six-coordinate with two trans

ligands. The spectroscopic properties of this porphyrin such as diamagnetism make them suitable for chemical study [120]. Phthalocyanines have the same characteristics as porphyrin, however its absorption bands are in the red region of the spectrum at (670-770) nm which good to light delivery and allows deeper retention into tissue and treat deep or large tumors.

2.4. Part Four: Application

As mentioned earlier, when exposed cancer cells are treated with porphyrins or phthlocynines" as photosentizier" (to the specific wavelength of light) a number of reactions take place. A very important product that can result from these reactions are the reactive oxygen species, which causes cytotoxicity and kills the tumour cell. There are many areas that require investigating such as intracellular localisation, cell viability studies and cytotoxicity of dendrimers as drug delivery agent.

Chapter 3

Results and Discussion

Part 1: The synthesis neutral water-soluble PAMAM dendrimers and the significance of secondary interactions on encapsulation.

3.1 Water soluble PAMAM dendrimers as solubility enhancer.

The polyamidoamine (PAMAM) dendrimer is a well-known macromolecule with many medical applications. Dendrimers have a globular, uniform structure and internal amine groups, which are useful for encapsulating different types of hydrophobic and acidic drugs [121].

The purpose of this part of the project was to determine the ability of the dendrimer to improve solubility via secondary metal to amine coordination. Water-soluble dendrimers have proved to be capable of improving drug solubility [89,122]. Despite these abilities, their synthesis and purification can be difficult and time consuming to achieve [123]. Nonetheless, we suggest PAMAM dendrimers as drug delivery systems, because compared to other dendrimers, their synthesis is much easier. Amine terminated PAMAM dendrimers are water soluble, but depending on concentration and generation, display haematotoxicity and cytotoxicity in the physiological environment. PAMAM dendrimers with ester terminate groups are not toxic, but they are not soluble in water; however, they are rapidly hydrolysed in the physiological environment, which produces carboxylic acids enabling solubilisation. At neutral PH, some acids are deprotonated to have a negative charge that may limits binding to cells (which also have a negative charge). Thus, conversion into neutral polar terminal groups is an inevitable demand to suit the standards of drug delivery carriers.

For this work, ester-terminated PAMAM dendrimers were converted to hydroxyl-terminated PAMAM dendrimers using a modified version of the original procedure devised by Newkome et al. Previous work by the Twyman group used the same procedure and conversion results were successful. Initially, ester-terminated PAMAM dendrimers (half-generation) were synthesised. Ethylenediamine (EDA) was used as a core, providing the primary and tertiary amine within the dendrimer structures. This was followed by the synthesis of amines terminated PAMAM dendrimers (whole generation). Once ready, the range of G 0.5 to G 4.5 terminal ester PAMAM dendrimers were converted to 12 OH and 96 terminal hydroxyl OH groups respectively.

3.2. Synthesis of PAMAM dendrimers

PAMAM dendrimers were chosen, as they are easy to synthesise and functionalise. The divergent approach was selected because this method has proved effective in generating PAMAM dendrimers. This method requires the smallest generation to be formed; starting from (G 0.5), extending to larger generation dendrimers (G4.5); successive reactions create higher

generations. The preparation of PAMAM dendrimers involves the repetitive sequence of two simple reactions; 1,4 Michael addition to form ester-terminated PAMAM dendrimers followed by an amination reaction for amine terminated PAMAM dendrimers [124]. The 1,4 Michael addition step occurs using methyl acrylate (acting as the alpha-beta unsaturated carbonyl compound). The carbonyl substituent has an electron-withdrawing effect on the alkene, generating a δ positive on the terminal carbon, which is eventually stabilised by resonance. Therefore, the β carbon becomes electropositive, consequently exposing it to nucleophilic attack from EDA. After the first step has finished, a second Michael reaction takes place. The mechanism of the 1,4-Michael addition is shown in Figure 3.1.

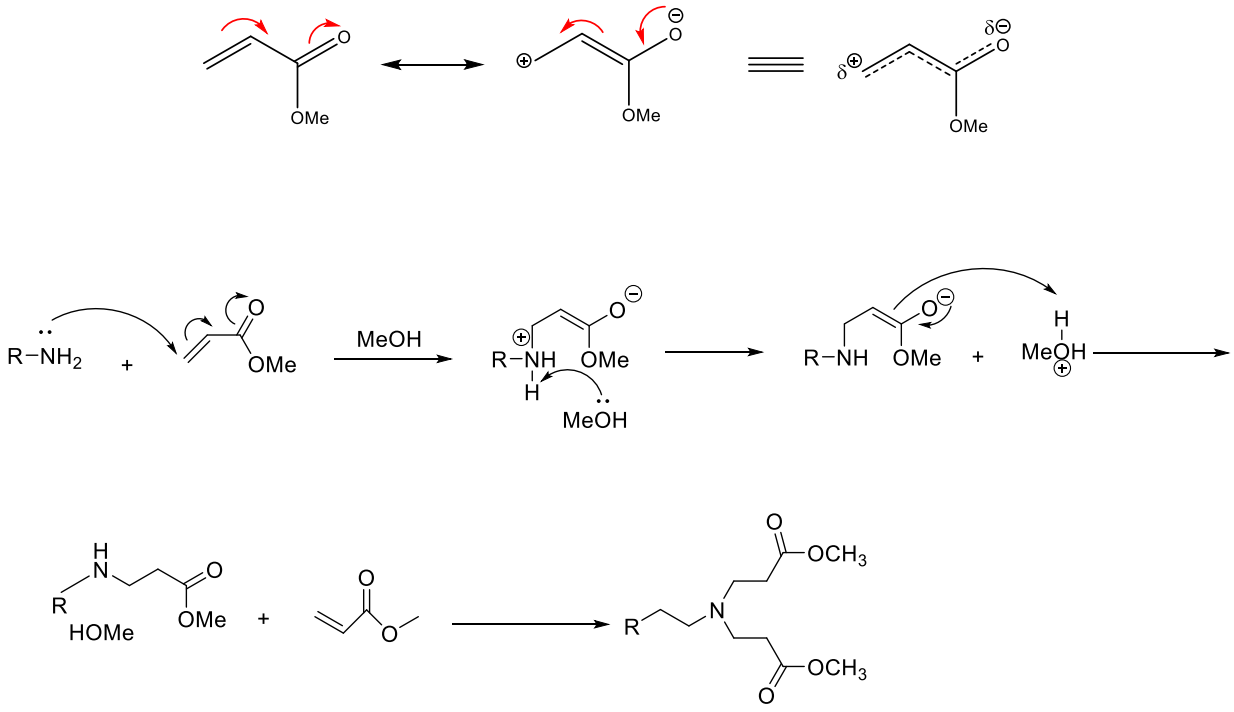

Scheme 3.1. Mechanism of 1,4 Michael addition step

When the 1,4 Michael addition is complete, the second step takes place. In this step, the nitrogen lone pair from EDA acts as a nucleophile, attacking the positive carbonyl carbon from the methoxy group. The intermediate that forms is then protonated by the second *terminal* amine. After that, the methoxy group is converted to a good leaving group and the positive charge is removed via deprotonation, resulting in the final product and alcohol. This step is called the amination reaction and is shown below in Scheme (3.2). These two steps are then repeated to

build up the size of the dendrimer. The process is described in more detail within the following sections.

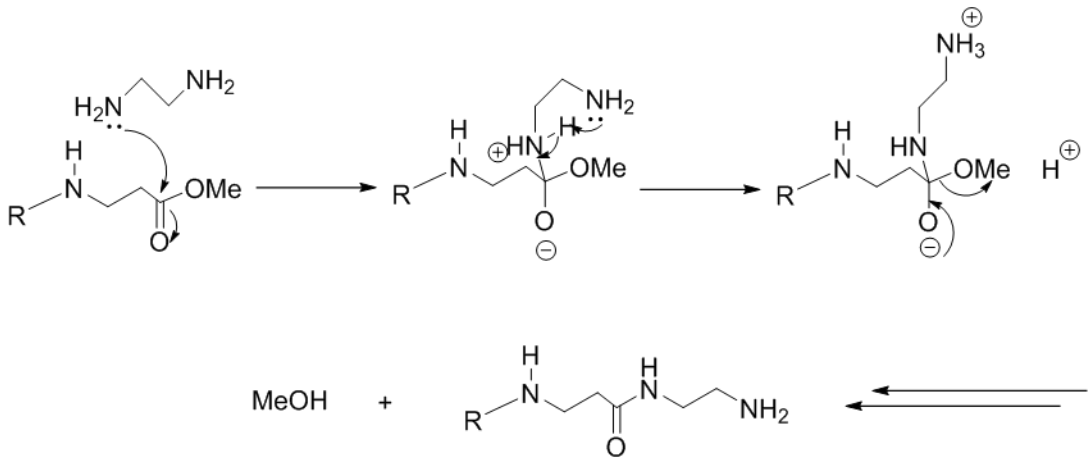

Scheme 3.2. Mechanism of amidation reaction step

3.2.1 Synthesis of half generation PAMAM dendrimers

Half-generation dendrimers were synthesised by adding an excess of MA (four equivalent of the methyl acrylate per ester group) drop wise to ethylene diamine (EDA), or the previous whole generation dendrimer dissolved in methanol at 0°C. The procedure is shown in scheme 3.3 using as G0.5 as an example. After that, the solution was stirred at room temperature. The amount of methyl acrylate that was added increased according to the increasing size of the dendrimer, but it was kept constant relative to the number of amines. The time taken by the reaction to be completed was determined by the size of generation; after each generation, small amounts of reaction solution were taken and analysed by ^{1}HNMR to check if the reaction was complete or not. It took 24 hours for the synthesis of G0.5, three days for the synthesis of G1.5, five days for the synthesis of G2.5, seven days for the synthesis of G3.5 and nine days for G4.5. The most important step was at the end of the reaction, in which any starting material had to be removed to avoid any side reactions occurring during the synthesis of the next generation. Subsequently, excess methyl acrylate was removed from the solvent by rotary evaporator. Spectroscopy (^{1}H NMR) was employed to confirm that MA was fully removed. By following reduction is size of the alkene peaks at 6.15 ppm and 6.37 ppm. The product was then placed under ultra-high vacuum to ensure complete removal; the yield of dendrimers was as viscous

oil products. The viscosities of dendrimers increased with increased size of the PAMAM dendrimers; also, the colour gradually became darker.

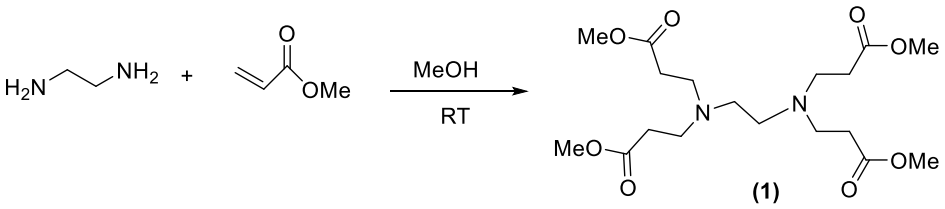

Scheme 3. 3. Synthesis of G0.5 PAMAM dendrimer

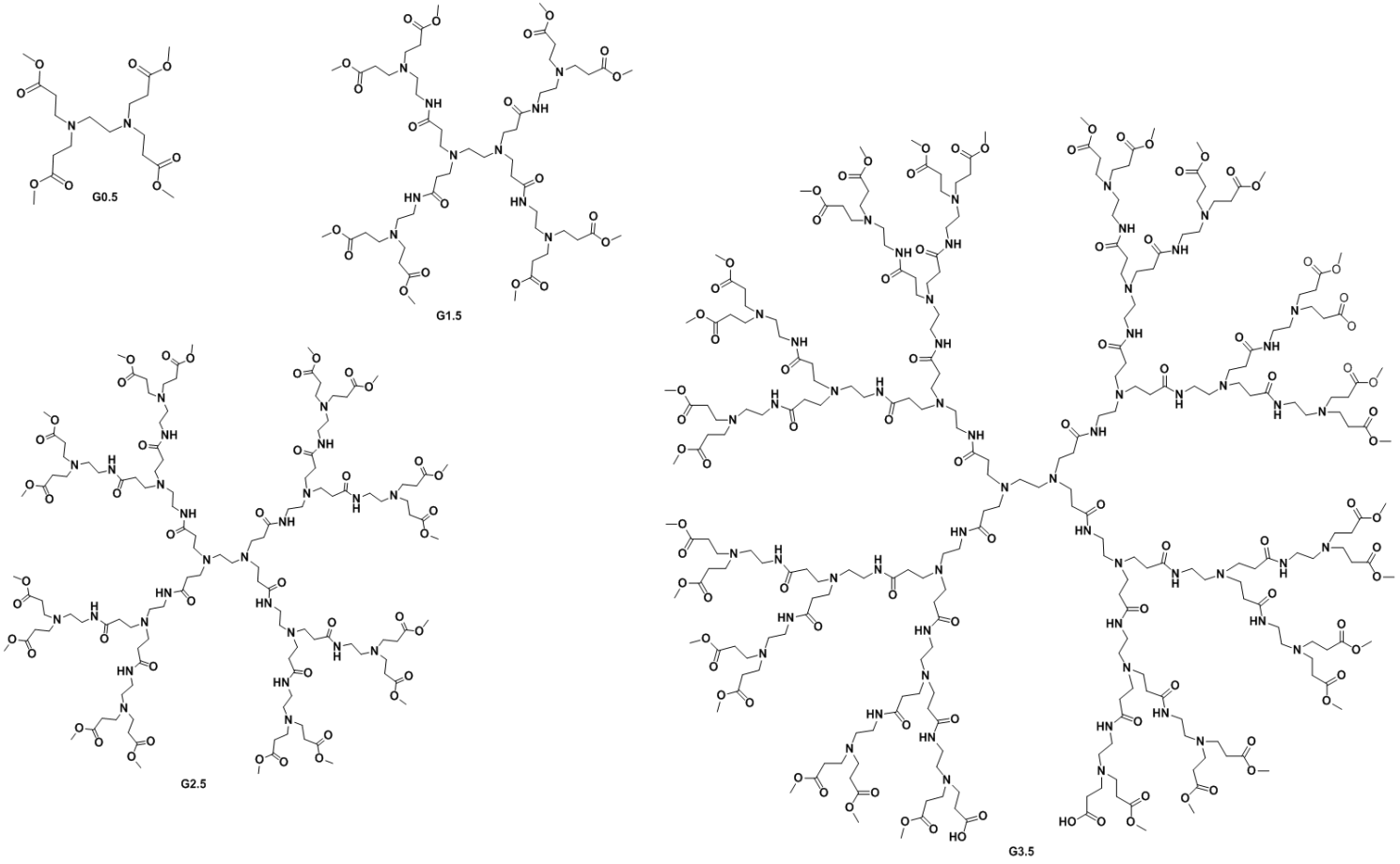
G0.5
G1.5
G2.5
G3.5

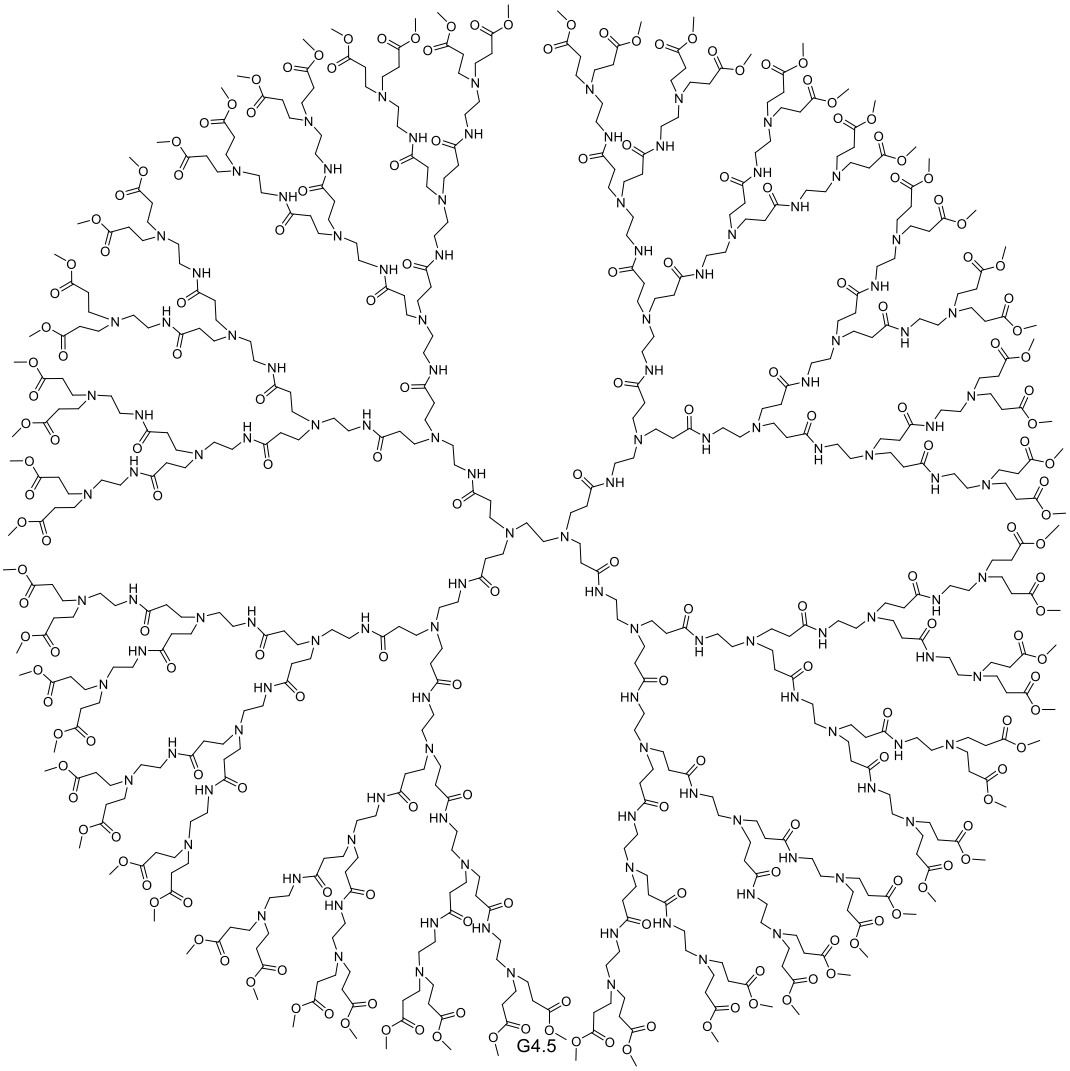

Figure 3.4. Structure of Half-generation PAMAM dendrimers .

3.2.2 Synthesis of whole generation PAMAM dendrimers

The whole generation PAMAM dendrimers were synthesised by adding an excess of EDA to ester-terminated PAMAM dendrimer solutions drop wise at 0° C. It was then stirred at room temperature. The scheme is shown in scheme 3.5 The success of the reaction depends on the use of an excessive amount of EDA (20 equivalents of EDA per ester group); this is to guarantee that the reaction reaches completion, obtaining homogeneous dendrimers and avoiding unfavourable side reactions. Generally, it was observed that the time taken for the reaction to produce the whole generation dendrimers took longer than the half-generation dendrimers; and the amination reaction was much slower than the previous 1,4-Micheal reaction. Once the reaction was complete, the excess EDA was removed using an azeotropic mixture of toluene and methanol in a 9:1 ratio. At this stage, it was important to remove EDA completely as it bonds to amide or amine groups of the dendrimers making it much harder to remove than methyl acrylate as. The next section (3.1.4) will describe the purification procedure. The washing process was continued until this peak was no longer visible in the spectrum. The scheme of Synthesis of whole generation PAMAM dendrimers is shown in scheme 3.5.

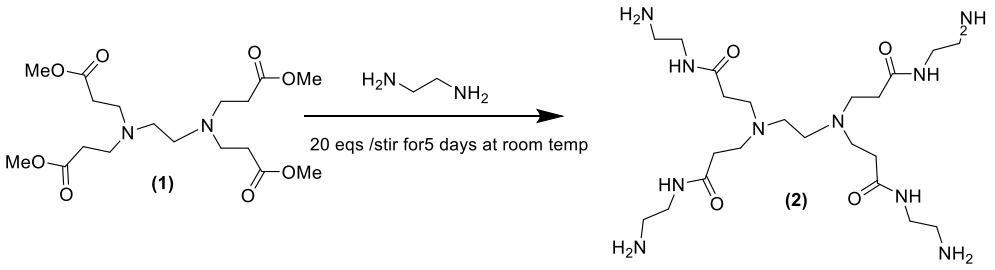

Scheme 3.5 . Synthesis of whole generation PAMAM dendrimers

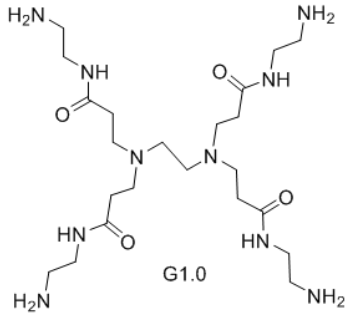
G1.0

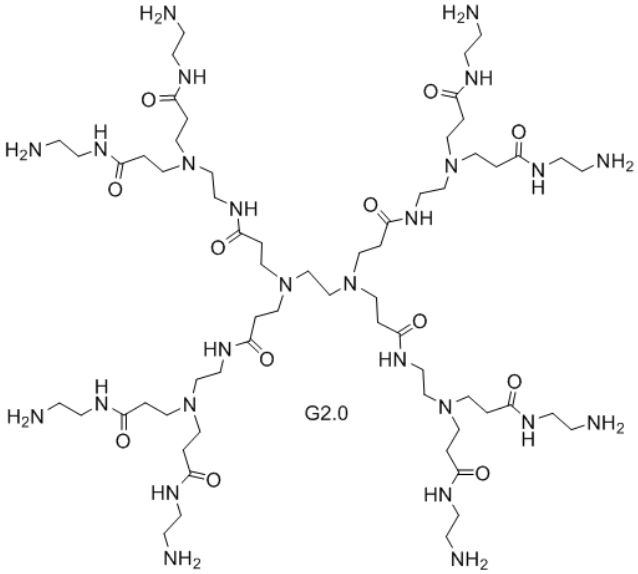
G2.0

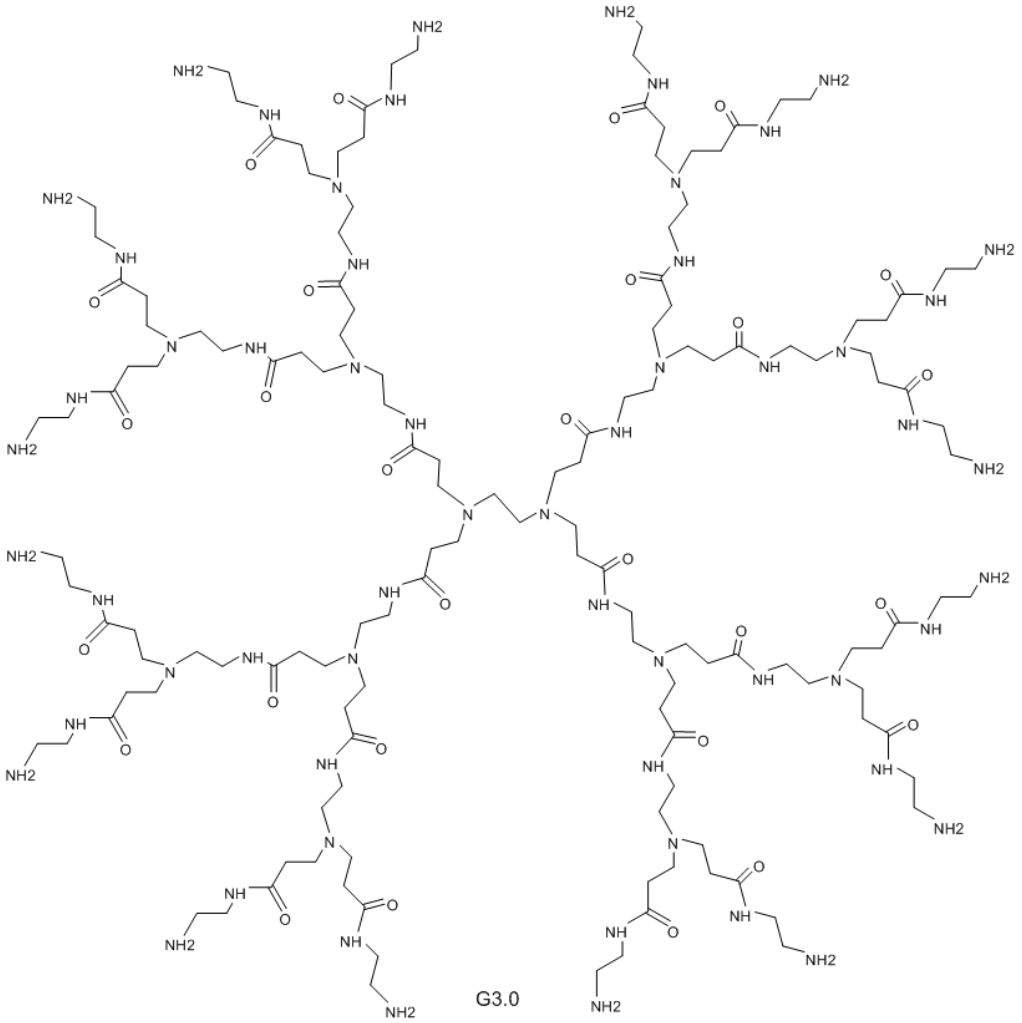
G3.0

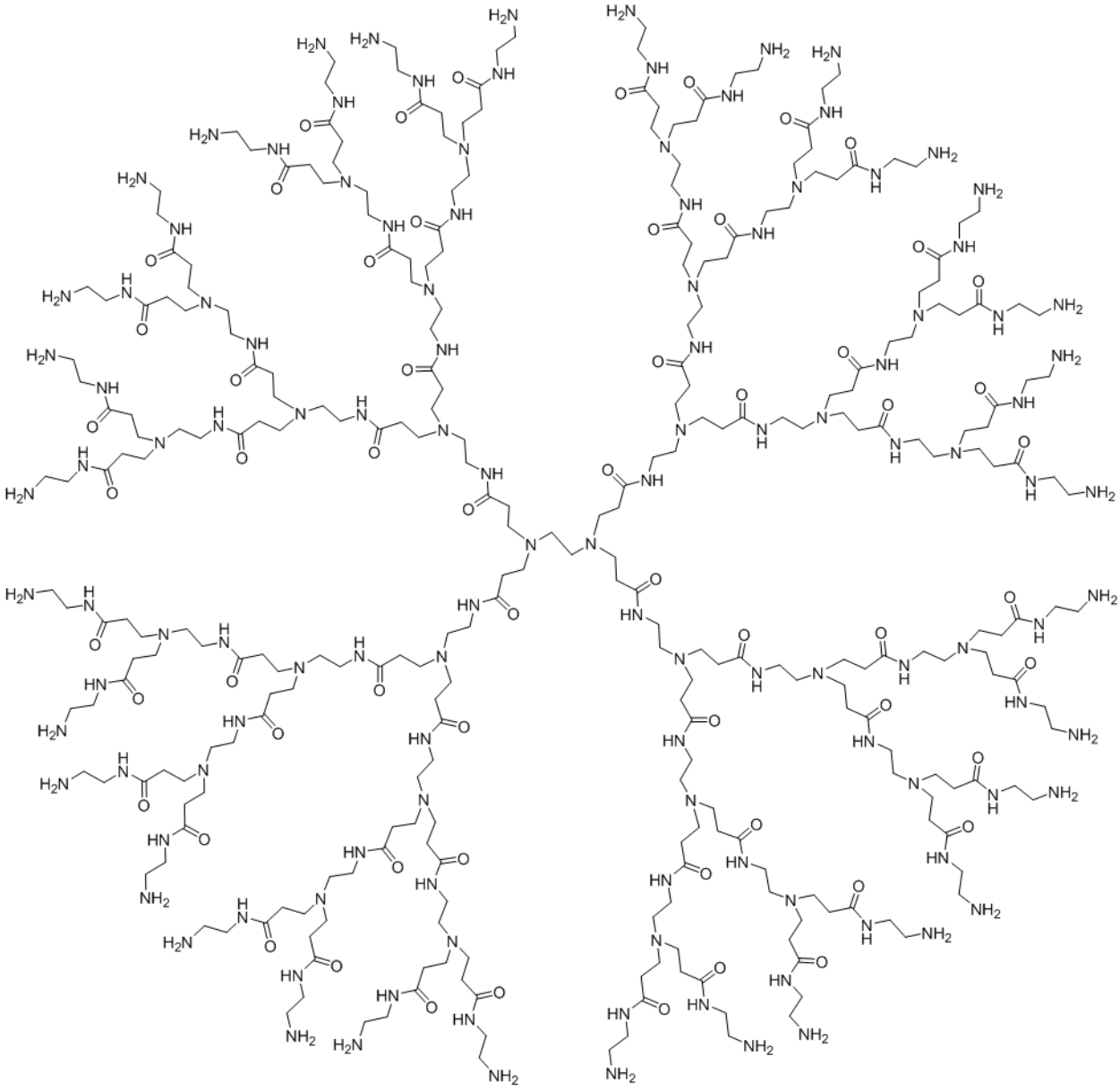

Figure 3.6. structures of whole -generation PAMAM dendrimers .

3.2.3 Purification of PAMAM dendrimer

Purification of the dendrimer is a necessary step to remove the excess amount of reactants from the final products, because their presence causes defects in the next generation. The Michael addition produced the half-generation, and the purification process was simple. The excess methyl acrylate was removed by rotary evaporator at 40 ^{o}c. The amination reaction produced the whole generation and the purification stage of amine terminated PAMAM dendrimer is more difficult. Incomplete purification of ethylenediamine (EDA) can lead to increasing impurities. The residues of excess EDA guides to the production of the desired dendrimer, but also the smaller dendrimer during the Michael addition which are difficult to separate from each other, because of the similar their structure. With more clarity, this occurs when unremoved of excess EDA act as a new core therefore will interact with MA to produce undesired G0.5 by-products (see scheme 3.7). Hence, the molecular weight distribution of dendrimers will be broad as result of these mixtures. Moreover, there side reactions may occur as a result of incomplete purification of EDA, such as cross-Linking products or cyclisation compounds. Scheme 3.5 shows the side reactions caused by residual of Ethylene Diamine.

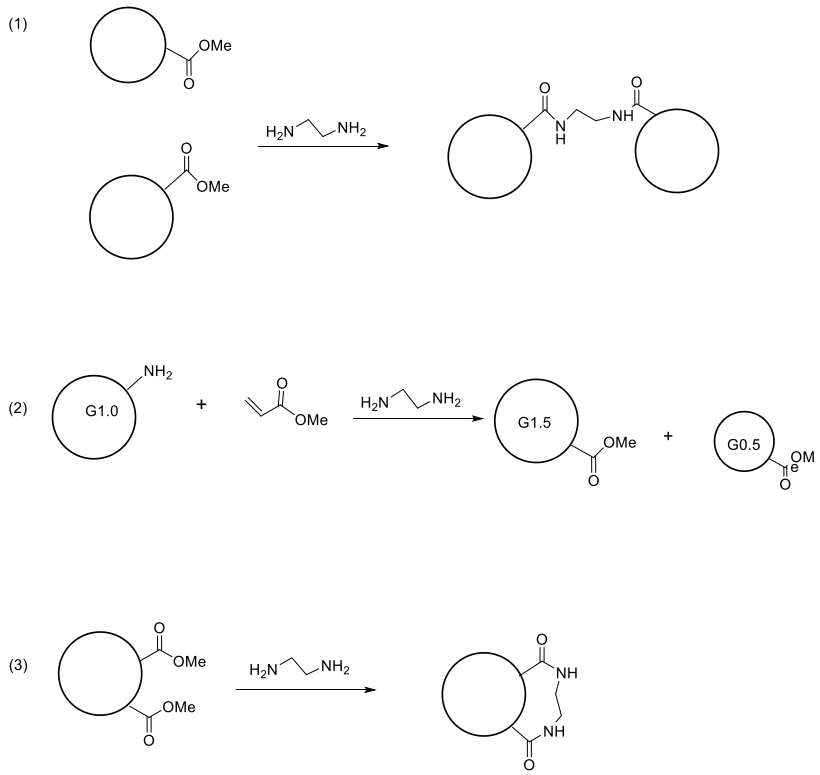

Scheme 3.7. Side reactions caused by non-removal of EDA in dendrimer, (1) Cross-Linking resulted from Intermolecular Reaction and (2) By-Product (3) Cyclisation

The reason for difficult purification is a result of strong hydrogen bonds between the dendrimer and ethylenediamine (EDA). Methanol is a good competitor for hydrogen bonds, and can displace excess EDA. However, the low boiling point of methanol compared to EDA is an obstacle in the process, as methanol is removed before all of the EDA when using a rotary evaporator. Therefore, the azeotropic solution was used in the ratio 9:1 from toluene and methanol, the whole PAMAM dendrimer was washed several times with this mixture until the peak of EDA (a singlet peak at 2.7) no longer in the ^{1}H NMR spectrum.

3.3 Characterisation of PAMAM dendrimers

The most important tools used in the analysis of dendrimers are mass spectrometry: ^{1}H NMR, ^{13}C NMR, and infrared (IR) spectroscopy. ^{1}H NMR can be used effectively for all generation dendrimers. The spectra of the G0.5 dendrimer showed four different peaks; there is a unique and singlet peak at 3.69 ppm in the half-generation dendrimers that corresponds to 12 methoxy protons. Two triplet peaks at 2.77 ppm and 2.46ppm correspond to the two methylene-proton groups in the dendrimer; the peak of the core protons (EDA) exists at 2.55 ppm (Figuer 3.4).

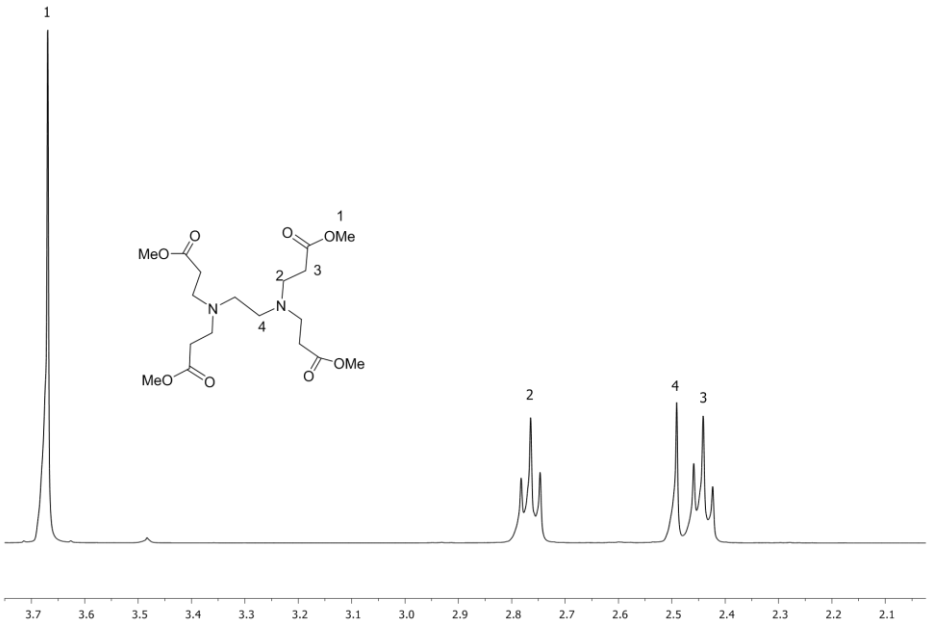

Figure 3.8. ^{1}H NMR Spectra for G 0.5 PAMAM dendrimer with four ester terminal

All spectra of high half-generation dendrimers (from G1.5 up to G4.5) show a singlet peak at 4.90 ppm, representing the amide NH protons. However, as the size of the generation increases, some of the peaks appear broader and overlap. Nevertheless, the terminal methoxy groups at 3.69 ppm were always present in the half-generation PAMAM dendrimers (Figure 3.8).

^{13}C NMR was used to confirm the dendrimer structures; the G0.5 showed one peak for ester carbonyl at 173.4 ppm and the G1.0 dendrimer had one peak at 173.9 ppm for the amide carbonyl. Meanwhile higher half generations have two peaks in the carbonyl region. As for the higher whole generation dendrimers, they also have two peaks, which come from the interior amide and exterior amide carbonyls. In all of the ^{13}C NMR spectra, there are peaks between 52.7– 32.2 ppm, confirming the large number of CH_2-proton environments for all generation PAMAM dendrimers. Where the higher generation has the largest number of different carbon peaks, using ^{13}C helps to confirm the structure and it is the best way to determine the presence of EDA. IR spectroscopy helps in the determination of the functional groups present in the structure of the PAMAM dendrimer and can be used to help confirm success as the process develops from half- to full-generation dendrimers. For example, half generations have a peak present at about 1735cm^{-1} for the ester (ester C=O) and a second peak at around 1640 cm^{-1} for the amide carbonyl. The whole generation dendrimers have only one peak around 1640 cm^{-1} for the amide carbonyl.

Mass spectrometry is a particularly useful tool for examining dendrimers with regards to the presence of any structural defects. Dendrimers have structural uniformity that give precise molecular weights. Electrospray ionisation mass spectrometry (ES-MS) was applied for the smaller generation (G -0.5 and G1.0) PMAM dendrimers (less than 1000). Matrix-assisted laser desorption ionisation (MALDI) was employed to determine the mass of the larger dendrimer [125,126]. The obtained value for the molecular ion peaks for all dendrimer generations were the same as the molecular weights calculated from the structure, which supports the product purity. The molecular ion peak values for each dendrimer half- and full-generation are shown in Table 3.1.

Dendrimer Generations	Molecular Formula	Terminal Groups	Expected Molecular Weight	Obtained Molecular Weight
G0.5	$C_{18}H_{32}N_2O_8$	4	404	405
G1.0	$C_{22}H_{48}N_{10}O_4$	4	516	517
G1.5	$C_{54}H_{96}N_{10}O_{20}$	8	1205	1205
G2.0	$C_{62}H_{128}N_{26}O_{12}$	8	1429	1430
G2.5	$C_{126}H_{224}N_{26}O_{44}$	16	2804	2805
G3.0	$C_{142}H_{288}N_{58}O_{28}$	16	3256	3278
G3.5	$C_{270}H_{480}N_{58}O_{92}$	32	6004	6010
G4.0	$C_{302}H_{608}N1_{22}O_{60}$	32	6904	6913
G4.5	$C_{558}H_{992}N_{122}O_{188}$	64	12411	11630

Table 3.1 The molecular weight of PAMAM dendrimer generations from (G-0.5 to G-4.5)

3.4 Synthesis of hydroxyl-terminated PAMAM dendrimers

The hydroxyl-terminated PAMAP dendrimers (neutral terminal groups) were synthesised by modifying the ester-terminated (half-generation) dendrimers. The method for converting the dendrimer ester-terminated groups into dendrimer hydroxyl end groups was carried out using a modified Tomalia PAMAM synthesis. This reaction included the addition of tris and an excess of potassium carbonate to the PAMAM dendrimers terminated ester groups dissolved in DMSO. The ester groups were converted into hydroxyl groups via amidation reaction, which has been explained in this chapter. The lone pair on the nitrogen of the tris base acting as a nucleophile attacks the electrophilic C of the ester C=O to produce the PAMAM dendrimer with hydroxyl terminal (Scheme3.9).

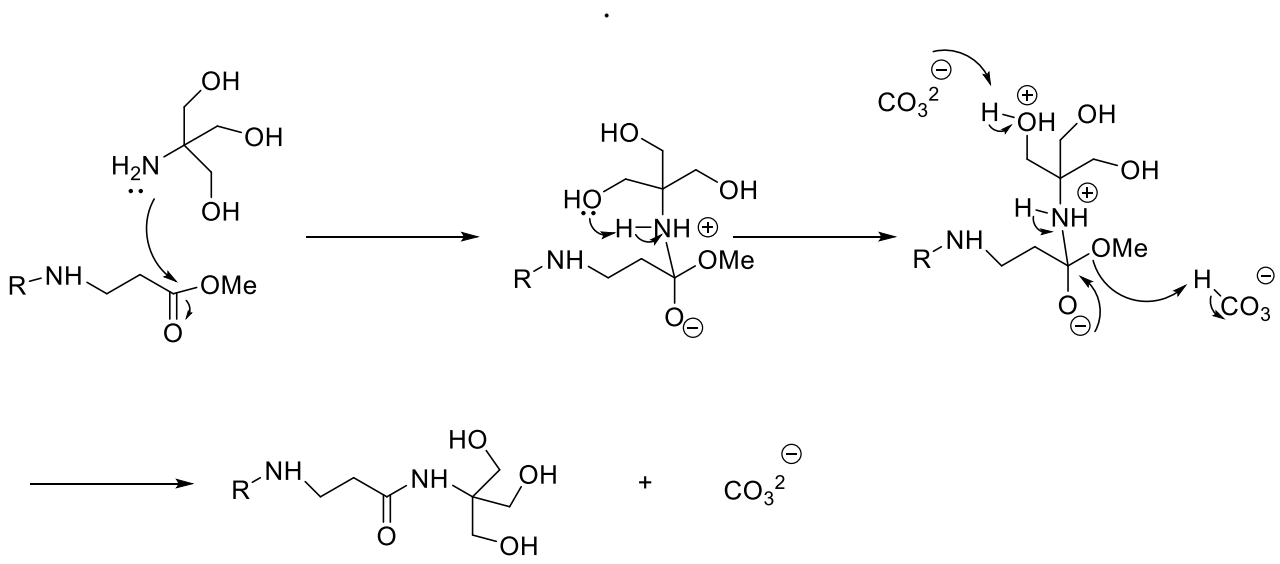

Scheme 3.9. Addition of tris (hydroxymethyl) amino methane (TRIS) groups

3.4.1 Procedure for synthesis of TRIS terminated PAMAM dendrimers

The dendrimers with terminal ester groups were dissolved in anhydrous dimethyl sulfoxide. This solution was added dropwise to a stirred suspension of anhydrous potassium carbonate and tris in anhydrous dimethyl sulfoxide. The reaction mixture was stirred at 50° C for 72 hours under a nitrogen environment. The reaction mixture was cooled to room temperature, then filtered to remove excess solid reagents. The anhydrous DMSO was removed by vacuum distillation at 50° C. The crude product was a thick opaque oil; hereafter it was dissolved in a minimum volume of water and then precipitated with acetone. The purification was repeated at least twice to fully eradicate the unreacted reactants and guarantee good purity. After this, the product was placed in a vacuum oven overnight to dry. The final product was a pale viscous oil of the hydroxyl-terminated PAMAM dendrimers. The same procedure was used to synthesise dendrimers up to G 3.5 with 96 hydroxyl (OH) end groups.

3.4.2 Characterisation of hydroxyl-terminated PAMAM dendrimer.

Similar to PAMAM dendrimers, the hydroxyl-terminated PAMAM dendrimers were characterised by numerous tools including mass spectroscopy, ^{1}H NMR, ^{13}C NMR and IR. Initially, ^{1}H NMR spectroscopy was utilised to verify the conversion of the terminal groups. The spectrum of the OH- terminal PAMAM dendrimers were compared with the spectrum of

the ester-terminated PAMAM dendrimers. The spectrum of the OH- terminal PAMAM dendrimers showed a slight broadening of the peaks and a small shift to a lower chemical shift, with none of the OCH3 peaks at 3.68 being visible. For example, the spectrum of the G1.5 dendrimers with eight hydroxyl terminal groups, indicated a singlet at 3.65 ppm, corresponding to the methylene protons adjacent to the terminal hydroxyl groups Figure 3.10. Compared to other methylene groups, these protons present as peaks in higher chemical shift regions

because they are de-shielded by more electronegative oxygen atoms. Even though the methylene peak adjacent to the terminal hydroxyl groups restricted with a similar chemical shift to the OCH_3 proton peak, the integral of the methylene proton peak was larger and matched the other peaks in the spectrum, which strongly indicated conversion of the terminal groups. This is due to the large number of methylene protons in the OH-dendrimer structure. The spectrum exhibits a triplet at 3.18ppm, representing the NHCH2CH2N proton. Furthermore, there were also three multiplet peaks displayed in the spectrum; the first peak was at 2.75 ppm corresponds to (NCH_2CH_2CO), which experiences greater deshielding because they get closer to tertiary amine groups; the second peak at 2.55 ppm contributed methylene protons of EDA core and 2.33 ppm for NCH_2CH_2CO. With growing generation sizes, overlapping of peaks tends to be more complex, becoming broad and hard to interpret.

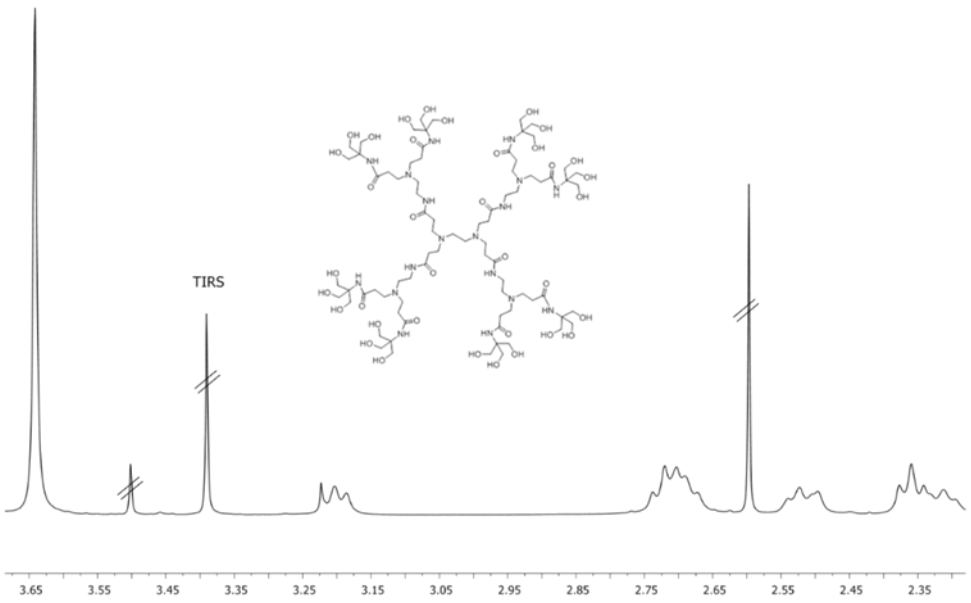

Figure 3.10 1H NMR spectra of G1.5 Hydroxyl terminated of the PAMAM dendrimer

Mass spectrometry is very valuable tool for the characterisation of PAMAM- OH terminal dendrimers. The spectra for PAMAM-OH G0.5 gave peaks with correct molecular ion (761) (MH+), also the G1.5 OH dendrimer shows a peak that was expected at (1956) (MK^+). The spectra of PAMAM-OH G2.5 and G3.5-OH, showed peaks at 4171 and 8149 respectively, however, they did not display the expected molecular ion at 4233, 8862 respectively. The reason may be structural defects occurring during their synthesis with part of the methoxy groups not converting into hydroxyl groups resulting from the loss of some ester groups by hydrolysis. Mass spectrum, especially for the largest dendrimer, G4.5OH, was very much anticipated and the peak was very broad which could be due to the large number of hydroxyl terminal groups on the PAMAM-OH dendrimer. The difference in expected and found M+ could indicated that up to 7 TRIS groups did not add. However, NMR integration showed the correct value for the terminal CH_2 groups of the terminal TRIS units, confirming that all esters had been converted. Therefore, at this stage we are unsure why the mass spec data does not show a molecular ion, but we have observed poor mass spec data for other large dendrimer systems. Overall we are convinced that the reaction was successful.

The ^{13}C NMR spectrum of the dendrimer hydroxyl terminal groups shows all expected regions of the spectrum. The spectrum shows peaks at 174.3 ppm for the interior amide and 175.2 ppm for the exterior amide. The ^{13}C NMR spectrum did not display the peak of the CH_3 group, indicating complete removal, confirming the successful addition of the hydroxyl groups. For the carbons adjacent to the terminal hydroxyl groups, peaks were revealed at 62.0, 61.5. In addition, there were other peaks at 59.8, 51.2, 49.1, 43.2, 41.5, 36.8 and 32.7, which correspond to the carbons of the C-NH, CH_2-N, CH_2 (core) and CH_2CO. Infrared spectroscopy was also used to confirm the conversion of ester terminal groups to OH-terminated dendrimers. The IR spectra of all the hydroxyl-terminated dendrimers displayed a broad peak at 3272 cm^{-1} indicating the presence of terminal hydroxyl groups and the sharp peak at 1640 cm^{-1}, corresponded to the amide carbonyl. However, the ester peak at 1735 cm^{-1} was no longer visible, which confirmed the conversion of the ester terminal groups into amide.

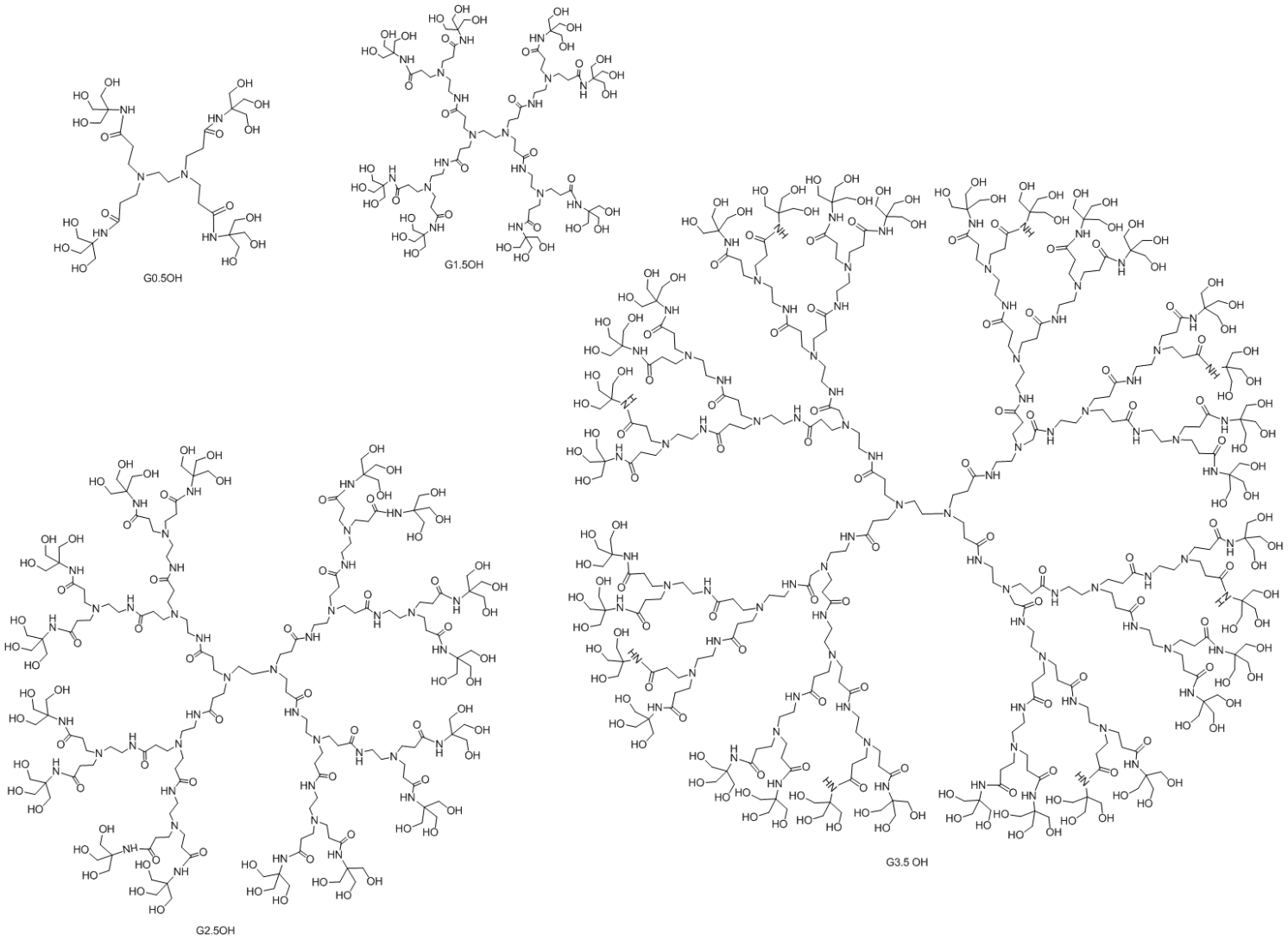

Figure 3.11. Hydroxyl-terminated PAMAM dendrimers

3.5 Encapsulation studies

We wanted to determine the concentration effect of dendrimer on encapsulation ability. Specifically, to see whether or not there was linear relationship between dendrimer concentration and encapsulation.

We initially decided to use a real drug to assess the efficiency and ability of the dendrimer to improve the solubility of the hydrophobic drug. Ibuprofen was selected, the main reason for studying this drug is that it is a common drug to test delivery systems we can compare our results to theirs. Although it has poor solubility which leads to a low bioavailability [1]. However, this is not a major problem, main problem is deliver to specific sites [127]. Its molecular weight is 206.29 g/mole, molecular formula is $C_{13}H_{18}O_2$ and chemical structure containing a carboxylic group made the ibuprofen partially soluble in water 21.0 mg/L [128]. In addition, this molecule is UV active as a result of this, so its solubility in solution can be effortlessly measured. The peak of Ibuprofen selected to use is the one at 263 nm (Q band) which has a smaller intensity, it is much easier to monitor than the sort band [129].

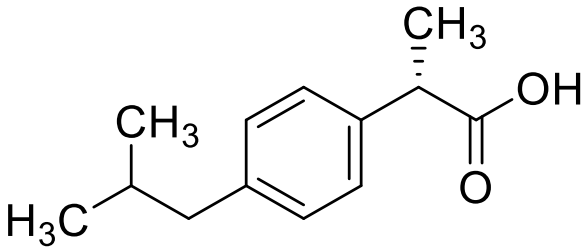

Figure 3.12. Structure of ibuprofen

To test solubility ibuprofen was added to a solution of TRIS buffer with a concentration 0.01 M and a pH 7.4. The encapsulation process was made at room temperature. Prior to the procedure, the extinction coefficients (Ɛ) of the Ibuprofen were determined from a Beer-Lambert plot. Because ibuprofen does not dissolve significantly in water, the Beer Lambert study was carried out using MeOH as the solvent. The extinction coefficient, was found to be 150 $dm^3\ mol^{-1}\ cm^{-1}$. The solubility of ibuprofen was first measured without the dendrimer. This experiment was carried out using the same steps that would be used for the dendrimer

encapsulation experiments discuses later. Specifically, ibuprofen was dissolved in methanol, followed by removal of the methanol. TRIS buffer (pH 7.4, 0.01M) was added and solution filtered to remove the excess ibuprofen. The maximum solubility of ibuprofen (using this method) was found to be 1.13×10^{-4} M. This inherent, or background solubility was subtracted from any future dendrimer enhanced solubility.

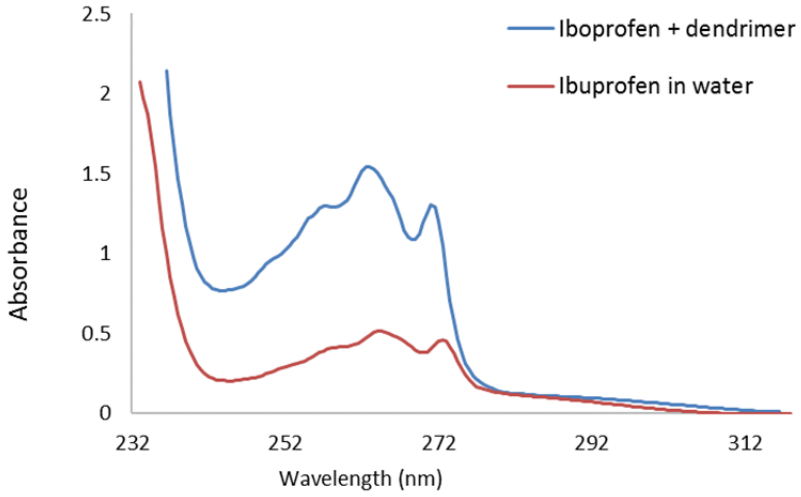

Figure 3.13. UV-Vis spectra of maximum solubilised ibuprofen in buffer and a buffer solution of PAMAM dendrimer [1×10^{-4}]

In the dendrimer encapsulation process, the dendrimer/drug complex was made via the co-precipitate technique. This method involved dissolution of the ibuprofen molecules and dendrimer in methanol. Following this, the solvent was removed using a rotary evaporator to obtain a PAMAM dendrimer/drug co-precipitate. Tris Buffer (pH 7.4, 0.01M) was added and the solutions were filtered to remove the excess insoluble drug molecules. The soluble complex solution was then measured using UV-Vis to determine the concentration of drug from a Beer Lambert analysis (absorption at 263 nm). To compensate for any base line draft direct absorption was not used. instead, Δ absorptions values were used wavelength from 264 to 268 nm.

As stated earlier, water soluble PAMAM dendrimers were successfully synthesised different generations with 24OH, 48 OH, and 96OH terminal groups. The first step was to determine the effect of dendrimer size on the encapsulation process. In order to achieve this, encapsulation was carried using concentration 1.00 x 10^{-4} M of PAMAM dendrimers with an excess ibuprofen. The above encapsulation processes were followed and the encapsulated concentration value of

all samples was determined by dividing the absorbance by the extinction coefficient (ε) of ibuprofen. Furthermore, loading per mole of the ibuprofen encapsulated within hydrophobic voids of hydroxyl PAMAM dendrimer was determined by dividing the concentration of ibuprofen by the concentration of dendrimer.

OH-dendrimers Generation	Concentration of dendrimer	Final concentrations of encapsulated Ibuprofen	Loading
1.5	1×10^{-4} M	2.00×10^{-4} M	2
2.5		4.00×10^{-4} M	4
3.5		27.0×10^{-4} M	27
Concentration of dendrimer in buffersolution $=1.00 \times 10^{-4}$ M. *No dilution was needed in this study			

Table 3.2. The final concentrations of ibuprofen upon encapsulation within G1.5, G2.5, and G3.5OH terminated PAMAM dendrimers.

From the results shown in the table 3.2 we can clearly observe effect of size generation of dendrimers on the solubility of ibuprofen. For G1.5 dendrimers with 48OH groups, only two moles of ibuprofen. can be incorporated within the hydrophobic voids of the dendrimers. As for the G2.5 dendrimers with 24OH groups, only four moles of ibuprofen were encapsulated in their dendritic box. When the upper generation (G3.5 96 OH groups) used, thirty moles of ibuprofen were accumulated inside the dendrimers.

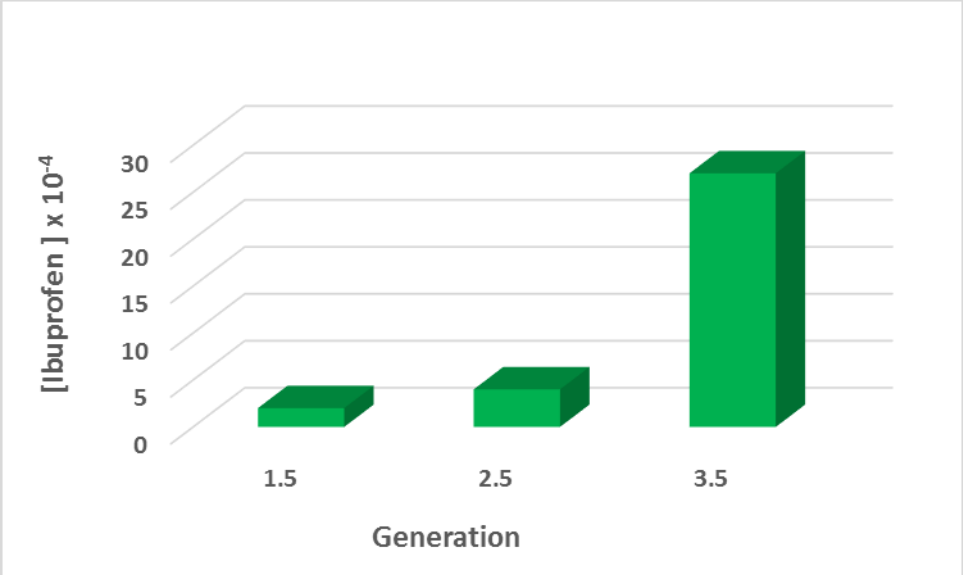

Figure 3.14. Increased concentration of encapsulated ibuprofen after encapsulation with different Size of PAMAM dendrimers.

Though the concentration increased with increased size of the dendrimers, there was no big difference from G1.5OH-dendrimers to G2.5OH-dendrimers, also both of them not much increased with respect to solubility. However, a higher generation (G3.5) exhibited higher solubility of ibuprofen and the concentration of the ibuprofen was hugely increased (Figure 3.14) compared with G1.5OH-dendrimers and G2.5OH-dendrimers, smaller dendrimers have no definition inter structures is flat, no hydrophobic pockets. However, the G3.5 is controlled "space" a well-defined with a hydrophobic inter. As a result of the of this study, the G3.5 is the best size dendrimer to encapsulate ibuprofen. After studying the effect of dendrimer size on encapsulation capacity, the study sustained with the relation between dendrimer concentrations and drug encapsulated, but before this we need to determine best initial concentration can be used to get the maximum loading of dendrimer. To achieve this, the G3.5- HO PAMAM dendrimer with a molecular weight of 8149g/mole and four different concentrations of the ibuprofen (1.00×10^{-3}, 5.00×10^{-3}, 1.00×10^{-2} and 5.00×10^{-2}) were used. The concentration of the drug encapsulated of all samples was calculated by dividing the absorbance by the extinction coefficient of ibuprofen. A typical result is clearly shows that the dendrimer can enhance the solubility. Different loading of guest molecule for a different concentrations of drug is shown in Table 3.3.

Dendrimer concentration	Initial drug concentration	Ibuprofen encapsulated concentration	Loading of ibuprofen per dendrimer
1.00×10^{-4}	1.00×10^{-3}	3.91×10^{-4}	4
	5.00×10^{-3}	18.7×10^{-4}	18
	1.00×10^{-2}	27.1×10^{-4}	27
	5.00×10^{-2}	25.7×10^{-4}	26
Concentration of G3.5 dendrimers in buffer is 1.00×10^{-4} Concentration of ibuprofen in buffer without dendrimer is 1.13×10^{-4} M			

Table 3.3. Solubility of ibuprofen in TRIS buffer solution for different concentrations of drug encapsulated in PAMAM dendrimer [1.00×10^{-4}]

The experiment studied different concentrations of ibuprofen (1.00×10^{-3}, 5.00×10^{-3}, 1.00×10^{-2} and 5.00×10^{-2}). The concentration of the drug encapsulated of all samples was calculated by

dividing the absorbance by the extinction coefficient of ibuprofen. A typical result is clearly shows that the dendrimer can enhance the solubility.

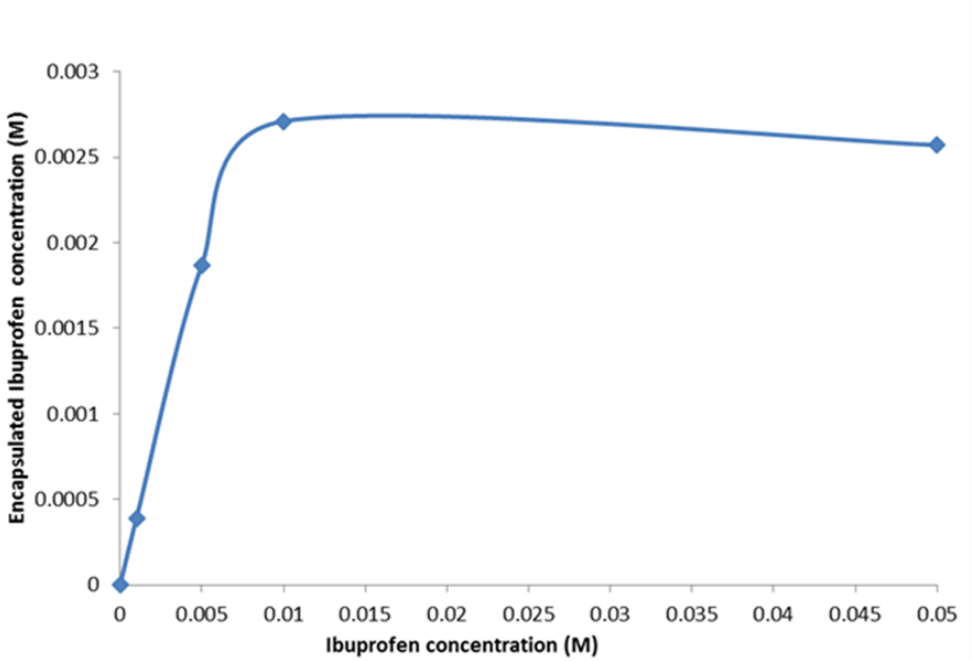

Figure 3.15. Encapsulated ibuprofen with dendrimers concentration of 1.00×10^{-4} M

The loading per mole of the PAMAM dendrimer was calculated by dividing the concentration of encapsulated ibuprofen by the concentration of the dendrimer, this was determined to be 27 ibuprofens per dendrimer. The increase in solubility of the drug was significant and is evidence of the ability of the dendrimer to encapsulate ibuprofen within their hydrophobic cavities. Moreover, a second interaction could occur between the acidic parts of ibuprofen and the tertiary amines inside the dendrimer may explains why so much ibuprofen is encapsulated Figure 3.16.

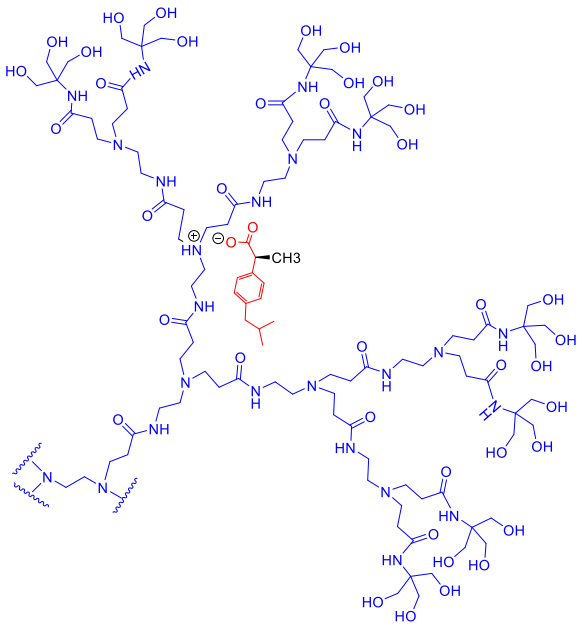

Figure 3.16. Encapsulation via a secondary electrostatic/acid base (ion pairing interaction). Only one dendrimer arm shown for clarify

There is also the probability that ibuprofen can form hydrogen bonds with the internal amide/amine units. This will provide another interaction to support and strengthen the hydrophobic and acid/base interaction. To test the importance of H bonding /salt we involved naphthalene as it does not have a carboxylic functional group in its structure.

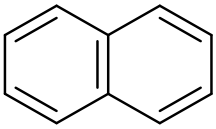

Figure 3.17. Structure of naphthalene

The study was conducted using G3.5 PAMAM dendrimer with concentration 1.00×10^{-4} to encapsulate an excess of naphthalene Figure 3.17. The encapsulation result (data not shown) showed that only a small number of these molecules could be trapped in the cavities of the dendrimer. the solubility of naphthalene increased but it was low (1.21×10^{-6}) and loading 0.0121naphthalene per dendrimer was less than one compared with ibuprofen molecules which showed high loading, 27 ibuprofens per dendrimer. This result provides strong evidence for the importance of carboxylic acid group in providing secondary interaction.

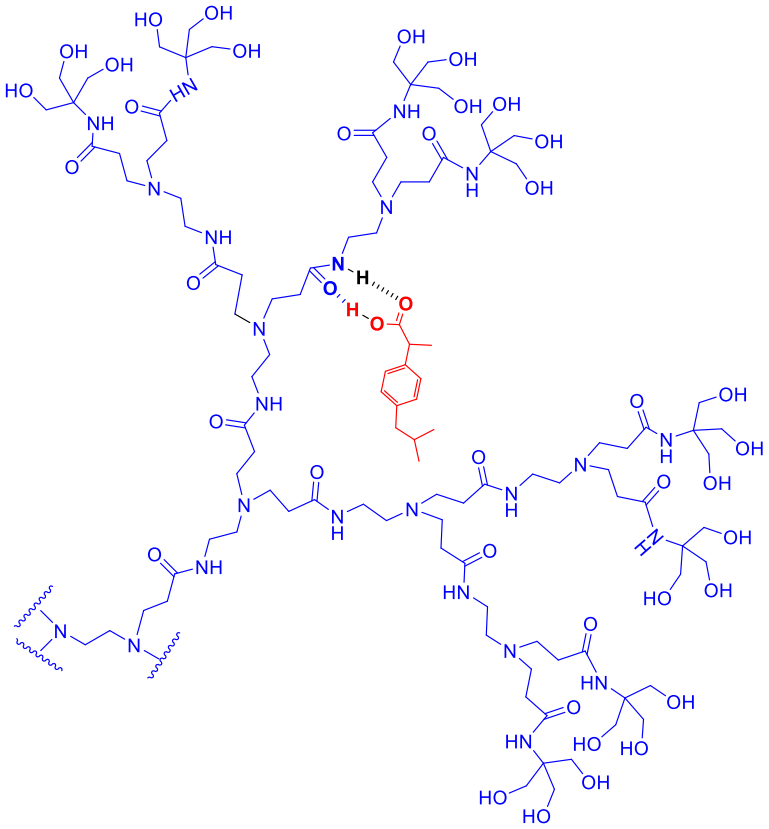

Figure 3.18 The possible hydrogen bonding interaction between dendrimer and ibuprofen.

Having worked out the maximum amount of drug that could be encapsulated within the G3.5 dendrimers. The next experiment was designed to determine if this was consistent for all dendrimer concentrations. That is, could the dendrimer solubilise more ibuprofen at higher dendrimer concentration and, could the dendrimer still encapsulate 27 ibuprofens per dendrimer at higher concentrations. To study G3.5, four different concentrations of G3.5 OH PAMAM dendrimer were prepared, these were (1x 10^{-4} M, 2x 10^{-4} M, 4x10^{-4} M and 6x 10^{-4} M) and used to encapsulate an excess amount of ibuprofen (higher 27 than the found in the previous experiment). The final concentration value of the encapsulated ibuprofen and the number of Ibuprofen encapsulated inside G3.5 dendrimers at various concentrations is shown in Table 3.4.

Table 3.4 dendrimer concentrations in solution and encapsulated ibuprofen in different concentrations of dendrimer

Dendrimer concentration	Concertation of encapsulated ibuprofen[M]	Loading per dendrimer
1.00×10^{-4}	27.3×10^{-4}	27
2.00×10^{-4}	40.0×10^{-4}	20
4.00×10^{-4}	80.0×10^{-4}	20
6.00×10^{-4}	85.0×10^{-4}	14

The G3.5 hydroxyl PAMAM dendrimer has 30 internal and basic amines groups and the maximum determined loading per dendrimer is 27 ibuprofens. This suggest that most of the internal amines have formed a salt. The fact that 30 ibuprofens were not encapsulated is probably due to steric, particularly, the two amines at the EDA core. However, from the above results, it can be observed that although the solubility of ibuprofen does not increase with increasing concentration of dendrimers, the amount of ibuprofen encapsulated within each dendrimer decrease with increase dendrimer concentrations. This is not what we expected. We expected that as concentration increased then the amount of encapsulated ibuprofen would increase increasingly.

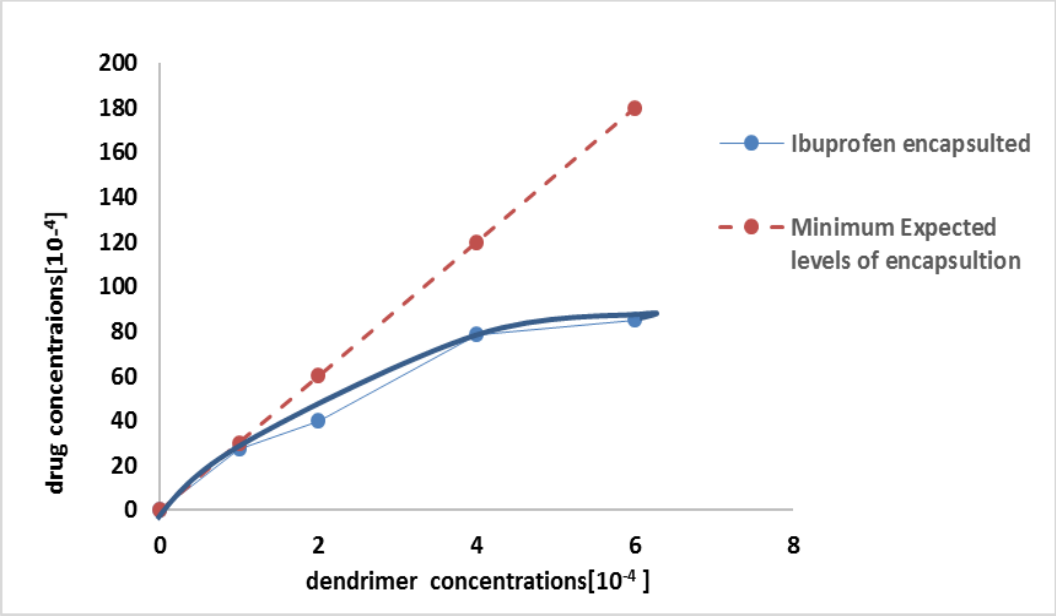

Figurer 3.19 The solubility of ibuprofen increased with increased concentration of G3.5 PAMAM dendrimer and minimum expected levels of encapsulation.

The above graph (Figurer3.19) showed the relationship between the PAMAM dendrimer concentration and solubility of ibuprofen after encapsulation. It is not a completely linear relationship, because the increase in solubility does not follow the increase in concentrations of the polymer.

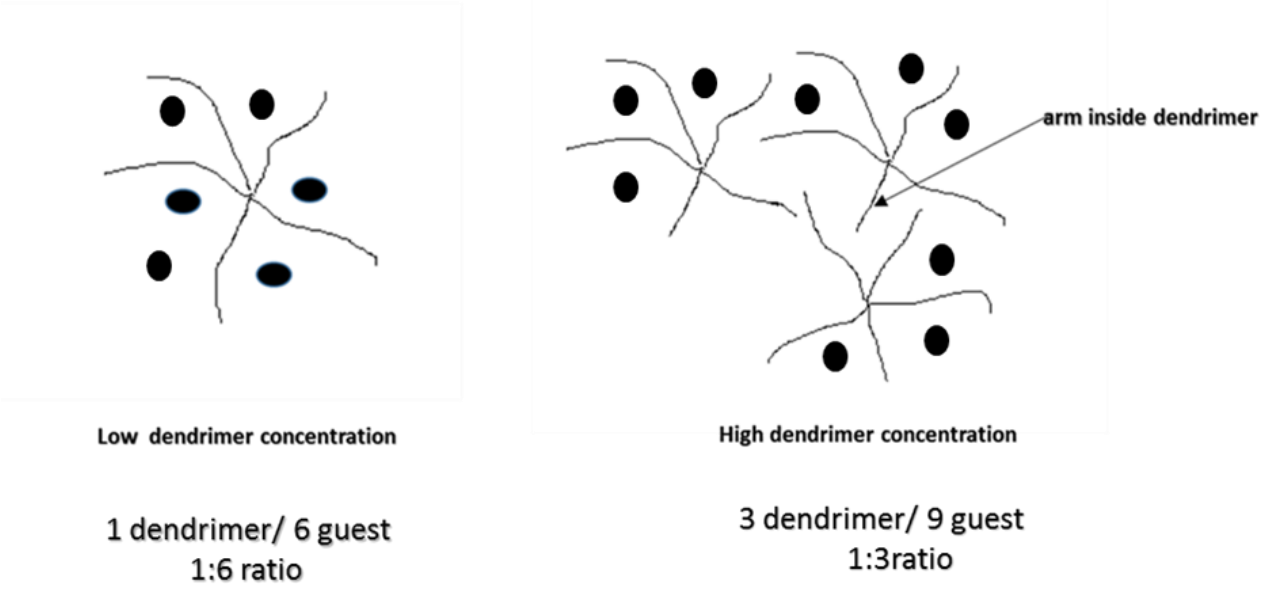

Figurer 3.20 Representation of possible encapsulation process at low concentration and possible arm inside dendrimer at high concentration.

The reason for reduced encapsulation is probably due to aggregation at high the concentrations. We suggest that the dendrimer arms can interpenetrate, and hinders the ibuprofen encapsulation. If this was the case, we should be able to detect larger species at higher concentrations. To test this, light scattering (DLS) was used to measure the intensity and the size of scattered light of particle at a given concentration. The DLS result showed an aggregation of G3.5 PAMAM dendrimer at 1.00×10^{-4}. Specifically, a peak at 206 nm confirms the produce of a large species. We also see a peak at 5.5nm, which corresponds to the non-aggregated structure (Figure 3.21).

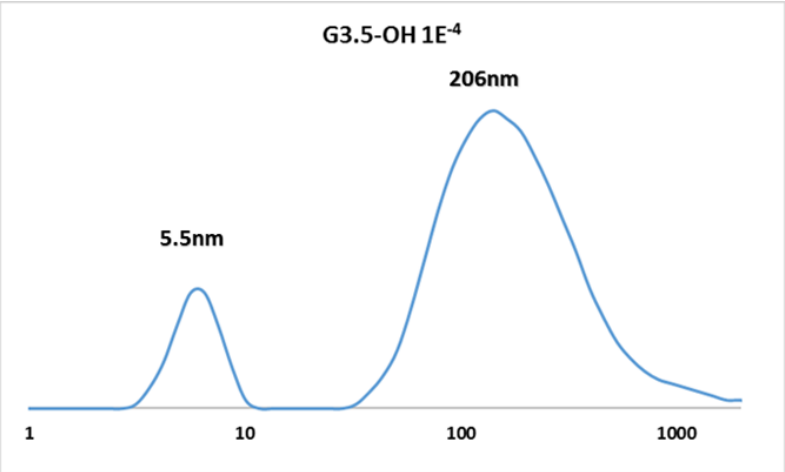

Figure 3.21 Aggregated structures at 1.00×10-4 M, a peak at 206nm confirms the produce of a large species and a peak at 5.5nm for non-aggregated structure.

3.6 PAMAM dendrimers for encapsulation of Ps for PDT

Having demonstrated that secondary H bonding and acid/base interaction led to increased encapsulation, the next step of the investigation was to determine the effect of coordination the process of encapsulation. This work presents a comparison between a simple tetraphenyl porphyrin (TPP) and metal porphyrin, zinc tetraphenylporphyrin (ZnTPP). We were interested in porphyrins due to their use as Ps in PDT.

3.6.1 Encapsulation of TPP within hydroxyl terminated PAMAM dendrimers via non-covalent (hydrophobic interaction)

Simple porphyrins are macrocyclic molecules [6,130] with four pyrrole rings linked together in as a conjugated system. Porphyrins are highly coloured molecules; the name originates from the Greek word meaning purple [123]. It is also referred to as free base porphyrin (i.e. without a metal) and has 22π-electrons in the macrocycle, 18 of which are delocalized in an aromatic ring which makes it very stable. It can coordinate metal ions inside its core which affect its electronic system [130]. The UV/Vis spectrum of porphyrin is characterised by a band around 400 nm (Soret band) and four Q bands at 515 nm, 551 nm, 592 nm and 645 nm. Porphyrins have other unique properties, for instance, they exhibit strong absorption and emission at wavelengths which make these chromophores suitable as photosensitizers.

3.6.2 Synthesis of tetraphenylporphyrin (TPP)

Tetraphenylporphyrin (TPP) was synthesised by the addition of pyrrole and benzaldehyde to refluxing propionic acid in a round bottom flask equipped with a condenser [131]. The reaction mixture was heated to reflux for 30 minutes and then allowed to cool; the product was filtered and washed with hot methanol followed by hot water to remove undesired impurities.

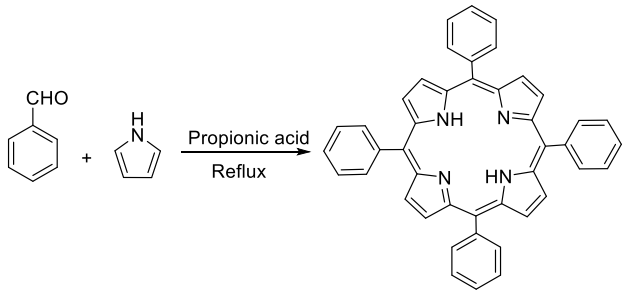

(4)

Scheme 3 .22. Synthesis of tetra phenyl porphyrin (4)

^{1}H NMR spectroscopy was the main tool used in the characterisation of TPP. The spectra showed a highly shielded peak at -2.71 ppm corresponding to the NH inner protons, this is because their location within the shielding area of the porphyrin which confirming the presence of a porphyrin (figure). In addition to that, three peaks at 8.89ppm (8 protons) from the β-pyrrolic protons, 8.23ppm (8 protons) and 7.75 ppm (12 protons) from the ortho and para-aromatic phenolic protons respectively(figure). UV-Vis spectra confirmed the successful synthesis of the compound, the Soret band at 418 nm and four Q bands at 515 nm, 551 nm, 592 nm and 645 nm. Further characterisation by mass spectrometry (ES-MS), displayed the molecular ion peak (MH^{+}) at the expected mass 615. Following the synthesis of the TPP, the next stage was to encapsulate it within the dendrimer's interior (hydrophobic interaction). TPP is a hydrophobic aromatic macrocycle; it's insoluble in water which makes it a good choice to determine the polymer's ability to improve solubility. The most intense absorption peak for TPP, its Soret band at 418 nm was monitored to determine the level of encapsulation.

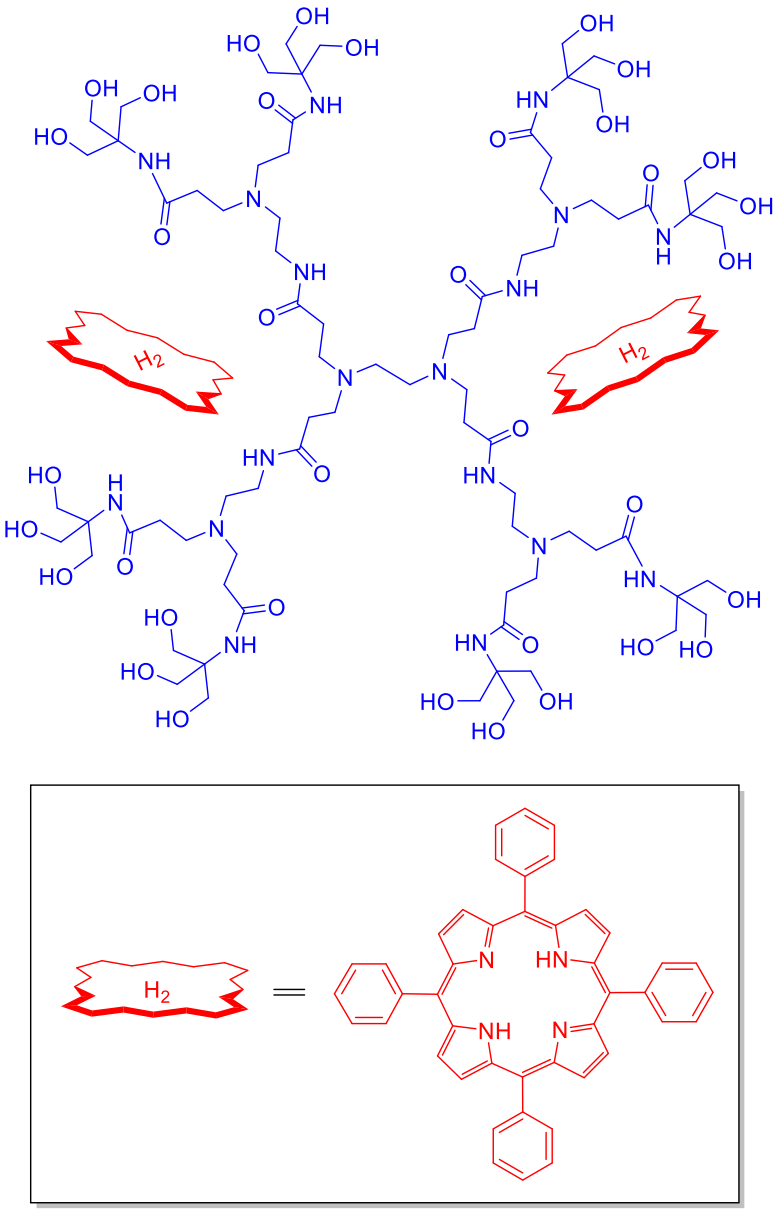

Figurer 3.23 Free-base porphyrin encapsulated in hydroxyl PAMAM dendrimer

Generally, the encapsulation process involved mixing both the guest and host in a soluble solvent however, there is difficulty finding a good solvent for both the dendrimer and TPP. This is due to the fact that TPP is a very hydrophobic molecule which does not dissolve in polar solvents. this meant we had to physically mix the two samples in methanol. The encapsulation of TPP within the dendrimer occurred by mixing an excess amount of solid TPP with a concentration of $1x10^{-4}$ PAMAM-OH dendrimer (24 OHs, 48 OHs and 96 OHs) in methanol. After a short time, the methanol was removed under vacuum resulting in a dendrimer-porphyrin co-precipitate. These complexes were dissolved in a TRIS buffer solution (pH 7.4, 0.01M), so

that the final concentration of dendrimer was 1×10^{-4}. The solution was filtered and the final product was a pale red complex solution. This colour indicated that encapsulation had been successful. Confirmation and quantification of encapsulation was carried out using UV/Vis. The extinction coefficient (Ɛ) was determined graphically from a Beer-Lambert plot and found to be 6.3×10^{-4} M^{-1} cm^{-1}. The final concentrations of the encapsulated free base porphyrin within all generations are shown in the table 3.5.

Dendrimer Generation	Concentration of dendrimer	Concentrations of encapsulated TPP x 10^{-6}	Loading ratio of dendrimer to TPP
1.5OH	1 x 10^{-4}	0.20	500:1
2.5OH		0.22	465:1
3.5OH		0.280	357:1

Table 3.5. TPP loading per mole of dendrimer with concentration of 1.00 x 10^{-4} M (G1.5, G2.5, G3.5OH).

Overall, the data above shows a very low efficiency of TPP encapsulation by neutral hydroxyl dendrimers. The small difference in the concentrations of encapsulated TPP between the generations (24 OH and 48 OH and 96 OH) were the result of increased hydrophobicity and size compared with small molecules. The proportion of loading between OH PAMAM dendrimers and TPP was <1 as shown in the table 3.5.

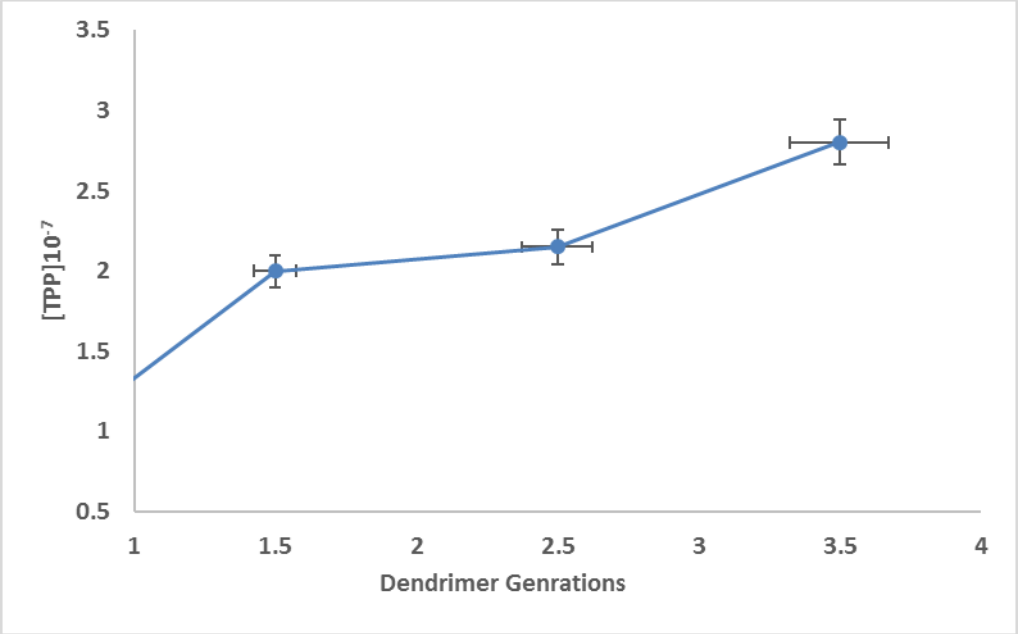

Figurer 3.24. Encapsulated TPP concentration with different molecular weights of PAMAM dendrimer.

The graph (3.24) shows an upward trend in TPP concentration, with G3.5 binding the best. However, all loading were extremely poor, with encapsulation levels lower than one TPP per 350 dendrimers. The reason for the low encapsulation could be due to the low solubility of TPP in any solvent that could also dissolve the dendrimers. This meant that the co-precipitate method was not effect and encapsulation relied on simply “mixing“ the TPP and dendrimers (that is, not much of the TPP was ever in solution).

3.7 Increasing solubility of encapsulation via coordination (second interaction)

As a result of the low encapsulation, we wanted to include a second type of interaction to improve the loading capacity of the polymer. To maximise interactions, we decided to use zinc tetraphenylporphyrin (ZnTPP) as this could form additional coordination bonds with the dendrimers internal amines. Zinc tetraphenylporphyrin (ZnTPP) is easily synthesised by the insertion of zinc into TPP; after losing its two inner protons, the zinc metal forms a coordination complex with the four nitrogen atoms of the porphyrin ring.

3.7.1 Synthesis of Zinc tetraphenylporphyrin (ZnTPP).

Zinc Tetraphenylporphyrin (ZnTPP) was synthesised in a reaction of tetraphenylporphyrin (TPP) with zinc acetate in chloroform for an hour. The mixture was then purified using filtration and rotary evaporation techniques; the end product was a fuchsia coloured compound.

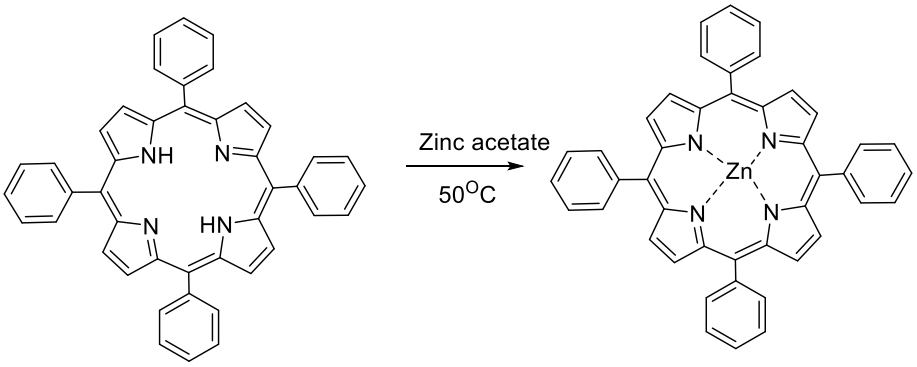

(4) (5)

Figurer 3.25. synthesis of Zinc tetraphenylporphyrin (ZnTPP) (5)

Insertion of zinc metal into TPP was confirmed using various techniques. The ^{1}H NMR spectrum showed an absence of the highly shielded peak at -2.75 ppm which relates to inner protons of porphyrin compound. Also, there was one singlet peak at 8.97 ppm corresponding to pyrrolic βH and two other peaks at 8.26 ppm and 7.81 ppm corresponding to the ortho, meta and para-phenylic protons. Mass spectroscopy (ES-MS) showed a molecular ion peak (MH^{+}) at 678, which agreed with the calculated molecular weight. More evidence was obtained from the UV-Vis spectrum which displayed the wavelength of maximum absorption (Soret band) at 419nm and two weak Q bands at 548 nm, and 678 nm; a reduction from the four bands observed in the spectrum of free base porphyrin. The following step was to encapsulate ZnTPP within PAMAM dendrimers via coordination.

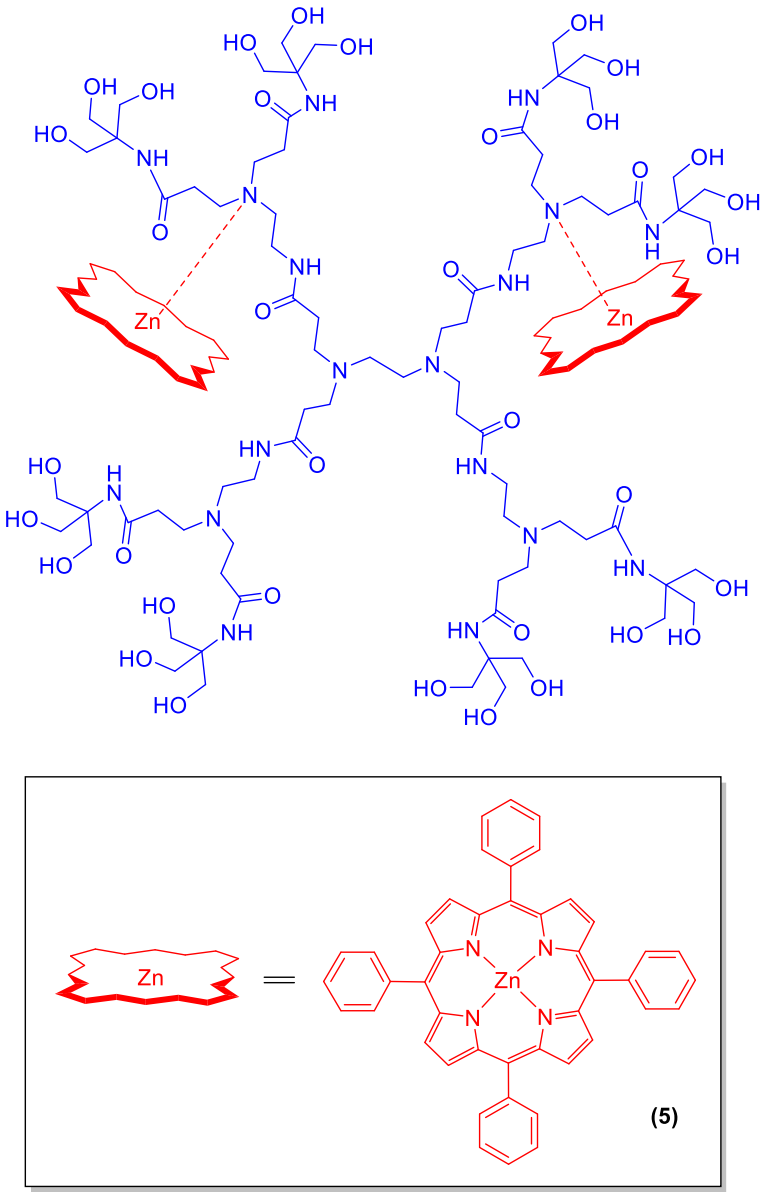

Figurer 3.26. Shows additional interaction provided by coordination

The same procedure for TPP encapsulation was applied, resulting in complex solutions that were a darker in colour than the TPP complex solutions; indicating increased encapsulation. Measurements were performed by UV/Vis spectroscopy to determine the concentration of the zinc porphyrin encapsulated by the OHs PAMAM dendrimers and a large porphyrin peak was detected at λmax = 418 nm. The extinction coefficient (Ɛ) was calculated as 263499 M^{-1} cm^{-1} and used to calculate the concentration of the encapsulated porphyrin. The data of PAMAM-OH-ZnTPP is shown in table (3.6).

Dendrimer Generation	Concentration of dendrimer	Concentrations of Encapsulated Zn TPP x 10^{-6}	Loading ratio of dendrimer and ZnTPP
1.5OH	1 x 10^{-4}	2.0	50:1
2.5OH		4.0	25:1
3.5OH		8.0	12:1

Table 3.6. Solubility of ZnTPP in TRIS buffer solution with different generations of PAMAM dendrimer.

As the dendrimer generation increased, there was a noticeable increase in the encapsulated ZnTPP concentration; For example, for the G 1.5OH, the ratio of dendrimer to zinc was 50:1 and this ratio increased to 25:1 for the G2.5 was used. The highest loading ratio was recorded for the G3.5OH dendrimer, which was found to be 12 dendrimers per ZnTPP. which shows that one molecule of the dendrimer can incorporate one molecule of ZnTPP. From the data, all dendrimer generations have the ability to encapsulate drug ZnTPP within their hydrophobic cavities, but the loadings were still low. However, comparing like for like with the free base porphyrins, we observed significantly higher loadings for the metallized porphyrins.

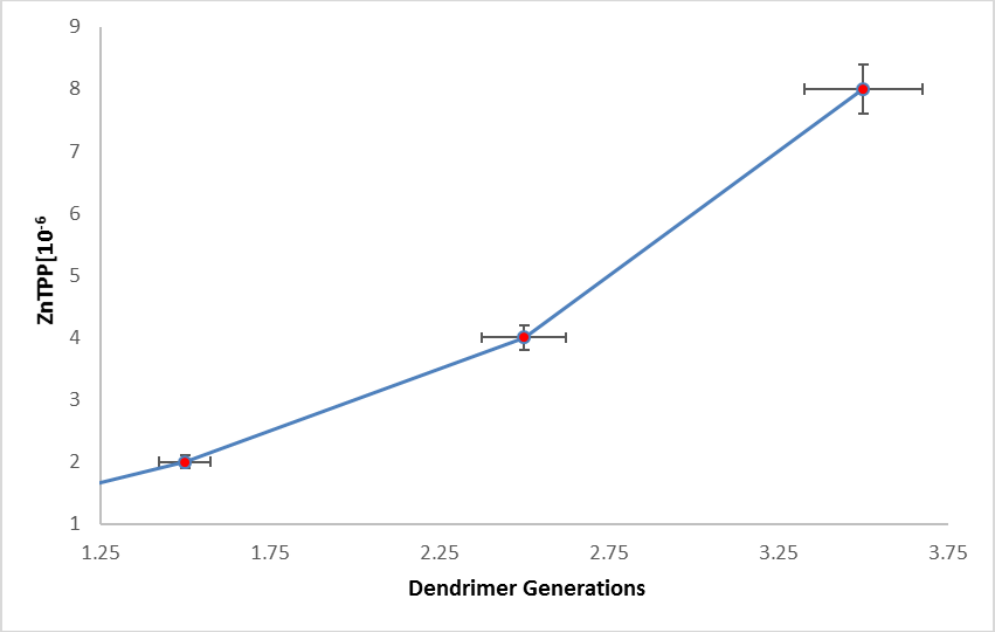

Figurer 3.27. Increased solubility of ZnTPP with increased size of PAMAM dendrimer.

The graph shows the concentration of ZnTPP plotted against the generation of dendrimer where each generation has a concentration of 1.00 x 10^{-4} M. For all generations, the ZnTPP concentration increase was roughly linear, we see the increase in solubility, is almost we move from G1.5 to G3.5 solubility double at each generation. This is evidence that the use of the second interaction has a significant effect to improving the encapsulation result and increasing the solubility. After encapsulation of these hydrophobic systems, a comparison was made between them to investigate the effectiveness of the type of interaction and improve the solubility of hydrophobic molecules. The solubilisation behaviour of the PAMAM dendrimer depends on the types of interactions between the host and guest molecules. For the purpose of comparison, all generations of PAMAM dendrimers with a concentration of 1.00 x10^{-4} M were used and the loading values for TPP and ZnTPP are tabulated in the table 3.7.

Dendrimer generation	[TPP]×10^{-6}	[ZnTPP] × 10^{-6}	Coordination effect [ZnTPP] / [TPP]
1.5OH	0. 2	2.0	10
2.5OH	0. 22	4.0	18
3.5OH	0. 28	8.0	28

Table 3.7. Comparison of the coordination effect on the solubility enhancement of ZnTPP and TPP.

From the results presented in table 3.6, we can say that encapsulation of ZnTPP using water soluble PAMAM dendrimers has better results compared to the encapsulation results of free base TPP. The final concentrations showed that the non-covalently incorporated porphyrin (TPP) in the PAMAM dendrimer had very low loading due to poor solubility and only one possible interaction (hydrophobic interaction). However, the non-covalently incorporated ZnTPP in the dendrimer showed much higher loading concentrations across all generations; this was due to secondary interactions (coordination bonds). The coordination effect on solubility can be represented by the increased concentration of the ZnTPP with respect to TPP. The table shows that for G3.5 OH dendrimer, there is a 28 times increase in solubility as result of coordination. This study into the encapsulation process was relatively successful and further work is needed to investigate other encapsulation techniques. These techniques play a

significant role in improving hydrophobic drug solubility. There is no question that secondary interactions significantly improve encapsulation. However, even though a big improvement in solubility was observed, the ratio of dendrimer to porphyrin was too low. For example, the best result using the G3.5OH and ZnTPP, required 12 dendrimers to 1 porphyrin. To improve this ratio, we proposed to design a molecule where porphyrin coordination was involved in the synthesise of the dendrimer. This would ensure that every dendrimer would have a porphyrin. The design and synthesise is described in the next chapter.

Chapter 4

Results and Discussion

Part 2: Self-assembled porphyrin cored dendrimers as a PDT sensitizer.

As mentioned earlier, the aim of this section of the project is to develop a self-assembled targeting system for Photodynamic Therapy.

4.1 PAMAM Dendron Systems

In order to achieve this aim, it was necessary to synthesise different generations of ester-terminated groups PAMAM dendrons. The chemical and physical properties of PAMAM ester dendrons, such as their degree of branching and size, can be controlled. It is their globular structure, interior void spaces and the large numbers of end groups that makes them an attractive option for our drug delivery system. PAMAM dendrimers would be synthesised (as previously described) using two iterative steps. The first step involves a 1,4 Michael addition using methyl-acrylate to give a half-generation ester-terminated groups. The second step is an amination reaction to produce whole generation PAMAM dendrons terminated with amine groups. The first and second steps can be repeated to give large generation PAMAM dendrons. Both methods are explained below.

The difference between the synthesis of PAMAM dendrimer and PMAMA dendrons is a reactive focal point. To synthesise half generation PAMAM dendrons, β-alanine was used as dendron core; the acid group of β-alanine was bonded with tin to form the self-assembled complexes. In this reaction, β-alanine was dissolved in methanol as first step, forming a zwitterion; this was unreactive to methyl-acrylate scheme. Consequently, potassium carbonate was added as a base in order to deprotonate the ionised β-alanine, which can then react with methyl-acrylate to produce the ester-terminated dendrons (Scheme 4.1)

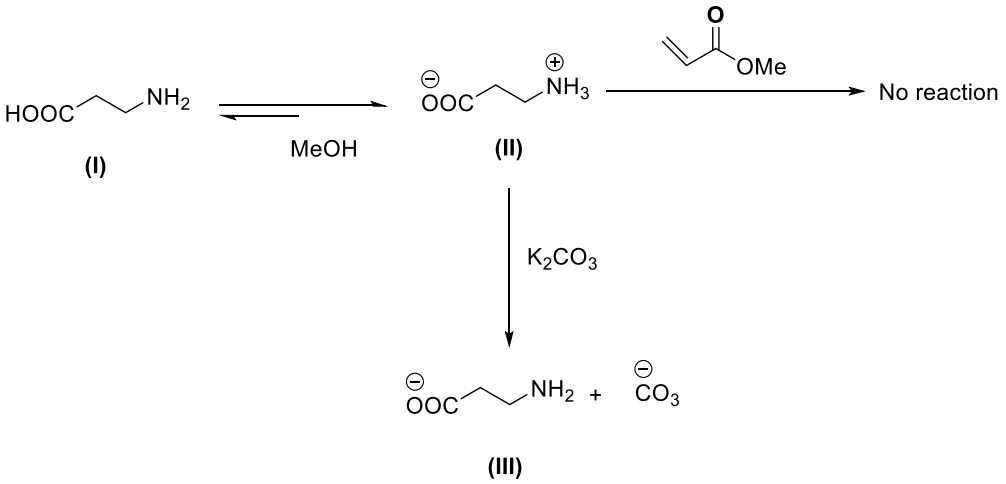

Scheme 4.1. The Reaction of β-alanine with Potassium carbonate

4.1.1 Synthesis of G0.5 acid cored Dendron with 2 ester groups.

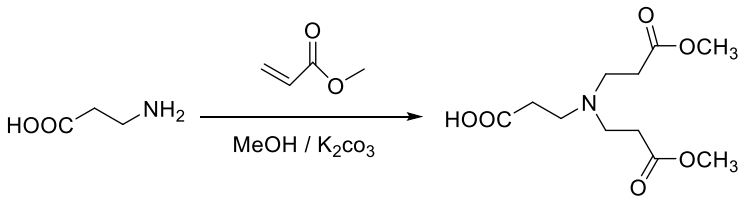

(6)

Scheme 4.2 synthesis of PAMAM dendron with two ester end groups.

The synthesis was initiated by adding potassium carbonate to a solution of β-alanine and methanol. This was followed by the addition of four equivalents of methyl-acrylate at 0˚C. The reaction mixture was then left to stir at room temperature for one day. The unreacted reagent and solvent were removed by the rotary evaporator to give the purification dendron. The product was analysed by ^{1}H NMR mass spectroscopy and IR spectroscopy to ensure the reaction was complete. The spectrum of the G 0.5 dendrons (2) with ester terminal groups has five characteristic peaks, when $CDCl_3$ was used as solvent (figure 3.4). The integral of the ^{1}H NMR of dendrimers provides information about their structures, indicating that they have highly symmetric structures.

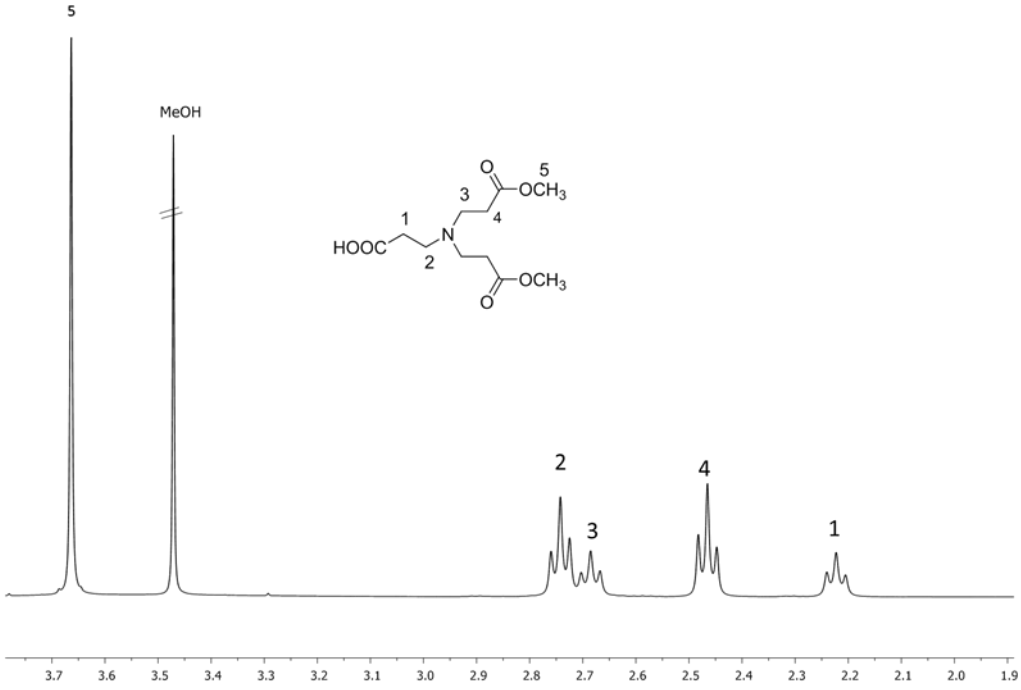

Figure 4.3. ^{1}H NMR of G-0.5 dendron (D-CDCl3, 400MHz) (6).

A singlet peak at 3.68 ppm corresponds to the six methoxy protons (5) in Figure 4.3. This peak is exclusive to the half generation PAMAM dendrons. The other four peaks are triplets: the first at 2.22 ppm, for the two methylene protons closer to the acid core of the dendron (1); the second at 2.47 ppm, for the four methylene protons next to the ester group (4); the third at 2.63 ppm, from the two methylene protons closer to tertiary amine group (3); and the fourth peak at 2.72 ppm, for the four equivalent methylene protons (2). This last peak was more deshielded due to its location, closer to the tertiary amine groups. As for the G1.5, it had the same peaks, in addition to the presence of the peak of amide proton (NH) at 4.92 ppm. ^{13}C NMR spectroscopy was used to confirm the structure of G0.5 ester-terminated dendron. The ^{13}C NMR spectrum showed a peak at 178.3ppm, representing the carbon of an acid group, and a peak at 173.7 ppm, corresponding to a methoxy carbonyl. All higher half generations show a peak at 172.1 ppm, attributed to a carbonyl amide carbon (Figure 4.4).

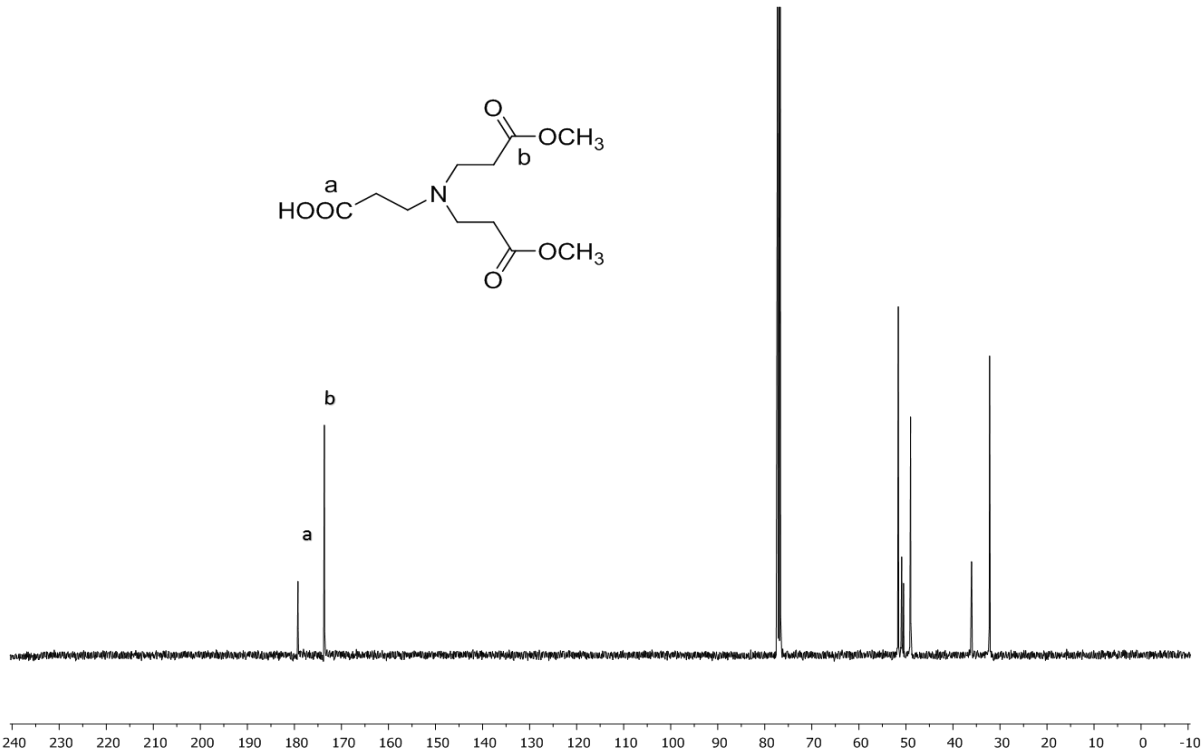

Figure 4.4. ^{13}C NMR of G-0.5 dendron (D-CDCl3, 400MHz) (6).

Mass spectrometry is another system for characterizing dendrons; this technique can incorrectly indicate the existence of defects in the sample which may not be present in the actual sample structure, and are in fact a product of ionization. This spectrum of G0.5 shows the molecular ion peak at 262 (MH^+). The spectrum of G 1.5 showed the molecular ion (M+H) at 662, and (M+K) at 700. FTIR spectroscopy helps to determine the functional group in the dendron structure; the main functional group in the half generations is a methoxy group. The spectrum demonstrated the presence of this peak at 1729 cm^{-1}, though this signal is not visible for whole dendron generations. This is evidence of the conversion of ester-terminated groups to amine-terminated end groups.

4.1.2 Synthesis of G2.5 dendron with 8 terminal ester groups

The method used to synthesise G0.5 dendron was followed, although potassium carbonate was not added to the dendron solution. The amine-terminated PAMAM dendron G2.0 was dissolved in methanol. At 0^oC methyl-acrylate was added dropwise to the dendron solution. The reaction

mixture was left to stir at room temperature. Once completed, the solvent and methyl-acrylate were removed by the rotary evaporation system. Scheme 4.3 showed the conversion of the G2.0 dendron ester-terminated groups to the G2.5 dendron ester-terminated group

.

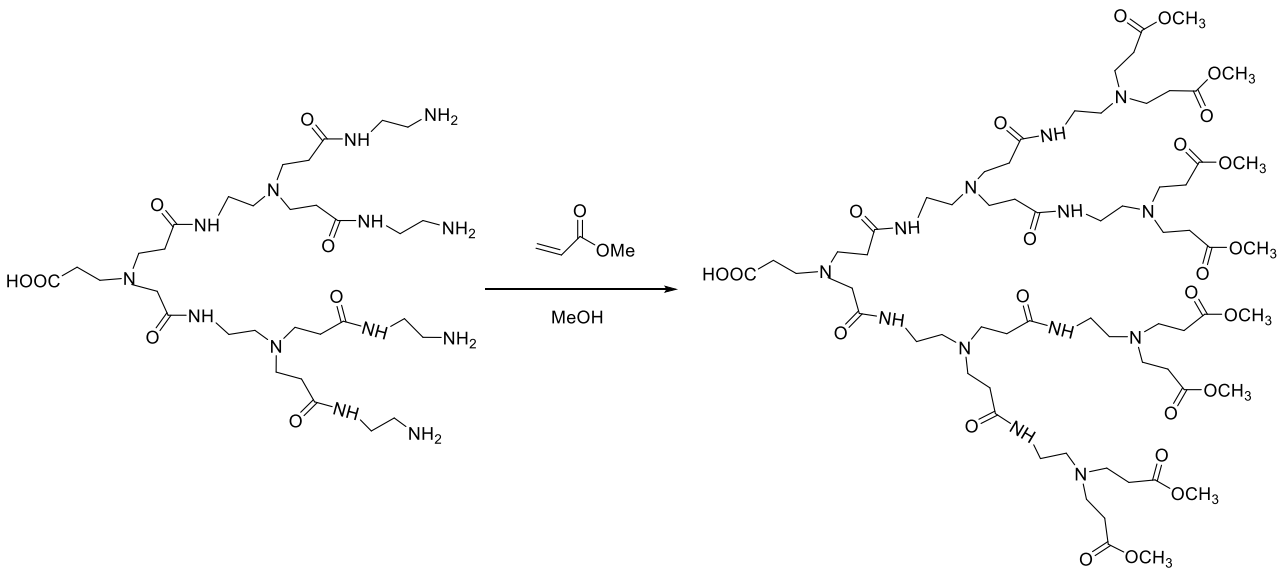

Figure 4.5 Synthesis of PAMAM dendron with eight ester end groups.

The PAMAM dendron G 2.5 with 8 terminal OMe terminal groups was analysed using ^{1}HNMR; the spectrum has a strong peak group at 3.66 ppm from the ester terminal, which suggests the structure of the desired compound. There is also a triplet peak at 2.28 ppm, which is attributed to the methylene protons next to the acid core of the dendron. In addition, the absence of peaks

between 5.51 - 6.51 ppm in the spectrum demonstrates the complete removal of methyl-acrylate. Integration values match the theoretical values of the structure, and this is strong evidence for that the formation of G2.5 PAMAM dendron has taken place (Figure 4.6).

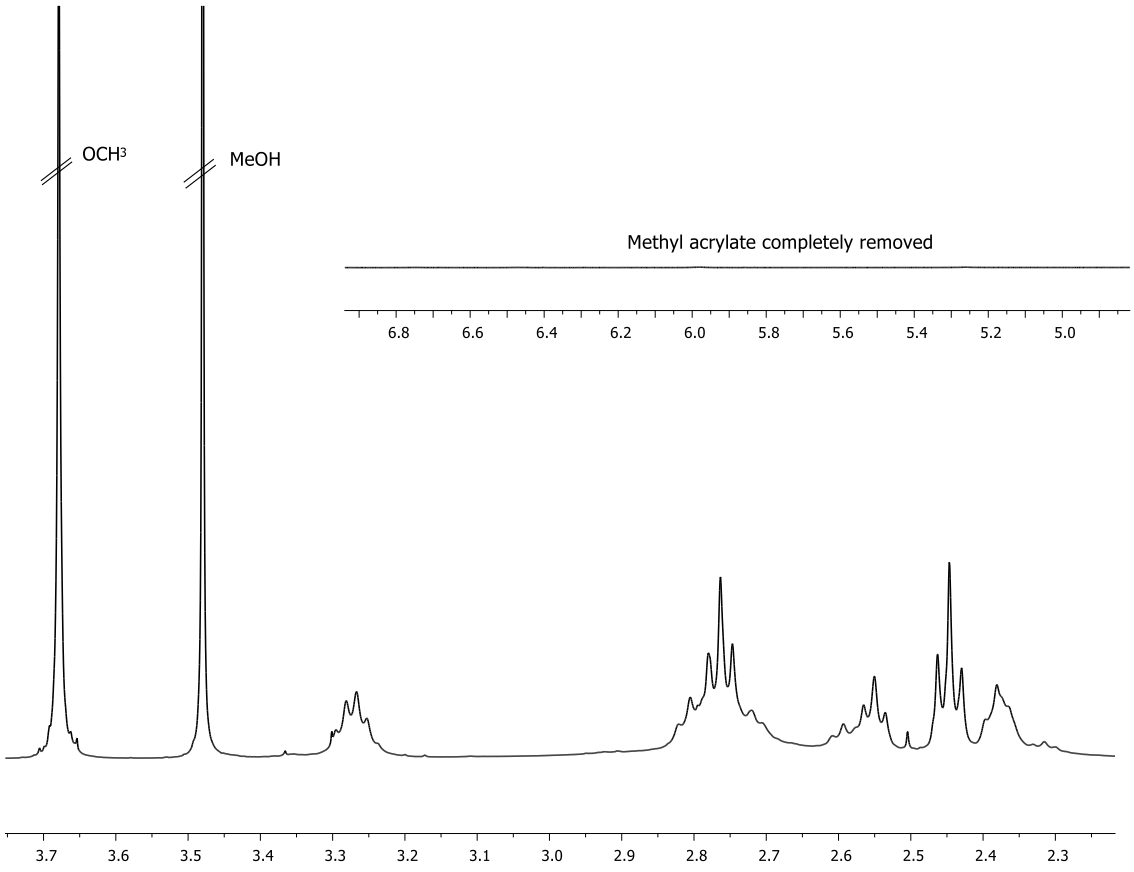

Figure 4.6 ^{1}H NMR of PAMAM dendron with eight ester end groups.

The ^{13}C NMR spectrum displays three different carbonyl peaks at 179.7 ppm, 173.1 ppm, and 172.3 ppm, from acid carbon, ester carbon and amide carbon respectively. The mass spectrometry spectrum of the G2.5 exhibits the peak due to $(M+H)^{+}$ at 1463, which suggests that the MALDI-TOF mass spectroscopy is extremely useful tool to investigate dendrimers. IR spectroscopy was the another tool applied to investigate the G2.5 dendron: the spectrum presented a noteworthy peak at approximately 1729 cm^{-1} for carbon carbonyl ester dendrons, and another peak at 1638 cm^{-1} for the amide carbonyl. The structure of a half generations PAMAM dendrimers with ester terminal groups are shown below (Figure 4.7).

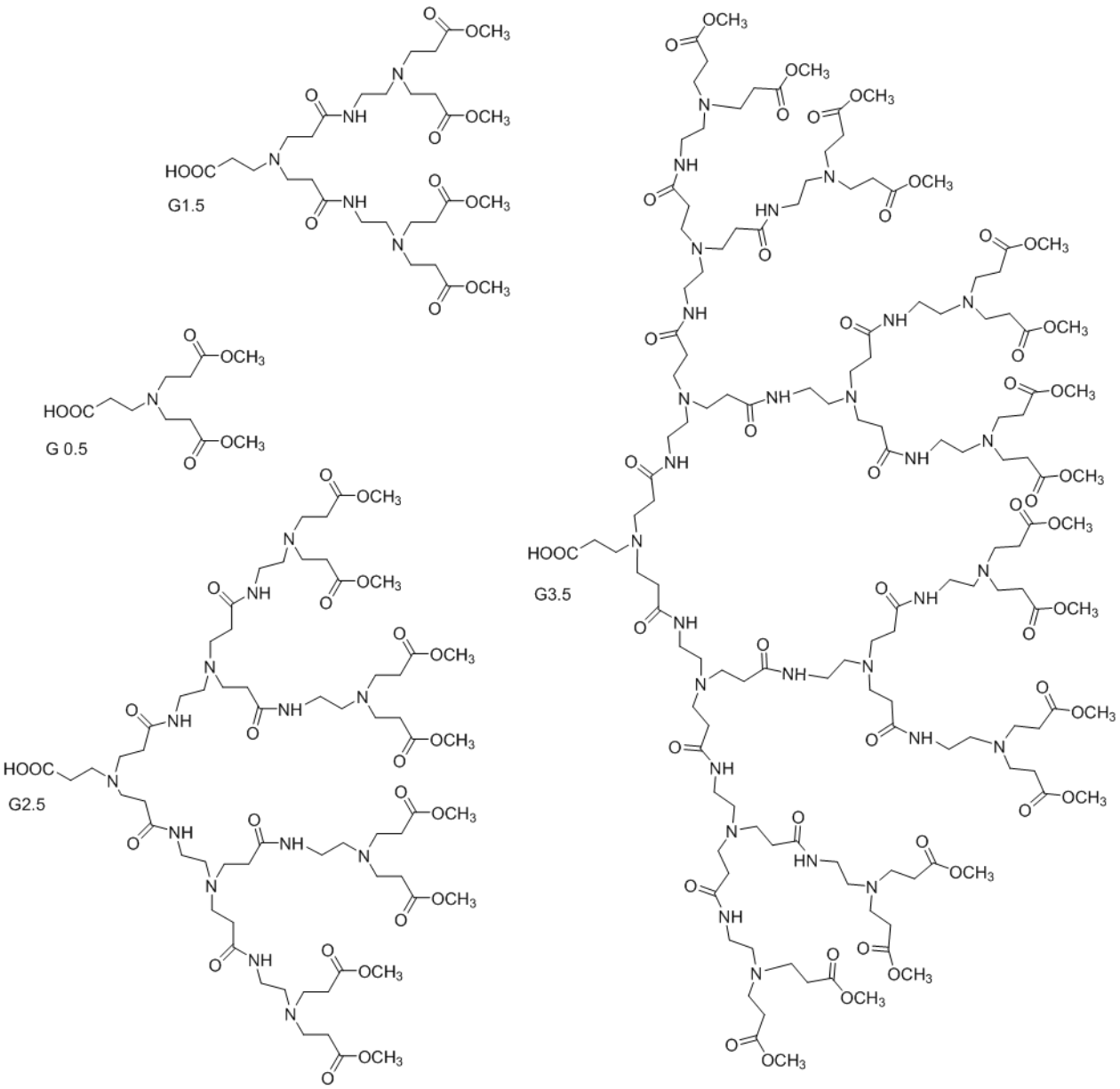

Figure 4.7. Half-generation PAMAM dendrons.

4.1.3 Synthesis of whole generations PAMAM dendrons

The whole generations PAMAM dendrons were synthesised by an amination reaction. The same procedure for synthesising full generation PAMAM dendrimers was followed to produce dendrons with amine-terminated groups Scheme 4.5. The period of reaction depended on the formed generation (from two to eight days).

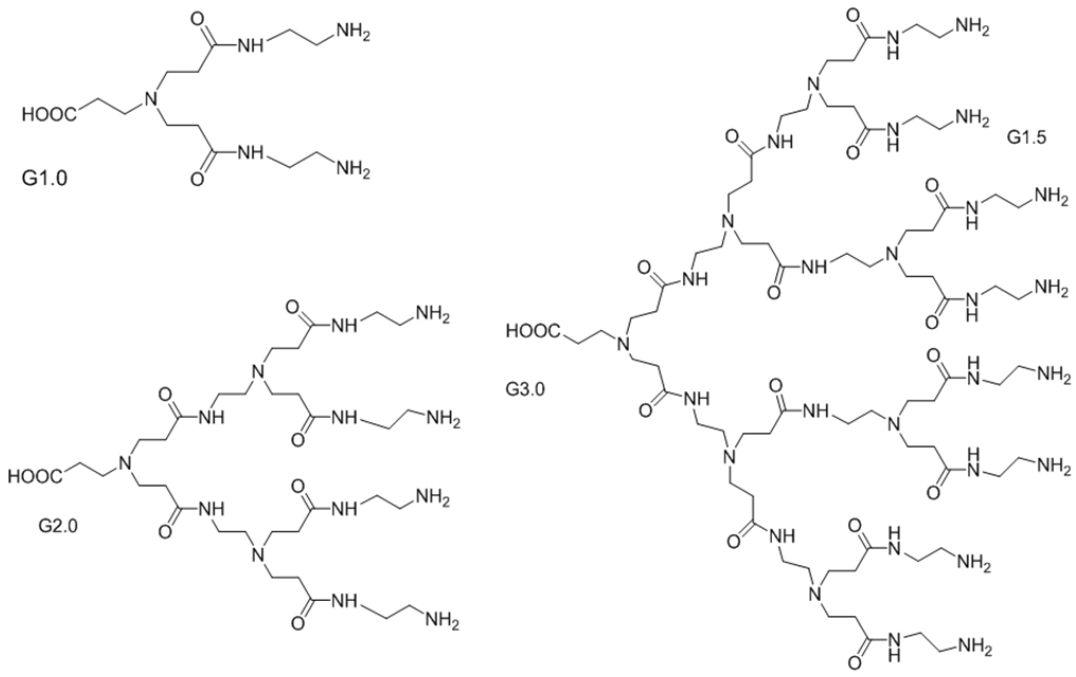

Figure 4.8. Whole -generation PAMAM dendrons.

4.1.4 Synthesis of G 1.0 amine-terminated PAMAM dendrons

The G1.0 PAMAM dendron with two amines was synthesised by dissolving the G0.5 in methanol. This was followed by the drop-wise addition of ethylene diamine (in excess) at 0˚C The reaction mixture was left to stir for 2 days. On completion, the excess EDA was removed using an azeotropic solution and rotary evaporation. The whole generation PAMAM dendron was formed as a dark honey oil.

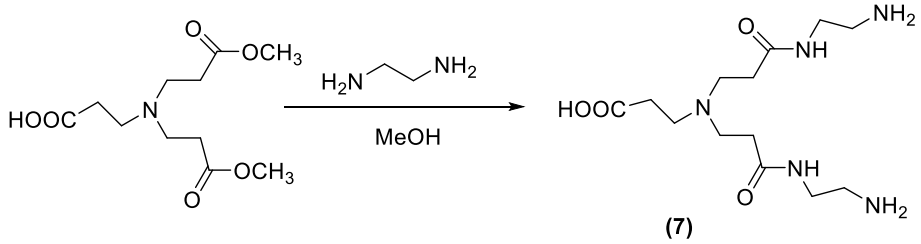

Scheme 4.9. synthesis of PAMAM dendron with two amine end groups (3).

The purification of amine dendrons is an important step after synthesis (the method is explained in purification of amine-terminated PAMAM dendrimer in chapter). It requires several washings in order to completely remove EDA and to avoid unfavourable side reactions. Structural defects in dendrons and unwanted by-products could result if any EDA, as shown in the next Scheme 4.10.

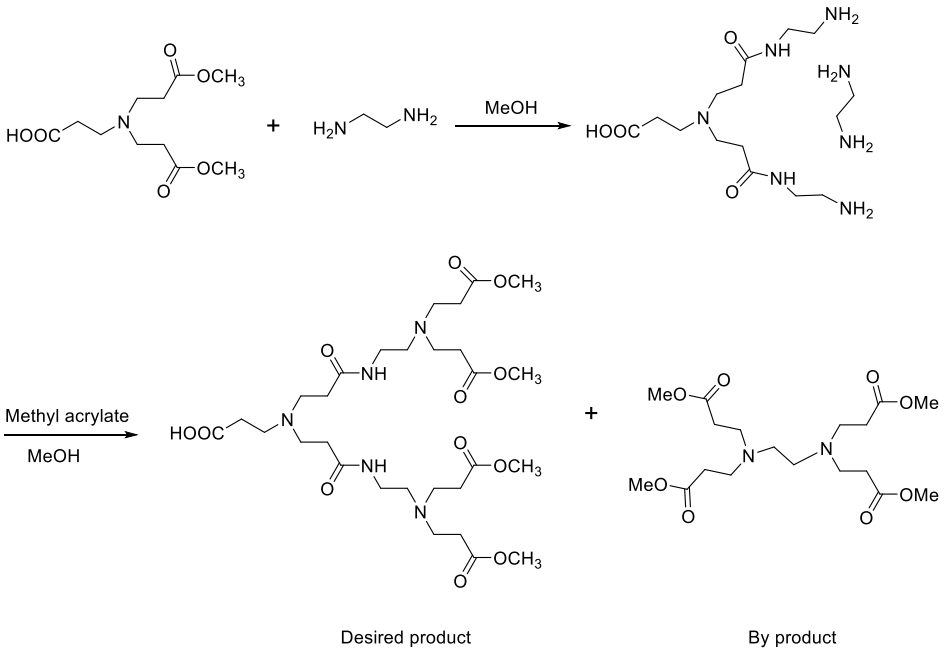

Scheme 4.10. Unfavourable side reaction resulted by products

The formation of G1.0 amine-terminated PAMAM dendrons was confirmed by several spectroscopy techniques. The ^{1}H NMR spectra presented all peaks as expected. The disappearance of the methoxy peak at 3.65 ppm suggests that there was formation of G1.0 dendrons terminal amine group as shown in Figure 4.1. Mass spectroscopy was a viable tool: the spectrum indicated the expected molecular ion peak (MH^{+}) at 662. On the other hand, a larger amine dendron with 4 amine groups (G2.0) showed two peaks corresponding to (MH^{+}) at 662, and (MK^{+}) at 813. The final analysis was made using FTIR spectroscopy. The amine terminal dendrons presented two characteristic peaks in spectra; the amide peak at 3220 cm^{-1} and amide carbonyl peak came at 1625 cm^{-1}.

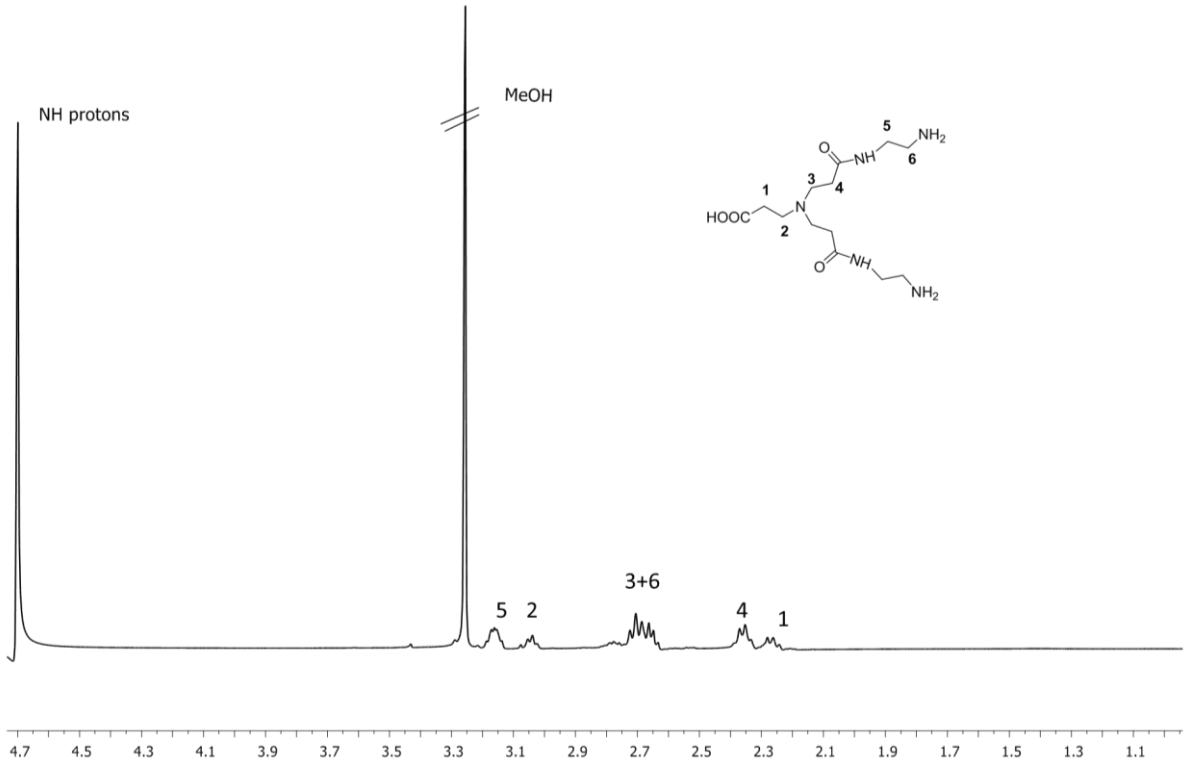

Figure 4.11. [1]HNMR of G1.0 PAMAM dendrimer with two amine groups (D2O,400MHz)

4.1.5 Synthesis of G 3.0 amine-terminated PAMAM dendrons

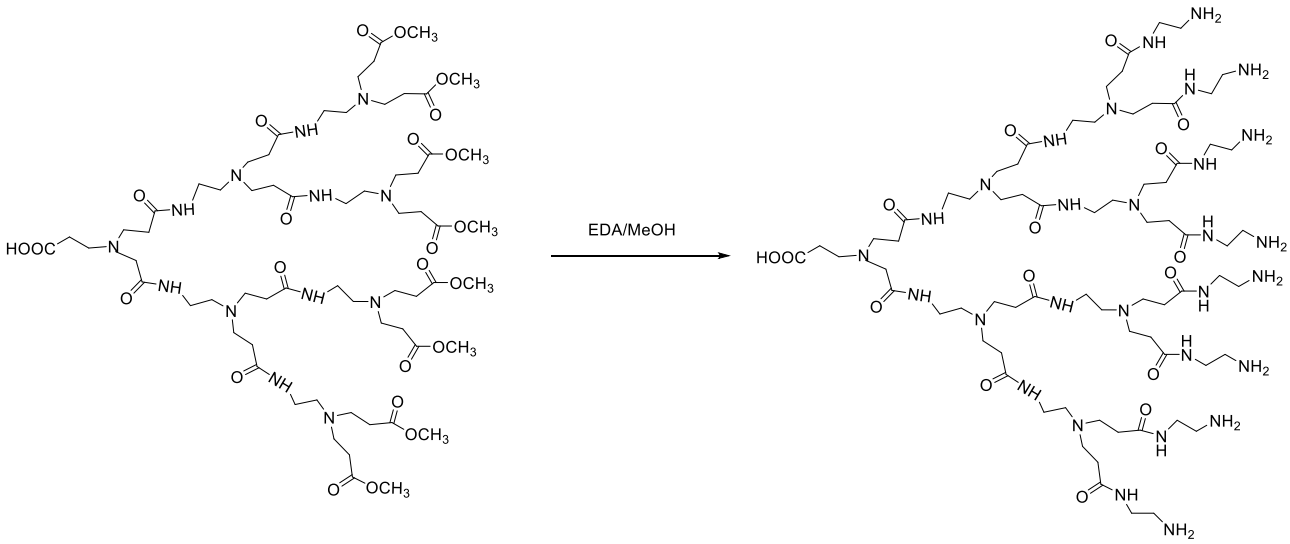

Scheme 4.12. Synthesis of PAMAM dendrons with eight amine end groups.

G2.5 PAMAM dendron was synthesised using an amination reaction as explained in the previous chapter (the synthesis of whole generation PAMAM dendrimers). The ^{1}H NMR spectrum of higher generation dendrons overlapped and was difficult to interpret because of the increasing number of protons associated with the increase of generation. But these spectra confirm our findings due to their chemical shift and their integration. Also, the methoxy peak is not visible, which confirms the successful production of the required compound.

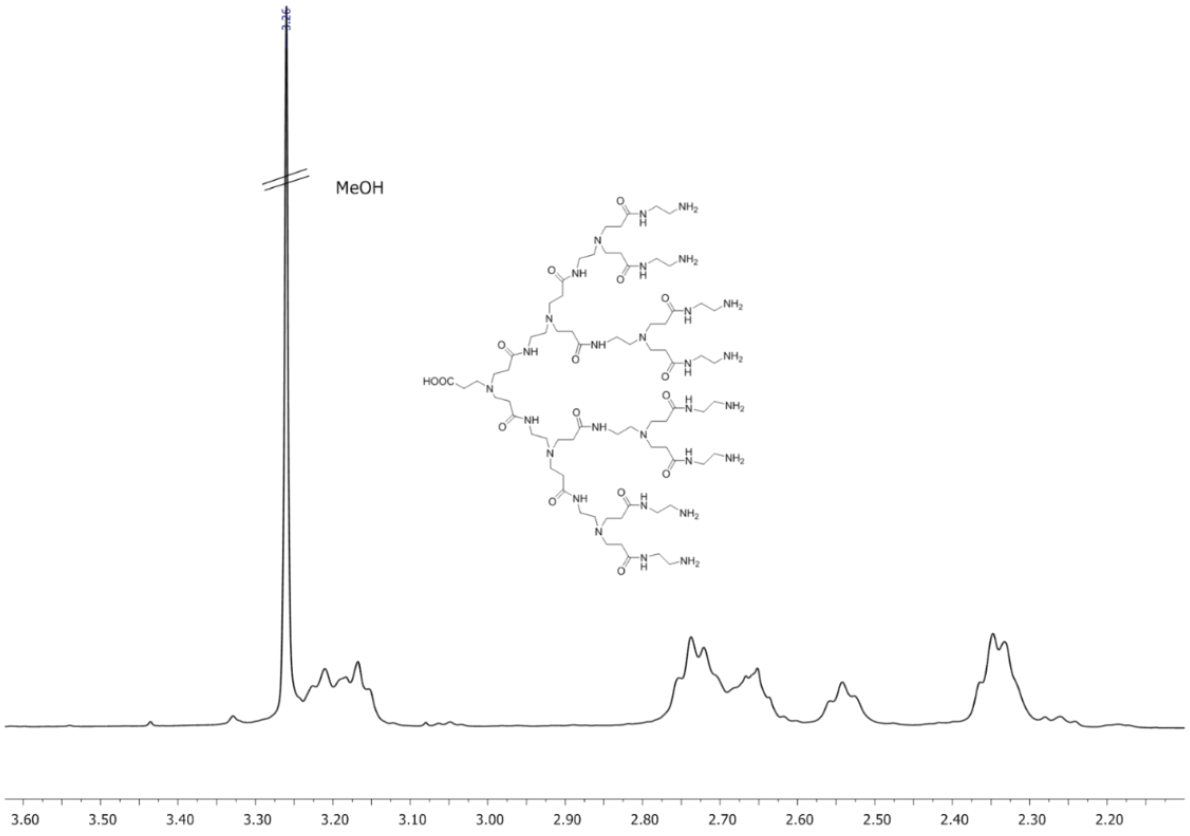

Figure 4.13. 1HNMR of G2.0 PAMAM dendrimer with eight amine groups (D2O,400MHz)

The ^{13}C NMR spectrum displays three carbonyl peaks at 179.1, 175.3, and 174.4ppm, from the acid core, exterior amides and interior amine respectively. Also, the mass spectrometry (MALDI-TOF-MS) spectrum of the G 3.0 (8 terminal amine groups) dendron displayed the molecular ion peak (MH^{+}) at 1688 and another peak for calcium salt at 1727 ($M+Ca^{+}$).

4.2 Photosensitizers (PSs) (porphyrin and phthalocyanine) for PDT

For PDT we need to obtain or synthesise a suitable photosensitizer. They are many kinds of light-absorbing chromophores used as photosensitizers, such as; porphyrin [63], chorine, heme, phthalocyanine, naphthalocyanine and acridine. These compounds are shown in Figuer 4.14. Photosensitizers often have low water solubility, which makes them hard to use therapeutically. Consequently, their use in vitro or in vivo is challenging. Our approach is to encapsulate them inside another molecule using non-covalent interactions, such as electrostatic, coordination, H-bonding, or π-πinteractions. In this work we will use coordination to self-assemble-dendrimer based PDT sensitizers.

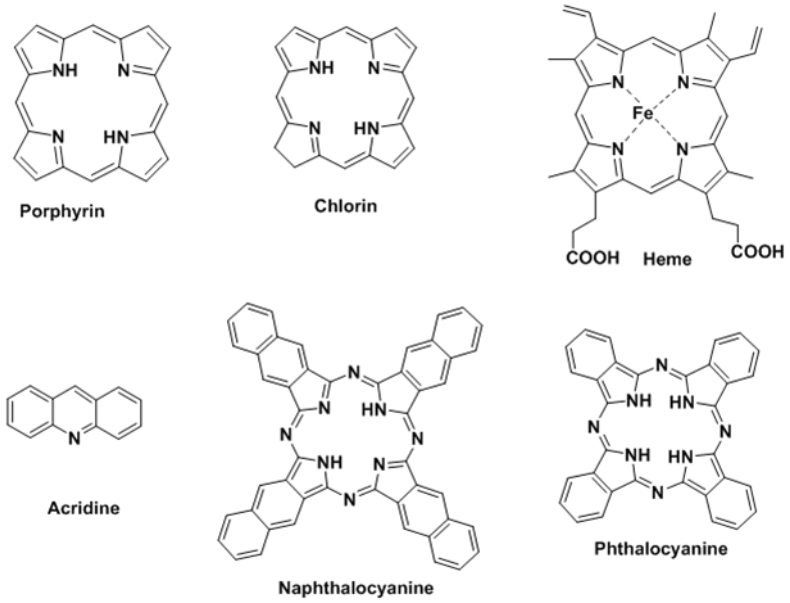

Figure 4.14. Structural representations of porphine, Chlorin, Heme, Acridine, Naphthalocyanine and Phthalocyanine

Porphyrins and phathlocynins were selected as our sensitizers, as they absorb light in the visible region of the spectrum or in the near infrared region. They are also easy to synthesis, have a high stability and they have an internal cavity which can accommodate a range of metal ions, including Sn(IV), which six-coordinate and two axial ligands [132]. Sn(IV) porphyrin is particularly suitable because of the oxophilic nature of Sn(IV), which facilitates complexes with carboxylate and aryloxide axial anions. Once tin has been inserted into the porphyrin or phthalocyanine, it can coordinate to the carboxylic core of our dendrons to form a large self-assembled photosensitizer.

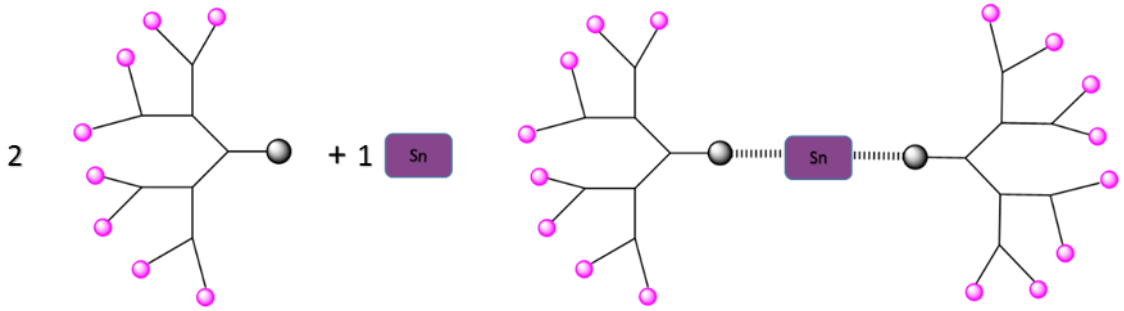

Figure 4.15. Representation of self-assembly between dendron core and Sn(IV) porphyrin

Ester terminated PAMAM dendrons will be used as these are biocompatible and are reported to be non-toxic in living organs [2]. Hydrolysis of esters by water at neutral pH is extremely slow. This is due to lone pair conjugation, which lowers the electrophilicity of the carbonyl carbon. In addition, water is a poor nucleophile. However, we have previously shown that esters at the periphery of large dendrimers can be hydrolysed faster as a result of an internal catalytic process [133]. This autocatalytic process involves the internal amid groups, which are capable of interacting with and stabilizing the charged tetrahedral intermediates. This stabilization results in a lowering of the activation energy and therefore a faster reaction (Scheme 4.16). If this auto catalytic process occurs for our dendrons, we will be able to avoid the use of acid or base catalysts, which could compromise the complex's stability. Therefore, the process of solubilising the complex will simply involve adding the ester terminated complex to a buffer solution and stirring until soluble. It's worth pointing out that it's not necessary at this (proof of principle) stage to hydrolyse all of the terminal esters, just enough of them to ensure sufficient solubility in water.

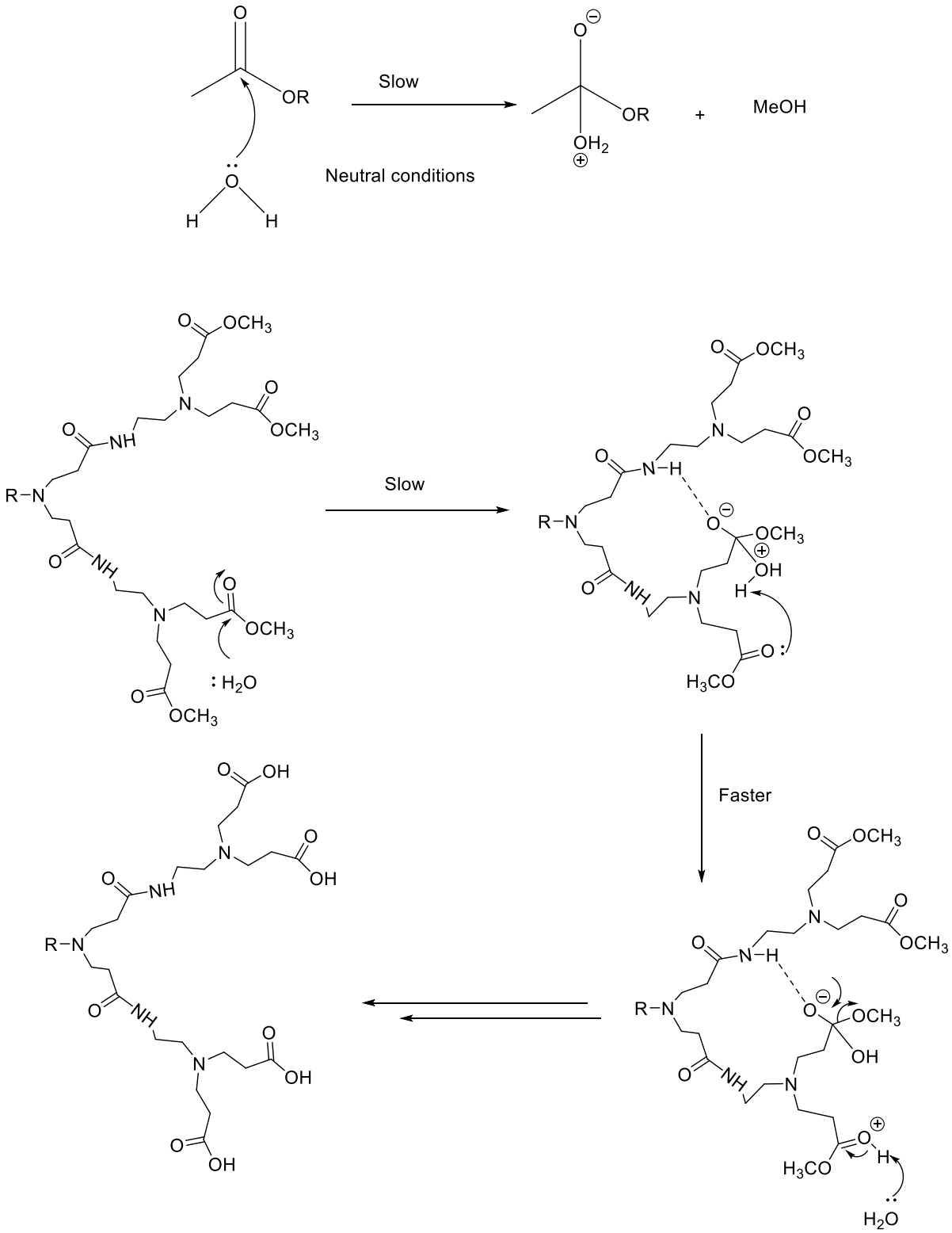

Scheme 4.16. The neutral hydrolysis reaction for polyester

4.2.1 Synthesis of dihydroxy tetra phenyl porphyrin tin (1V) [$Sn(OH)_2TPP$].

There is more than one method to synthesis Sn(IV) porphyrin, the most common and convenient method for the insertion of Sn(IV) was accomplished using the method described by Arnold et al [120,134] which generally produces the $SnTTP(Cl)_2$ which converts to the hydroxy derivative. Sn (IV) porphyrin was synthesized by refluxing tetra-phenyl porphyrin with excess $SnCl_2$ in pyridine for one hour. The temperature was reduced to 50 ^{0}C, ammonia was then added cautiously, and the solution stirred for one hour. Vacuum filtration was applied to get the precipitates, which was washed with water. However, the precipitates were contaminated with grey material. The crude products were washed with chloroform, which dissolved the Sn(IV) porphyrin. The mixture was filtered and the filtrate was dried over anhydrous sodium sulphate to remove water. The filtrate was concentrated and passed through a short neutral alumina column with activity V, using chloroform as eluent. Alumina is basic and contains OH groups, these will exchange for the Cl ligands in the $Sn(TPP)Cl_2$ complex, to give the $SnTPP(OH)_2$ complex. To make sure that the produce is pure, a recrystallization was carried out using chloroform and hexane.

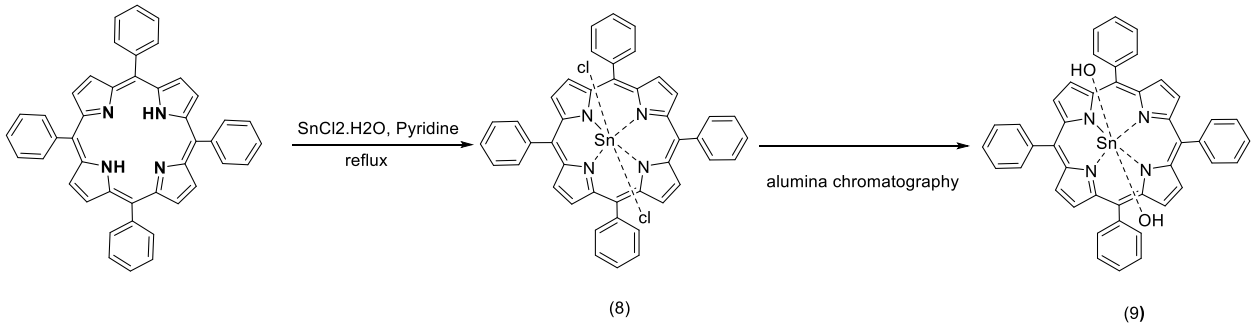

Scheme 4.17. leading to the synthesis of $Sn(OH)_2$

In ^{1}H NMR spectrum, the existence of axial hydroxyl groups should be visible appears as a broad signal ~ minus 7 ppm, as reported the literature [131,] However, in our spectra, this proton was not visible, possibly because of exchange with the solvent. Additional conformation of metalation is obtained because there are satalite peaks from the tin isotopes (^{117}Sn and ^{119}Sn (have I = 1/2, with a 7.6 and 8.6% abundance respectively). Figuer 4.18 shows the spectrum, which has a broad singlet at 9.16 ppm, attributed to the β-pyrrole protons which possess a sharp peak with the isotope satellite signals clearly visible. In addition, ^{1}H NMR the chemical shift is useful in distinguishing between the chloro or hydroxo ligands The spectrum also shows two

multiples around 8.39 and 7.80 ppm, corresponding to the ortho and meta protons on the phenyl ring.

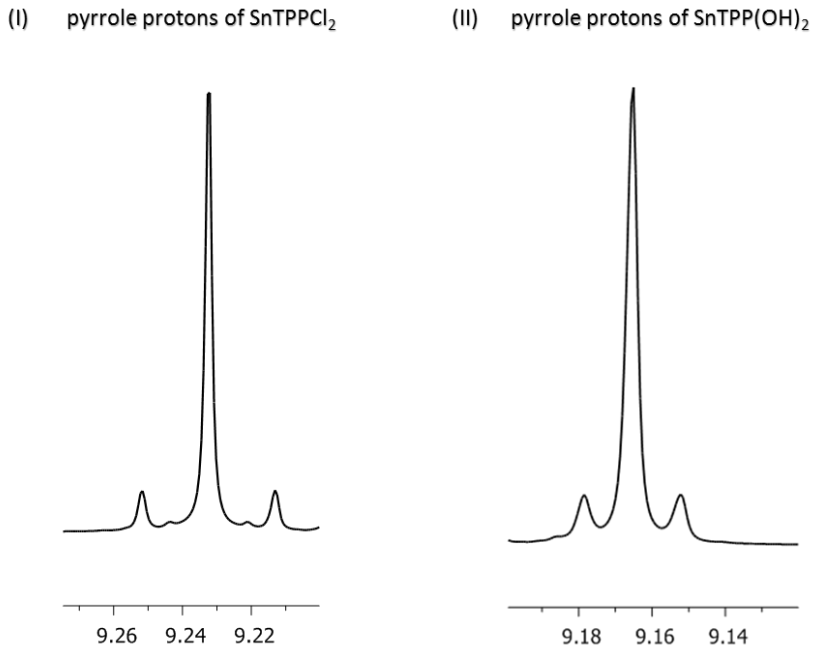

Figuer 4.18.^{1}H NMR spectrum showing peaks for (i) pyrrole protons with satellites for $SnTPPCl_2$ (8) and (ii) pyrrole protons with satellites $SnTPP(OH)_2$ (9)

Finally, absence of a peak from the strongly shielded NH protons at -2.72 ppm, conforms successful metalation and synthesis of $SnTPP(OH)_2$, Figure 4.19. The MALDITOF spectrum of $SnTPP(OH)_2$ showed a molecular ion peak [M-OH^+] at 749 which agreed with the values in the literature [132,134.] Further characterisation was carried out by UV-Vis spectroscopy. The spectrum had the distinctive absorption for the Soret band at 427, and two Q bands at 562, 601(Figure 4.20) which supports the successful synthesis of $Sn(OH)_2$ [135,136].

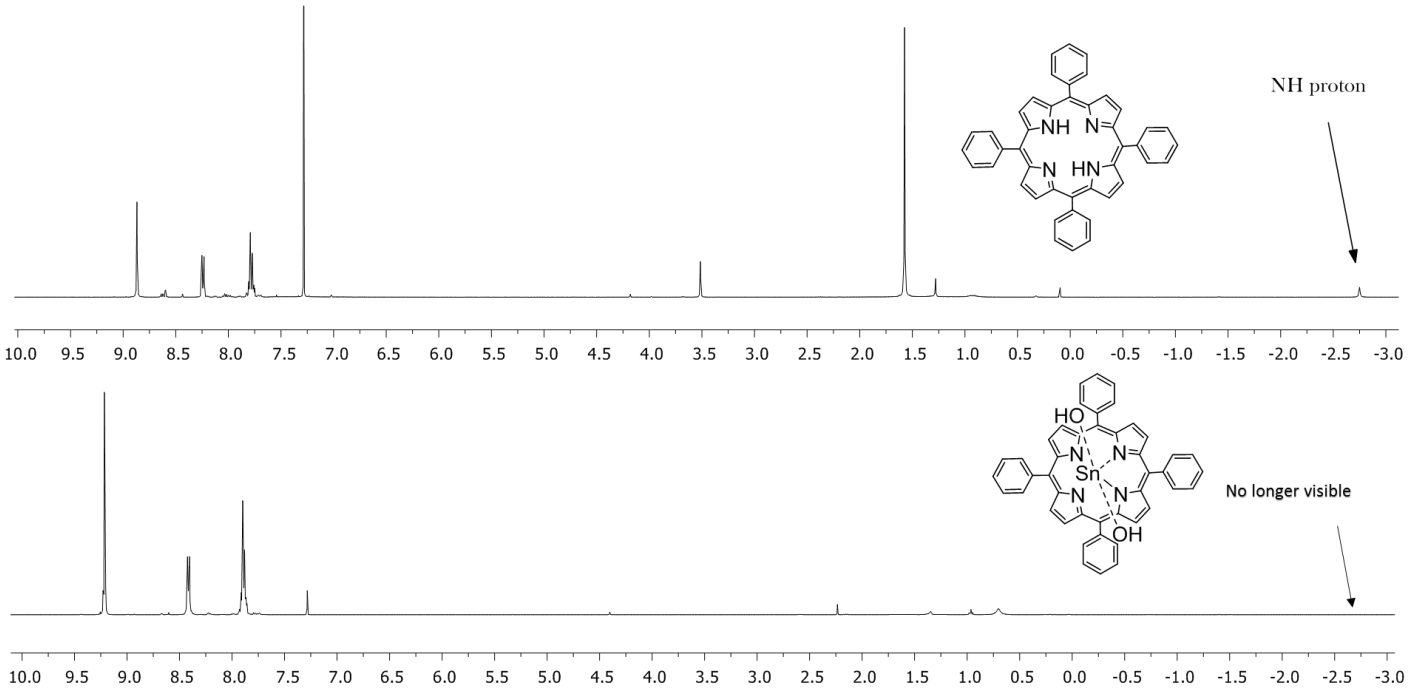

Figuer 4.19.^{1}H NMR spectrium of porphyrin(4) with $SnTPP(OH)_2$ (9) recorded in CDCl3

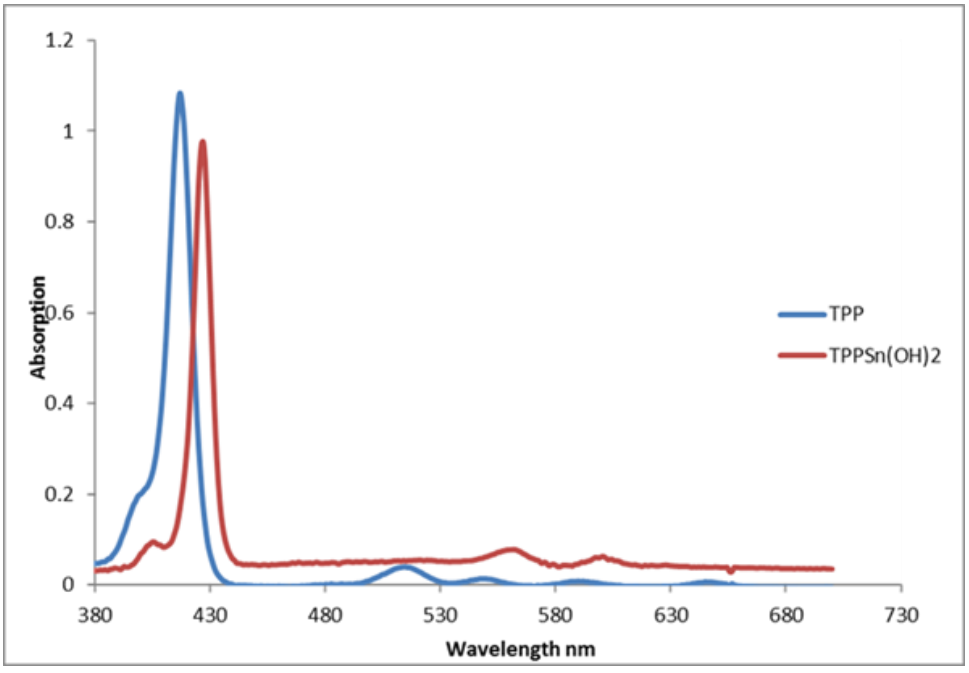

Figure 4.20. Comparison between absorption spectrum of TPP and $SnTPP(OH)_2$ recorded in CH_2Cl_2.

The IR is a very valuable tool which used to demonstrate the presence of the hydroxyl group that was not showed when used ^{1}HNMR (could be due to exchange with deuterium from $CDCl_3$ solvent). The spectrum of the compound shows two peaks at 3622, 3147 nm corresponding to the hydroxyl ligands.

Depending on the nature of the Sn(IV) TPP, which has a high affinity to oxygen donor ligands, and due to the oxophilic nature of the Sn(IV) centre, the complexes with carboxylate axial anions are easily obtained [132,137138]. Scheme (4.21) shows the presumed mechanism for the formation of tin-carboxylate complexes. So, for the structural confirmation of self-assembly of dendron with tin porphyrin, the Sn(IV) TPP treated with an excess of carboxylic acids.

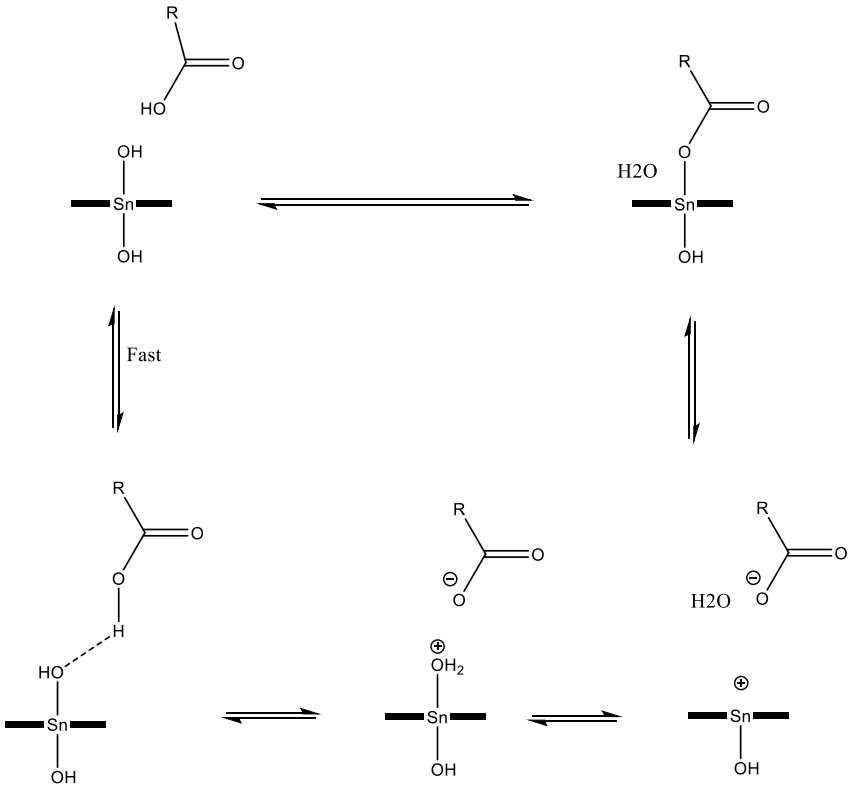

Scheme 4.21. Mechanism of formation for tin carboxylate complexes

4.3 Self-assembly of dendron with porphyrin as targeting system for Photodynamic therapy.

In order to accomplish photosentizier for PDT, self-assembly between the tin porphyrin and the dendron was achieved. It was obtained by adopting a supramolecular approach. In order to increase drug loading and the grantee 2:1 ratio between dendron and porphyrin, the coordination chemistry was applied and a strong intermolecular interaction metal coordination with dendrons was created. Attempts were made to synthesis self-assembly between tin porphyrin and ligand (carboxylic acid core of dendron). At first, self-assembly between tin porphyrin and G 0.5 PAMAM dendron was unsuccessful which may have been because the G 0.5 PAMAM dendron was hydrolysed prior to use (G 0.5 PAMAM dendron made of period). Following this, the second attempt with a G 0.5 PAMAM dendron was a success. Self-assembly between different half generations of PAMAM dendrons and the $Sn(OH)_2TPP$ were made by dissolving tin(IV) porphyrin and different generations of ester terminated PAMAM dendrons in chloroform for a period of 1 hour. The self-assembly with G1.5, G2.5 and G3.5 with Sn(IV) porphyrin were obtained by employing the same procedure. Porphyrin assemblies involving only Sn(IV)–O coordination are presented in Figure 4.22.

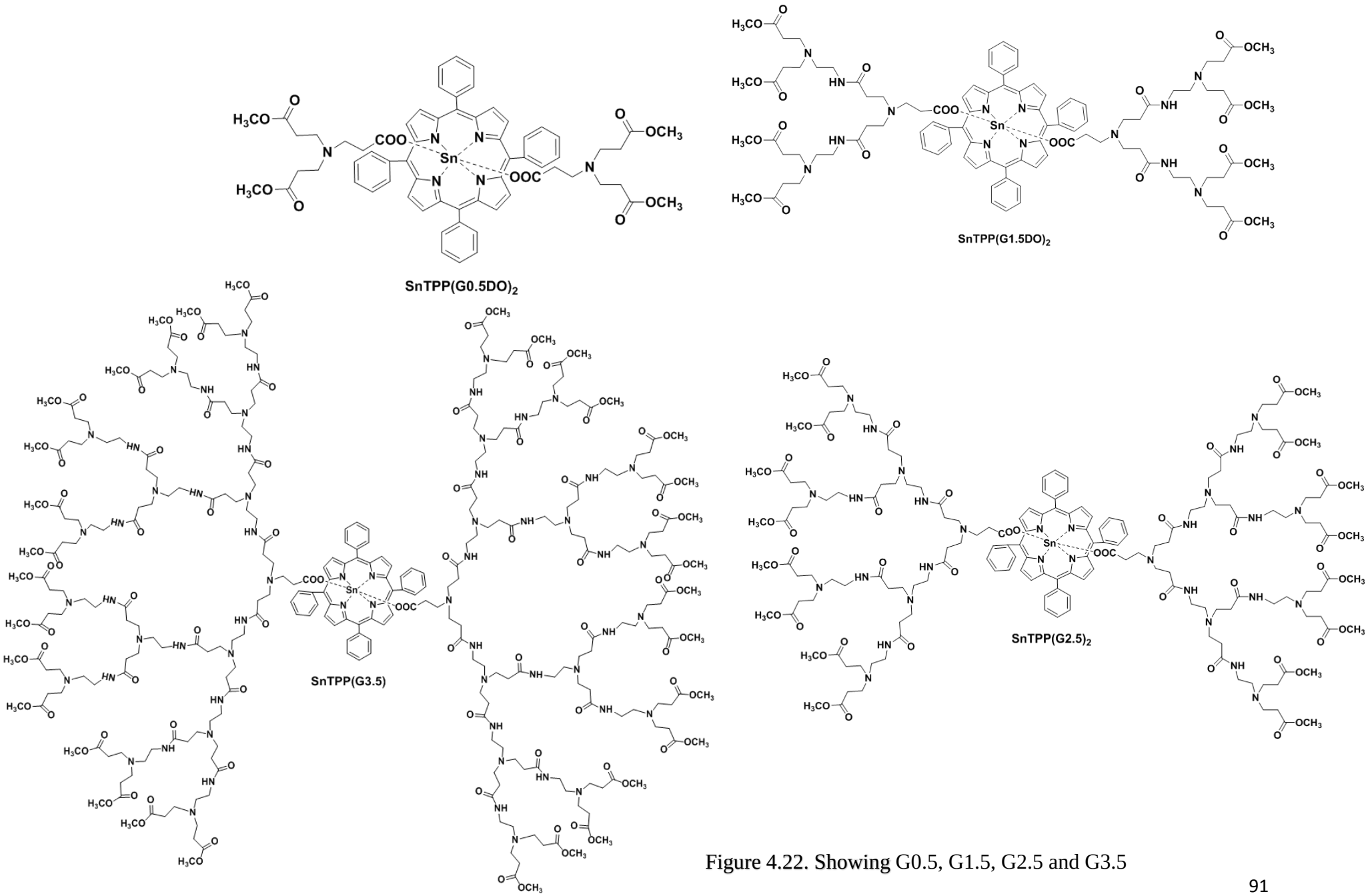

Figure 4.22. Showing G0.5, G1.5, G2.5 and G3.5 PAMAM dendrons

4.3.1 Self-assembly of dendron G-0.5 with $Sn(OH)_2TPP$

The porphyrin dendron complex was synthesised in a round bottom flask, 1 equivalent of dihydroxy tetraphenylporphyrin) tin(IV) and 2 equivalents of dendron G-0.5 were dissolved in 5 mL $CHCl_3$. The reaction mixture was stirred for an hour, followed by passing the reaction mixture through a small plug of anhydrous sodium sulphate so as to remove the water. Next, the solvent was removed via a rotary evaporator and a purple sticky compound was obtained. The process of forming the self-assembled complex **10** [$SnTPP(G0.5DO)_2$] is shown below in Scheme 4.23.

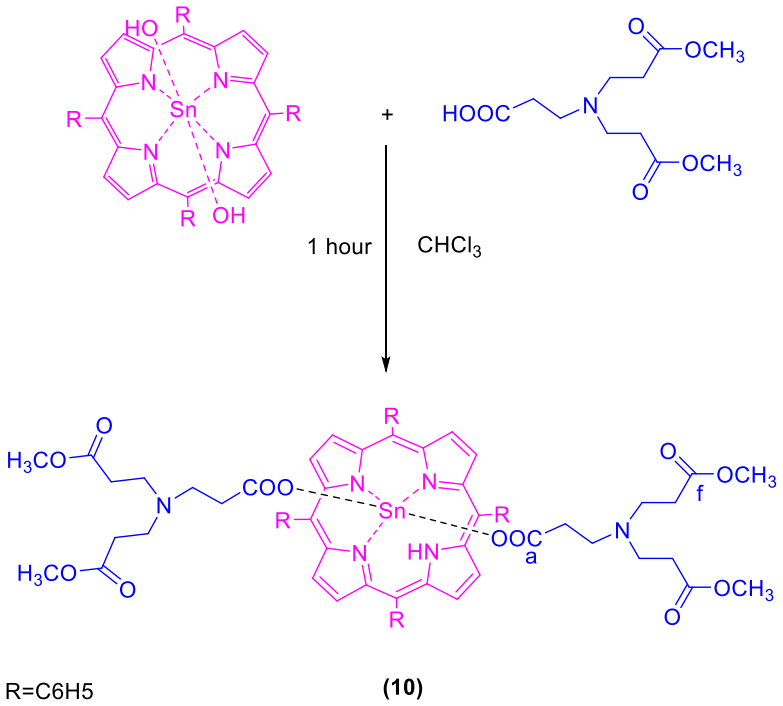

Scheme 4.23. of formation of [$SnTPP(G0.5DO)_2$] complex (10)

As stated above, a selection of $SnTPP(OH)_2$ was used for the self-assembled complex due to the fact that tin metal can be easily inserted in the porphyrin, while the oxophilic nature of tin (IV) helps to bond carboxylic acid in the dendron core and the porphyrin. In addition, TPPSn $(OH)_2$ has zero solubility in water. The aqueous solubility of $SnTPP(OH)_2$ complex was compared with the self-assembled dendron-tin porphyrin complexes $SnTPP(G)_2$. $SnTPP(OH)_2$ was completely insoluble, whilst the smallest self-assembled dendron $SnTPP(G0.5)_2$ was only sparingly soluble. However, the three biggest dendrons $SnTPP(G1.5)_2$ - $SnTPP(G3.5)_2$ offered some solubility. Within this series it was evident that larger the Dendron, then the better the

solubility. The UV spectrum of the self-assembled SnTPP(G2.5)$_2$ is presented in Figure 4.24 and has a maximum concentration of 3.0x10^{-6} M. Additional characterisation was performed by employing FTIR spectroscopy. The spectra displayed peaks at 1656-1592 cm^{-1} and 1439-1463 cm^{-1} which confirmed the binding of carboxylate ligands to tin atoms. Further evidence was provided from the UV-Vis spectrum which displayed a small shift of B band from 427 to 424 nm utilising chloroform as a solvent. The UV-Vis spectrum of SnTPP G2.5)$_2$ is used here as an example.

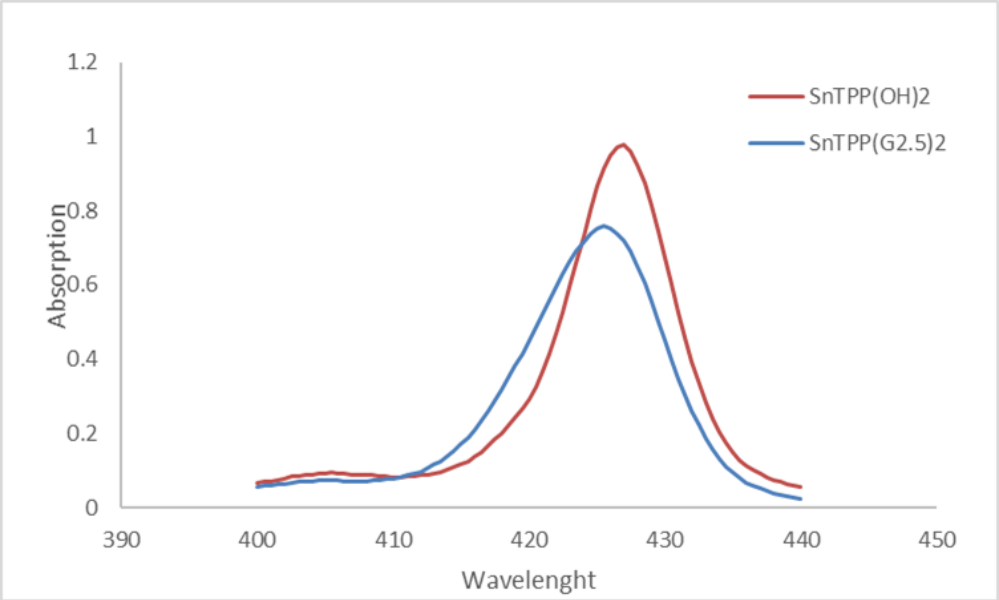

Figuer 4.24. UV-Vis spectrum of TPPSn(OH)$_2$ in CH_2Cl_2 and sthe uv spectrum of SnTPP(G2.5)$_2$ recorded in water.

Preliminary characterisation of SnTPP(G0.5)$_2$ was obtained via NMR spectroscopy using $CDCl_3$ as solvent. The analysis carried out by ^{1}H NMR spectroscopy contained a large singlet at 3.67 ppm from the terminal methoxy hydrogens of ester group PAMAM dendron (in spectra 1, Figure 4.25) that was integrated as twelve protons, which confirmed the existence of the two axial dendron ligands in the complex. Furthermore, the spectra revealed that the methylene protons next to the core had moved up field (spectra 2, Figure 4.25), (from 2.21ppm in dendron to -0.76 ppm in the complex) as they were now located in the porphyrin's shielded region. The results of the experiment therefore confirmed that SnTPP(G0.5)$_2$ was successfully synthesised.

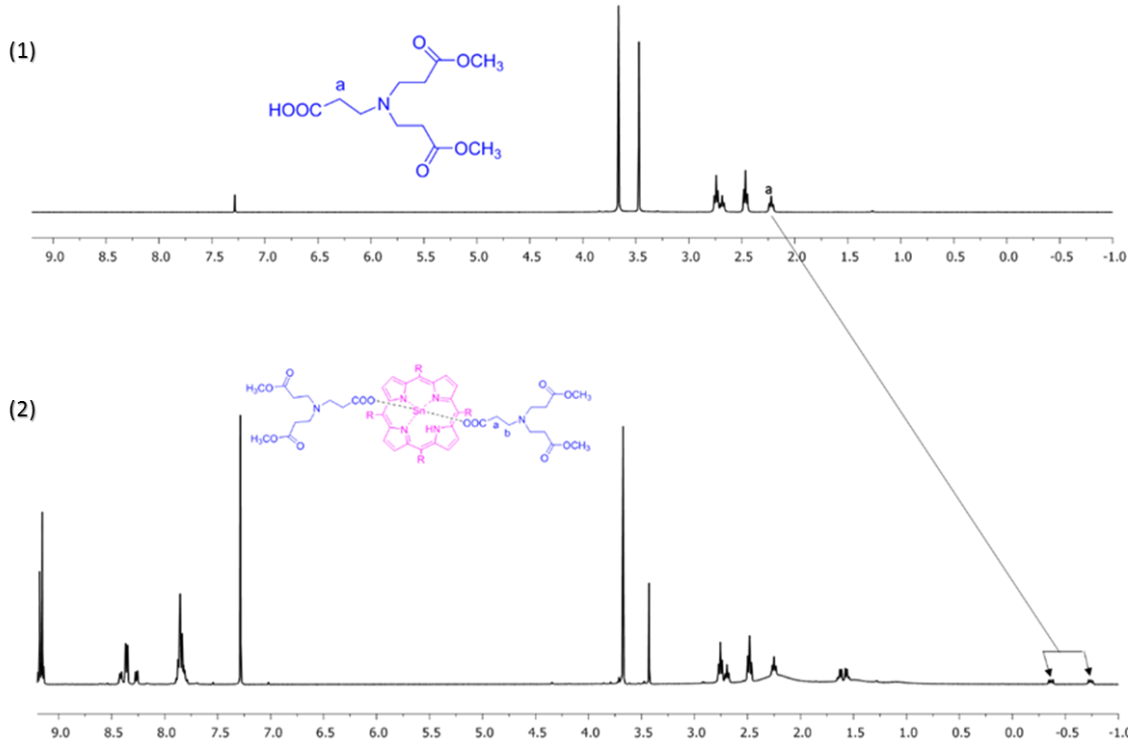

Figure 4.25. 1H NMR spectrums of G0.5 (1) and complex of SnTPP (G 0.5)2 (clear up field shift of proton shown by arrows) in CDCl3

Further confirmation of the self-assembled structure was carried out via ^{13}C NMR spectroscopy. A single carbonyl peak in the spectrum of G0.5 dendron at 179.29 ppm, which comes from the acid carbonyl group, was shifted to 168.35ppm in the complex, which is shown in spectra (4) Figure 4.26. In addition, instead of the expected single peak within the carbonyl region of the SnTPP(G0.5)$_2$ spectrum, two peaks are now visible, Figure 4.26, spectra (4). This is due to slow rotation, which results in slightly different conformers being present, as shown schematically in Scheme 4.11. However, when the NMR was recorded at 50°C, only one peak could be seen, confirming that conformational motion had speeded up, and only an average structure recorded by NMR; endorsing the existence of slow conformational motion at room temperature Figure 4.27.

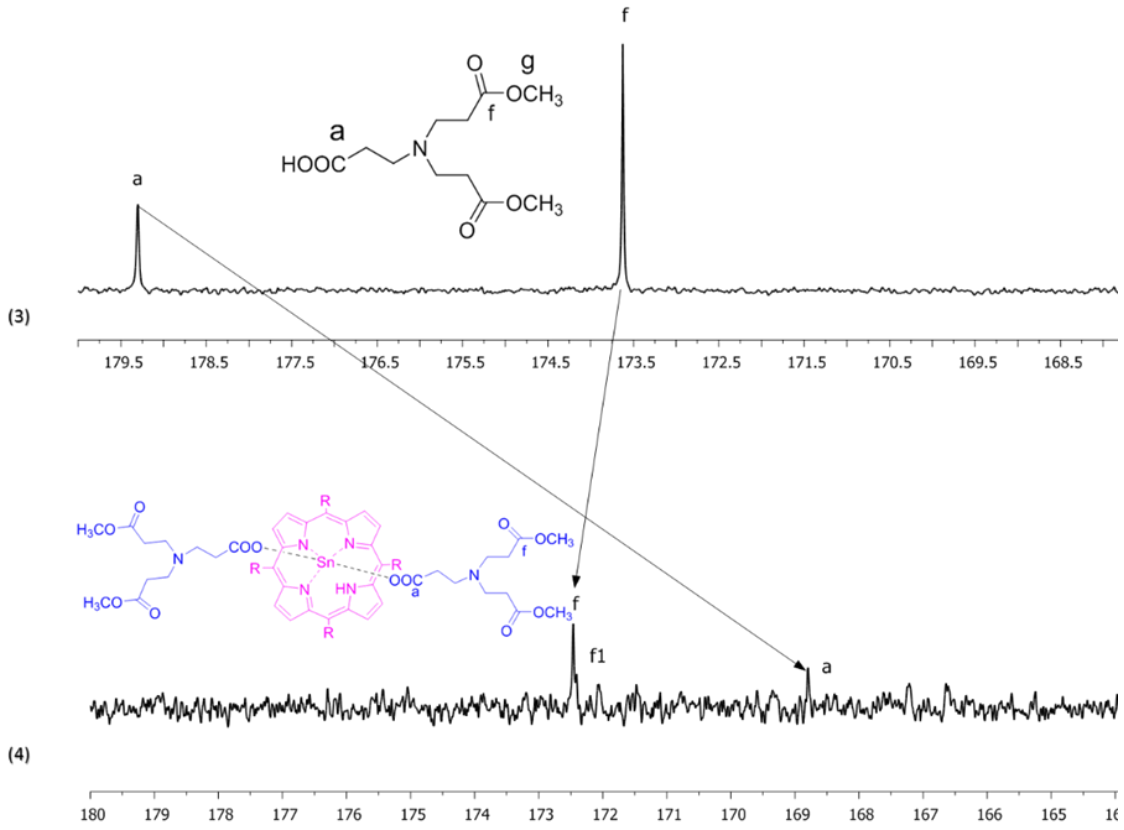

Figure 4.26. Changes in ^{13}C spectrum of G0.5 dendron before (3) and after (4) self-assembly of dendron G-0.5 with $Sn(OH)_2TPP$

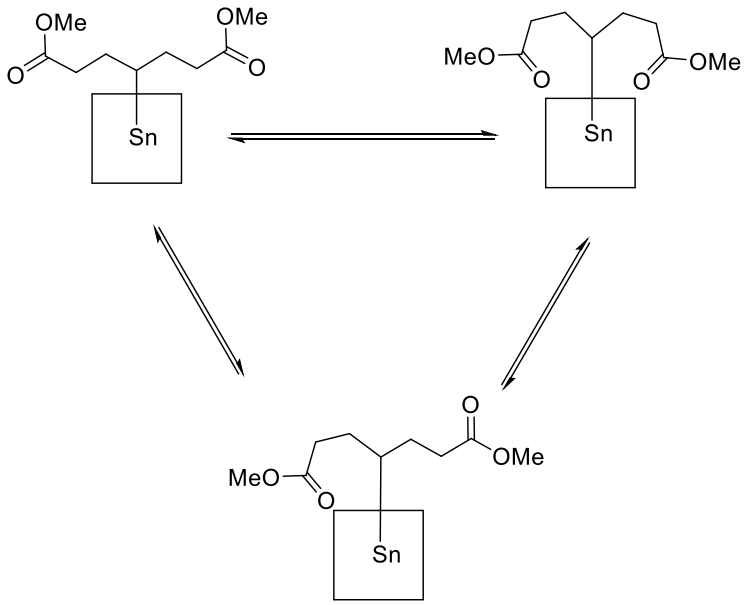

Scheme 4.27. Some of the dynamic conformations for the terminal ester carbonyls in $SnTPP(G0.5DO)_2$

Mass spectroscopy (MALDI-TOF-MS) was employed to further analyse the compound. However, the spectra failed to display molecular ion for the $(M\text{-}L_2)^+$ complex, with two ligands. It only revealed an molecular ion that corresponded to the species with a single ligand attached; $(M\text{-}L)^+$ at 991. Although this was surprising (as the NMR data confirmed two ligands were attached), it turns out that this is not uncommon. Studying the literature reveals that the majority of reported tin complexes do not have a molecular ion for the $(M\text{-}L_2)$ species, with most only showing a molecular ion for species with a single ligand attached; $(M\text{-}L)^+$. This was supported by studies (carried out by Kuljit Dyal) on the simpler complex, diacetoxo(5,10,15,20-tetraphenylporphyrin) tin(IV). As with our complex, the mass spectrum only showed peaks for the species with a single ligand attached; $(M\text{-}L)^{+\cdot}$ However, the X-Ray of the crystal structure clearly showed that two ligands were attached (Figure 4.28).

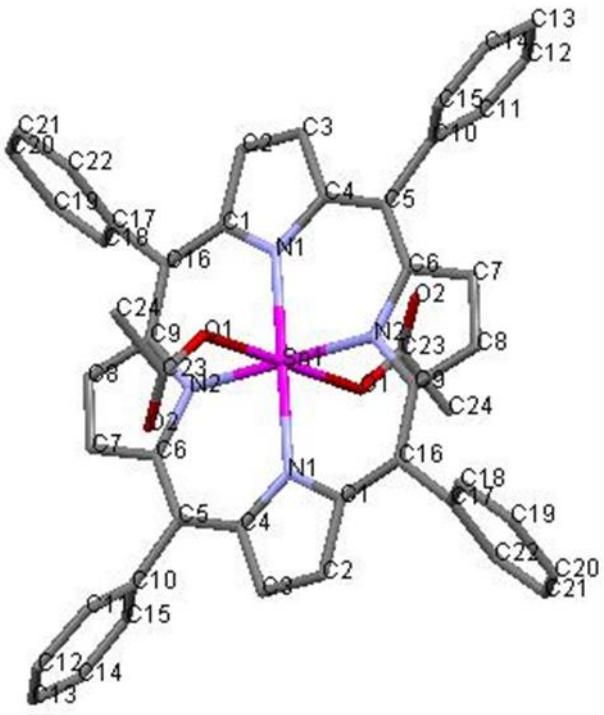

Figure 4.28. Crystal structure of diacetoxo(5,10,15,20-tetraphenylporphyrin) tin(IV)

Therefore, taking all of the data into account, we can clearly say that all compounds and complexes have been successfully synthesised. The molecular weights of complexes and key ^{13}C NMR data are shown Table 4.1.

Compound	Obtained molecular weight(M-L) gmol-1	Expect molecular weight gmol-1	C=O δ ppm
G0.5 PAMAM dendon	262	262	179.1
$TPPSn(G0.5DO)_2$	991	1252	168.35
$TPPSn(G1.5DO)_2$	1392	2051	168.7
$TPPSn(G2.5DO)_2$	2194	3655	168.9
$TPPSn(G3.5DO)_2$	3853(3793 CAL)	6853	167.7

Table 4.1. Molecular weights for compound (6), self-assembled complexes of different generation dendrons (10) and carbonyl chemical shift.

The self-assembled dendron-tin porphyrin complexes (Pporphyrin dendrimers) which was applied in this study have a maximum wavelength (Q-band) of about 599 nm which has limited tissue penetration effectiveness [138]. Consequently, tin phthalocyanine was selected for PDT, since it absorbs light in the higher wavelength area at 750 nm. As such, there is a strong possibility that the photosentizers (self-assembled dendron-tin phthalocyanine complexes) can be applied for PDT. This will be discussed in the next section.

4.4 Self-assembly between PAMAM dendrons terminal ester group and dichloride(phthalocyanine)tin(IV).

Phthalocyanines (Pcs) are similar to porphyrins in their photophysical and photochemical behaviour. Phthalocyanines have been widely studied as photosensitizers for PDT of cancer. Advantages such as their selectivity for cancerous cell and ability to yield reactive oxygen species are important features for successful PDT. Metallophthalocyanines can be obtained by hosting non-transition metal ions into the cavity of the phthalocyanines. They like porphyrins, metal provide the opportunity introducing two ligands(dendrons) at the axial positions to generate large complexes, with increased aqueous solubility [47].

Pcs have intense absorption in 650-750 nm (a long wavelengths), this is an important property to deliver the light (deep penetrate) to deep target tissue which is not easily accessible and this is the main reason to use Pcs in this work. Self-assembled complexes of G-0.5, G-1.5, G2.5 and G-3.5 with dihydroxy(5,10,15,20-tetraphenylporphyrin) tin(IV) are shown in Figure 4.29.

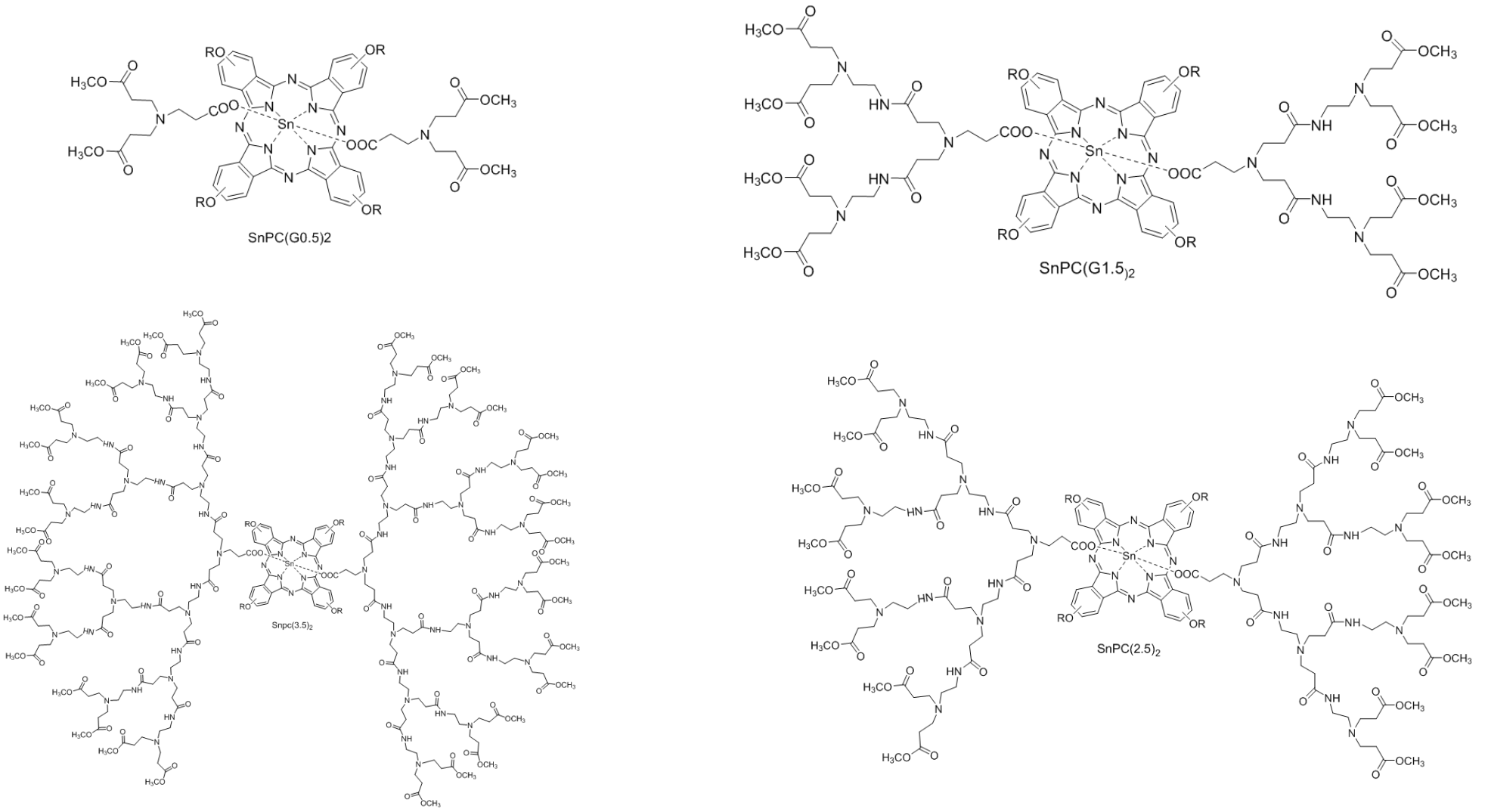

Figure 4.29 Self-assembled complexes of G-0.5, G-1.5, G2.5 and G-3.5 with dihydroxy (5,10,15,20-tetraphenylporphyrin) tin (IV).

4.4.1 Synthesis of 3-penyloxy phthalonitrile

Scheme (4.30) provides the synthetic pathways for the dichloride(Phthalocyanato)tin(IV) [115]. It is prepared by employing 3-penyloxy phthalonitrile as the start material. 3-penyloxy phthalonitrile as can be synthesised according to literature [140] from the reaction of 3-nitrophthalonitrile and n-pentanol in DMSO and anhydrous potassium carbonate. The reaction mixture was left to reflux for 4 hours under nitrogen. Once it had cooled, water was added and the reaction mixture was then vigorously stirred for an extra 10 minutes. The mixture was then filtered for collection and washed with water. The crude product was purified on a silica column with chloromethane as an eluent.

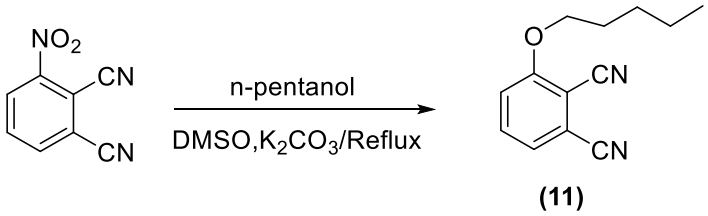

(11)

Scheme 4.30. Synthesis of 3-penyloxy phthalonitrile

The ^{1}H NMR spectrum of 3-penyloxy phthalonitrile revealed the presence of two triplets at 0.69 and 4.14, ppm which corresponds to methyl protons of n-pentanol and methelne protons next to oxygen and multiples at 1.54-1.35and 1.89-1.92 ppm corresponds to methelne protons of n-pentanol protons. In addition, there are three doublets at 7.65-7.62, 7.30-7.34 and 7.25-7.22 ppm which relates to phenyl protons. Mass spectroscopy was utilised and the spectrum revealed a molecular ion peak $(MH)^{+}$ at 215. Further characterisation to support successful synthesis of 3-penyloxy -1,2-dicyanobenzene was carried out by adopting the FTIR technique, while the IR absorption of the compound was revealed at band 2237 cm^{-1} for the vibration of cyano groups.

4.4.2 Synthesis of Tin(IV)dichlorophthalocyanine

The complex was synthesised by the employing the following procedure The synthesis began by dissolving the 3-Pentyloxy phthalonitrile in 1-CNP (1-chloronaphthalene). The reaction mixture was then stirred under nitrogen followed by the addition of tin (II) chloride and the mixture heated at 250 ^{o}C for a period of five hours. The reaction mixture was cooled at room temperature and was then purified by utilising a short column of silica and hexane as eluent to remove excess 1-CNP. The column was eluted with 4:1 dichloromethane/methanol. There were

three fractions; the second fraction contained the product Tin(IV) dichlorophthalocyanine **12** in 57% yield.

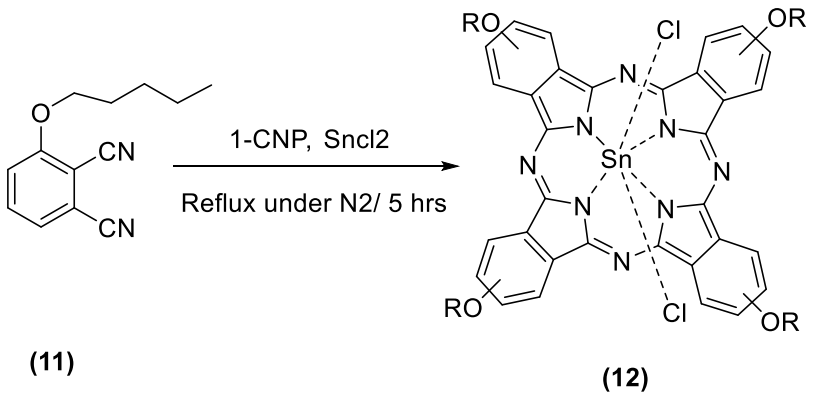

(11) **(12)**

Scheme 4.31. Synthesis of tin phthalocyanine

The structure of tin phthalocyanine was confirmed by ^{1}H NMR, MS, UV–vis, IR spectroscopy. MS (ESI) for the complex indicated a molecular ion with mass 1008, corresponding to the tin phthlocycnine minus one of its ligands $[M\text{-}Cl]^{+}$. The ^{1}H NMR spectrum of compound presented three multiplets at 9.34-9.16, 8.33-8.21, 7.88-7.80 from the phthalocyanine ring protons, which integrated as twelve protons. The peaks at 4.98-4.75 ,2.47-2.33, 1.87-1.53 and 1.23-1.01 were attributed to the n-pentyl protons of the side group and these integrated correctly as forty-four protons. The IR spectrum confirmed the conversion of 3-Pentyloxy phthalonitrile (start material) to tin phthalocyanine, as the peak from the nitrile stretch at 2237 cm^{-1} in the starting material, was no longer visible. The axial substituents ($Sn–Cl_2$) were visible as a peak at 875 cm^{-1}. Furthermore, the UV–vis spectrum showed the characteristic peak in the Q band at 751 and Soret band at 333 nm. All of the data indicates that the tin phthalocyanine synthesis had been successful synthesis. Following this, the next step would involve the self-assembling of tin phthalocyanin with dendrons as a photosentizier for PDT.

4.4.3 Self-assembly of tin(phthalocyanato)dichloride with G.0.5 PAMAM dendron.

The preparation of self-assembled complexes between tin Phthalocyanine and different generations of the PAMAM dendrons terminal ester groups would be carried out using an

identical procedure to that described for the self-assembly of tin porphyrin system. A self-assembled complex between $SnPCCl_2$ and G- 0.5 PAMAM dendron ester terminal group was prepared by taking tin phthalocynin (1 equivalent), G0.5 dendron (2 equivalent) and mixing together in chloroform. The mixture was stirred at room temperature for an hour and passed through a small plug of anhydrous Na_2SO_4. The solvent was removed by rotary evaporation to produce the complex **13** as a green sticky solid (Scheme 4.32).

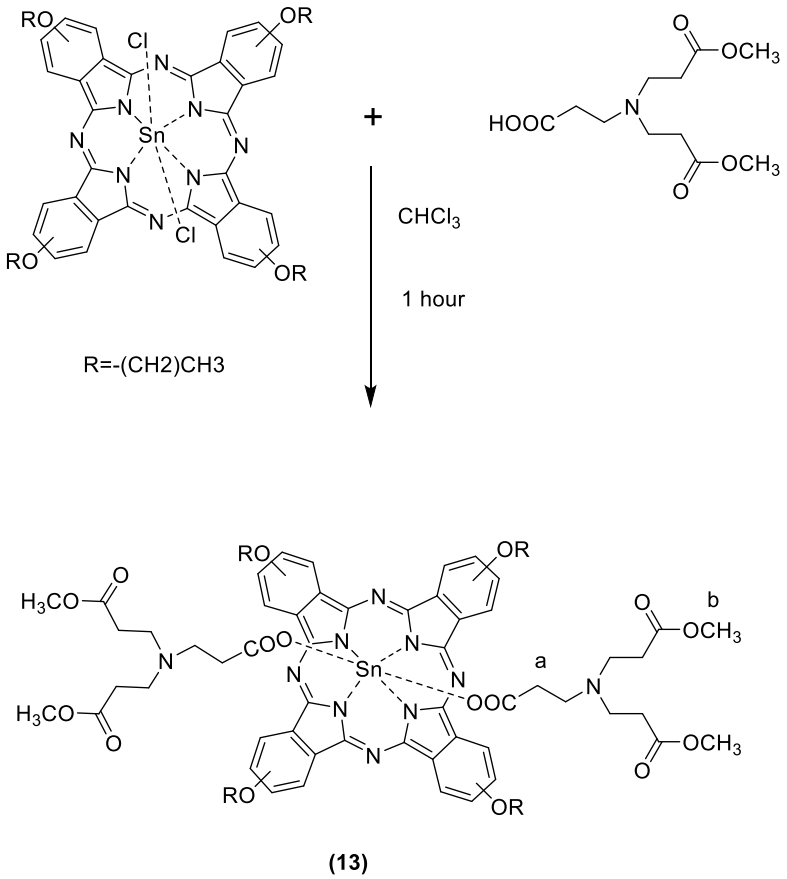

Scheme 4.32. self-assembly complex between tin Phthalocynin and G-0.5 dendron (13)

The characterisation of the SnPC $(G0.5)_2$ began with a ^1H NMR spectroscopy. The spectrum contains various distinctive peaks, including a singlet at 3.68 ppm. This integrated for 12 protons and corresponds to the methoxy protons on the terminal ester. A singlet at -0.2 was assigned as the methylene protons next to core. These protons resonate at this up field position as they are positioned within the shielding area of phthalocynin, which gives good evidence for proposed structure **13**. The other important peaks include multiplets for the aromatic groups, at 7.71-7. 89 ppm, 8.21-8.30 ppm, and 9.14-9.35 ppm, which integrate for a total of 12 protons (Figure 4.33).

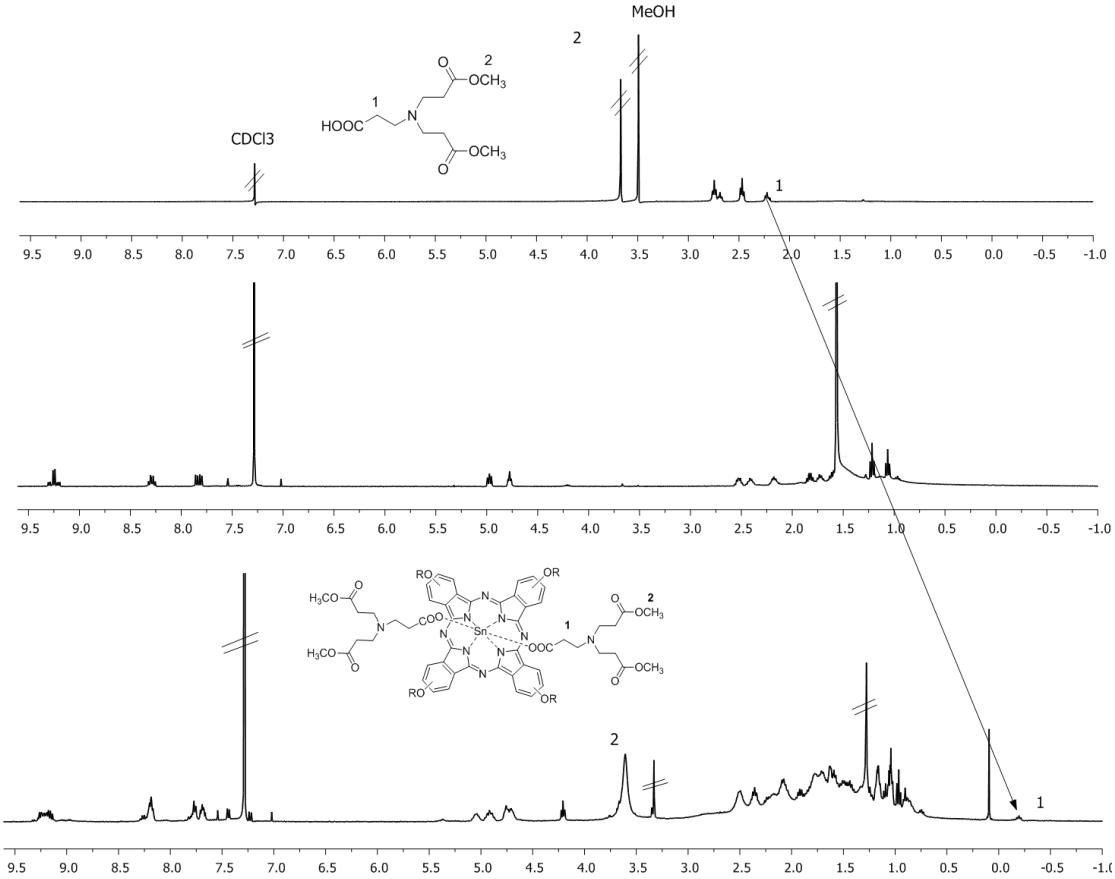

Figure 4.33 – ^1H NMR of dendron G-0.5, (SnPC $(OH)_2$ and self-assembled complex (SnPC $(G0.5)_2$)

Other support was received from mass spectroscopy in which (MALDI-TOF-MS); the spectra revealed a molecular ion peak at 1237 ($M\text{-}L^+$). The UV-Vis spectroscopy indicated the presence of the Q band, which shifted from 744 nm to 740 nm, the blue shift of the Q bands could be due

to interaction between the dendrons and Pcs (the binding method of tin atom with carboxylate dendrons) (Figure 4.34).

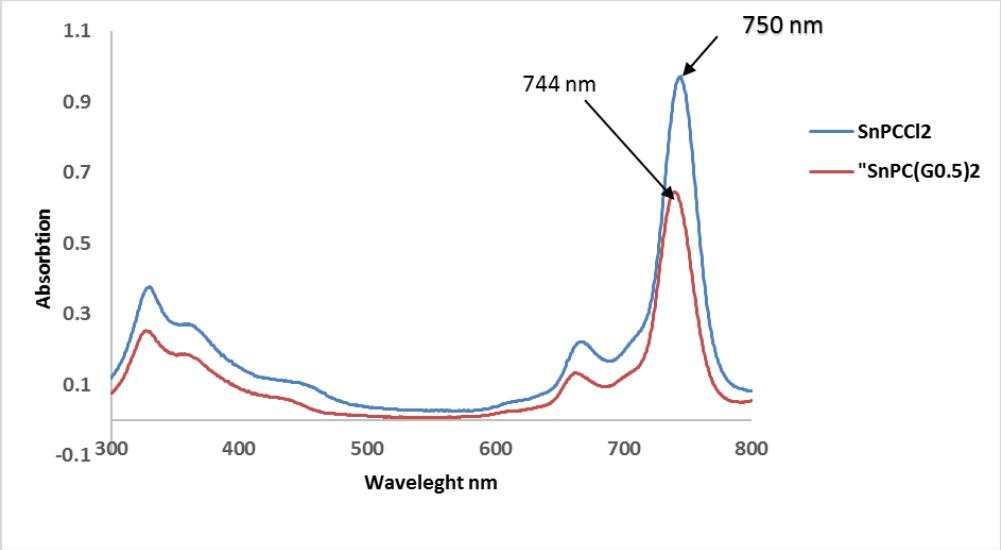

Figure 4.34. UV/Vis a spectrum of SnPcCl2 and SnPc(G0.5)2 13 in CH2Cl2

Also the confirmation was made via FTIR spectroscopy, the spectrum displayed the presence of peaks at 1585 cm^{-1}, 1645 cm^{-1} and 1463 cm^{-1} which indicate to the binding method of tin atom with carboxylate dendrons. Tin phthalocyanine have specific UV/vis spectrum with two strong absorption peaks in DCM, one in the UV region at around 350 nm (sort band) and second one in the Vis region from 600-760 nm.

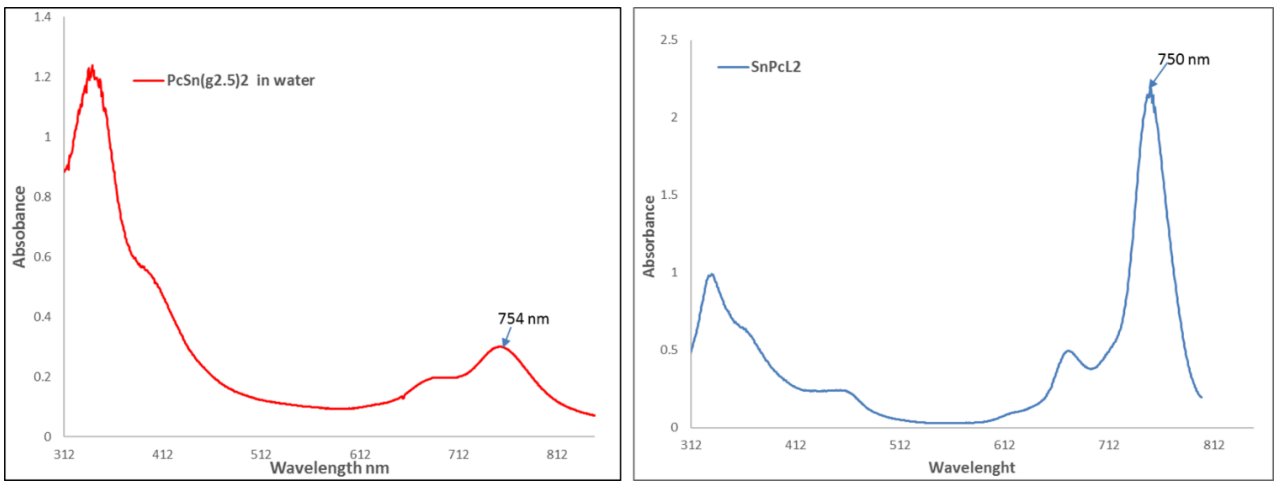

Figure 4.35. The different between UV/vis spectrum of compound of SnPc complexes **13** in water (left) and $SnPcCl_2$ in dichloromethane (right).

The tin phthalocyanine complexes are water soluble, which is good and a requirement for PDT. However, when recorded in water, the spectra are very different to those obtained in organic solvent. The spectrum of complex **13** in water is different to that obtained in DCM, Figure 4.35 and is a result of aggregation. We had assumed that the steric bulk of the dendrons would prevent aggregation (which was the case for the porphyrin systems), but clearly this was not the case. Presumably the coordination chemistry is different to that occurring within the porphyrin systems, resulting in the phthlocycanines having a stronger desire towards aggregation. This could come about from the increased hydrophobic nature, or stronger π–π interactions between the phthlocyanines. The literature describes two principle geometries for aggregation, which are referred to as either H or J- aggregates and correspond to a face-to-face or side-by-side conformation respectively. Considering the fact that phthlocyanines without ligand are completely insoluble in water, we can conclude that at least one ligand remains. As such, we can propose possible structures for the aggregate, which are shown schematically in Figure 4.36. The first possibility arises from the initial loss of a dendron ligand (mass spectrometry has already shown that the second ligand is labile), which would be followed by a face-to-face or edge-to-face interaction/aggregation. This possibility is shown on the left of Figure 4.36. Alternatively, both ligands remain, but are not big enough to prevent powerful hydrophobic and π–π interactions from taking place. This possibility is shown on the right of Figure 4.36. Although the ligands may not big enough to prevent aggregation, there size should prevent J aggregation, which is more sensitive to larger axial ligands. It is possible to distinguish these two conformations using UV spectroscopy. In both cases the peak around 350 nm increases (and becomes the largest peak), whilst the peak around 750 nm is significantly reduced. However, a J aggregate results in a shift to longer wavelength. On the other hand, H aggregate result in a shift to shorter wavelength. If we look at the aqueous spectrum of complex **13**, we notice a peak at 754 nm and a peak at shorter wavelength (665 nm), corresponding to the non-aggregated and H-aggregated structures respectively. There is no evidence of a peak at longer wavelength, allowing us to dismiss the possibility of the unlikely J aggregates. Next we did quick experiment to see if we could recover the dendrimer complex from the water by extraction with DCM. However, the organic fraction was colourless and did not have any peaks in the phthlocyanine's UV regions. We also looked at the aqueous phase from the extraction, which retained its colour and gave the same UV structure (before extraction). Interestingly, aggregation can be beneficial to the clinical application of PDT However, as the largest peak

was now at the shorter wavelength of 350 nm, we did not test these compounds as photosensitizers [141-143].

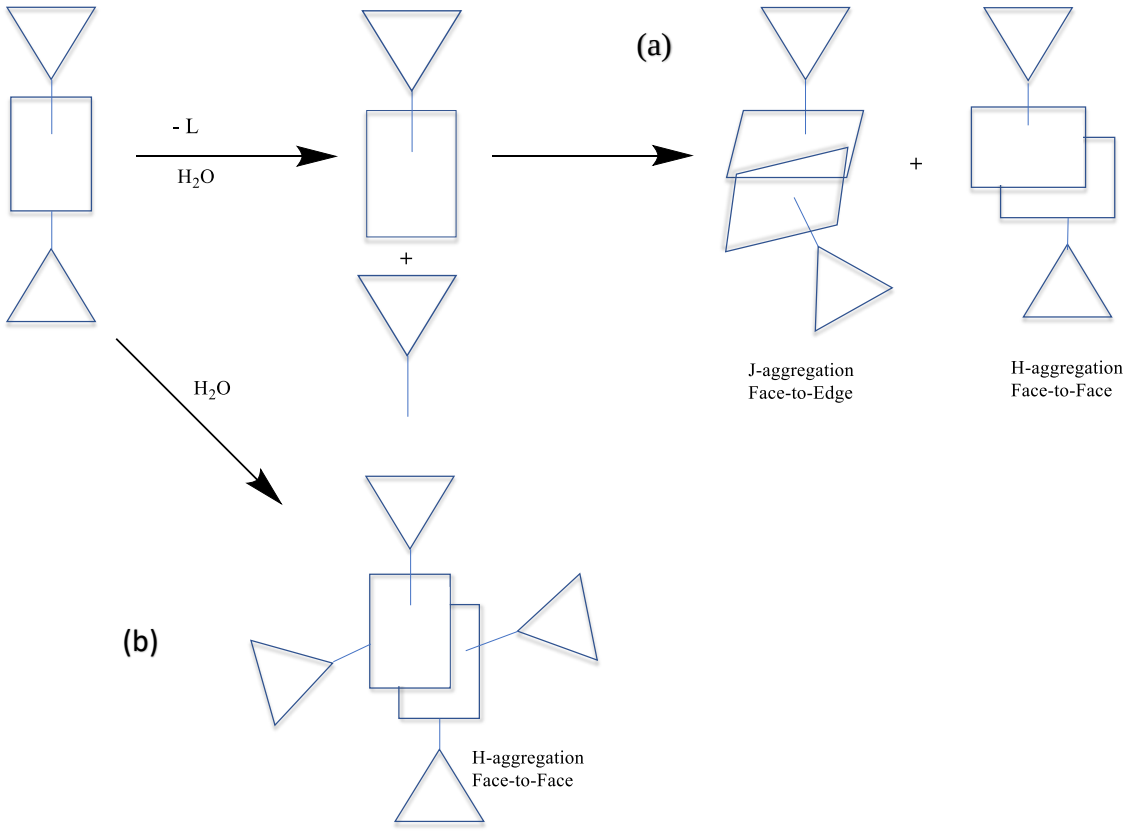

4.36 The aggregation possibilities of the soluble water phthalocynins (10) in aqueous solution

4.5 Intracellular Localization.

In order to exploit dendrimers so as to allow greater cellular delivery of drugs, it is vital to investigate the transformation of dendrimers into cells, along with the cytotoxicity of dendrimers as a drug delivery agent. Despite our prior knowledge that anionic dendrimers do not result in haemolysis and cytotoxicity [112]. In order to test the self-assembled drug as PS, cell viability assay, intracellular localisation and concentrations of photosensitizer that lead to

structure photo damage require evaluation. At this stage, all these investigations require a soluble product which can easily pass into cells. Unfortunately, we did not achieve the concentration required to complete these tests. Easter determined that polyamidoamine dendrimers have partially hydrolysed PAMAM dendrimers. All complexes give a low concentration (1×10^{-7}M) when dissolved in a buffer solution (PH 7.4). Only one sample was submitted to the medical school for further testing, while third generation ester dendrimer porphyrin was presented in 16 ester groups. The complex was evaluated as a novel, supramolecular class of photosensitizer for PDT by applying DMSO as a solvent. The intracellular localisation of the tin porphyrin complex $SnTPP(G2.5)_2$ in cells was tested by using confocal microscopy. The images 4.37 produced clearly showed cellular uptake of the compound, Figure 4.22. The images also revealed that the complex did not enter the nuclease. The punctate staining is likely endosomal/lysosomal in origin, which is often seen with lipophilic compounds. For photodynamic therapy, lysosomal staining is advantageous as apoptotic death rather than necrotic death is associated with lysosomal localization.

The low solubility was a hindrance to completing the rest of the experiments which can be carried out after employing the method to hydrolyse all of the ester in future research.

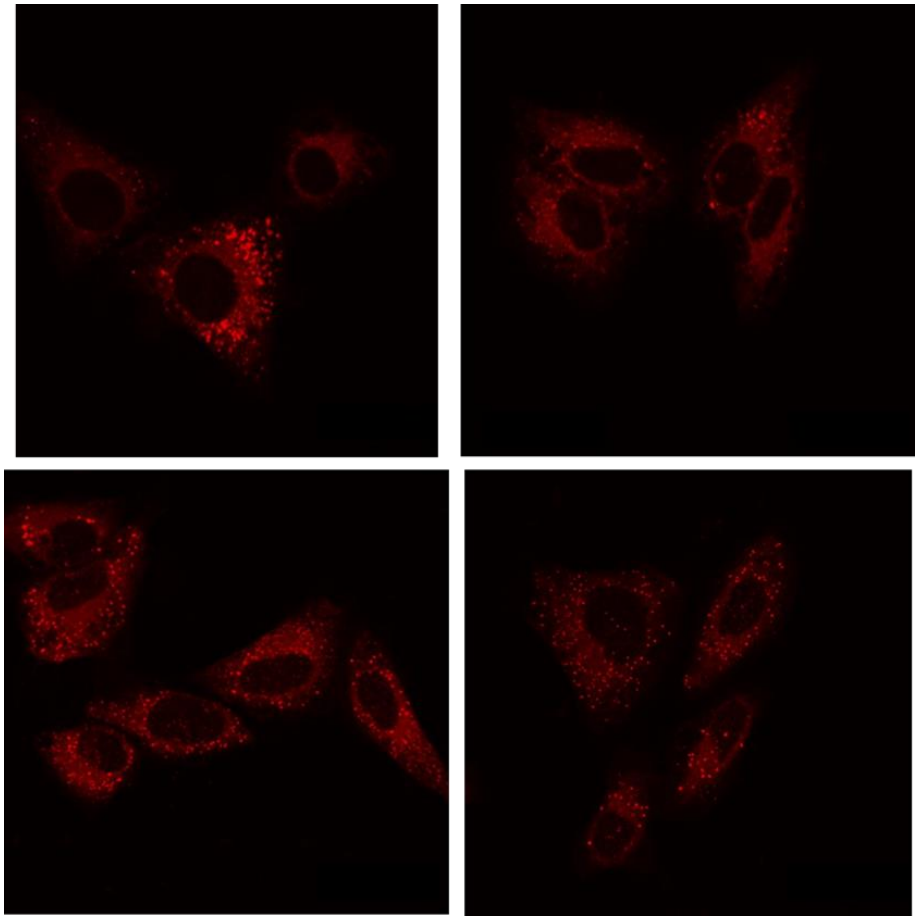

Figure 4.37. Confocal laser scanning microscopy images of HeLa cells treated with $SnTPP(2.5DO)_2$

The photosensitizer concentration for PDT was not achieved when we used the PAMAM dendrons terminated ester groups, because there are no surfaces hydrolysed enough to form a spherical shape to encapsulate the porphyrin and the hydrophobic areas become exposed to water, leading to a slight improvement in solubility compared to $SnTPP(OH)_2$. However, as time is the limited we tried to improve solubility by converting the ester terminal dendron to hydroxyl terminated dendrons.

4.6 Synthesis and Purification of PAMAM-OH Dendron

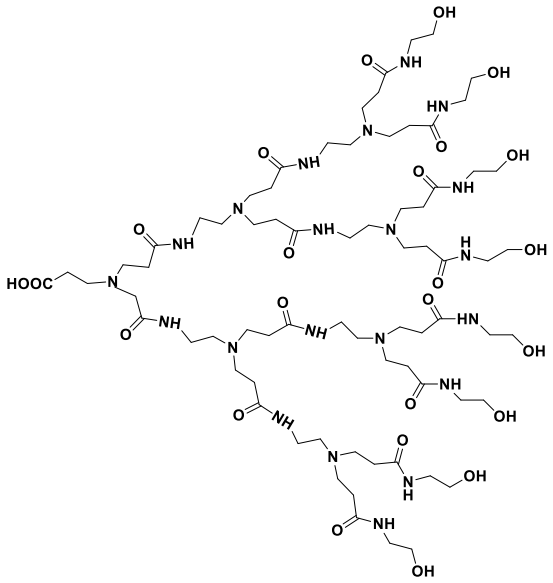

(14)

Scheme 4.38. Synthesis G2.5 hydroxyl PAMAM dendrons

The synthesis of OH-dendron was achieved following the same procedure of synthesis OH-dendrimers, but using ethanolamine instead of the tris. The half generation dendrimer was dissolved in minimum amount of DMSO, then ethanolamine and potassium carbonate was added to the solution. Each ethanolamine molecule contains one primary amine functional group, which can react with one ester group of dendrons. The reaction mixture was left to stir and reflux at 50 ^{o}C for three days. The product was purified by removing solids by filtration to give the hydroxyl dendrimers in DMSO. Precipitation using acetone gave the crude product as as thick paste. Purification by repeated precipitation from the minimum amount of water using acetone gave the neutral hydroxyl dendrons, followed by freeze drying. ^{1}H NMR, ^{13}C NMR, IR and mass spectrometry were applied to analyse neutral hydroxyl terminated dendrons The spectrum of this compound is very similar to full generation dendrons, but there is a small difference shows in spectra of the hydroxyl dendrons, the methylene protons that are adjacent to terminal amines in spectrum of full generation dendrons were no longer visible. In addition to

a new triplet peak in higher chemical shifts at about 3.55 ppm for methylene protons, which are adjacent to terminal hydroxyl groups (Figure 4.39).

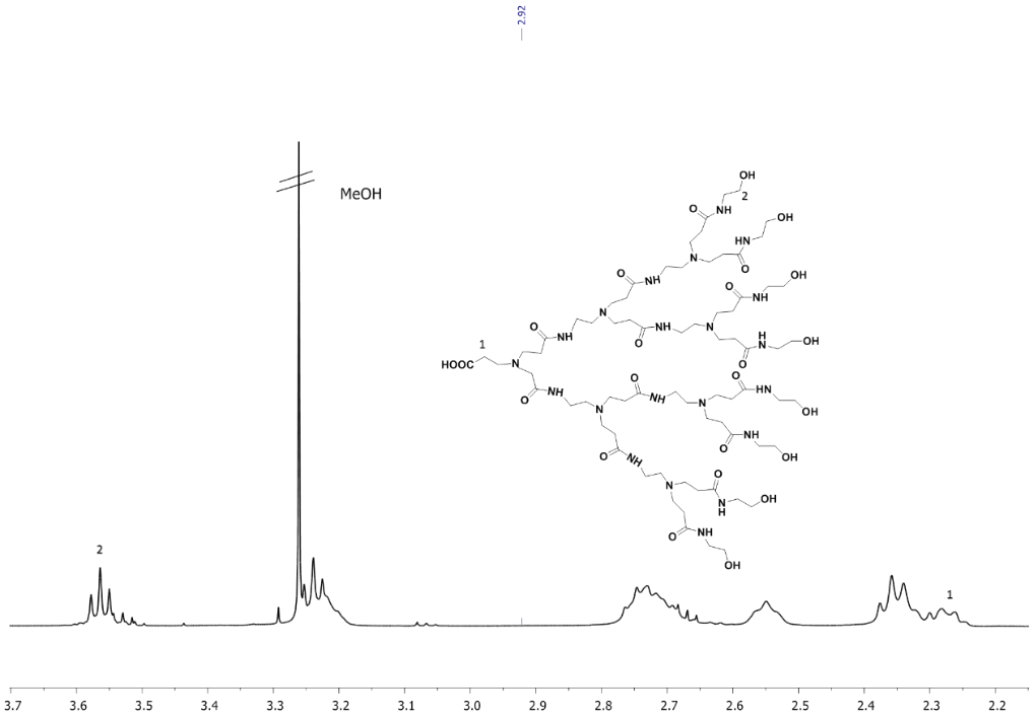

Figure 4.39- The ^{1}H NMR Spectrum (MeOD, 400 MHz) of hydroxyl PAMAM dendron (G- 2 .5)

The mass spectrum of, the dendrimer with 8 OH terminal groups displayed two peaks at 1694 and 1733 corresponding to MH^{+} and MK^{+} respectively. IR spectroscopy was a further technique used to confirm this compound. The spectrum of neutral hydroxyl dendron did not display the peaks for external ester C=O and C-O, which indicates the conversion of the terminal ester groups to the desired hydroxyl terminal groups. Further proof came from the existence of the broad peak at 3230 cm^{-1}, due to the hydroxyl groups. Unfortunately, we were unable to synthesise the SnTPP complex, because we did not find a common solvent that could or dissolve the polymer and the porphyrin.

Chapter 5

Conclusion & future work

Conclusion & future work

The focus of recent scientific research has been to improve the issues associated with the effectiveness of drugs used for numerous diseases. In nanomedicine, one of the strategies used to overcome challenges, such as poor solubility and poor absorption, is to use a drug delivery system. Several drug delivery systems have been advanced, such as, dendrimers, block copolymers and linear polymers. In this study, hydrophobic drugs were encapsulated within dendrimers to enhance solubility, as they are advanced macromolecule nanocarriers with globular architecture, well-defined structure, hydrophobic interior and hydrophilic external.

The synthetic approach, adapted in this studied, generated the successful synthesis of a series of dendrimers. The ester-terminated PAMAM dendrimers (half generations) and amine-terminated PAMAM dendrimers (full generations) with different sizes were synthesised, ranging from G 0.5 to G 4.5. Michael addition followed by amination was used; these two steps were recycled to obtain the desired generations of PAMAM dendrimers. A water soluble PAMAM dendrimer was created by converting the ester terminated groups of the dendrimers to hydroxyl-terminated groups producing hydroxyl-terminated PAMAM dendrimers (12 OH, 24 OH, 48 OH, and 96 OH). In the initial study, tests were conducted to determine the polymer's ability to encapsulate the drug ibuprofen, and determine which generation bound best (based on size and dense packing). For this investigation, three different generations were used (G1.5, G2.5, G3.5) at a concentration of 1×10^{-4} M. The level of dendrimer loading varied from one generation to the next. The results demonstrated that the solubility enhancement behaviour of G3.5 dendrimers was the best, compared to smaller, the G2.5 and G 1.5 (as expected). Larger dendrimers can provide well defined spaces for guest molecule within the dendritic box.

The solubility of the encapsulated drug using the G3.5 water soluble PAMAM dendrimers increased with dendrimer concentration. This study was expected to show the number of encapsulated drug molecules increased linearly as concentration increased but this did not occur. The study revealed that a maximum of twenty-seven ibuprofen molecules incorporated in the internal cavities of dendrimers at concentration 1×10^{-4} M. Which roughly corresponds to the number of internal amines. At higher dendrimer concentrations, the concentration of encapsulated ibuprofen plateaued. As the dendrimer concentration increases, aggregation starts to occur, involving interpenetration, which reduces the space insides the dendrimer for drug molecules. It is clear that the polymer concentration is an important factor to consider when encapsulating hydrophobic molecules. Another element that can effect on the aqueous

solubility of the hydrophobic drug is the pH of the buffer (medium) [144145]. However, because of the limited time, these influencing elements were not studied.

Porphyrins have been assessed as suitable photosensitisers for photodynamic therapy. Due to its unique characteristics such as simple synthesis, strongly absorbs at 400 nm (B band) and between 600 and 800 nm (Q band, useful for PDT), their ability to yield singlet oxygen efficiently, and thermal stability. Drawbacks related to these compounds are a lack of solubility at physiologic conditions and poor targeting for cancerous cells. In this section of the study, PAMAM dendrimers were used to improve the solubility and carry the drug to the diseased tissues. Non-covalent encapsulation method was applied for a comparison between tetraphenyl porphyrin (TPP) and zinc tetraphenylporphyrin (ZnTPP) to determine the effect of coordination interaction to improve the use of dendrimers as a drug delivery system. Different generations (24 OH, 48 OH and 96 OH terminal end groups) of PAMAM dendrimers were utilised. The result of the comparison determined that ZnTPP displayed greater solubility (high loading) than TPP (low loading). For example, G3.5 OH dendrimer, there is a 28 times increase in solubility, this was due to secondary interactions between guest and host. In the case of ZnTPP. It forms an additional coordination bond with the dendrimers internal amines, which improved the dendrimers use as host molecules. On the other hand, the solubility of TPP was lower because of hydrophobic interaction between TPP and hydrophobic (internal) cavities so, this strategy had a poor drug loading capacity. The study proved that the size of the dendrimer affected the loading capacity, dendrimer with 96 OH terminal end groups had the highest loading of ZnTPP, found to be 12 dendrimers per ZnTPP. Dendrimer with 48 OH, loading was 25 dendrimers per ZnTPP more than the G 1.5 OH which was only 50 dendrimers per ZnTPP.

The success of coordination to improve encapsulation led us towards designing a molecule where porphyrin coordination was involved in the synthesis of the dendrimer; this would ensure that every dendrimer would have a porphyrin. Self-assembled drugs for PDT were achieved by synthesis of acid core PAMAM dendrons, up to generation G3.5, as the carrier. The synthesis of dendrons was similar to that used to obtain PAMAM dendrimers but used a β-alanine core instead. The Sn(IV) porphyrins are ideal scaffolds for the construction of axial bonding style assemblies [146]. The tin cored porphyrin system $SnTPP(OH)_2$ was successfully synthesised and used for self-assembled drugs. Self-assembly was achieved between dendron containing ester-terminated dendrons and $SnTPP(OH)_2$. Self-assembly complexes demonstrated that the non-incorporation strategy using coordination binding is a simple synthesis, stoichiometry is 2:1

polymer to drug. Solubility improved from zero to 1.0 $x10^{-7}$ but is still too low to for PDT assesmal.

Deeper penetration of light delivery would improve the efficacy of PDT in tumour treatment. Tin phthalocyanine ($SnPcCl_2$) would be a suitable core unit; it strongly absorbs at 670–770 nm which is in the red region of the spectrum, suitable for PDT [9]. Phthalocyanine is insoluble in biological systems so is unable to act as a photosensitizer unaided; solubilisation of the axial ligands on the central metal could overcome this problem. The self-assembled systems of different generations of the ester-terminated dendrons and tin phthalocyanine were proposed. The tin cored phthalocyanine system $SnPC(Cl)_2$ was synthesised. Self-assembly between dendron containing ester groups and $SnPC(Cl)_2$ were successfully achieved. The solubility behaviour of the phthalocyanine complexes was investigated by UV/vis spectroscopy; the complexes formed higher aggregates in aqueous solution.

In an attempt to improve polymer solubility, G2.5 ester-terminated dendrons were converted to G2.5 hydroxyl-terminated dendrons. Analysis using ^{1}H NMR, ^{13}C NMR, IR, and mass spectrometry confirmed the synthesis of G2.5 OH was successful. Self-assembly between dendron containing hydroxyl-terminal group and $SnTPP(OH)_2$ was not possible due to problems with solubility.

In general, the aims of this study haven't been completely fulfilled. Future work try and be to problems overcome by synthesising a larger generation of dendrons which contains more terminal groups enabling them to surround the surface and prevent aggregation, However, synthesis of dendrons, their purification and characterisation is very difficult. The ^{13}C NMR spectrum showed a small acid core carbonyl peak in small generation complexes, but in larger generations, no peak will be visible. ^{1}H NMR already showed overlap, which makes it hard to interpret [2]. Consequently, the future work of this research would include an investigation into the use of hyperbranched polymers, to produce a soluble system. The challenge with a HBP system is how to control the molecule weights, in a healthy organism the renal threshold is in the range of 30–50 kDa [39], a very narrow disparity will be required.

Also further work could include the concentration of the terminal groups into solubilizing groups before or after complex formation. Alternatively, additional research may be carried out within the Twyman research group to study the hydrolysis process. Further research should involve PDT studies, toxicity test for both complexes with porphyrin and phthalocyanine.

Chapter 6

Experimental

6.1 Solvents and reagents

Many chemicals and reagents used in this project were obtained from commercial sources (mainly from Sigma-Aldrich) and used directly without further purification. Dry solvents were taken from the Chemistry Department at university of Sheffield.

6.2 Instrumentation

NMR Spectroscopy

Deuterated solvents used for sample preparation for both ^{1}H NMR and ^{13}C NMR analysis were purchased from Sigma Aldrich. Both spectrums of ^{1}H NMR and ^{13}C NMR were recorded using a Bruker AV 400MHz instrument Chemical shifts of spectrums are estimated in ppm, the NMR spectra were examined using Topspin 3.0 NMR software.

Fourier Transform Infrared (FTIR) Spectroscopy

All FT- IR samples were analysed neat on a Perkin-Elmer Paragon 1000 FT-IR

spectrophotometer with integral Dura Sample IR-II.

Mass Spectrometry

Mass Spectrometry equipment was used to determine the mass of compounds. Two types of mass spectrometers were used; Electrospray Ionisation Mass Spectrometry (ES-MS), and Matrix Assisted Laser Desorption Ionisation Time of Flight (MALDI-TOF) mass spectrometry. ES-MS was used for low molecular weight products (less than 1000 Da) and recorded using a Micromass Prospec spectrometer. MALDI-TOF was used for a high molecular weight compound (more than 800 Da) and carried out using dithranol or dihydroxy benzoic acid matrices on Bruker III mass spectrometer.

UV-vis spectroscopy

The UV/Vis absorbance was recorded by an Analytik Jena AG Specord S-600 spectrophotometer and Software (WinASPECT) was used for UV/Vis analysis.

PH Meter

The pH of the buffer solution was measured using a pH Meter 3030 from UEN way. The system was calibrated using pH 4.0 and pH 10.0 standard buffer solutions.

Dynamic light scattering (DLS)

Hydrodynamic diameters of dendrimers in aqueous solutions were determined by dynamic light scattering (DLS). The DLS instrumentation consisted of a Malvern Zetasizer NanoZS Model ZEN 3600 instrument operating at 25˚C with a 633-nm laser module. All determinations were made in triplet.

Confocal:

The slides were imaged using a nikon A1 confocal with excitation at 643 nm and emission registered in the window 700 nm +/- 35 nm and using a 63x oil objective lens.

6.3 Synthetic and Experimental Procedures

6.3.1 General procedure for synthesis of half generation PAMAM dendrimers

In a round bottom flask, a whole generation PAMAM dendrimer (or ethylene diamine, EDA, in the case of synthesizing PAMAM G0.5 dendrimer) was dissolved in methanol and stirred then methyl acrylate in an excess amount was added to the solution drop wise at 0°C for 40 minutes. The reaction was stirred overnight at room temperature. For a given amount of time, depending on the generation of dendrimer in question, unreacted methyl acrylate and methanol was removed by rotary evaporator and the ultra-high vacuum was used for definite purity of the product from traces of the reactants and the solvent.

6.3.2 General procedure for synthesis of whole generation PAMAM dendrimers

The general procedure was followed to synthesis a full generation dendrimer PAMAM dendrimers. In a round bottom flask, the ester terminated intermediate generated previously was dissolved in methanol, then EDA was added drop wise over a period of 30 minutes to a stirred

solution at 0 °C, the reaction was stirred at room temperature for a given amount of time depending on the number of generation of dendrimer. The solvent was removed via rotary evaporation at 45 °C, following this, and the purification steps (described in 3.1.4) were carried out to yield the product.

6.3.3 Synthesis of PAMAM dendrimer with 4 terminal OMe terminal groups

In a 500 mL round bottom flask, the ethylene diamine EDA (5.18g, 0.08mol) was dissolved in methanol (50 mL) and stirred using a magnetic stirrer then methyl acrylate in an excess amount (50.22g, 0.052mol) was added to the solution drop wise at 0°C for 40 mins. The reaction was stirred overnight at room temperature. Unreacted methyl acrylate and methanol was removed by rotary evaporator and ultra-high vacuum was used for definite purity of the product from traces of the reactants and the solvent, the product was a yellow honey coloured oil (Yield 30 g, 88 %).

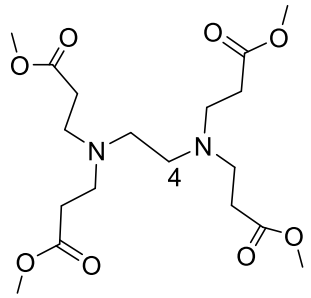

ES-MS, 405 (MH^+), calculated 405gmol^{-1}. ^{1}H NMR (MeOD, 400 MHz): δ 3.69 (s, 12H), 2.76 (t, 8H), 2.55 (s, 4H), 2.49 (t, 8H); ^{13}C NMR (MeOD, 400 MHz) δ ppm 173.1, 51.3, 50.5, 49.4, 47.5, 31.8; FTIR (cm^{-1}) 2953, 2826, 1730 (Ester carbonyl).

6.3.4 Synthesis of PAMAM dendrimer with 4 amine terminal groups

In a 500 mL round bottom flask, the 4 terminal OMe terminal groups (13.46g, 0.04mol), which was produced from the previous step, was dissolved in methanol (40 mL). EDA (97.88g,1.62

mol) was then added drop-wise at 0°C. The reaction mixture was stirred at room temperature for 5 days. The excess of EDA and solvent was then removed through washing the mixture using a solution of an azeotropic mixture of 9:1 toluene: methanol. This purification process was repeated numerous times until all EDA was completely removed. The product was placed under ultra-high vacuum for 5 hours. The product was honey coloured oil (Yield 12.2g, 0.023mol,74 %).

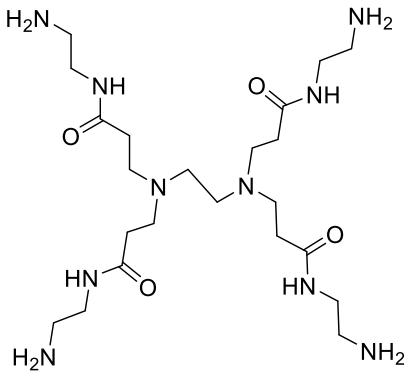

ES-MS, 517 (MH)^{1}H NMR (MeOD, 400 Mhz): δ 4.93 (s, 4H), 3.69(s, 8H), 3.33-3.27 (mm, 16H), 2.81-2.41 (m, 20H). ^{13}C NMR (MeOD) δ ppm 173.5, 51.1, 49.9, 48.2, 38.1, 33.3. FTIR λ (cm^{-1}) 328 (amide, N-H, Stretch), 3071 ,2953 (C-H sp^3), 2859, (, 1636 (amide, C=O stretch), 1546,1436 (CH_2 bend), 1356 ,1283, 1112, 1030, 940.

6.3.5 Synthesis of PAMAM dendrimer with 8 OMe terminal groups

In a round bottom flask, the PAMAM dendrimer with 4 amine terminal groups (5.02g, 9.72 mmol) was dissolved in methanol (50 mL). Then, methyl acrylate (14.66g, 0.18mol) was added to the mixture solution drop-wise over 40 minutes at 0°C. The reaction mixture was stirred at room temperature for 3 days. After that, excess amount of methyl acrylate was removed by rotary evaporator at 40°C. The PAMAM dendrimer with 8 OMe terminal groups was placed under ultra-high vacuum for 5 hours. The product was obtained as a sticky orange oil (Yield 10.1g, 84 %).

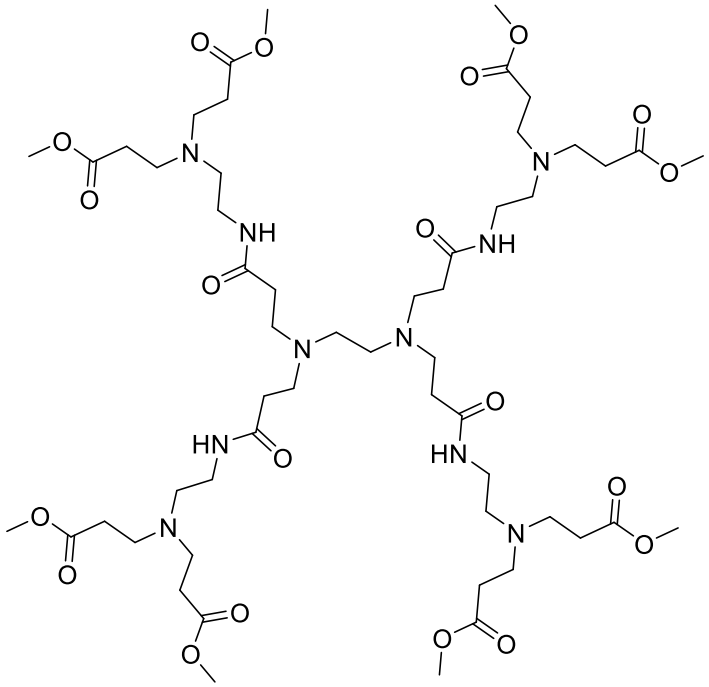

MALDI-TOF: 1205 (MH^+) (calculated, 1206 $gmol^{-1}$): ^1H NMR (MeOD, 400 MHz): δH 4.91 (s, 4H), 3.69 (s, 24H), 3.39-3.21(m, 24H), 2.87-2.35 (mm, 44H): ^{13}C NMR (MeOD, 400 MHz) δ ppm 173.3, 173.2, 52.4, 50.7, 49.8, 49.1, 37.1, 32.2, 31.9; FTIR (cm^{-1}) 3311 (N-H, amide stretch), 2953, 2878, 1736 (C=O, ester), 1649 (C=O, amide), 1538(N-H, amide bend), 1438 (CH_2 bend).

6.3.6 Synthesis of PAMAM dendrimer with 8 NH_2 terminal groups

In 250 mL a round bottom flask, the PAMAM dendrimer with 8 OMe terminal groups (8.82g, 7.32mmol) was dissolved using methanol (50 mL) then EDA (68.28g, 1.14mol) was added to the dendrimer solution drop-wise over 40 minutes. The reaction mixture was stirred at room temperature for 8 days. After the reaction was completed, the reaction mixture was washed with an azeotropic solution (500 mL) of toluene and methanol (ratio 9:1) to remove EDA via a rotary evaporation system at 40^oC. Then the product was washed with methanol (60 mL). The purification process was repeated until the EDA was wholly removed. Lastly, the product was placed under ultra-high vacuum for 5 hours. The product of PAMAM dendrimer with 8 NH_2 terminal groups was a very viscous deep orange oil (Yield 8g, 78 %).

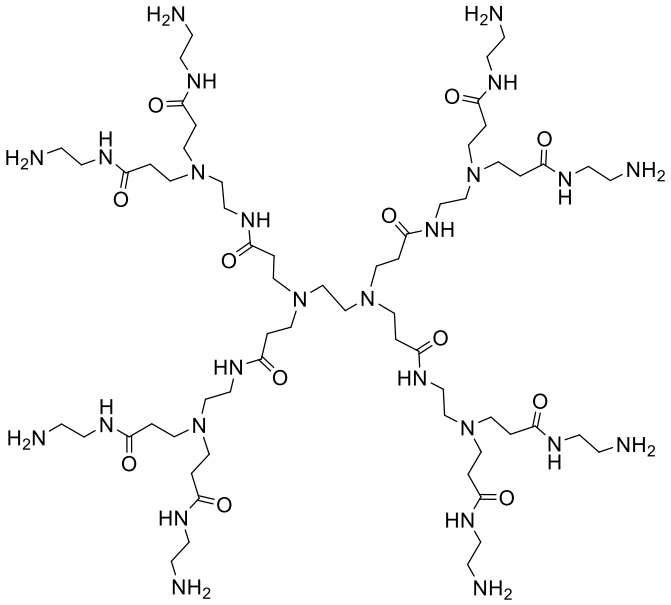

ES-MS, 1429 (MH^+).^{1}H NMR (MeOD, 400 MHz) δ, 4.91 (s, 4H), 3.65(s, 8H), 3.40-3.21 (m, 24H), 2.88-2.26 (mm, 76H). ^{13}C NMR (MeOD): 172.2, 50.7, 48.3, 46.1, 40.2, 35.9, 32.0, 31.7. FTIR (cm^{-1}) 3277 (N-H, amide stretch), 3078, 2938 (C-H, sp3 stretch), 2866, 1647 (C=O, amide), 1560 (N-H, amide bend), 1463, 1438, 1360, 1287, 1201, 1128, 1033.

6.3.7 Synthesis of PAMAM dendrimer with16 OMe terminal groups.

In a round bottom flask, the PAMAM dendrimers with 8 NH_2 terminal groups (6.2g, 0.043mol) were dissolved in methanol (50 mL). Methyl acrylate was added to a solution (14.1g, 0.16mol) drop-wise over 30 minutes at 0^{o}C. After that, the reaction mixture was stirred at room temperature for 4 days, the solvent and unreacted methyl acrylate was removed by rotary evaporator at 40^{o}C. The liquid product was placed under ultra-high vacuum for 5 hours, the PAMAM dendrimer with 16 OMe terminal groups was a viscous deep orange coloured oil (Yield 6.2 g, 70%).

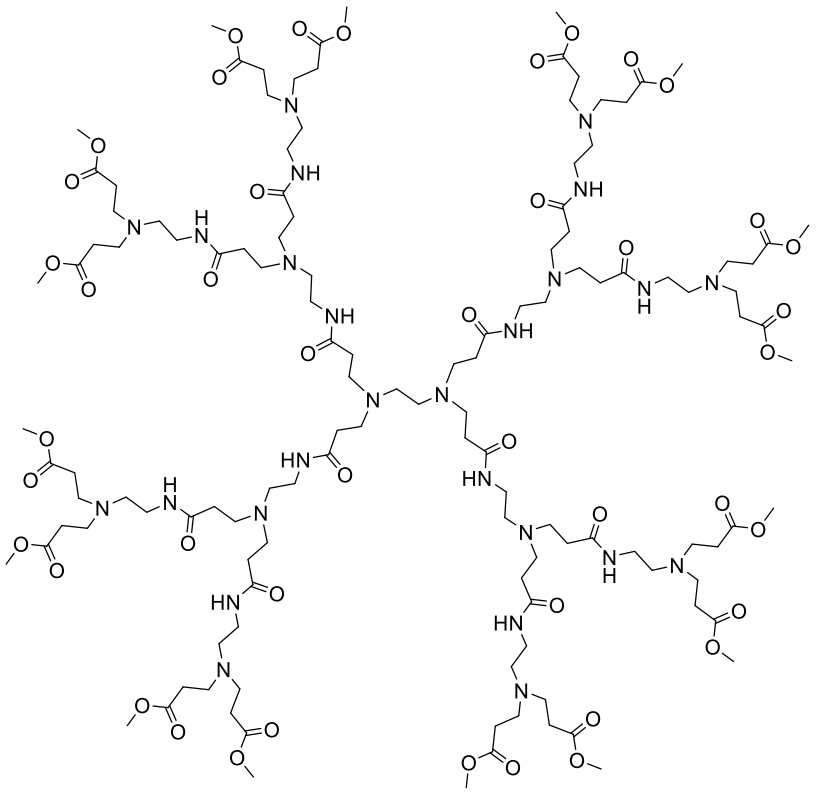

TOF MALDI-MS, 2804(MH^+), 2828 (MNa^+): ^{1}H NMR (MeOD, 400MHz) δ 4.91 (s, 12H, NH), 3.68 (s, 48H), 3.37-3.22 (m, 12H), 2.91-2.32 (mm, 152H); ^{13}C NMR (MeOD, 400MHz) δ ppm 173.2, 173.3, 52.4, 50.8, 49.1, 48.3, 37.6, 33.1, 32.1; FTIR (cm^{-1}) 3297 (N-H, amide stretch), 2952 (C-H, sp^3 stretch), 2837, 1737 (C=O, ester), 1647 (C=O, amide), 1550 (N-H, amide bend), 1438 (CH_2, bend), 1200, 1045.

6.3.8 Synthesis of PAMAM dendrimer with16 NH_2 terminal groups

In 250mL a round bottom flask, the PAMAM dendrimer with16 OMe terminal groups (4.36g, 1.56mmol) was dissolved in methanol (50 mL). Then the EDA (18.2g, 0.3mol) was added drop-wise over 30 minutes at 0^{o}C. The reaction solution was stirred at room temperature for 9 days. The product solution was then washed with azeotropic solution (500 mL) of toluene and methanol (ratio 9:1) to remove EDA by rotary evaporator at 40^{o}C then the product was washed

with methanol (60 mL). The product was placed under ultra-high vacuum for 6 hours to obtain a PAMAM dendrimer with16 NH_2 terminal groups as very viscous deep orange coloured oil (Yield 4.4 g, 87%).

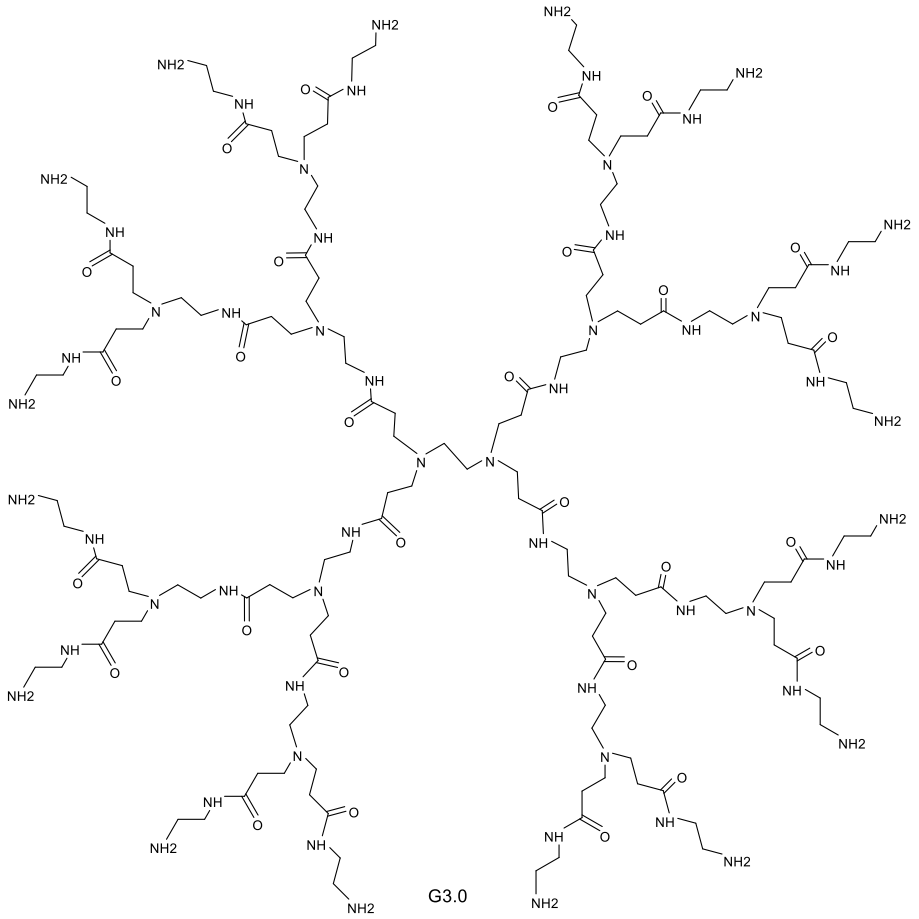

TOF MALDI-MS, 3257 (MH^+). ^{1}H NMR (MeOD, 400MHz) δH 4.93 (s, 28H), 3.55-3.2(m, 112H), 2.9-2.2 (mm, 116H) ^{13}C-NMR (MeOD, 400MHz) δ ppm 173.7, 173.5, 52.1, 49.9, 47.4, 41.2, 40.3, 37.1, 33.4, 33.2; FTIR (cm^{-1}) 3367, 3291 (N-H, amide stretch), 3092 (C-H, sp^3 stretch), 2949, 1638 (C=O, amide), 1560 (N-H, amide bend), 1486 (CH_2, bend), 1323, 1154, 1038.

6.3.9 Synthesis of PAMAM dendrimer with 32 OMe terminal groups

In a round bottom flask (500mL), the PAMAM dendrimers with 16 NH_2 terminal groups (3.36g, 0.01mol) were dissolved in methanol (40 mL). Methyl acrylate (5.84g, 0.08mol) was then added drop-wise over a period of 30 minutes at 0^oC. The reaction mixture was stirred at room temperature for 5 days. A rotary evaporation system was used to remove solvent at 40^oC. The product was placed under ultra-high vacuum for 8 hours to obtain PAMAM dendrimer with 32 OMe terminal groups as really sticky orange coloured oil (Yield 3.6g, 58%).

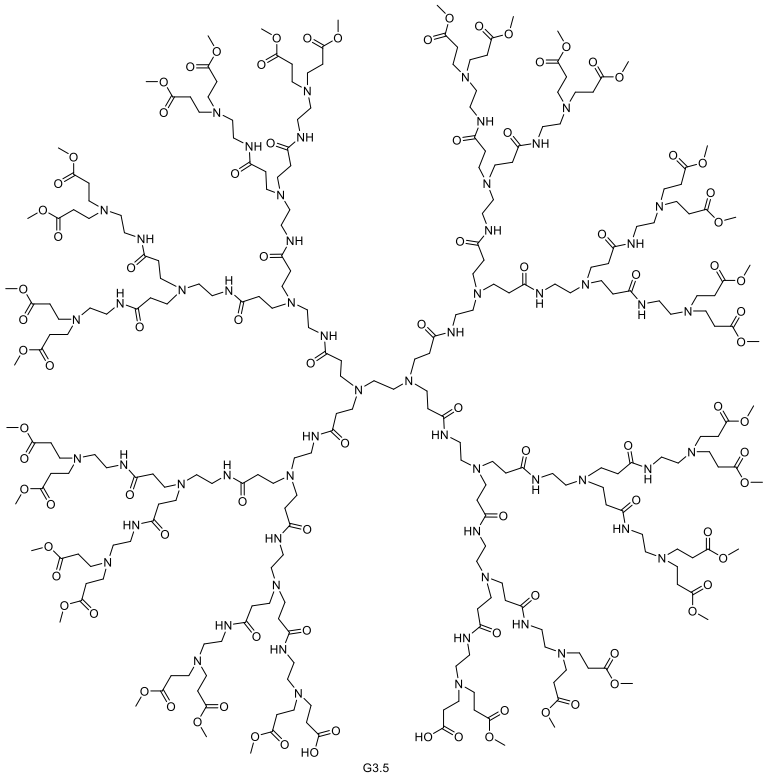

TOF MALDI-MS, 6012 (MH^+) ^1H NMR (MeOD, 400MHz) δ 3.68 (m, 96H), 3.39-3.26 (m, 56H), 2.89-2.36 (mm, 300H); ^{13}C-NMR (MeOD, 400MHz) δ ppm 174.4, 173.5, 52.7, 52. 51.3, 49.7, 49.0, 37.3. 37.2, 33.4, 32.1; FTIR (cm^{-1}): 3298 (N-H, amide stretch), 2953 (C-H, sp^3 stretch), 2833, 2105, 1734 (C=O, ester), 1643 (C=O, amide), 1549 (N-H, amide bend), 1439 (CH_2, bend), 1361, 1263, 1200, 1043.

6.3.10 Synthesis of PAMAM dendrimer with 32 NH_2 terminal groups

In a round bottom flask 500mL the previously synthesised PAMAM dendrimer with 32 NH_2 terminal groups (4.72g, 0.81 mmol) was dissolved in methanol (60 mL). The EDA (23.375g, 0.39mol) was added drop-wise over 30 minutes. The reaction mixture was stirred for 10 days at room temperature. The resulting solution was washed by an azeotropic solution (500 mL) of

toluene and methanol (ratio 9:1) to remove EDA via a rotary evaporation system at 40 ^{o}C. The product was then washed with methanol. The purification procedure was repeated until the EDA was totally removed. PAMAM dendrimer with 32 NH_2 terminal groups was placed under ultra-high vacuum for 6 hours to obtain PAMAM dendrimer as very sticky orange coloured oil (Yield 3.34g, 90%).

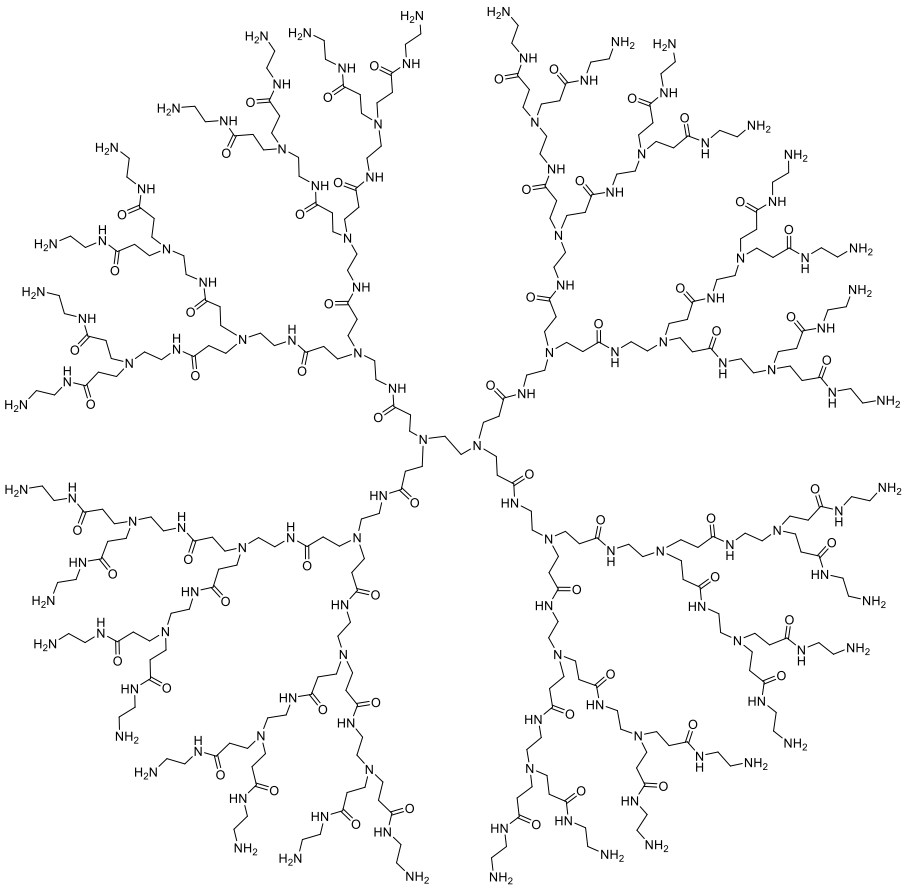

TOF MALDI-MS, 6913 (MH^+);^{1}H NMR (d d4-MeOH, 400MHz) δH 3.54-3.17 (m, 240H), 2.89-2.19 (mm, 132H) ^{13}C-NMR (MeOD, 400MHz) δ ppm 173.6, 173.1, 52.0, 49.3, 47.4, 41.5, 40.6, 37.3, 33.1, 33.0; FTIR (cm^{-1}) 3282 (N-H, amide stretch), 3089, 2943 (C-H, sp^3 stretch), 2852, 1640 (C=O, amide), 1557 (N-H, amide bend), 1467 (CH_2, bend), 1324, 1155, 1042.

6.3.11 Synthesis of PAMAM dendrimer with 64 OMe terminal groups

In a round bottom flask, the PAMAM dendrimer with 32 NH_2 terminal groups (3.34g, 0.485mmol) was dissolved in methanol (50 mL). At 0^oC methyl acrylate (8.125g, 0.095 mol) was added drop-wise over 40 minutes. The reaction mixture was stirred at room temperature for 7 days. Unreacted methyl acrylate and the solvent was removed by rotary evaporator at a temperature of 40^oC. The product was located under ultra-high vacuum for 6 hours to yield PAMAM dendrimer with very sticky deep honey coloured oil (Yield 5.1 g, 85%)

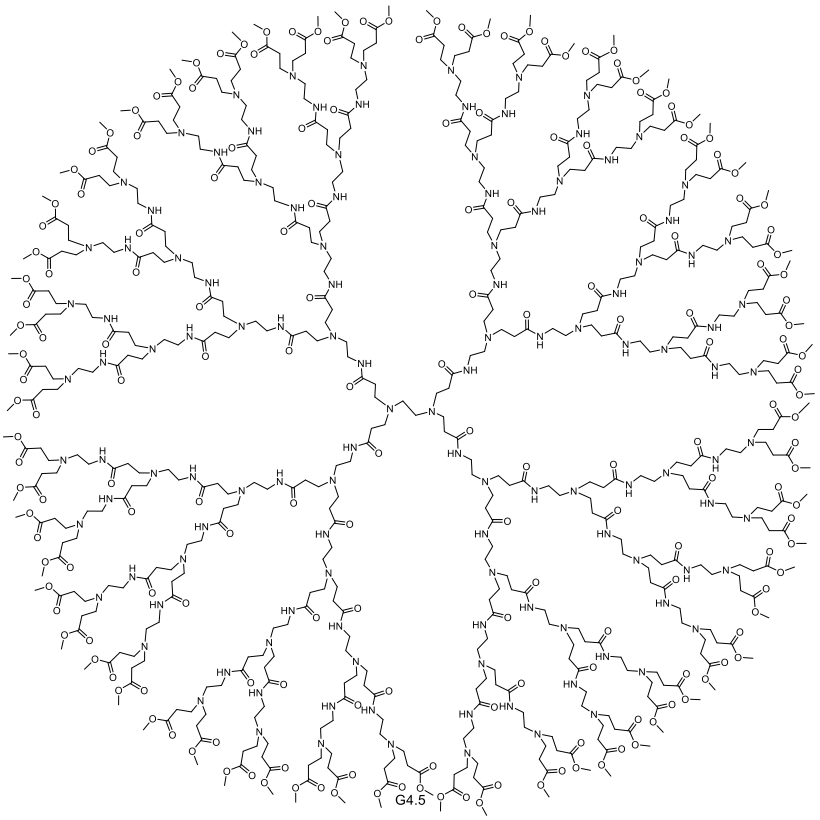

TOF MALDI-MS, found 11630 (MK^+); ^1H NMR (MeOD, 400MHz) δ 3.68 (s,192H), 3.39-3.26 (m, 120H) 2.89-2.36 (mm, 500H);^{13}C NMR (MeOD, 400MHz) δ ppm 174.3, 173.6, 52.6, 52.2, 51.1, 49.7, 49.1, 37.5, 37.2, 33.5, 32.2; FTIR (cm^{-1}) 3410 (N-H, amide stretch), 2932 (C-H, sp^3 stretch), 2840, 1723 (C=O, ester), 1640 (C=O, amide), 1568(N-H, amide bend), 1437 (CH_2, bend), 1202, 1041.

6.3.12 General procedure for converting half generation PAMAM dendrimers to PAMAM dendrimer terminal hydroxyl groups

All glassware was dried in the oven overnight to avoid undesirable hydrolysis from moisture. The half generation PAMAM dendrimer was dissolved in dry DMSO. This was added to a suspension of tris-(hydroxymethyl) aminomethane (TRIS) and oven dried potassium carbonate. This solution was allowed to a stir under nitrogen environment for period depending on the size of half generation at 50^{o}C. Once completed, distillation process was used to remove the solvent from the reaction mixture. The resulting product was dissolved in very little water and then precipitated in a quantity of acetone (300mL). This process was repeated three times, then the PAMAM dendrimers terminal hydroxyl groups was collected and placed in oven to dry.

6.3.13 Synthesis of hydroxyl-terminated PAMAM dendrimers (0.5 G with 12 OH group)

A general procedure was followed to synthesise a G 0.5 with 12 OH group. The half generation PAMAM dendrimer (5g, 12.35mmol) in dry DMSO (3mL) was added into TRIS solution (8.95g, 0.05m) and anhydrous potassium carbonate (10.4g, 0.05) in dry DMSO (7mL). The solution was stirred under a nitrogen environment for 72 hours at 50^{o}C. This was followed by a purification process as described in the general procedure (Yield 0.24g, 6.3%).

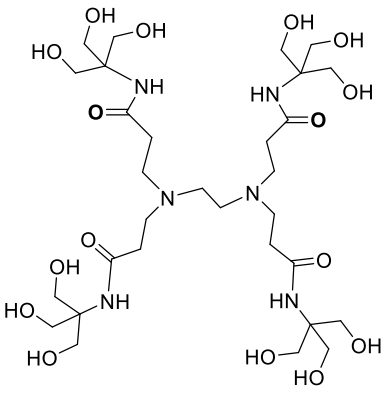

ES-MS 761 (MH+), ^{1}H NMR (D_2O,400Mhz) δ 3.60 (s, 24H), 2.72 (t, 8H),2.53 (s, 4H), 2.35 (t, 8H);^{13}C NMR (D2O, 400Mhz) δ ppm 175.4, 174.4, 62.0, 60.5, 51.8, 48.8; FTIR (cm^{-1}) 3274

(OH), 2938 (C-H sp^3), 1636 (amide C=O), 1548 (amide N-H bend) 1461 (CH_2 bend) 1370, 1260, 1121, 1044, 1017;

6.3.14 Synthesis of hydroxyl-terminated PAMAM dendrimers (1.5 G with 24 OH groups)

A general procedure was followed to synthesise a G 0.5 with 12 OH group. The half generation PAMAM dendrimer (4.2g,3.5mmol) in dry DMSO (3mL) was added into TRIS solution (3.8g, 31.4mmol) and anhydrous potassium carbonate (4.34g, 31.45mmol) in dry DMSO (7mL). The solution was stirred under a nitrogen environment for 72 hours at 50°C. Followed by a purification process as described in the general procedure (Yield 2.95g, 43%).

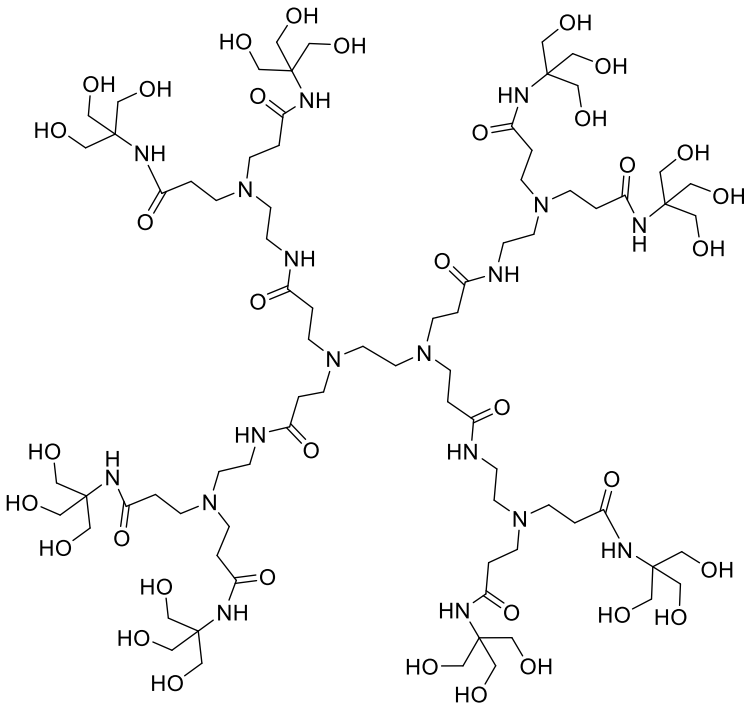

MALDI-TOF MS 1917, (1956) (MK^+); ^{1}H NMR (D_2O,400Mhz) δ 3.61 (s, 48H), 3.23(t, 8H), 2.71 (m, 24H), 2.50 (m, 12H), 2.30 (m, 24H); ^{13}C NMR (D_2O), δ ppm 175.1, δ 174.2, δ 61.5, δ 59.8, δ 51.2, δ 49.1, δ 43.2, δ ,41.5, δ 36.8, δ 32.7. FTIR (cm^{-1}) 3270 (OH), 2943 (C-H

sp^3), 1631 (amide C=O), 1555 (amide N-H bend), 1455 (CH_2 bend), 1391, 1245, 1128, 1041, 1019

6.3.15 Synthesis of hydroxyl-terminated PAMAM dendrimers (2.5 G with 48 OH Groups)

A general procedure was followed to synthesis a G 0.5 with 12 OH group. The half generation PAMAM dendrimer (5g, 1.8mm) in dry DMSO (3mL) was added into TRIS solution (3.75, 30.95mmol) and anhydrous potassium carbonate (4.25,30.8mm) in dry DMSO(7mL). The solution was stirred under a nitrogen environment for 96 hours at 50^{o}C. This was followed by a purification process as described in the general procedure (Yield 0.7g, 8.9%).

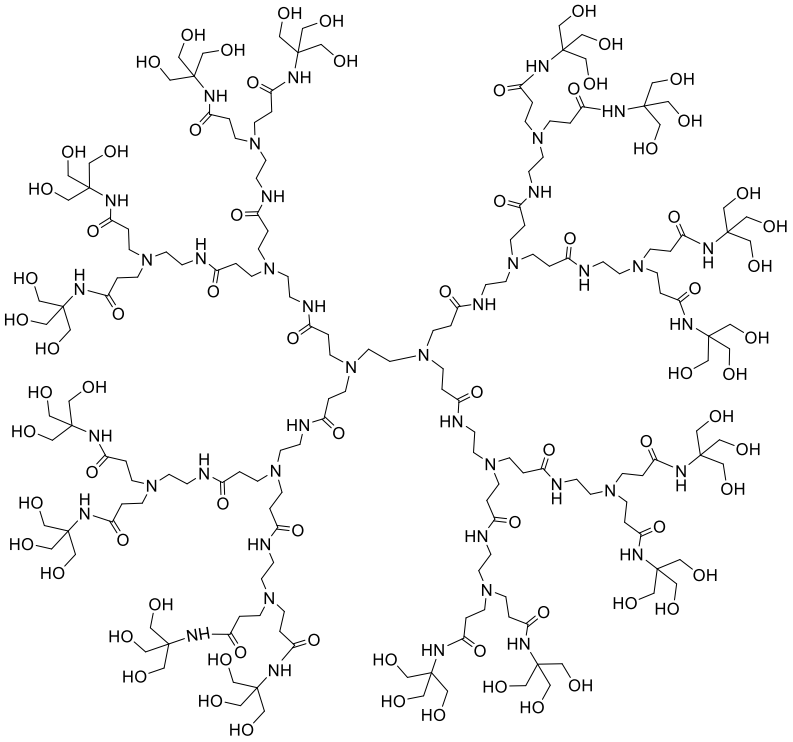

MALDI-TOF MS, found 4171; ^{1}H NMR (D_2O,400Mhz) δ 3.61 (s, 96H), 3.2 (t, 24H), 2.73 (m, 56H), 2.53 (m, 28H), 2.35 (m, 56H); ^{13}C NMR (D_2O,400Mhz), δ ppm 175.1, 174.2, 61.5, 59.8,

51.2, 49.1, 43.2, 41.5, 36.8, 32.7. FTIR (cm^{-1}) 3270 (OH), 2943 (C-H sp^3), 1631 (amide C=O), 1555 (amide N-H bend), 1455 (CH_2 bend), 1391, 1245, 1128, 1041, 1019.

6.3.16 Synthesis of hydroxyl-terminated PAMAM dendrimers (3.5 G with 96 Groups)

A general procedure was followed to synthesis a G 0.5 with 12 OH group. G 3.5 PAMAM dendrimer (3.95g, 0.65mm) in dry DMSO (3mL) was added into TRIS solution (3.8g, 31.2mmol) and anhydrous potassium carbonate (3.25g,31.2mmol) in dry DMSO (7mL). The solution was stirred under a nitrogen environment for 5 days at 50ºC. This was followed by a purification process as described in the general procedure (Yield 0.7g, 8.9%).

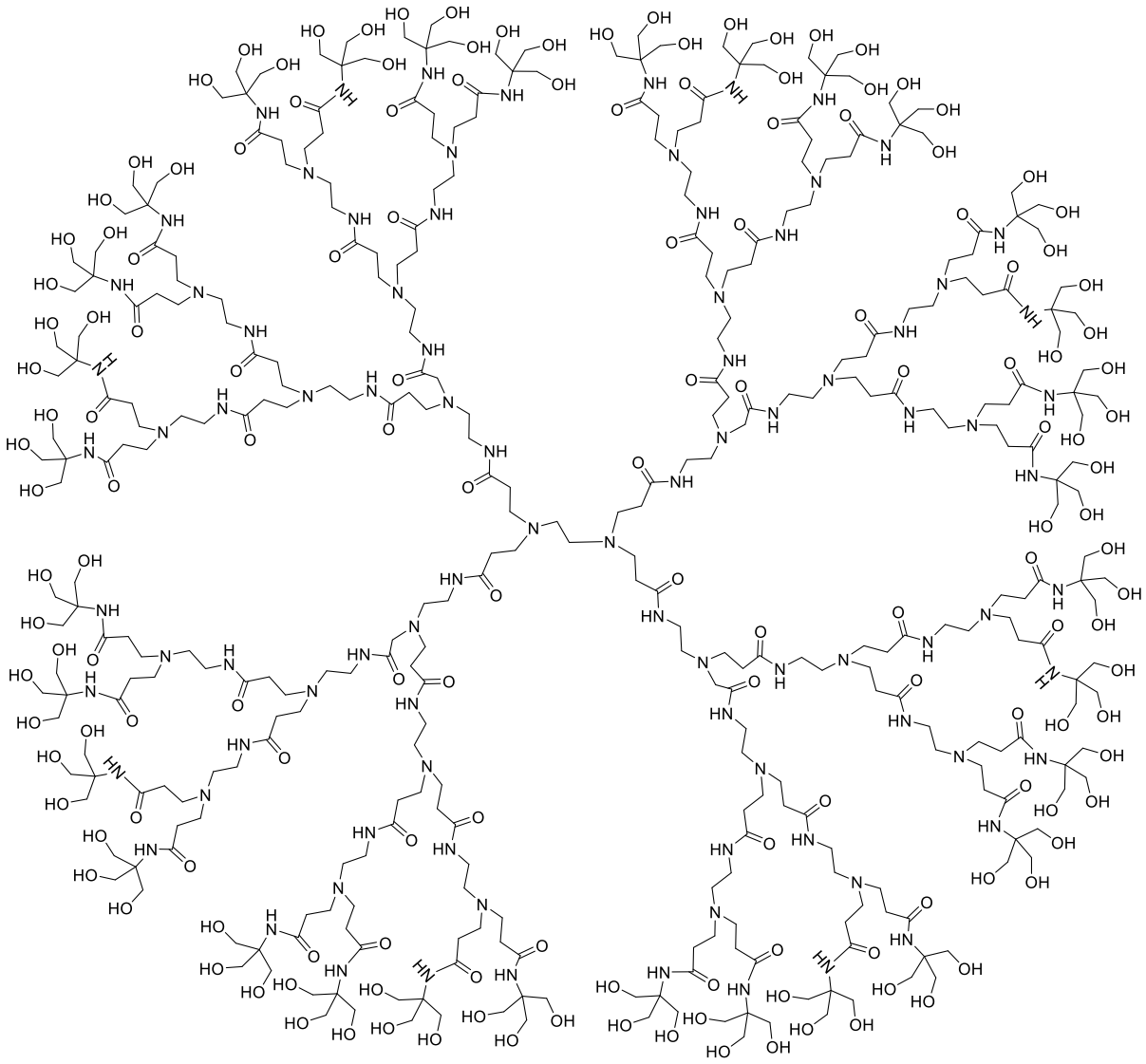

MALDI-TOF MS found 8149, ^{1}H NMR (D_2O,400Mhz) δ 3.61 (s, 96H), 3.2 (t, 24H), 2.73 (m, 56H), 2.53 (m, 28H), 2.35 (m, 56H); ^{13}C NMR (D2O), δ ppm 175, 174.2, 61.5, 59.8, 51.2, 49.1, 43.2, 41.5, 36.8, 32.7; FTIR (cm^{-1}) 3276 (OH), 2932 (C-H sp^3), 1629 (amide C=O), 1549 (amide N-H bend), 1451 (CH_2 bend), 1359, 1244, 1128, 1023.

6.3.17 Synthesis of hydroxyl-terminated PAMAM dendrimers (4.5 G)

A general procedure was followed to synthesis a G 4.5 with 12 OH group. G 4.5 PAMAM dendrimer (3g, 0.241mmol) in dry DMSO (3mL) was added into TRIS solution (2.3g. 0.019mol) and anhydrous potassium carbonate (2.3g ,0.017mol) in dry DMSO (7mL). The solution was stirred under a nitrogen environment for 7 days at 50^{o}C. This was followed by a purification process as described in the general procedure.

MALDI-TOF MS, found 17426, FTIR λmax 3279 (OH), 2944, 284 (C-H sp^3), 1630 (amide C=O), 1558 (amide N-H bend), 1459(CH_2 bend), 1393, 1247, 1120, 1042, 1021.

6.3.18 Beer-Lambert experiment ibuprofen

A series of Me-OH solutions of ibuprofen with different concentrations was prepared. UV/Vis spectroscopy was used to measure the absorbance of ibuprofen, the Δ absorptions values were used at wavelength from 264 to 268 nm. A Beer-Lambert Plot was shown the relationship between absorbance and concentrations of ibuprofen.

6.3.19 Procedure for encapsulation of ibuprofen

Preparation of 1×10^{-4} M of G1.5 PAMAP dendrimers with 24 OH (3) methanolic solution.

4.8mg of G1.5 hydroxyl PAMAM dendrimer was dissolved in 25 mL of methanol to prepare the concentration 1×10^{-4} M.

Preparation of 1×10^{-4} M of G2.5 PAMAP dendrimers with 48 OH (3) methanolic solution.

10 mg of G2.5 hydroxyl PAMAM dendrimer was dissolved in 25 mL of methanol to prepare the concentration 1×10^{-4} M.

Preparation of four different concentrations of G3.5 PAMAP dendrimers with 96 OH (3) methanolic solution.

Four different concentration 1.00, 2.00, 4.00 and 6.00 (x 10^{-4}) M of hydroxyl PAMAM dendrimers were made to encapsulate ibuprofen molecules. 20 mg, 40 mg, 81mg and 122 mg of the polymer was dissolved in 25 ml of methanol to prepare above concentrations.

Preparation of four different concentrations of ibuprofen

103mg, 21mg, 10mg, and 2mg of ibuprofen was dissolved in 10 mL of methanol to give the ibuprofen methanolic solution with 5×10^{-2}, 1×10^{-2}, 5×10^{-3} and 1×10^{-3} M respectively

6.3.20 Preparation of 0.01M tris(hydroxymethyl) aminomethane buffer solution.

1.21g of tris was dissolved in 1L of distilled water to prepare the concentration of 0.01M. The pH of the Tris buffer was monitored by a pH metre. To obtain a pH of 7.4, hydrochloric acid was slowly added to the solution until the pH of the solution was adjusted.

6.3.21 Procedure for encapsulation ibuprofen within dendrimer (dendrimer (24 OH, 48 OH, 96 OH terminal groups).

Each hydroxyl PAMAM dendrimer (G1.5, G2.5, G3.5) was mixed with 100 mg of ibuprofen in methanol, the concentrations of dendrimers for all generations were kept to be the same (1×10^{-4} M). After this, the solution was physically mixed for 5 mins then the solvent was removed by rota evaporator. Finally, for each generation, the dendrimer/ibuprofen complex was dissolved into TRIS buffer solution (10 mL) Each sample was measured by UV-Vis spectroscopy and concentration was worked out from the absorbance

6.3.21 Synthesis of Meso-Tetraphenylporphyrin(TPP)

In a 500mL around contains refluxing propionic acid (250 mL), the Freshly. pyrrole (7.01mL, 0.101 mole) and benzaldehyde (10.02g, 80mmol) were added and stirred for 30 min. After that, the mixture cooled at room temperature the reaction mixture was filtered under vacuum and washed thoroughly with methanol, hot distilled water. This synthetic approach required

purification via silica gel chromatography using chloroform as mobile phase to get pure compound of meso-tetraphenyl porphyrin (2.82 g, 19%) as a purple powder.

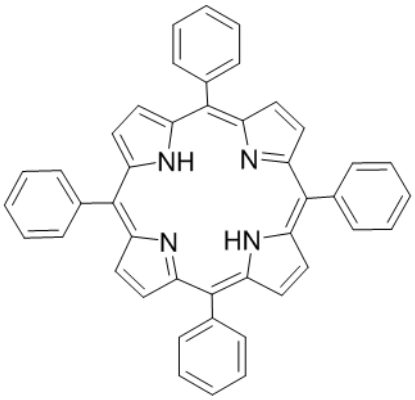

(TPP)

ES-MS 615 (MH^+), ^{1}HNMR ($CDCl_3$, 400 MHZ) δ 8.7(s, 8H, Pyrrolic – CH), 8.24(8H, dd, Phenylic o-CH), 7.78 (m, 12H), -2.75 (s, 2H, NH) ^{13}C NMR ($CDCl_3$, 400 MHZ) δ ppm 137.19, 134.5, 126.6, 120.9; FTIR (cm^{-1}) 3319 (amine N -H stretch), 3013 (aromatic and alkene, C-H stretch), 1675, 1224, 748, 695; UV absorbance ($CHCl_3$) λmax¬ (nm) 418, 515.5, 551, 592, 645.

6.3.22 Synthesis of Zinc Tetraphenylporphyrin (ZnTPP)

Tetraphenylporphyrin (TPP) (500mg) and chloroform were added into a round bottom flask and left for stirring until TPP completely dissolved. Zinc acetate (1.5g) was added to TPP solution at 50^0C. The reaction mixture was stirred for 20 minutes. Once completed, the reaction mixture was allowed to cool at room temperature and filtered to remove zinc acetate. the solvent was by rotary evaporator and the Fuchsia compound (Yield 0.50g, 90 %) was obtained.

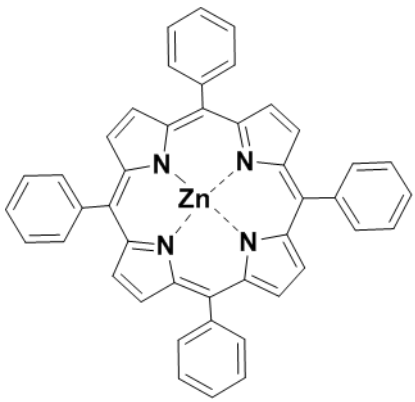

(ESI-MS) 678 (MH^+), and (calculated 678 $gmol^{-1}$) ^1H NMR (D-$CDCl_3$, 400M Hz) δ 8.97(s, 8H pyrrolic β-H), 8.26 (d, J = 7.9 Hz, 8H phenolic o-CH), 7.81(d, J = 8.3 Hz, 12H, phenolic m,p-CH); ^{13}C NMR (D-CDCl3, 400MHz) δ ppm 150.2, 142.8, 134.4, 132.0, 127.5, 126.6, 121.1; FTIR (cm^{-1}): 2923(s), 2854 (s), 1463, 1377 (w), 1173 (w); UV/Vis Spectroscopy (nm): 418.5, 547.5, 678.

6.3.23 Beer-Lambert experiment for TPP and ZnTPP.

In volumetric flask, 27mg of TPP and ZnTPP were dissolved in DCM (1L) to prepare a stock solution. The UV spectrophotometer was used to measure the absorbance of compounds at their characteristic wavelengths (419nm) with methanol as the reference. Additional dilutions at different concentrations (M) were made to plot the Beer-Lambert graph.

6.3.24 Encapsulation of TTP and ZnTTP using a different generation of PAMAM dendrimer

Each PAMAM hydroxyl dendrimer (24OH, 48OH, and 96OH) was mixed with one equivalent of TPP in methanol. These solutions were physically mixed for 5 minutes then the solvent was removed by rotary evaporator. After that, 3mLof tris buffer solution 0.01M was added to the complex and filtered, the absorbance of the solutions was measured by UV/Vis spectroscopy at 418nm.

6.3.25 Synthesis of PAMAM Dendron G-0.5 with 2 terminal OMe terminal groups

β-alanine (2g,0. 022moles) and potassium carbonate (3.11g, 0.022moles) were dissolved in methanol (40 mL) in a 250mL round bottom flask. Then methyl acrylate (5.8g, 0.065moles) was added drop wise to the solution in flask at 0^oC. The reaction mixture was stirred at room temperature for 24 hours. After completion of the reaction, filtered and excess methyl acrylate was removed by evaporation. Next, the product was placed under high vacuum for 6 hours. The

PAMAM dendron G-0.5 with 2 terminal OMe terminal groups was obtained (5.2g, 88 %) as white viscous oil.

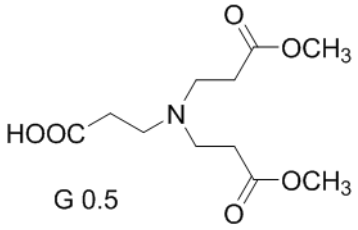

The compound was confirmed by; ES-MS: 262 (MH^+); ^{1}HNMR ($CDCl_3$, 250MHz), δ 3.67(s, 6H, OCH3), 2.23 (t, 2H, J = 7.0 Hz), 2.47 (4H, t, J = 7.0 Hz), 2.63 (2H, t, J = 7.3 Hz), 2.72 (4H, t, J = 7.0 Hz); ^{13}C - NMR ($CDCl_3$, 400MHz) δ ppm 179.29, 173.65, 51.64, 50.83, 49.04, 36.00, 30.22; FTIR (cm^{-1}): 3262 (acid-OH), 2953 (C-H-sp^2), 2826 (C-H-sp^3), 1729(ester carbonyl group), 1636, 1554, 1436, 1358, 1176, 1080 (-C-N stretch).

6.3.26 Synthesis of PAMAM dendron G-1.0 with 2 terminal NH_2 terminal groups

In a 500 mL round bottom flask, G0.5 PAMAM dendron (5g, 0.0191moles) was dissolved in methanol (40 mL), the addition of EDA (28.8g, 0.477mol) was made drop-wise over 30 minutes at 0^{o}C. At room temperature, the reaction mixture was stirred for 5 days. After the reaction was completed, the product was purified, to remove excess EDA, using 9:1 azeotropic mixture of toluene: methanol, this was then washed with methanol. The purification step was repeated until the EDA was totally removed. The product was placed under high vacuum for 4 hours to yield G1.0 PAMAM dondron (4.9g, 80 %) as a sticky honey coloured product.

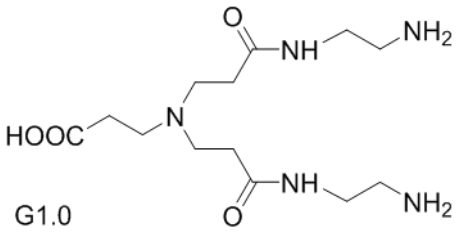

The compound was confirmed by; ES-MS:318(MH^+), ^{1}HNMR ($CDCl_3$, 400MHz) δH ,3.10(4H, t, J = 7.0 Hz) 3.04 (2H, t, J = 7.0 Hz), 2.75-2.55 (8H, m), 2.32 (4H, t J = 7.0 Hz) 2.21 (2H, t, J = 7.0 Hz); ^{13}C NMR (D_2O, 400MHz) δ ppm 180.46, 48.1.3, 43.92, 41.9, 39.6, 35.36, 32.94; FTIR λ max (cm^{-1}): 3220(acid OH), 3052, 2930(CH - sp^2), 2099(CH - sp^3), 1625(amide carbonyl group), 1555(amide NH bend), 1540 (amine), 1471(CH_2 bend), 1302, 1240.

6.3.27 Synthesis of PAMAM Dendron G-1.5 with 4 terminal OMe terminal groups

G1.0 PAMAM Dendron (3g, 9.4mmole) was dissolved in methanol (30mL) in a 250 mL round bottom flask. To this solution, methyl acrylate (4.25g, 0.047moles) was added drop-wise over 30 minutes at 0^{o}C. Then the reaction mixture was stirred at room temperature for 2 days. Excess methyl acrylate and methanol were removed by rotary evaporation. The product was dried under high vacuum for 4 hours to obtain final product (4.5g ,72%), as sticky deep honey coloured oil.

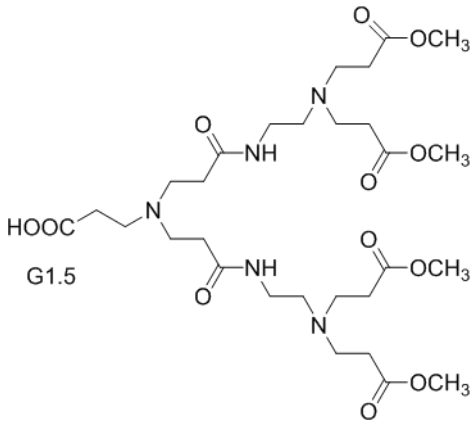

The compound was confirmed by; ES-MS: 662(MH^+), 700 (MK^+); ^{1}H NMR(d - CDCl3 , 400MHz) δ 3.67(s, 12H, OCH3), 3.09-3.17 (2H, m), 2.75 (12H, t J = 7.0 Hz) 2.53 (6H, t J = 7.0 Hz), 2.43 (8H, t, J = 7.0 Hz,), 2.36 (4H, t) 2.21(2H, t J = 7.0 Hz); ^{13}C NMR(d-CDCl3, 400MHz) δ ppm 178.9, 173.3,172.4, 52.7, 51.7, 48.9, 37.8, 32.5; FTIR (cm^{-1}), 3291(acid O-H stretch), 2952(CH - sp^2), 2823(CH - sp^3), 1649 (amide carbonyl stretch), 1731(ester carbonyl), 1566, 1436 (acid carbonyl stretch), 1386(acid O-H bend), 1260, 1030 (- C -N stretch).

6.3.28 Synthesis of PAMAM dendron G 2.0 with 4 terminal NH2 terminal groups

In a 500 round bottom flask, G1.5 PAMAM dendron (3g, 4.5mmole) was dissolved using methanol (30 mL). EDA (13.65,0227mole) was added to the dendron solution drop-wise over 30 minutes at 0^{o}C. The reaction mixture was stirred at room temperature for 7 days until completion of the reaction. The azeotropic mixture (toluene and methanol 9:1) was used to remove EDA by rotary evaporation. Then the product was washed with methanol, this process was repeated until the EDA was fully removed. Then, the product was dried under high vacuum for 4 hours, G2.0 PAMAM dendron was achieved (3g, 86%), as a white sticky coloured oil.

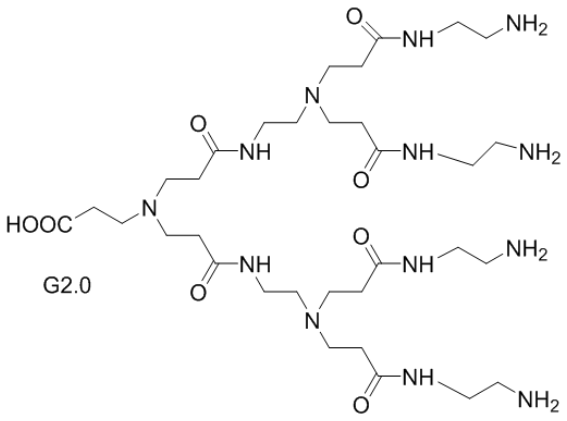

The compound was confirmed by ES-MS: 774 (MH^{+}), 813(MK); ^{1}H NMR(D_2O, 400MHz),δ 3.144 (4H, t, J = 7.0 Hz), 3.088 (8H, t, J = 7.0 Hz), 2.71-2.57 (m, 14H), 2.54 (8H, t, J = 7.0 Hz,) 2.46 (4H, t, J = 7.0 Hz), 2.27(12H, t, J = 7.0 Hz,), 2.2 (2H, t, J = 7.0 Hz); ^{13}C NMR(D_20 , 400MHz) δ ppm 180.9, 175.1, 174.6, 51.0, 48.9, 48.6, 48.1, 41.1, 39.6, 36.6, 34.2, 32.6; FTIR (cm^{-1}) 3258 (amide stretch), 3066 (acid OH), 2927 (CH - sp^2), 2880 (CH - sp^3), 1631(amide carbonyl bend), 1556 (amide bend), 1476, 1431 (carbonyl stretch), 1334 (acid O - H bend), 1152(amine C-N).

6.3.29 Synthesis of PAMAM dendron G 2.5 with 8 terminal OMe terminal groups

G2.0 PAMAM dendron (3g, 3.8mmole) was dissolved in methanol (50mL) in a round bottom flask. Methyl acrylate (3.34g, 0.039moles) was added drop-wise over 30 minutes at 0^{o}C. Then, the reaction mixture was stirred at room temperature for 2 days. Excess methyl acrylate and methanol were removed by rotary evaporation. The product was dried under high vacuum for 4 hours to obtain the final product (2.1g ,37%), as a sticky deep honey coloured oil.

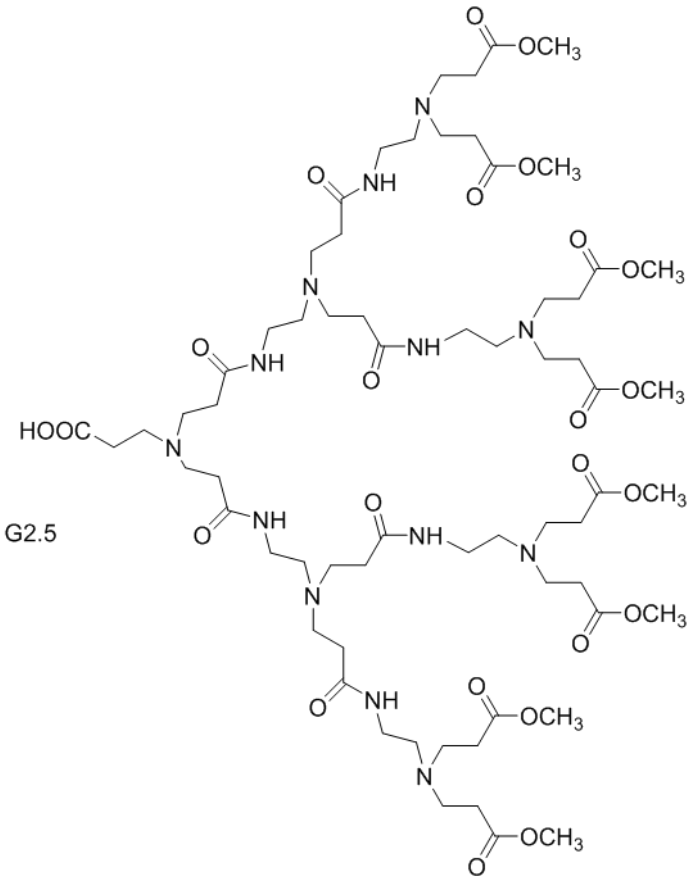

The compound was confirmed by; ES-MS,1463(MH^+); ^{1}HNMR (d-$CDCl_3$, 400MHz) δ 3.67 (24H, s), 3.23-3.3 (12H, t, J = 7.0 Hz), 2.78-2.58 (42H,mm)), 2.41 (16H, t J = 7.4 Hz), 2.39-2.35 (12H, br m, 2.2(2H ,t, J = 7.0 Hz); ^{13}C-NMR (d-CDCl3, 250MHz) δ ppm179.7, 173.1, 172.3, 172.0, 52.9, 51.7, 50.8, 49.4, 49.2, 37.2, 33.6, 32.7; FTIR λ max(cm^{-1}) 3273 (acid O - H stretch), 2953 (CH-sp^2), 2824 (CH-sp^3), 1729(ester carbonyl), 1638(amide carbonyl stretch), 1540, 1435 (acid carbonyl stretch), 1363(acid O-H bend), 1195(-C-N stretch), 1030.

6.3.30 Synthesis of PAMAM dendron G 3.0 with 8 terminal NH2 terminal groups

In a 500 round bottom flask, G2.5 PAMAM dendron (2g, 1.3mole) was dissolved in methanol (40 mL). EDA (7.66, 0.125mole) was added to the dendron solution drop-wise over 30 minutes at 0^{o}C. The reaction mixture was stirred at room temperature for 7 days until completion of the reaction. The azeotropic mixture (toluene and methanol 9:1) was used to remove EDA by rotary evaporation. Then, the product was washed with methanol. This process was repeated until the EDA was fully removed. Afterward, the product was dried under high vacuum for 4 hours, G3.0 PAMAM dendron was yield as white sticky coloured oil

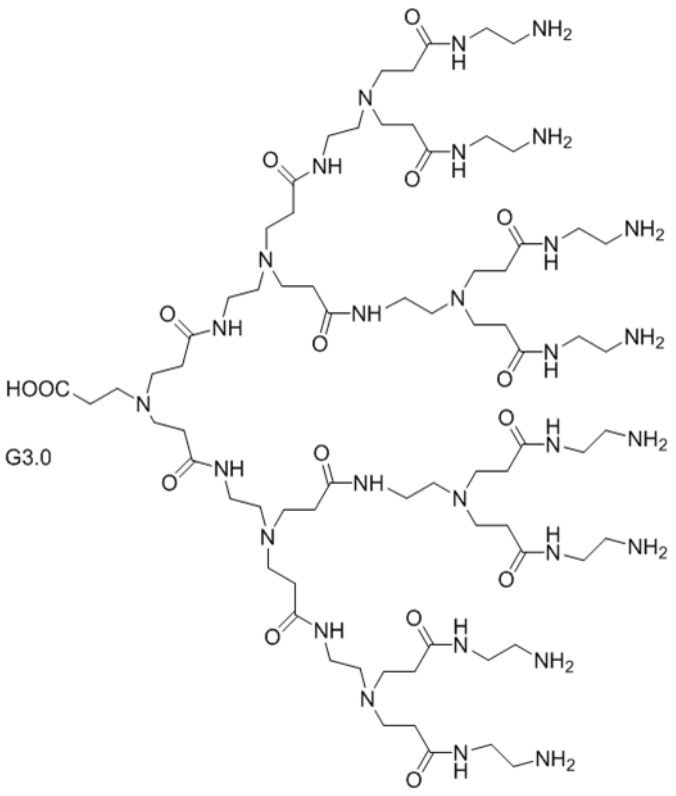

MS -MALDI-TOF,1688 (MH^{+}), ^{1}H NMR (D_2O, 400MHz) δ 3.19 (12H, t, J = 7.0), 3.1 (16H, t, J = 7.0 Hz,), 2.62-2.71(30H, m), 2.52-2.58 (16H, m), 2.48 (12H, t, J = 7.0 Hz), 2.28(28H, br m), 2.21 (t, J = 7.0 Hz, 2H); ^{13}C NMR (D20, 400MHz) δ ppm 181.1, 175.3, 174.7, 164.8, 164.2,

51.8, 48.3, 43.9, 41.3, 39.7, 36.2, 32.6; FTIR (cm^{-1}) 3260 (amide stretch), 3061(acid OH), 2929(CH-sp^2), 2822(CH-sp^3), 1632(amide carbonyl bend), 1547(amide bend).

6.3.31 Synthesis of PAMAM dendron G 3.5 with 16terminal OMe terminal groups

In a 250 mL round bottom flask, G3.0 PAMAM dendron (2.5g, 1.5 mmole) was dissolved in methanol (40mL). Methyl acrylate (2.55, 0.061moles) was added drop-wise over 30 minutes at 0^{o}C. Then, the reaction mixture was stirred at room temperature for 4 days. Excess amounts of methyl acrylate and methanol were removed by rotary evaporation. The product was dried under high vacuum for 4 hours to obtain the final product (3.98g, 92%), as a sticky deep honey coloured oil.

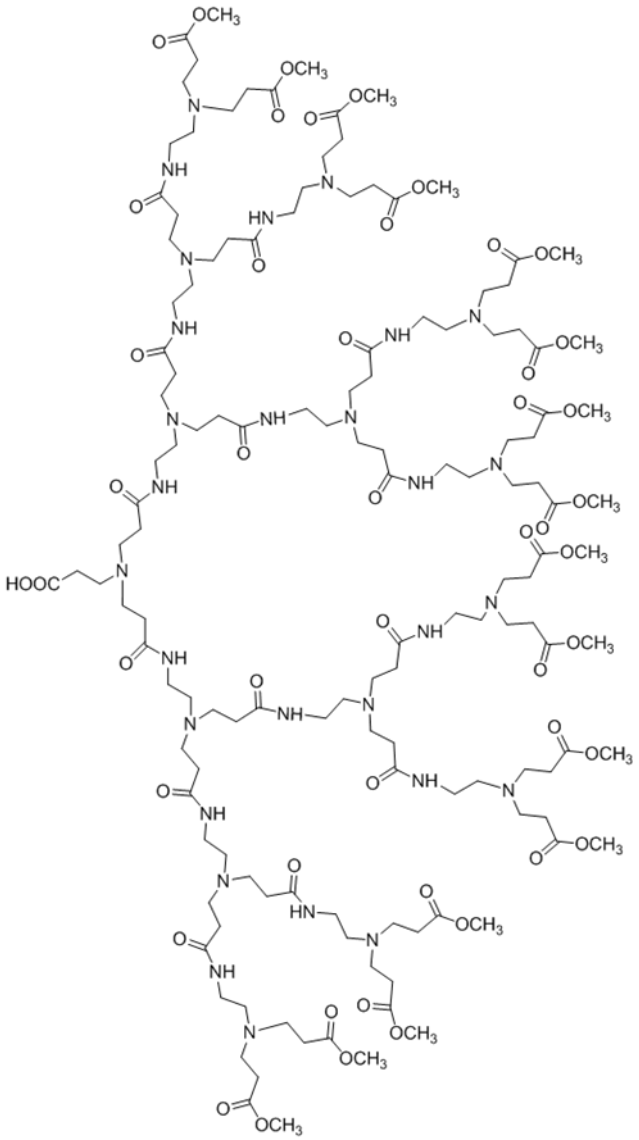

ES-MS: 3064(MH^+),^{1}HNMR($CDCl_3$, 400MHz) δH 3.66(48H, s), 2.20-2.36(br m, 2H)2.36-2.3 (66H, br, m,)2.41(24H, t, J = 7.0 Hz), 2.77-2.48(60H,m), 3.09-3.15(28H, m); 13C-NMR(CDCl3, 400MHz) δc 178.42, 176.9, 173, 172.67, 52.7, 51.7, 50.54, 49.24, 48.96, 32.7, 32.22, 32.2, 31.52; FTIR λ max (cm-1) 3283(acid O - H stretch), 2953(CH - sp^2), 2831(CH - sp^3), 1638(amide carbonyl stretch), 1730(ester carbonyl), 1532, 1436.14(acid carbonyl stretch), 1358,(acid O - H bend), 1199(-C-N stretch), 1041.

6.3.32 Synthesis of Di-hydroxytetraphenylporphyrintin (1V) [Sn(OH)2TPP]

Tetraphenylporphyrin (500mg, 0.8mmoles) was dissolved in pyridine (50mL) and tin (II) chlorodedihydrate (400 mg, 0.026mmole) was added to the TPP solution. The reaction mixture was heated at refluxing at115^{o}C for 1 hour. After that, the solution was cooled at 50^o C and then concentrated ammonia NH_3 (25mL) was added very cautiously. The reaction was stirred for another hour, then, distilled water (300mL) was added to the reaction mixture, filtered and washed with water. Following this, the compound was dried by suction, and dissolved in chloroform (120mL) that dissolves the purple product, leaving a brown residue of tin salts. The reaction mixture was dried with anhydrous Na_2SO_4 and concentrated to 10 mL by a rotary evaporator. Hereafter, the concentrated mixture was passed through a short column of neutral alumina (100g) in chloroform, the $CHCl_3$ was used as elute and the purple band was concentrated to 6mL. Hexane (100mL) was sensibly layered on top of the $CHCl_3$ solution, the flask was closed by stopper, and the mixture left to crystallize for 2 days. The product was filtered, washed by hexane, and the dried product (0.27g, 43%) was purple crystals.

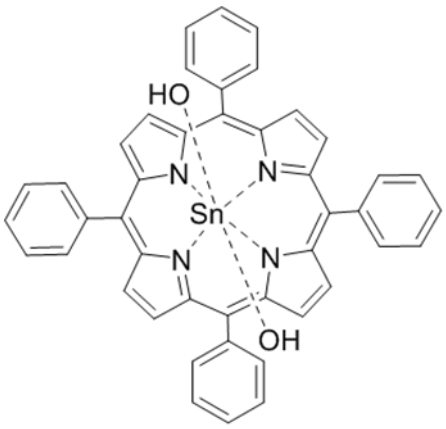

$TPPSn(OH)_2$

MALDI-TOF-MS; obtained 749 ($M\text{-}OH^+$) the compound had identical ^{1}HNMR properties to those reported by Arnold (d - $CDCl_3$, 400MHz) δ 9.17 (8H, s, β-pyrrol H), 8.30-8.39 (8H, m, ortho Ar-H), 7.80-7.86 (12H, meta and para Ar-H); ^{13}C -NMR (d - $CDCl_3$, 400MHz) δ ppm 144.6, 142.0, 132.0, 131.4, 126.0, 125.8, 122.0; FTIR (cm^{-1}); 3622, 3108, 2921, 1651, 1595, 1466, 1038, 1068; UV/Vis Spectroscopy: 427, 562, 601.

6.3.33 Self-assembly of PAMAM dendrons (2 terminal ester terminal groups) with dihydroxytetraphenylporphyrintin(1V) [$Sn(OH)_2$TPP]

In a 25 mL round bottom flask, G-0.5 PAMAM Dendron with 2 terminal ester terminal groups (42 mg, 0.16 mmol), and $TPPSn(OH)_2$ (60 mg, 0.08 mmol) were dissolved in $CHCl_3$ (5 mL) and stirred at room temperature for an hour. After this, the mixture was passed through a small plug of anhydrous Na_2SO_4 (0.3g) into a round bottom flask. The solvent was removed by rotary evaporator. The product (0.095g, 94%) was obtained as a sticky purple coloured oil.

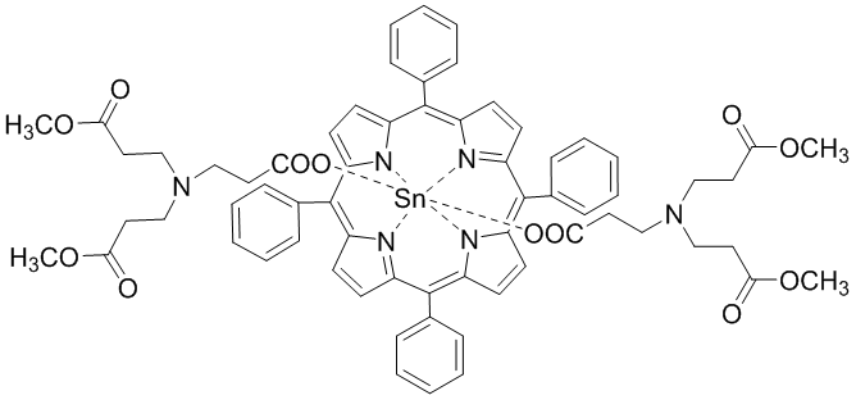

MS-(MALDI-TOF): 991$(M\text{-}G\text{-}0.5)^+$ (obtained) and 1261(calculated); ^{1}HNMR(d - $CDCl_3$,400MHz) δ 3.68 (12H, s), -(0.71-0.76) (1H ,m), -(0.34-0.39) (1H, m), 0.85-0.94 (m, 2H), 1.59-1.54 (4H, m), 1.32 (2H, br s), 2.49 (6H,t, J = 7.0 Hz), 2.76-2.68 (8H, m), 7.88-7.83 (12H, m), 8.4-8.2 (8H, m), 9.13-9.17 (8H, m); ^{13}C NMR(d -$CDCl_3$, 400MHz) δ ppm 173.3, 168.3 146.7, 141.2, 135.0, 132.7, 128.3, 127.8, 121.4, 51.9, 48.9, 47.9, 32.3, 31.4, 26,85, 22.8; UV–vis ($CHCl_3$): λ max (nm); 424, 517, 560, 600.

6.3.34 Self-assembly of PAMAM Dendrons (4 terminal ester terminal groups) with dihydroxytetraphenylporphyrintin(1V) [Sn(OH)2TPP]

In a 25 mL round bottom flask, G-1.5 PAMAM Dendron with 4 terminal ester terminal groups (106mg, 0.16 mmol) and $TPPSn(OH)_2$ (60mg, 0.08mmol) were dissolved in $CHCl_3$ (5mL) and stirred at room temperature for an hour. After this, the mixture was passed through a small plug of anhydrous Na_2SO_4 (0.3g) into a round bottom flask. The solvent was removed by rotary evaporator. The product (120mg, 73%) was obtained as a sticky purple oil.

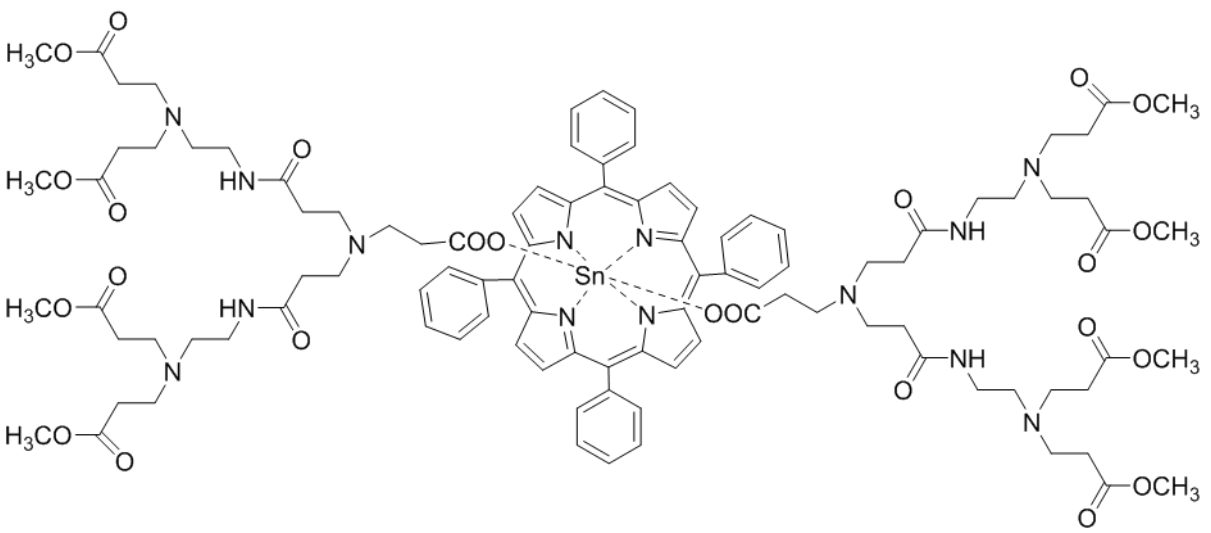

MS-(MALDI-TOF): 1392(M-G-1.5$^+$) (obtained) and 2054(calculated); ^{1}HNMR(d - $CDCl_3$, 400MHz) δ 3.70 (s, 24H), -(0.69-0.74) (m, 1H,), -(0.34-0.39) (m, 1H), 0.94-0.85 (m, 1H,), 1.56 (t, J = 6.9 Hz, 4H), 2.26 (t, J = 6.8 Hz, 6H), 2.83-2.45 (m, 38H), 2.2(t, J = 7.2 Hz, 4H), 2.42 (t, J = 6.9 Hz, 4H), 3.32-2.91 (mm, 8H), 7.80-7.91 (m, 12H), 8.20-8.41 (m, 8H), 9.24 (s, 8H); ^{13}C-NMR(d-$CDCl_3$, 400MHz) δ ppm 173.0, 168.7, 146.7, 141.3, 135.1, 132.5, 128.2, 126.9, 121.2, 51.6, 48.9, 47.6, 32.2, 31.8, 29.7, 21.3; UV–vis ($CHCl_3$): λ max (nm) ;424, 518, 559, 599.

6.3.35 Self-assembly of PAMAM Dendrons (8 terminal ester terminal groups) with dihydroxytetraphenylporphyrintin(1V) [$Sn(OH)_2TPP$]

In a 25 mL round bottom flask, G-2.5 PAMAM Dendron with 4 terminal ester terminal groups (234 mg, 0.16 mmol) and $TPPSn(OH)_2$ (60 mg, 0.08 mmol) were dissolved in $CHCl_3$ (5 mL) and stirred at room temperature for an hour. After this, the mixture was passed through a small plug of anhydrous Na_2SO_4 (0.3g) into a round bottom flask. The solvent was removed by rotary evaporator. The product (0.195g, 66%) was obtained as a sticky purple oil.

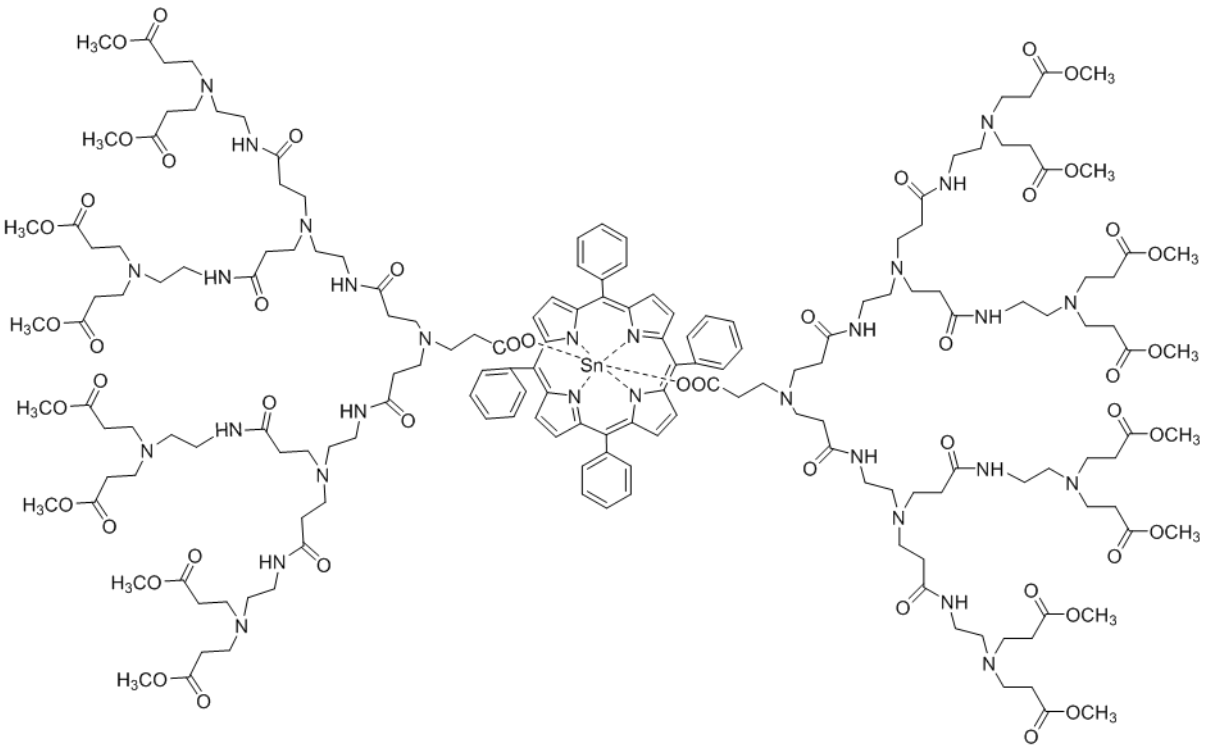

MS-(MALDI-TOF) 2194(M-G2.5^{+}) (obtained) and 3654 (calculated) ; ^{1}HNMR (d - $CDCl_3$, 400MHz) δ 3.64 (48H, s), -0.90 (1H , t, J = 7.0 Hz), -0.31 (1H , t, J = 7.8 Hz), 1.31 (2H ,t, J = 7.4 Hz), 1.45 (2H, t, J = 7.0 Hz), 2.09-2.14 (6H, m), 2.21-2.43 (54H, mm), 2.46-2.56 (26H , m), 2.48-2.75(76H, m), 3.03-3.12 (6H,m), 3.10-3.26 (16H ,m), 7.81-7.90(12H, m), 8.21-8.42 (8H, m), 9.08-9.19 (8H, m); ^{13}C - NMR(d - $CDCl_3$, 400 MHz) δ ppm 173.1, 168.9, 147.1,146.5, 141.1, 135.1, 132.8, 128,5, 127.6, 121.4, 51.8, 51.7, 49.0, 37.0, 32.2, 31.9, 29,7, 21.3; UV–vis ($CHCl_3$): λ max (nm) 424, 517, 559, 598.

6.3.36 Self-assembly of PAMAM dendrons (16 terminal ester terminal groups) with dihydroxytetraphenylporphyrintin(1V) [Sn(OH)$_2$TPP]

In a 25 mL round bottom flask, G-3.5 PAMAM Dendron with 4 terminal ester terminal groups (490mg, 0.16mmol) and TPPSn(OH)$_2$ (60 mg, 0.08 mmol) were dissolved in $CHCl_3$ (5mL) and stirred at room temperature for an hour. After this, the mixture was passed through a small plug of anhydrous Na_2SO_4 (0.3g) into a round bottom flask. The solvent was removed by rotary evaporator. The product (0.39, 71%) was obtained as a sticky purple oil.

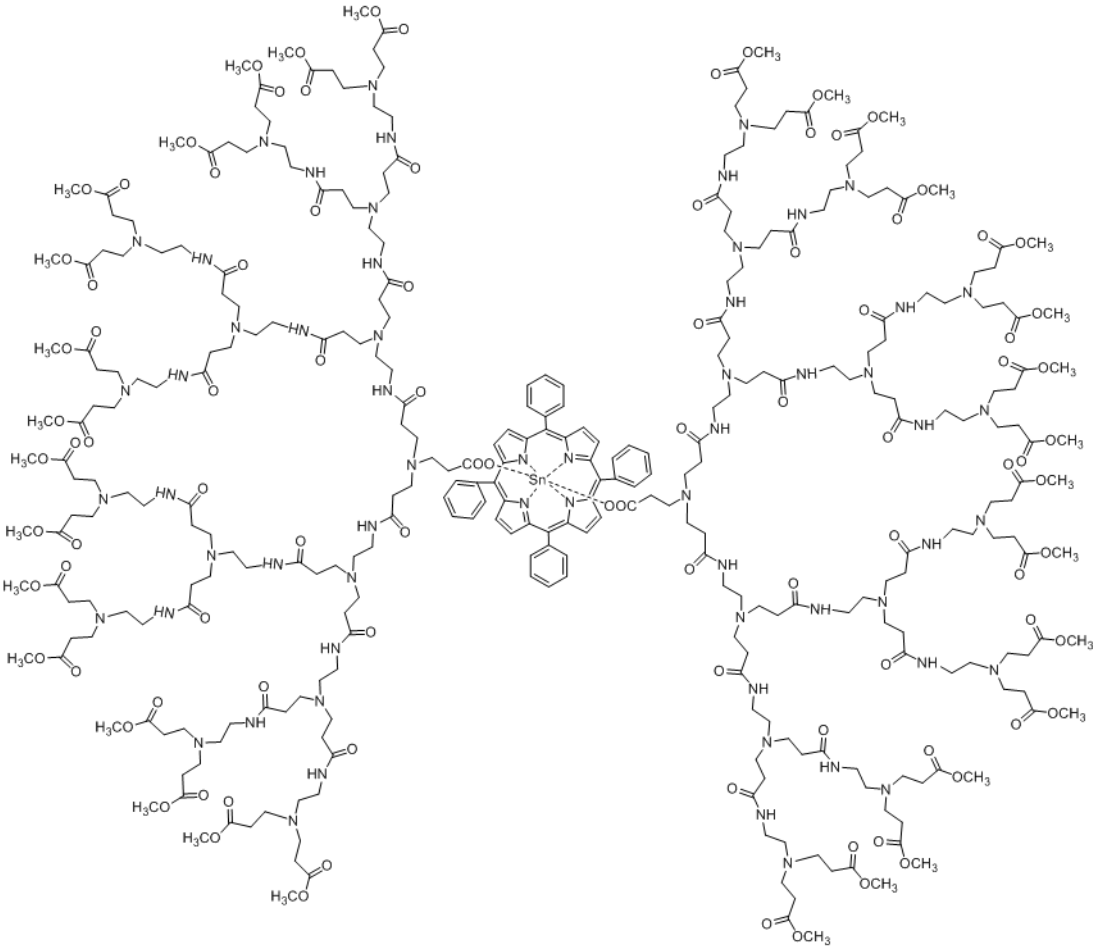

MS-(MALDI-TOF) 3853 (obtained) and (calculated) ; ^{1}H NMR(d - $CDCl_3$, 400MHz) δ 3.64 (96H, s), -0.95(1H, t, J = 7.0 Hz), -0.31(1H, t, J = 7.8 Hz), 0.8 (4H, t, J = 7.4 Hz), 1.30 (4H, t, J = 7.4 Hz), 1.47 (8H, t, J = 7.0 Hz), 2.09-2.15 (12H, m), 2.22-2.44 (122H, mm), 2.48-2.58 (178H, m), 2.47-2.8 (168H, m), 3.07-3.11 (6H, m), 3.19-3.27 (48H, m), 7.84-7.90 (12H, m), 8.21-8.40 (8H, m), 9.08-9.16 (8H, m); ^{13}C NMR(d - $CDCl_3$, 250 MHz) δ ppm 172.2, 168.7, 148.2,146.9, 141.5, 140.8, 132.0, 128.2 , 127.8, 126.3, 53.3, 51.9, 52.2, 49.3, 36.6, 34.04, 31.0, 29,7, 22.4; UV–vis ($CHCl_3$): λ max (nm) 424, 516, 559, 601.

6.3.37 Imaging protocol

A stock solution of the compound was made at 5mM in DMSO Sterilised coverslips (15mm by 15mm) were placed flat in 6 well dishes. Cells (HeLa) were seeded at 150,000 cells/well in cell culture media (DMEM with 10 % FCS) and left to adhere overnight in the incubator (37 ºC, 5% CO_2). The compound was diluted into the cell culture media (DMEM with 10% FCS) to the staining concentration (2 μM) and added to the cells (2 mL/well) and left for 2 hours in the

incubator. The cells were washed (3 X with PBS) and the cells were fixed using paraformaldehyde (4% in PBS, 1 mL/well, 20 mins) and the cells were washed again (3 X PBS) before the coverslips were mounted onto glass microscope slides (immu-mount).

6.3.38 Synthesis of 3-pentyloxy phthalonitrile

3-Pentyloxy phthalonitrile was synthsised by addition of 3-Nitrophthalonitrile (1g, 5.77mmol) and 1-pentanol (1.25mL, 11.54mmol) to 12mL of DMSO contained in 100mL dry round bottom flask under a nitrogen atmosphere. The reaction mixture was stirred for 5 minutes and potassium carbonate (1.6g, 11.54mmol) was added to the reaction mixture, then reaction was left to reflux for 4 h at 90^{o}C. After this, the reaction mixture was cooled and water (150mL) was added. The solution was stirred strongly for 15 minutes at room temperature. The reaction mixture was then filtered and washed with water. The crude product was purified on silica-gel column with chloromethane to give a pure compound (0.34, 27%).

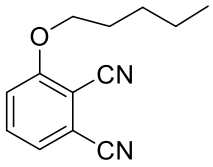

ES-MS, 215(MH^+)^{1}HNMR(d-$CDCl_3$,400MHz) δ 7.65-7.62 (1H, dd), 7.368-7.342 (1H, dd), 7.25-7.22 (1H, d), 4.14 (2H, t), 1.89-1.92 (m, 2H), 1.54-1.35 (m, 3H), 0.96 (t, 2H, J = 7.2 Hz); ^{13}C-NMR(d-$CDCl_3$, 400MHz) δ ppm 161.51, 135.3,134.4, 130.0, 124.9, 122.0, 117.1, 116.0, 115.4, 113.1, 104.9, 69.9, 28.4, 27.9, 22.31, 13.9; FTIR λ max(cm^{-1}): 3087(s), 2958(s), 2934, 2861, (alkyl H-C-H stretch), 2237, 2226 (-C-N- stretch), 1579.3, 1397, 1472.28 (alkane bend), 1052 (ester stretch), 795.26 (aromatic bend).

6.3.39 Dichloride-tetra-(α-pentyloxy) tin(IV) phthalocyanine

3-Pentyloxy phthalonitrile (429mg, 4mmol), and tin(II)chloride (190.0mg, 1mmol) were dissolved in 5 mL 1-chloronaphthalene (1-CNP) and then the reaction mixture was refluxed at 250^{o}C for 5 hours under nitrogen. After that, the reaction mixture was cooled and

chromatographed with hexane to remove 1-CNP. The column was then eluted with dichloromethane. The solvent was removed via rotary evaporator and the product was obtained and washed with hot methanol to yield a dark green product.

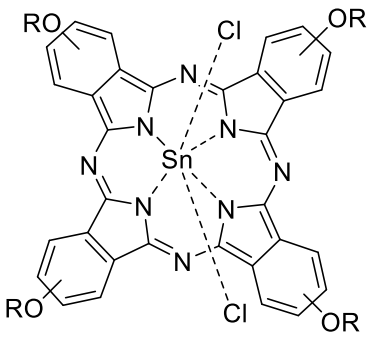

ESI-MS:1008 ($M\text{-}Cl^{+}$) (obtained), 1044 (calculated): ^{1}H NMR (d - $CDCl_3$, 400 MHz) δ 9.34-9.16 (4H, m), 8.33-8.21 (4H, m), 7.88-7.80 (m, 4H), 4.98-4.75 (dm, 8H), 2.47-2.33 (m, 8H), 1.87-1.53 (m, 16H), 1.23-1.01(dm, 12H); ^{13}C -NMR (d-$CDCl_3$, 400MHz) δ ppm 157.9, 152.1, 148.2, 134.4, 116.6, 114.4, 110.0, 104.0, 70.9, 57.3, 29.7, 29.0, 28.6, 27.7, 23.0, 13.9 ; FTIR (cm^{-1}); 3198, 2927, 2858 (w), 1583 (s), 1489, 1466, 1336, 1266.4, 1231, 1116, 1075.8, 874; UV–vis ($CHCl_3$): λ max (nm) 347, 676, 744.

6.3.40 Self-assembly of 2 terminal OMe terminal groups PAMAM dendrons with tin(phthalocyanato)dichloride

In a 25mL round bottom flask, G-0.5 PAMAM dendron (5mg, 0.02mmol) and, $SnPc(Cl)_2$ (10 mg, 0.01mmol) were dissolved in $CHCl_3$(10 mL). The reaction mixture was stirred at room temperature for an hour. After that, the mixture was passed through a small plug of anhydrous Na_2SO_4 (0.5g) into a round bottom flask. The solvent was removed by rotary evaporator to give product as very a sticky green coloured oil.

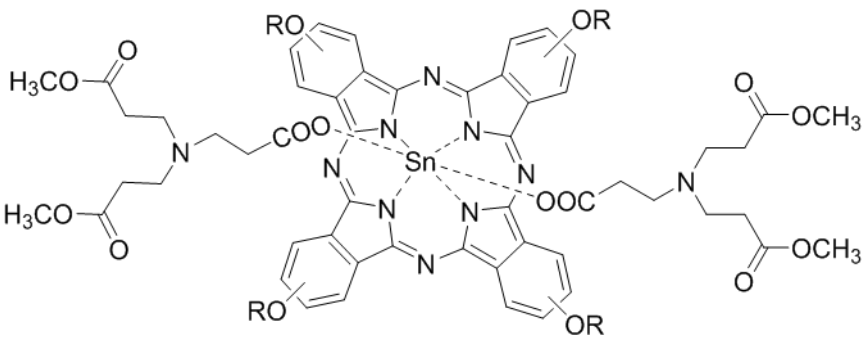

The structure of complex was confirmed by, MS- MALDI-TOF: 1237 (M-G0.5^{+}) (obtained), 1497(calculated). 1H NMR (d - CDCl3, 400MHz) δ - (0.12-0.2) (m,1H), 0.71-0.80 (t, 2H), 0.99-1.21 (mm, 16H), 1.54-2.10 (m, 27H), 2.18 (s, 4H), 2.28-2.60 (m, 13H), 3.67 (s, 12H), 4.69 -5.11(m, 6H), 7.71-7.89 (m, 4H), 8.21-8.30 (m, 4H), 9.14-9.35 (m, 4H). 13C-NMR (D - CDCl3, 400MHz) δ ppm 172.8, 157.3, 153.6, 143.3, 132.4, 119.9, 111.0, 71.8, 70.7, 58.9, 51.3, 48.3, 40.3, 29.5, 27.9, 22.8, 21.6, 14.1; FTIR (cm^{-1}): 2850, 2819 (w), 1728 (s), 1639, 1588(s), 1531, 1479, 147; 1248; UV–vis (CHCl3): λ max (nm) 327, 664, 740.

6.3.41 Self-assembly of 4 terminal OMe terminal groups PAMAM dendrons with tin(phthalocyanato)dichloride

Using a 25 mL round bottom flask, G-1.5 PAMAM dendrons (13.2mg, 0.02mmol) and, $SnPc(Cl)_2$ (10 mg, 0.01mmol) were dissolved in $CHCl_3$(10mL). The reaction mixture was stirred at room temperature for an hour. After that, the mixture was passed through a small plug of anhydrous Na_2SO_4 (0.5g) into a round bottom flask. the solvent was removed by rotary evaporator to give product as a very sticky green oil.

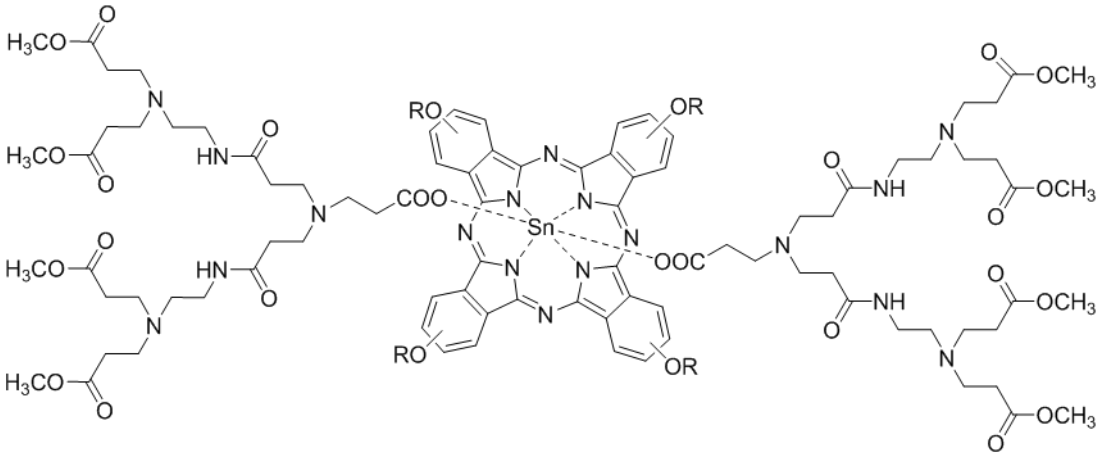

The structure of the complex was confirmed by MS- MALDI-TOF :1636(M-G1.5^{+}) 100% ,(2030) 25% (obtained) and 2296 (calculated) .^{1}H NMR(d - $CDCl_3$, 400MHz) δ -(0.70-0.72) (3H, m), 0.86-0.89 (18H, m), 1.46-1.38 (8H, m), 1.47-1.54 (24H, m), 2.08-2.199 (20H, m), 2.45-2.28 (36H, m),3.60 (24H, s), 4.63-4.72 (6H, m), 7.70-7.74 (4H, m), 8.20-8.23 (4H, m), 9.16-9.21(4H, m); ^{13}C - NMR(d-$CDCl_3$, 400MHz) δc173.1, 172.48, 171.94, 166.63, 154.09, 153.5, 145.73, 145.19, 136.26, 131.91,129.79,127.9 118.6, 115.6, 69.3, 53.07, 49.39, 49.2, 48.3, 46.8, 36.9, 36.8, 33.0, 32.7, 32.6, 32.4, 30.5, 29.8, 28.8, 28.2, 28.1, 23.0, 22.7, 14.31; FTIR λ max(cm)$^{-1}$: 2853, 2825(w), 1731(s), 1643, 1590(s), 1537, 1493, 1435 ; UV–vis (CHCl3): λ max (nm) 328, 668, 745.

6.3.42 Self-assembly of 8 terminal OMe terminal groups PAMAM dendron with tin(phthalocyanato)dichloride

Using a 25 mL round bottom flask, G-2.5 PAMAM dendrons (29.24mg, 0.02mmol) and $SnPc(Cl)_2$ (10mg, 0.0mmol) were dissolved in $CHCl_3$(10mL). The reaction mixture was stirred at room temperature for an hour. After that, the mixture was passed through a small plug of anhydrous Na_2SO_4 (0.5g) into a round bottom flask. The solvent was removed by rotary evaporator to yield a product as a very sticky green coloured oil.

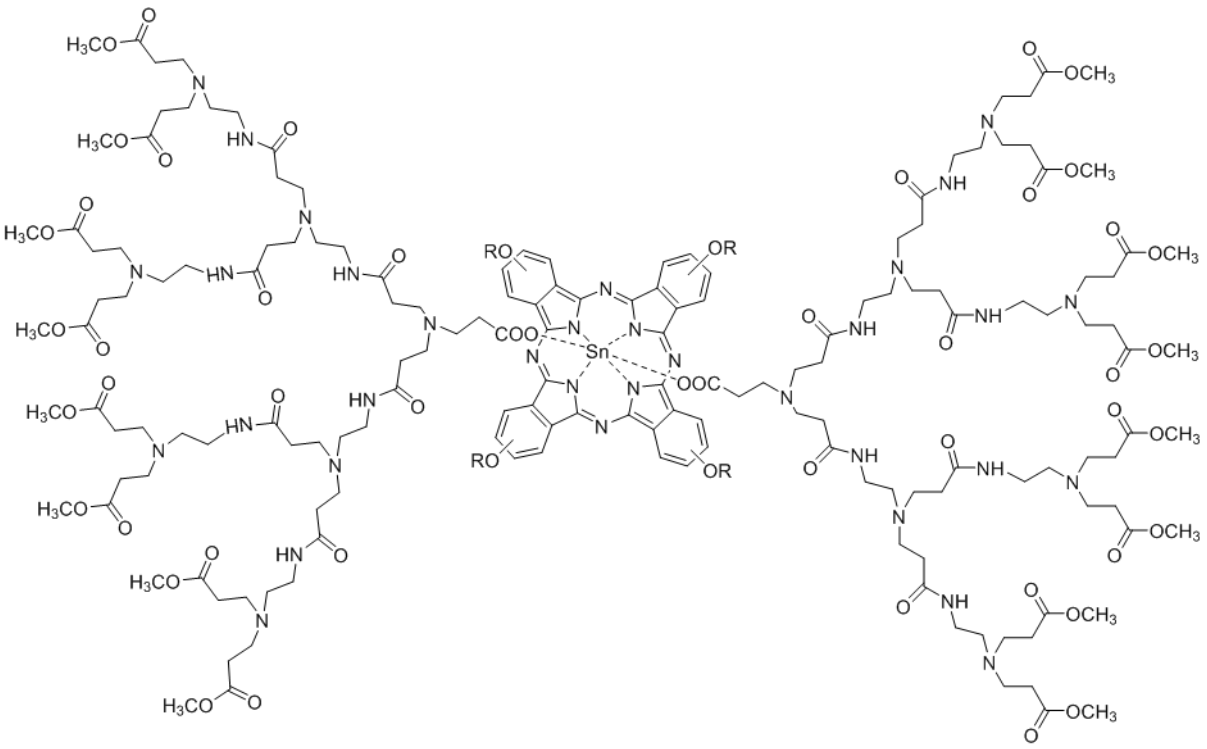

MS-MALDI-TOF: 2436 (M-L) (found), 4898 (calculated), ^{1}H NMR(d - $CDCl_3$, 400MHz) δ 0.7-0.805 (4H, m), 0.93-0.99 (6H, m), 1.4-1.62 (22H, m), 2.2-2.7 (118H, mm), 3.04-3.2 (28H, m), 3.24-3.6 (34H, m), 4.3-4.99 (6H, m), 7.70-7.81(4H, m), 8.26-8.1(4H, m), 8.9-9.2 (4H, m); ^{13}C – NMR (d - $CDCl_3$, 400 MHz) δ ppm 173.3, 172.8, 170.0, 152.5, 147.1,139.5, 131.5, 129.1, 115.9, 113.4,104.0, 69.5, 67.3, 56.0, 49.2, 42.0, 37.1, 29.9, 21.9, 14.3 ; FTIR λ max(cm^{-1}): 2853, 2825 (w), 1731 (s), 1643, 1590 (s), 1537, 1493, 1435; UV–vis ($CHCl_3$): λ max (nm) 328, 667.5, 744.5.

6.3.42 Self-assembly of 16 terminal OMe terminal groups PAMAM dendrons with tin(phthalocyan)dichloride

Using a 25mL round bottom flask, G-3.5 PAMAM dendron (61.28mg, 0.02mmol) and $SnPc(Cl)_2$ (10mg, 0.01mmol) were dissolved in $CHCl_3$(10mL). The reaction mixture was stirred at room temperature for an hour. After that, the mixture was passed through a small plug of anhydrous Na_2SO_4 (0.5g) into a round bottom flask. The solvent was removed by rotary evaporator to give product as very sticky green oil.

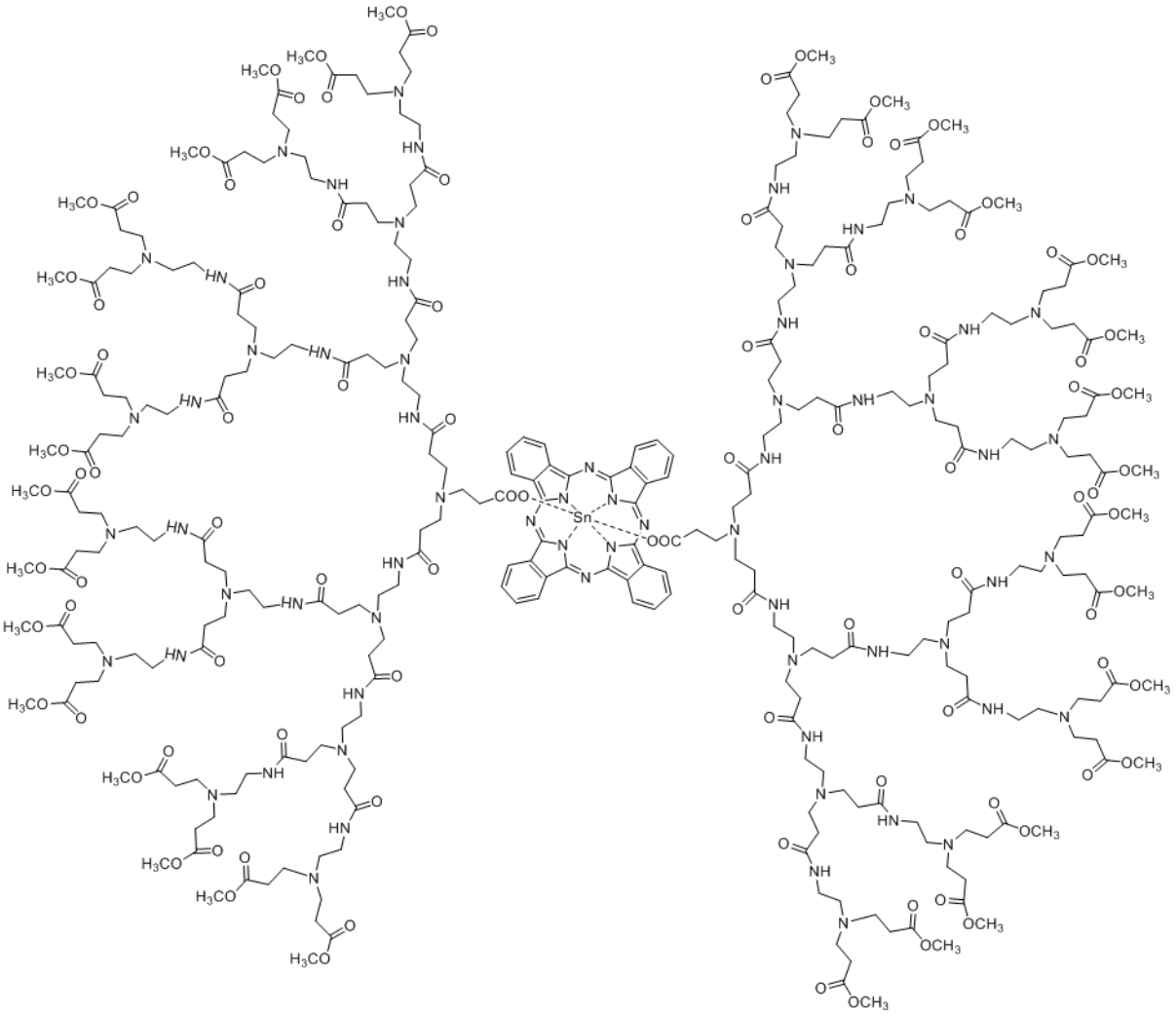

MS-MALDI-TOF: 3096 (obtained),7100(calculated), ^{1}H NMR(d - $CDCl_3$, 400MHz) δ 0.61-0.84(8H, m), 0.85-0.98 (12H ,m), 1.55-2.22 (22H ,m), 2.25-2.88 (234H, mm), 3.23-3.37(56H, m), 3.56-3.66(35H, m), 4.3-5.25 (12H, m), 7.70-7.80 (4H, m), 8.22-8.31 (4H, m), 8.91-9.3(4H, m); ^{13}C – NMR (d - $CDCl_3$, 400 MHz) δ ppm 173.9, 173.3, 172.0, 159.0, 152.9, 151.2, 145.81, 136.74, 135.4, 125.31, 119.23, 117.08,113.39,100.92, 70.0, 69.5, 53.31, 52.88, 51.56, 49.84, , 48.9, 36.6, 32.9, 29.2, 28.4, 27. 1, 22.3, 14.3; FTIR λmax$(cm)^{-1}$: 2853, 2825 (w), 1731 (s), 1643, 1590 (s), 1537, 1493, 1435; UV–vis (CHCl3): λ max (nm) 327, 664, 740.

6.3.44 Synthesis and Purification of PAMAM-OH Dendron

In a round bottom flask, G2.5 PAMAM ester terminal dendron (2.34g, 0.83mmol) was dissolved in minimum amount of DMSO (5ml). The ethanolamine (1.05g, 0.017mol) and potassium carbonate (2.35g, 0.017mol) were added and the reaction mixture was stirred and

refluxed at 50^{o}C for 3 days under nitrogen condition. Then, the solution was filtered to remove any remaining solid substances. After this, the filtered product was washed twice by acetone and the acetone layer was poured off and the obtained product was dissolve in minimum quantity of distilled water. Following this, the dissolved compound was precipitated using acetone and left to settle for 2 hours. Then, the acetone layer was poured off and the product was then dried using rotary evaporator and ultra-high vacuum. Lastly, the product was dried by freeze dryer to obtain the desired product G2.5 PAMAM dendron with eight-OH end groups (2.56g, 92.9 %) as viscous orange oil.

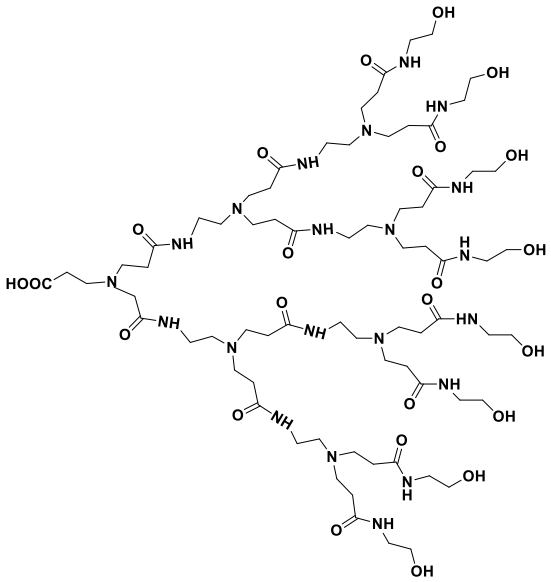

(14)

TOF MALDI-MS, 1694 (MH^+);^{1}H NMR (D2O, 400 MHz), δ 3.57 (16H, t, J= 5.47 Hz), 3.23 (28H, m), 2.74 (28H, t, J=6.80), 2.52 (12H, t, J= 6.66), 2.35 (56H, t, J =7.17 Hz); ^{13}C NMR (D2O, 400MHz,), δ ppm 175.1 (C=O), 174.6 (C=O), 59.9, 51.3, 49.0 ,41.4, 38, 36.8 ,32.7; FTIR (cm^{-1}) 3297 (N-H, amide stretch), 2949, 1639 (C=O, amide), 1556 (N-H, amide bend), 1441, 1320, 1069, 1091.

Chapter 7

References

References

1. C. Yiyun, X. Tongwen, European journal of medicinal chemistry, 2005, **40**, 1188-1192.
2. J. A. K. Twibanire and T. B. Grindley, Polymers, 2014, **6**, 179-213.
3. H. Min, Y. Z. Heng, X.Y. Li, J. D. Zhi, J. Z. Rui, L. Yu, European Journal of Organic Chemistry, 201, **36**, 7271-7277.
4. G. Thomas, Medicinal chemistry, John Wiley and Sons, 2011.
5. C. Wischke, S.P. Schwendeman, International Journal of pharmaceutics, 2008, **364**, 298-327.
6. S. S. Lucky, K. C. Soo, Y. Zhang, Chemical reviews, 2015, **115**, 1990-2042.
7. S. Kannan , P. Kolhe , V. Raykova, M. Glibatec , R. M. Kannan, M. L . Lai and D. Bassett Journal of Biomaterials Science, Polymer Edition. 2004, **15**, 311-330.
8. A. Juarranz, P. Jaen, F. S. Rodriguez, J. Cuevas, and S. Gonzalez, Clinical and Translational Oncology, 2008, **10**, 148-154.
9. M. Ethirajan, Y. Chen, P. Joshi and R. K. Pandey, Chemical Society Reviews, 2011, **40**, 340-362.
10. Y. Cheng, A. C. Samia, J. D. Meyers, I. Panagopoulos, B. Fei, and C. Burda, Journal of the American Chemical Society, 2008, **130**, 10643-10647.
11. M. Dabrzalska, M. Zablocka, S. Mignani, J. P. Majoral, B. K. Maculewicz, International journal of pharmaceutics, 2015, **492**, 266-274.
12. A. Weiss, J. R. v.Beijnum, D. Bonvin, P. Jichlinski, P. J. Dyson, A. W. Griffioen, P. N. Sliwinska, Journal of cellular and molecular medicine, 2014, **18**, 480-491.
13. Y. H. Jeong, H. J. Yoon and W. D. Jang, Polymer journal, 2012, **44**, 512-521.
14. P. Agostinis, K. Berg, K. A. Cengel, T. H. Foster, A. W. Girotti, S. O. Gollnick, S. M. Hahn, M. R. Hamblin, A. Juzeniene, D. Kessel, M. Korbelik, J. Moan, P. Mroz, D. Nowis, J. Piette, B. C. Wilson, J. Golab, CA, a cancer journal for clinicians, 2011, **61,** 250-281.
15. G. M. F. Calixto, J. Bernegossi, L. M. d. Freitas, C. R. Fontana, and M. Chorilli, A review Molecules, 2016, **21,** 342.
16. J. Bhaumik, A. K. Mittal, A. Banerjee, Y. Chisti, and U. C. Banerjee, Nano Research, 2015, **8**, 1373-1394.
17. H. Maeda, G. Y. Bharate, J. Daruwalla, European Journal of Pharmaceutics and Biopharmaceutics, 2009, **71**, 409-419.
18. S. H. Battah, C. E. Chee, H. Nakanishi, S. Gerscher, A. J. M. Robert, and C. Edwards, Bioconjugate chemistry, 2001, **12**, 980-988.
19. G. M. F. Calixto, J. Bernegossi, L. M. d. Freitas, C. R. Fontana and M. Chorilli, Molecules, 2016, **21**, 342.
20. R. Elena, Journal of Photochemistry and Photobiology B: Biology., 1997, **37**, 189-195.
21. Z. Hu, Y. Pan, J. Wang, J. Chen, J. Li, L. Ren, Biomedicine and pharmacotherapy., 2009, **63**, 155-164.
22. J. Moan, Lasers in Medical Science, 1986, **1**, 5-12.
23. J. Voskuhl ,U. Kauscher, M. Gruener, H. Frisch, B.Wibbeling, C. A. Strassert, and B. J. Ravoo, Soft Matter, 2013, **9**, 2453-2457.

24. F. Danhier, O. Feron,V. Preat, Journal of Controlled Release, 2010, **148**, 135-146.
25. J.D. Byrne ,T. Betancourt, L. B. Peppas, Advanced drug delivery reviews, 2008. **60**, 1615-1626.
26. E. P. Herrero, A. F. Medarde, European journal of pharmaceutics and biopharmaceutics, 2015, **93**, 52-79.
27. P. S. Lai, P. J. Lou, C. L. Peng, C. L. Pai, W. N .Yen, M. Y. Huang, T. H. Young, M. J. Shieh, Journal of Controlled Release, 2007, **122**, 39-46.
28. V. Torchilin, Advanced drug delivery reviews, 2011, **63**, 131-135.
29. S. L. Mekuria, T. A. Debele and H. C. Tsai, RSC Advances, 2016, **68**, 63761-63772.
30. M. Schappacher, A. Deffieux, J. L. Putaux, P. Viville, and R. Lazzaroni, Macromolecules, 2003, **36**, 5776-5783.
31. B. A. R. Hassan, Overview on Drug Delivery System, Pharmaceut Anal Acta, 2012, **3,** 1.
32. J. Panyam, V. Labhasetwar, Advanced drug delivery reviews, 2003, **55**, 329-347.
33. K. Chen, S. Pan, X. Zhuang, H. Lv, S. Que, S. Xie, H. Yang, Y. Peng, Journal of Nanoparticle Research, 2016, **7**, 1-9.
34. J. Safari, Z. Zarnegar, Journal of Saudi Chemical Society, 2014, **18**, 85-99.
35. L. Y. Qiu, Y. H. Bae, Pharmaceutical research, 2006, **23**, 1-30.
36. J . Khandare, and M. Calderón, Nanoscale, 2015, **7**, 3806-3807.
37. J . Huwyler, D. Wu and W. M. Pardridge, Proceedings of the National Academy of Sciences, 1996, **93**, 14164-14169.
38. S. M. Barros, S. K.Whitake, P. Sukthankar, L. Avila, S. Gudlur, M. Warner, E. I. C. Beltrao, J. M. Tomich, Archives of biochemistry and biophysics, 2016, **596**, 22-42.
39. R. Haag, F. Kratz, Angewandte Chemie International Edition, 2006, **45**, 1198-1215.
40. C. M. Paleos, D. Tsiourvas, and Z. Sideratou, Molecular pharmaceutics, 2016, **13,** 2233-2241.
41. Y. Malam, M. Loizidou, A. M. Seifalian, Trends in pharmacological sciences, 2009, **30**, 592-599.
42. Y. Cheng, L. Zhao, Y. Li , and T. Xu, Chemical Society Reviews, 2011,**40**, 2673-2703.
43. V. T. Huynh, G. Hen, P. d. Souza, and M. H. Stenzel, Biomacromolecules, 2011, **12**, 1738-1751.
44. A. K. Patri, I. J. Majoros, J. R. B. Jr, Current opinion in chemical biology, 2002, **6**, 466-471.
45. A. N. Lukyanov, V . P. Torchilin, Advanced drug delivery reviews, 2004, **56**, 1273-1289.
46. R. V. Vasant, M. A. Hollinger, Drug delivery systems, CRC press, 2004.
47. C. K. Nguyen, N. Q. Tran, T. P. Nguyen, D. H. Nguyen, Advances in Natural Sciences: Nanoscience and Nanotechnology, 2017, **8**, 015001.
48. P. Kesharwani, K. Jain, N. K. Jain, Progress in Polymer Science, 2014, **39**, 268-307.
49. G. M. Dykes, Journal of Chemical Technology and Biotechnology, 2001,**76**, 903-918.
50. E. Mohammadifar, A. N. Kharat and M. Adeli, Journal of Materials Chemistry, 2015, **3**, 3896-3921.
51. D. A. Tomalia, J. M. J. Fréchet, Journal of Polymer Science Part A. Polymer Chemistry, 2002, **40,** 2719-2728.

52. M. Rolf, Angewandte Chemie International Edition, 2004, **43,** 1054-1063.
53. D. A. Tomalia, H. Baker, J. Dewald, M. Hall, G. Kallos, S. Martin, J. J. Roeck, Polymer journal, 1985, **17**, 117-132.
54. M. T. Morgan, M. A. Carnahan, C. E. Immoos, A. A. Ribeiro, S. Finkelstein, S. J. Lee, and M. W. Grinstaff, Journal of the American Chemical Society, 2003 ,**125**, 15485-15489.
55. Y. Kim, S. C. Zimmerman, Current opinion in chemical biology., 1998, **2** , 733-742.
56. A. K. Sharma, A. Gothwal, P. K esharwani, H. Alsaab, A. K. Iyer, U. Gupta, Drug discovery today, 2017, **22,** 314-326.
57. G. M. Dykes, Journal of Chemical Technology and Biotechnology, 2001, **76**, 903-918.
58. S. Mohanty, S. K. Biswal, International Journal of Pharmaceutical Research and Allied Sciences, 2015, **4**, 18-27.
59. D. A. Tomalia, H. Baker, J. Dewald, M. Hall, G. Kallos, S. Martin, J. Roeck, J. Ryder, P. Smith, Macromolecules, 1986, 19, 2466-2468.
60. Tomalia, D. A. Dendrimer-based drug delivery systems: from theory to practice, John Wiley and Sons, 2012.
61. C. C. Lee, J. A. MacKay, J. M. J. Fréchet and F. C. Szoka, Nature biotechnology, 2005, **23**,1517-1726.
62. U. Boas, J. B. Christensen and P. M. H. Heegaard, Journal of Materials Chemistry, 2006 ,**16**, 3785-3798.
63. B. M. Rosen, C. J. Wilson, D. A. Wilson, M. Peterca, M. R. Imam and V. Percec, Chemical reviews, 2009, **109**, 6275-6540.
64. J. W. Lee, S. C. Han, S. H. Yun, and S. H. Jin. Bull Korean Chem Soc, 2013, **34**, 971-974.
65. R. Esfand, D. A.Tomalia, Drug discovery today, 2001, **6**, 427-436.
66. B. Klajnert and M. Bryszewska, Acta biochimica polonica, 2001, **48**, 199–208.
67. A. V. Ambade, E. N. Savariar and S. Thayumanavan, Molecular pharmaceutics, 2005, **2**, 264-272.
68. A. Malik, S. Chaudhary, G. Garg and A. Tomar**,** Advances in biological research, 2012, **6**, 165-169.
69. G. R. Newkome, C. D. Shreiner, G. R. Newkome, D. S. Carol, Polymer, 2008 ,**49**, 1-173.
70. S. Svenson, D. A. Tomalia, Advanced drug delivery reviews, 2012 ,**64**, 102-115.
71. U. Singh, M. M. Dar and A. A. Hashmi, Oriental Journal of Chemistry, 2014. 30, 911-922.
72. Holister, Paul, C. R. Vas, and T. Harper, Technology White Papers, 2003, **6**, 1-15.
73. S. M. Grayson and J. M. J. Fréchet, Chemical Reviews, 2001,**101**, 3819-3868.
74. M. S. Kumar, M. Yuvaraj, P. Aruna, D. Koteeswaran and S. Ganesan, International Journal of Polymeric Materials and Polymeric Biomaterials, 2015, **64**, 519-525.
75. A. S. Saxena, S. A. Singh, International Journal of Research in Pharmacy and Science, 2012, **1**, 44-52.
76. R. Duncan, L. Izz, Advanced drug delivery reviews, 2005, **57**, 2215-2237.
77. S. K. Singh, G. K. Lohiya, P. P. Limburkar, N. B. Dharbale, V. K. Mourya, Asian Journal of Pharmaceutics, 2009, **3**, 178.

78. A. Z. Wilczewska, K. Niemirowicz, K. H. Markiewicz, H. Car, Pharmacological reports, 2012, **64**, 1020-1037.
79. N. Malik, R. Wiwattanapatapee, R. Klopsch, K. Lorenz, H. Frey, J. W. Weener, E.W. Meijer, W. Paulus, R. Duncan, Journal of Controlled Release, 2000, **65**, 133-148.
80. W. D. Jang, K. M. K. Selim, C. H. Lee, I. K. Kang, Progress in Polymer Science, 2009, **34**, 1-23.
81. K. Madaan, S. Kumar, N. Poonia, V. Lather, and D. Pandita, Journal of pharmacy and bioallied sciences, 2014, **6**,139.
82. V. P. Torchilin, Journal of controlled release, 2001, **73**, 137-172.
83. P. Stafstrom, E. Hjorth, Y. Zhang, O. C. J. Andre, S. G. Marquet, M. Schultzberg, and M. Malkoch, Biomacromolecules, 2017, **18**, 4323–4330.
84. R. J. Amir and D. Shabat, Chemical communications, 2004, **14**, 1614-1615.
85. B. N. Luna, L. A. Godínez, F. J. Rodríguez, A. Rodríguez, G. Z. L. Larrea, C. F. S. Ferreyra, R. F. M. Curiel, J. Manríquez, and E. Bustos, Journal of Nanomaterials, 2014, **2014**, 39.
86. E. Abbasi, S. F. Aval, A. Akbarzadeh, M. Milani, H. T. Nasrabadi, S. W. Joo, Y. Hanifehpour, K. N. Koshki, R. P. Asl, Nanoscale Research Letters, 2014, **9**, 9-247.
87. N. Nasongkla, B. Chen, N. Macaraeg, M. E. Fox, J. M. J. Fréchet and F. C. Szoka, Journal of the American Chemical Society, 2009, **131**, 3842-3843.
88. T. Garg, O. Singh, S. Arora, R. Murthy, Int J Pharm Sci Rev Res, 2011, **7**, 211-220.
89. A. E. Beezer, A. S. H. King, I. K. Martin, J. C. Mitchel, L. J. Twyman, C. F. Wain, Tetrahedron, 2003, **59**, 3873-3880.
90. J. M. J. Fréchet, Proceedings of the National Academy of Sciences, 2002, **99**, 4782-4787.
91. R. Jevprasesphant, J. Penny, R. Jalal, D. Attwood, N. B. Mckeown, A. D. Emanuele, International journal of pharmaceutics, 2003, **252**, 263-266.
92. G. Pan, Y. Lemmouch, E. O. Akala and O. Bakare, Journal of bioactive and compatible polymers, 2005, **20**, 113-128.
93. J. Amour, K. Twibanire, and T. B. Grindley, Polymers, 2014, **6**, 179-213.
94. L. J. Twyman, Tetrahedron Letters, 2000, **41**, 6875-6878.
95. M. Han, H. Y. Zhang, L. X. Yang, Z. J. Ding, R. J. Zhuang, and Y. Liu, European Journal of Organic Chemistry, 2011, **36**, 7271-7277.
96. M. Ooe, M. Murata, T. Mizugaki, K. Ebitani, and K. Kaneda, Nano Letters, 2002, **2**, 999-1002
97. A. Demanuele, D. Attwood, Advanced drug delivery reviews, 2005, **57,** 2147-2162.
98. V. Leiro, J. P. Garcia, H. Tomas, and A. P. PegoBioconjugate chemistry, 2015, **26**, 1182-1197.
99. O. Flomenbom, R. J. Amir, D. Shabat, J. Klafter, Journal of luminescence, 2005. **111**, 315-325.
100. M. E. Fox, F. C. Szoka, and J. M. J. Fréchet, Accounts of chemical research, 2009, **42**, 1141-1151.
101. E. R. Gillies, J. M. J. Fréchet, Drug discovery today, 2005, **10**, 35-43.
102. M. F. Neerman, H. T. Chen, A. R. Parrish, and E. E. Simanek, Molecular pharmaceutics, 2004, **1**, 390-393.
103. F. G. A. Johan, Jansen, E. W. Meijer and E. M. M. de Brabander-van den Berg Journal of the American Chemical Society, 1995,**117**, 4417-4418.

104. L. J. Twyman, A. E. Beezer, R. Esfand, M. J. Hardy, J. C. Mitchell, Tetrahedron Letters, 1999. **40**, 1743-1746.
105. J. B. Wolinsky, M. W. Grinstaff, Advanced drug delivery reviews, 2008, **60**, 1037-1055.
106. R. H. Müller, S. Runge, V. Ravelli, W. Mehnert, A. F. Thunemann, E. B. Souto, International journal of pharmaceutics, 2006, **317**, 82-89.
107. M. Gonçalves, D. Maciel, D. Capelo, S. Xiao, W. Sun, X. Shi, J. Rodrigues, H. Tomas, and Y. Li, Biomacromolecules, 2014,**15**, 492-499.
108. Y. Cheng, Z. Xu, M. Ma, T. Xu, Journal of pharmaceutical sciences, 2008, **97** ,123-143.
109. D. A. Bhagwat, J. I. Dsouza, International current pharmaceutical journal, 2012, **1**, 414-419.
110. U. Gupta, H. B. Agashe, A. Asthana, and N. K. Jain, Biomacromolecules, 2006, **7**, 649-658.
111. S. Samsudin, PhD thesis, University of Sheffield, 2012.
112. S. Kannan, P. Kolhe , V. Raykova , M. Glibatec , R. M. Kannan , M. L. Lai and D. Bassett, Journal of Biomaterials Science, Polymer Edition. 2004, **15**, 311-330.
113. A. M. Caminade, D. Yan and D. K. Smith, Chemical Society Reviews, 2015, **44,** 3870-3873.
114. H. Frey, R. Haag, Reviews in Molecular Biotechnology, 2002, **90**, 257-267.
115. K. K. Jain, Drug delivery systems, 2008, **437**, 1-50.
116. R. Giovannetti, In Macro to nano spectroscopy, InTech, 2012, **87**.
117. K. R. P. Daniel, J. S. Namban, L. R. Andrade, P. E. N. Souza, L. G. Paterno, R. B. Azevedo, M. A. G. Soler, European Journal of Pharmaceutics and Biopharmaceutics, 2016, **103**, 23-31.
118. J. W. Steed, R. T. David, W. Karl, Core concepts in supramolecular chemistry and nanochemistry. John Wiley and Sons, 2007.
119. I. A. Khodov. M. Y. Nikiforov, G. A. Alper, G. M. Mamardashvili, N. Z. Mamardashvili, O. I. Koifman, Journal of Molecular Structure, 2015, **1081**, 426-430.
120. T. D. Lash, J. L. Romanic, M. J. Hayes and J. D. Spence, Chemical Communications, 1999, **9** ,819-820.
121. G. W. Jin, H. Koo, K. Nam, H. Kim, S. Lee, J. S. Park, Y. Lee, Polymer, 2011. **2**, 339-346.
122. M. Jikei, M. A. Kakimoto, Journal of Polymer Science Part A, Polymer Chemistry, 2004, **42**, 1293-1309.
123. S. M. Grayson and J. M. J. Fréchet, Organic letters, 2002, **4,** 3171-3174.
124. S. P. Gautam, A. K. G. A. Sharma and T. G. Madhu, Global Journal of Medical research, 2013, **13**, 7-15.
125. L. Zhou, D. H. Russell, M. Zhao, and R. M. Crooks, Macromolecules, 2001,**34,** 3567-3573.
126. R. Muller, C. Laschober, W. W. Szymanski, and G. Allmaier, Macromolecules, 2007, **40**, 5599-5605.
127. P. Kolhe, E. Misra, R. M. Kannan, S. Kannan, M.L. Lai, International journal of pharmaceutics, 2003, **259**, 143-160.
128. R. R. Giri, H. Ozaki, Y. Takayanagi, S. Taniguchi, R. Takanami, International Journal of Environmental Science and Technology, 2011, **8**, 19-30.

129. D. P. Patel, R. R. Shah, A. P. Patel and P. K. Tank, Pharma Science Monitor, 2012, **3**,4.
130. F. Lodato, PhD thesis, University of Massey, 2006.
131. F. Wang, L. Xu, M. H. Nawaz, F. Liu and W. Zhang, RSC Advances, 2014, **106**, 61378-61382.
132. D. P, Arnold, J. Blok, Coordination chemistry reviews, 2004, **248**, 299-319.
133. F. Chiba, PhD Thesis, University of Sheffield, 2009.
134. L. Li and K. M. Huh, Biomaterials research, 2014, **18**, 19.
135. A. Guenet, E. Graf, N. Kyritsakas and M.W. Hosseini, W. Inorganic chemistry, 2010, **49**, 1872-1883.
136. D. Li, K. K. Huang, B. Hu, Z. Shi, G. Wang, S. H. Feng, Journal of Molecular Structure, 2009, **938**, 82-88.
137. J. C. Hawley, N. Bampos, J. K. M. Sanders and R. J. Abraham, Chemical Communications, 1998, **6**, 661-662.
138. M. Liu, J. M. J. Fréchet, Pharmaceutical science and technology today, 1999,**2**, 393-401.
139. N. Nishiyama, H. R. Stapert, G. D. Zhang, D. Takasu, D. L. Jiang, T. Nagano, T. Aida, K. Kataoka, Bioconjugate chemistry, 2003, **14,** 58-66.
140. Y. R. Peng, Y. H. Cao, P. F. Chen, X. X. Huang, Chinese Chemical Letters, 2008, **3**, 273-276.
141. C. Kantar, E. Ataci, S. Sasmaz, Turkish Journal of Chemistry, 2014, **38**, 1185-1200.
142. A. Atsay, A. Koca, M. B. Kocak, Transition metal chemistry, 2009, **34**, 877.
143. D. Roy, N. M. Dasa, N. Shakti and P. S. Gupta, P. S. RSC Advance, 2014, **4**, 42514-42522.
144. B. Devarakonda, R. A. Hill, M.M. Villiers, International journal of pharmaceutics, 2004, **284**, 133-140.
145. C. Yiyun, X. Tongwen, F. Rongqiang, European Journal of Medicinal Chemistry, 2005 ,**40**, 1390-1393.
146. A. Alka, Y. Pareek, V. S. Shetti, M. R. Rao, G. G. Theophall, W. Z. Lee, K. V. Lakshmi, and M. Ravikanth, Coordination Chemistry Reviews, 2012, **256**, 2816-2842.